THE UNIVERSITY OF MICHIGAN
OCT 5 - 1960
ENGINEERING

JOURNAL OF FLUID MECHANICS

VOLUME 9 PART 1

SEPTEMBER 1960

PUBLISHED BY

CAMBRIDGE UNIVERSITY PRESS

BENTLEY HOUSE, 200 EUSTON ROAD, LONDON, N.W. 1

AMERICAN BRANCH: 32 EAST 57TH STREET, NEW YORK 22, N.Y.

Price 30*s.* (*U.S.A.* $5.00)

The JOURNAL OF FLUID MECHANICS exists for the publication of theoretical and experimental investigations of all aspects of the mechanics of fluids, and is issued in four parts per volume.

EDITOR

DR G. K. BATCHELOR

Department of Applied Mathematics and Theoretical Physics, University of Cambridge, Free School Lane, Cambridge, England

ASSISTANT EDITORS

DR T. B. BENJAMIN, DR I. PROUDMAN, DR P. G. SAFFMAN

Department of Applied Mathematics and Theoretical Physics, University of Cambridge, Free School Lane, Cambridge, England

ASSOCIATE EDITORS

PROF. G. F. CARRIER

Pierce Hall, Harvard University, Cambridge 38, *Massachusetts, U.S.A.*

DR W. C. GRIFFITH

Research and Development Laboratory, Missile Systems Division, Lockheed Aircraft Corporation, Palo Alto, California, U.S.A.

M. J. LIGHTHILL

Royal Aircraft Establishment, Farnborough, Hampshire, England

PROF. R. R. LONG

School of Engineering, The Johns Hopkins University, Baltimore 18, *Maryland, U.S.A.*

Authors wishing to have papers published in the JOURNAL should communicate them to any one of the persons named above, choosing one in their own country where possible.

Authors are urged to ensure that their papers are written clearly and attractively, in order that their work will be readily accessible to readers.

Manuscripts should be typed in double spacing on one side of the paper only, with references listed at the end in alphabetical order of authors. Drawings should be done on a large scale in Indian ink on tracing cloth or drawing paper, the lettering being shown clearly in pencil for reproduction by the printer; the list of captions should be typed at the end of the manuscript. Proofs of papers from overseas will usually be despatched to authors by airmail. There is no charge for publication. Authors are entitled to receive 50 offprints of a paper in the JOURNAL free of charge, and additional offprints can be purchased if ordered in advance.

SUBSCRIPTIONS

The subscription price for a volume of four parts is £5. 10*s*. net, post free, payable in advance; separate parts 30*s*. net, plus postage. Subscriptions may be sent to any bookseller, or to the Cambridge University Press, Bentley House, 200 Euston Road, London, N.W.1.

Subscribers in the United States should send their orders to the Cambridge University Press, American Branch, 32 East 57th Street, New York 22, N.Y. The subscription price per volume is $18.50, post free, payable in advance; separate parts $5.00, plus postage.

Quotations for available back volumes and parts may be obtained on application to the Cambridge University Press.

On the generation of sound by supersonic turbulent shear layers

By O. M. PHILLIPS

Mechanics Department, The Johns Hopkins University, Baltimore

(Received 12 March 1960)

A theory is proposed to describe the generation of sound by turbulence at high Mach numbers. The problem is formulated most conveniently in terms of the fluctuating pressure, and a convected wave equation (2.8) is derived to describe the generation and propagation of the pressure fluctuations.

The supersonic turbulent shear zone is examined in detail. It is found that, at supersonic speeds, sound is radiated as eddy Mach waves, and as the Mach number increases, this mechanism of generation becomes increasingly dominant. Attention is concentrated on the properties of the pressure fluctuations just outside the shear zone where the interactions among the weak shock waves have had little effect. An asymptotic solution for large M is derived by a Green's function technique, and it is found that radiation with given frequency n and wave-number $\mathbf{k}$ can be associated with a corresponding critical layer within the shear zone.

It is found that $\overline{(p-p_0)^2}$ increases approximately as $M^{\frac{3}{2}}$ for $M \gg 1$ contrasting with the M^8 variation found by Lighthill for $M \ll 1$. The acoustic efficiency thus varies as $M^{-\frac{3}{2}}$ for $M \gg 1$, and as M^5 for $M \ll 1$, indicating a maximum acoustic efficiency for Mach numbers near one. The directional distribution of the radiation is discussed and the direction of maximum intensity is shown to move towards the perpendicular to the shear zone as M increases. The predictions of the theory are supported qualitatively by the few available experimental observations.

1. Introduction

The problem of acoustic radiation from turbulence has excited interest in recent years because of its relevance to questions of structural fatigue and human discomfort in high-speed aerodynamics. The problem was formulated by Lighthill (1952, 1954), and most subsequent work has been concerned with the application and extension of his technique to various flows at Mach numbers much less than one. A central point in Lighthill's formulation is the emergence of an exact analogy with classical acoustics. From the momentum and continuity equations of the fluid, he showed that the fluctuations in density ρ are described by the equation

$$\frac{\partial^2 \rho}{\partial t^2} - a_0^2 \nabla^2 \rho = \frac{\partial^2 T_{ij}}{\partial x_i \partial x_j}, \tag{1.1}$$

where a_0 is the speed of sound in the undisturbed medium and

$$T_{ij} = \rho u_i u_j + p_{ij} - a_0^2 \rho \delta_{ij}. \tag{1·2}$$

In this expression u_i represents the Cartesian velocity components, p_{ij} the stress tensor and δ_{ij} the Kronecker delta tensor.

If the right-hand side of (1.1) were zero, it would be the simple wave equation for the propagation of density fluctuations in a uniform acoustic medium. The full equation is identical with the equation governing sound propagation in an acoustic medium containing a distribution of quadrupole sources whose strength per unit volume is T_{ij}. It follows that there is an exact analogy between the density fluctuations in a real fluid in arbitrary motion and those in a uniform acoustic medium at rest; all the real fluid effects such as sound generation, convection, attenuation and the like are represented by a suitably chosen distribution of acoustic quadrupoles. This acoustical analogy has been powerful in the development of the subject, since it implies that we can use the terminology and concepts of classical acoustics, and the problem really reduces to finding from considerations of the flow dynamics the appropriate distribution $T_{ij}(\mathbf{x}, t)$.

If the Mach number of the flow is small, and this is the case with which most contributions have been concerned, T_{ij} can be approximated by $\rho_0 u_i u_j$; and a retarded potential solution of (1.1) can be written down. This ultimately leads to Lighthill's U^8 law for the intensity of the radiated sound when the Mach number $M \ll 1$. The restriction to low Mach numbers, though not inherent in the original analogy, becomes very important in the course of this analysis. It is involved first in the neglect of $\partial^2(p_{ij} - a_0^2 \rho \delta_{ij})/\partial x_i \partial x_j$ in (1.1) which corresponds physically to the neglect of the sound attenuation and of the variation in the speed of sound at different points in the flow. It is invoked again to replace the density factor in $\rho u_i u_j$ by ρ_0, the density of the undisturbed fluid. This is a good approximation if $(\rho - \rho_0)/\rho_0$ is small, but at high Mach numbers this may not be so. Without this approximation, the retarded potential 'solution' of (1.1) is an integral equation for ρ of a rather intractible kind. This alone would provide a considerable obstacle to extending the Lighthill formulation to high Mach numbers, but it would not be the only one. If $M \gg 1$, the lifetime of an eddy is comparable with, or shorter than, the time taken by a sound pulse to move across the eddy, and the retarded time effect could not at any stage be neglected. Despite this cascade of difficulties, attempts have been made by Ribner (in an unpublished note) and Lilley (1958) to extend the Lighthill approach to mean velocity Mach numbers of about 1·5 or 2, but this seems to be the limit. It has frequently been speculated that, for very large M, the acoustic efficiency might become constant, so that the sound intensity would be proportional to U^3. The author has been unable to find convincing reasons for this belief; it seems that the only reasonable statement of this kind that one can make is that the acoustic efficiency must be bounded above, so that the exponent of U must be less than or equal to 3.

It appears that if we are to be concerned with high Mach numbers, a new approach will be necessary, involving a reformulation of the problem from the beginning. An attempt towards this is made in the present paper. This will involve a reluctant abandonment of the acoustical analogy, and a discussion of the phenomenon as a flow problem at large Mach numbers.

It might be worth while at this point to set forth the detailed aims of this investigation. The first, of course, is to uncover the mechanism whereby sound is generated in a supersonic turbulent flow; it is found to be different from the one that dominates when $M \ll 1$. Secondly, we wish to find how the intensity of the sound field, its directional distribution and the radiated energy flux vary with the appropriate flow parameters, particularly the Mach number M. Associated with this is the question of radiation damping—does the loss of energy from the turbulence by radiation ever become such a large fraction of the energy supply that the turbulence itself tends to be damped out at very large Mach numbers? With these objectives in mind we propose to investigate the sound radiation from a turbulent shear zone, this particular flow being chosen for reasons of relative simplicity and convenience, and in the hope that the results might be experimentally verifiable in, say, the shear zones of a jet.

My first attempt to formulate the problem was in terms of density fluctuations, as in Lighthill's approach. This led to what can best be described as a convected wave equation rather similar to (2.8) below, in which the dependent variable was $\log(\rho/\rho_0)$. This overcame one of the difficulties in the Lighthill formulation in that the density did not occur explicitly on the right-hand side as it does in (1.1). However, the right-hand side consisted of two large terms whose relative importance was difficult to estimate—one involving vorticity fluctuations and one entropy fluctuations. This might indeed have been inferred *a priori* from the work of Chu & Kovasznay (1958) concerning the interactions among the various modes of motion at supersonic speeds. However, if the problem is expressed in terms of pressure fluctuations, this difficulty disappears and the right-hand side of our governing wave equation, (2.8) below, contains only a single dominant term, since pressure-entropy interactions are small.

2. The convected wave equation

In the present discussion, it will be assumed that the effects of gas dissociation and relaxation phenomena can be neglected. These approximations will probably be adequate in aeronautical problems (except in strong shock waves) if the stagnation temperature does not exceed about 2000° K. The equation of state for a perfect gas is

$$p = \mathscr{R}\rho T, \tag{2.1}$$

where $\mathscr{R}$ is the gas constant and p, ρ, T represent the pressure, density and temperature of the gas. In a fixed Cartesian reference frame, the equation of continuity is

$$\frac{1}{\rho}\frac{D\rho}{Dt} + \frac{\partial u_i}{\partial x_i} = 0, \tag{2.2}$$

and since the density can be considered a function of pressure and entropy S, this equation can be expressed alternatively as

$$\frac{1}{\rho}\left(\frac{\partial \rho}{\partial p}\right)_S \frac{Dp}{Dt} + \frac{1}{\rho}\left(\frac{\partial \rho}{\partial S}\right)_p \frac{DS}{Dt} + \frac{\partial u_i}{\partial x_i} = 0. \tag{2.3}$$

From the second law of thermodynamics,

$$dS = c_v \frac{dT}{T} + \left(\frac{\partial p}{\partial T}\right)_\rho d\left(\frac{1}{\rho}\right)$$

(Howarth, 1953, p. 45), where c_v is the specific heat at constant volume. Therefore

$$\left(\frac{\partial S}{\partial \rho}\right)_p = \frac{c_v}{T}\left(\frac{\partial T}{\partial \rho}\right)_p - \frac{1}{\rho^2}\left(\frac{\partial p}{\partial T}\right)_\rho$$
$$= -\rho^{-1}(c_v + \mathscr{R})$$
$$= -\frac{c_p}{\rho}, \tag{2.4}$$

from (2.1) and the equation $c_p - c_v = \mathscr{R}$, where c_p is the specific heat at constant pressure. Furthermore,

$$\left(\frac{\partial p}{\partial \rho}\right)_S = a^2 = \frac{\gamma p}{\rho},$$

where a is the local speed of sound and γ the ratio of specific heats, so that (2.3) can be expressed as

$$\frac{\partial u_i}{\partial x_i} = -\frac{1}{\gamma p}\frac{Dp}{Dt} + \frac{1}{c_p}\frac{DS}{Dt}. \tag{2.5}$$

The momentum equation for the fluid is

$$\frac{Du_i}{Dt} = \frac{1}{\rho}\frac{\partial p_{ij}}{\partial x_j}, \tag{2.6}$$

where p_{ij} represents the stress tensor which, for a Stokesian fluid, is of the form

$$p_{ij} = -p\delta_{ij} + \mu(e_{ij} - \tfrac{2}{3}\theta\delta_{ij}), \tag{2.7}$$

where δ_{ij} is the Kronecker delta, e_{ij} the rate of strain tensor and $\theta = \partial u_i/\partial x_i$ the fluid dilatation.

We now eliminate the linear velocity term between (2.5) and (2.6). Since

$$\frac{\partial}{\partial x_i}\frac{D}{Dt} \equiv \frac{D}{Dt}\frac{\partial}{\partial x_i} + \frac{\partial u_j}{\partial x_i}\frac{\partial}{\partial x_j},$$

it follows from (2.6) and (2.7) that

$$\frac{D}{Dt}\frac{\partial u_i}{\partial x_i} = -\frac{\partial u_j}{\partial x_i}\frac{\partial u_i}{\partial x_j} - \frac{\partial}{\partial x_i}\left(\frac{1}{\rho}\frac{\partial p}{\partial x_i}\right) - \frac{\partial}{\partial x_i}\left\{\frac{1}{\rho}\frac{\partial}{\partial x_j}[\mu(e_{ij} - \tfrac{2}{3}\theta\delta_{ij})]\right\}.$$

Operating on equation (2.5) with D/Dt, and subtracting the result from the last expression, we have

$$\frac{D^2}{Dt^2}\log\left(\frac{p}{p_0}\right) - \frac{\partial}{\partial x_i}\left\{a^2\frac{\partial}{\partial x_i}\log\left(\frac{p}{p_0}\right)\right\}$$
$$= \gamma\frac{\partial u_i}{\partial x_j}\frac{\partial u_j}{\partial x_i} + \gamma\frac{D}{Dt}\left(\frac{1}{c_p}\frac{DS}{Dt}\right) - \gamma\frac{\partial}{\partial x_i}\left\{\frac{1}{\rho}\frac{\partial}{\partial x_j}[\mu(e_{ij} - \tfrac{2}{3}\theta\delta_{ij})]\right\}, \tag{2.8}$$

since

$$\frac{1}{p}\frac{Dp}{Dt} = \frac{D}{Dt}\log\left(\frac{p}{p_0}\right); \quad \frac{1}{\rho}\frac{\partial p}{\partial x_i} = \frac{a^2}{\gamma}\frac{\partial}{\partial x_i}\log\left(\frac{p}{p_0}\right),$$

where p_0 is a convenient reference pressure.

Equation (2.8) provides the starting point of the present investigation. The terms on the left-hand side are those of a wave equation in a moving medium with a variable speed of sound, the partial time derivatives of the ordinary wave

equation being replaced by derivatives following the motion. The first term on the right-hand side represents the generation of pressure fluctuations by the velocity fluctuations in the fluid while the remaining terms describe the effects of entropy fluctuations and fluid viscosity. In contrasting these equations with those of Lighthill, it is evident that the effects of convection and variation in the local speed of sound are included here in the left-hand side of the equations, whereas in Lighthill's acoustic analogy, they were described in terms of a quadrupole distribution in an acoustic medium. In supersonic flow, neither of these effects can reasonably be ignored, whereas if $M \ll 1$, the variation of a^2 is likely to be small, and the convection effects can if necessary be included by a subsequent translation of our frame of reference. In both this and Lighthill's case, the direct effects of fluid viscosity and heat conductivity are likely to be unimportant as far as the sound generation is concerned, and under these circumstances the last two terms of (2.8) can be neglected, since

$$\rho T \frac{DS}{Dt} = \Phi + \frac{\partial}{\partial x_i}\left(\kappa \frac{\partial T}{\partial x_i}\right), \tag{2.9}$$

where Φ is the rate of energy dissipation per unit volume by viscosity and κ the fluid conductivity.

If we were to be concerned with the *structure* of the shock waves developed inside a turbulent fluid at high Mach numbers, then these terms certainly could not be neglected, since the internal structure of the shocks is determined by the balance between these diffusive and the convective effects. For a turbulent shear layer, however, there is the possibility that we might consider separately the processes of generation of the pressure waves and the subsequent development of the shocks. The pressure waves are generated inside the shear zone and they develop into weak or strong shock waves with increasing distance from the turbulent zone. The distance that the wave travels before the shock is fully developed is $\lambda p_0/p'$ (Lighthill 1956, § 5·2), where λ is the wavelength, p_0 the mean pressure and p' the root-mean-square fluctuation in pressure associated with the wave. If this distance is comparable with, or larger than, the shear zone thickness, a separation of the two processes is possible, and the diffusive effects can be neglected as far as the generation is concerned. We would expect that a theory based on this separation would reliably predict the pressure field just outside the shear zone for all wavelengths if p'/p_0 is small and for the larger wavelengths of the sound field if p'/p_0 is moderate.

3. The Fourier transform equation

Consider a turbulent shear zone in which the mean velocity $\overline{u_1}$ is a function of the x_3 position co-ordinate only. Suppose that the characteristic zone thickness is $2L$ and that $\overline{u_1}$ changes from $-U$ to U as x_3 moves from $-\infty$ to ∞. We seek to derive properties of the radiated pressure waves in terms of the velocity fluctuations of the shear zone, our primary concern being with values of U greater than a_0, the speed of sound at infinity. For the sake of analytical convenience we suppose further that all mean-point properties of the motion in the shear zone are

independent of x_1, x_2 and time t, being functions of x_3 alone, the position coordinate normal to the zone.

Neglecting the diffusive terms in (2.8), we obtain

$$\left\{\frac{D^2}{Dt^2}-\frac{\partial}{\partial x_i}a^2\frac{\partial}{\partial x_i}\right\}\log\left(\frac{p}{p_0}\right)=\gamma\frac{\partial u_i}{\partial x_j}\frac{\partial u_j}{\partial x_i}. \tag{3.1}$$

This equation† can be further simplified if we neglect on the left-hand side products of two fluctuating quantities with zero means, on the understanding that these will be small (in mean square) compared with the products of mean and fluctuating quantities. This neglects such physical processes as the convection and scattering of sound by the *turbulence*, and by variation of a^2 about its local mean value. We retain, however, besides the generation term, the processes of convection and refraction of the sound by the mean flow and by variation with x_3 of the local mean speed of sound. The latter may be important if there are significant variations in the mean temperature of the flow. Equation (3.1) then reduces to

$$\left\{\left(\frac{\partial}{\partial t}+\bar{u}_1\frac{\partial}{\partial x_1}\right)^2-\frac{\partial}{\partial x_i}\bar{a}^2\frac{\partial}{\partial x_i}\right\}\log\left(\frac{p}{p_0}\right)=\gamma\frac{\partial u_i}{\partial x_j}\frac{\partial u_j}{\partial x_i}, \tag{3.2}$$

or

$$\left\{\left(\frac{\partial}{\partial t}+\bar{u}_1\frac{\partial}{\partial x_1}\right)^2-\frac{\partial\bar{a}^2}{\partial x_3}\frac{\partial}{\partial x_3}-\bar{a}^2\frac{\partial^2}{\partial x_i^2}\right\}\log\left(\frac{p}{p_0}\right)=\gamma\frac{\partial u_i}{\partial x_j}\frac{\partial u_j}{\partial x_i}, \tag{3.3}$$

since $\bar{a}^2=\bar{a}^2(x_3)$. In many instances, the dominant term on the right-hand side is likely to result from the interactions of the large mean velocity gradient with the fluctuating velocity gradients, and the generation term can be approximated by

$$2\gamma\frac{\partial\bar{u}_1}{\partial x_3}\frac{\partial u_3}{\partial x_1}, \tag{3.4}$$

but for the present, the full expression will be retained.

It is of advantage to express (3.3) in dimensionless form. Let the instantaneous and mean velocities be given by

$$v_i=\frac{u_i}{U},\quad V=\bar{v}_1, \tag{3.5a}$$

and also

$$y_i=\frac{x_i}{L},\quad \tau=\frac{tU}{L},$$

$$A^2(y_3)=\frac{\bar{a}^2}{a_0^2},\quad M=\frac{U}{a_0}, \tag{3.5b}$$

where a_0 is a reference sound speed, say at $y_3=+\infty$ in the undisturbed fluid. If the mean stagnation temperature is the same on both sides of the shear zone, then

$$A(y_3)\to 1\quad\text{as}\quad y_3\to\pm\infty; \tag{3.6}$$

the limit as $y_3\to-\infty$ may be different otherwise.

† Since diffusive effects are neglected in this equation, $p\propto\rho^\gamma$ and (3.1) takes the alternative form

$$\left\{\frac{D^2}{Dt^2}-\frac{\partial}{\partial x_i}a^2\frac{\partial}{\partial x_i}\right\}\log\left(\frac{\rho}{\rho_0}\right)=\frac{\partial u_i}{\partial x_j}\frac{\partial u_j}{\partial x_i},$$

from which the familiar Lighthill form can be deduced immediately when $M\ll 1$.

The dimensionless form of (3.3) is thus

$$\left\{\left(\frac{\partial}{\partial\tau}+V\frac{\partial}{\partial y_1}\right)^2-\frac{1}{M^2}\frac{dA^2}{dy_3}\frac{\partial}{\partial y_3}-\frac{A^2}{M^2}\frac{\partial^2}{\partial y_i^2}\right\}\log\left(\frac{p}{p_0}\right)=\gamma\frac{\partial v_i}{\partial y_j}\frac{\partial v_j}{\partial y_i}, \tag{3.7}$$

which can be reduced to the normal form for y_3 (in which there is no first differential operator $\partial/\partial y_3$) by taking a new dependent variable

$$\zeta(\mathbf{y},t)=A(y_3)\log\left(\frac{p}{p_0}\right). \tag{3.8}$$

This yields

$$\left\{\left(\frac{\partial}{\partial\tau}+V\frac{\partial}{\partial y_1}\right)^2+\frac{A}{M^2}\frac{d^2A}{dy_3^2}-\frac{A^2}{M^2}\frac{\partial^2}{\partial y_i^2}\right\}\zeta(\mathbf{y},\tau)=\gamma A(y_3)\frac{\partial v_i}{\partial y_j}\frac{\partial v_j}{\partial y_i}$$
$$=G(\mathbf{y},\tau),\quad\text{say.} \tag{3.9}$$

The generation term G is significant only inside the turbulent shear zone, so that

$$G(\mathbf{y},\tau)\to 0\quad\text{as}\quad y_3\to\pm\infty. \tag{3.10}$$

Let us now define the generalized Fourier transforms (Lighthill 1958)

$$\left.\begin{aligned}\zeta(\mathbf{y},\tau)&=\iint\varpi(y_3,\mathbf{k},n)\exp\{i(\mathbf{k}.\mathbf{y}+n\tau)\}\,d\mathbf{k}\,dn,\\ G(\mathbf{y},\tau)&=\iint\Gamma(y_3,\mathbf{k},n)\exp\{i(\mathbf{k}.\mathbf{y}+n\tau)\}\,d\mathbf{k}\,dn,\end{aligned}\right\} \tag{3.11}$$

where $\mathbf{k}=(k_1,k_2)$ is a wave-number vector in the plane of the shear layer and the integrations are made over all values of $\mathbf{k}$ and frequency n.

The equation relating the generalized Fourier transforms ϖ and Γ that corresponds to (3.9) is

$$\frac{d^2}{dy^2}\varpi(y,\mathbf{k},n)+\left\{\frac{M^2}{A^2}(n+Vk_1)^2-k^2-\left(\frac{A''}{A}\right)\right\}\varpi(y,\mathbf{k},n)=-\frac{M^2}{A^2}\Gamma(y,\mathbf{k},n), \tag{3.12}$$

where the suffix on y_3 has been dropped, $k^2=k_1^2+k_2^2$, A and V are functions of y only, and $A''=d^2A/dy^2$.

4. Some simple deductions

Before we embark on a detailed analysis of equation (3.12), it might be worth while to discuss briefly the nature of the solutions that we expect in the region $|y|>1$ outside the shear zone. For $y>1$, $G(y)\simeq 0$, $A(y)\simeq 1$, $V(y)\simeq 1$, so that (3.12) becomes

$$\frac{d^2\varpi}{dy^2}+\{M^2(n+k_1)^2-k^2\}\varpi=0. \tag{4.1}$$

Since $\varpi(y)$ must be bounded as $y\to\infty$, the solutions to (4.1) must be either exponentially decreasing or oscillatory according as the coefficient of ϖ is negative or positive. Clearly the oscillatory solution corresponds to a radiated pattern of Mach waves, which for a given Mach number are associated with wave-numbers $\mathbf{k}$ and frequencies n such that

$$M^2(n+k_1)^2-k^2>0. \tag{4.2}$$

Let us consider the contribution to the radiated pressure field from the layer between $y = Y$ and $y = Y + \delta Y$ in the shear zone. The turbulent eddies in this neighbourhood are convected by the mean stream with velocity V_c, say, which is approximately equal to the local mean velocity at Y. If the flow is supersonic, it is sufficient to neglect for the moment the evolution of the eddy pattern as it is carried along, so that the frequency of the components of wave-number $\mathbf{k}$ is just the frequency with which the wave component is swept past the fixed observation point at a rigid convected pattern.† We therefore have

$$n = -k_1 V_c. \tag{4.3}$$

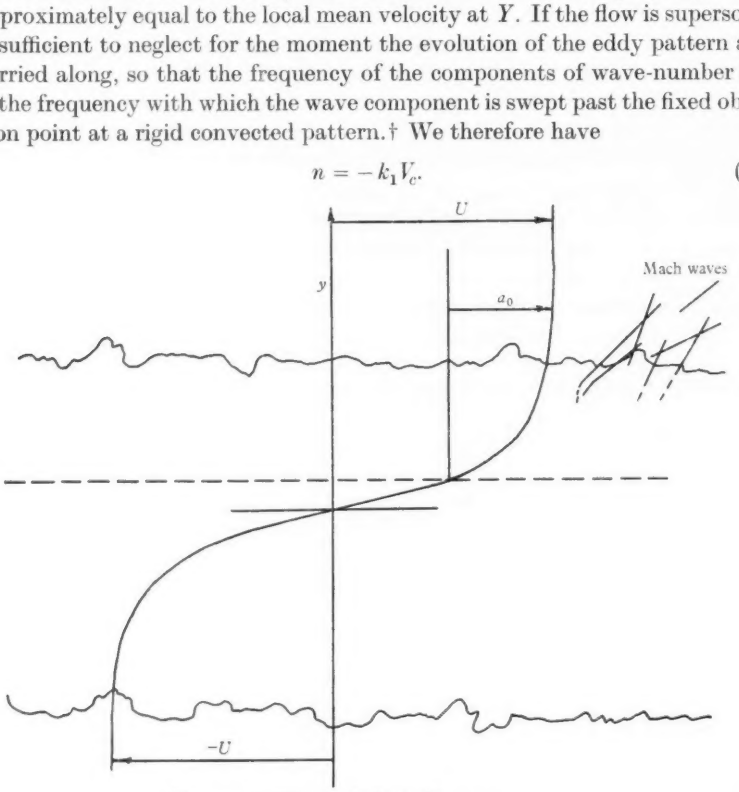

FIGURE 1. The turbulent shear zone.

The layer of the shear zone near Y, where the convection velocity is V_c, will therefore generate Mach waves on the side of the layer $y > 1$ with wave-numbers $\mathbf{k}$ such that

$$M^2 k_1^2 (1 - V_c)^2 > k^2.$$

If θ is the angle between the vector wave-number $\mathbf{k}$ and the direction of the mean velocity, then $\cos\theta = k_1/k$ and this condition becomes

$$\cos^2\theta > [M(1 - V_c)]^{-2}. \tag{4.4}$$

Radiated Mach waves will therefore be generated by some wave-numbers in those layers of the shear zone for which the difference between the mean velocity of the fluid outside the shear zone and the local eddy convection velocity is greater than the speed of sound outside the zone. Generation of Mach waves

† Notice that if the eddy convection velocity is subsonic, this approximation is much too coarse. As Lighthill (1952, 1954) has shown, sound is radiated in subsonic flow *only because* the convected eddy pattern does change as it is carried along.

in this way is somewhat analogous to their formation by thin bodies moving supersonically; they can be described conveniently as 'eddy Mach waves'. This is illustrated in figure 1, where the area below the dashed line, including the whole of the turbulent region in $y < 0$, represents the part of the shear zone which make some contribution to the eddy Mach waves in the fluid above the zone. Clearly, there is a corresponding region towards the upper side of the shear zone that is responsible for Mach wave generation in the fluid below the zone. The possibility that this effect might be important was suggested by Kramer (1955) among others, but hitherto no detailed analysis has been carried out.

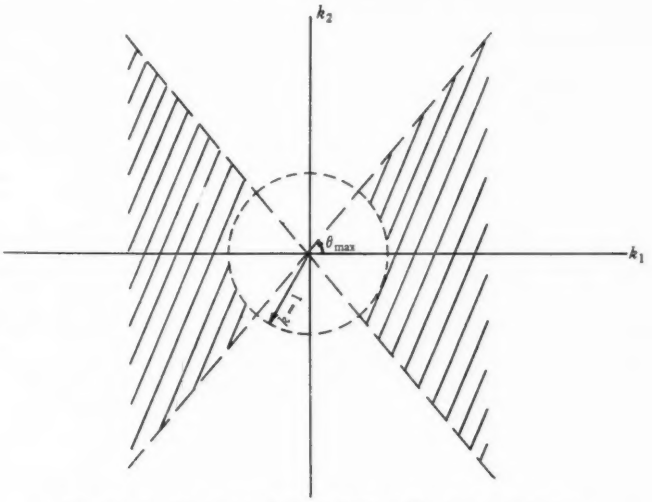

FIGURE 2. Wave-numbers radiating Mach waves from a given critical layer in the shear zone.

For a given layer where the convection velocity is V_c, the allowable wave-numbers for Mach wave generation are given by (4.4) and are indicated in figure 2 by the region inside the lines

$$\theta_{\max} = \cos^{-1}\{M(1-V_c)\}^{-1}.$$

However, the maximum eddy size in the shear layer is of order $6L$, or a little more, so that the smallest (dimensionless) wave-numbers present in the turbulence are of order 1 or a little less. We would therefore expect to find the wave-numbers of the radiated pressure field predominantly in the region $\theta < \theta_{\max}$, $k > 1$. As the Mach number increases, the critical angle $\theta_{\max}$ increases also, until at very high Mach numbers, almost all components of the turbulence are capable of radiating Mach waves.

The Fourier components whose wave-numbers lie at angles greater than $\theta_{\max}$ (whose convection velocities resolved in the direction of **k** are subsonic) are still of course capable of radiating some sound since their amplitides and phases change slowly as they are convected. Their contribution could be estimated in a manner analogous to that used by Lighthill (1952). However, if the Mach

number of the flow is substantially greater than one, their contribution is probably unimportant, and decreases with increasing M, since for most of the shear layer only a small part of the wave-number plane is excluded by the condition (4.4).

These geometrical considerations do not allow any quantitative predictions concerning the over-all intensity of the radiated field or its distribution among the wave-numbers indicated in figure 2. Such questions can be answered only by a more detailed analysis of (3.12).

5. The radiated pressure field

Equation (3.12) can be expressed as

$$\frac{d^2\varpi(y)}{dy^2}+\left\{M^2q^2(y)-k^2-\left(\frac{A''}{A}\right)\right\}\varpi(y)=-\frac{M^2}{A^2}\Gamma(y), \tag{5.1}$$

where

$$q(y)=\frac{n+k_1V(y)}{A(y)}. \tag{5.2}$$

If $|n|<|k_1|$,† then $q(y)$ passes through zero at some value of y, say Y such that

$$n+k_1V(Y)=0. \tag{5.3}$$

This equation defines the critical layer for a given n and $\mathbf{k}$ more formally than was possible by the intuitive arguments of the previous section, and it will be found that the radiation of frequency n and wave-number $\mathbf{k}$ does indeed originate from the region of the shear zone near Y. When M is large, the coefficient of the term containing $\varpi(y)$ has a small negative region (the subsonic region) near $y=Y$ where $q(Y)=0$. The two zeros are closely spaced, their separation being of order M^{-1}, and the coefficient becomes constant in y as $|y-Y|\to\infty$. This behaviour suggests that we transform (5.1) to the form

$$\frac{d^2\xi}{dz^2}+b^2z^2\xi=f(z), \tag{5.4}$$

where b is a large parameter (of order M) and b^2z^2 has a double zero at $z=0$ corresponding to the closely spaces zeros in $M^2q^2(y)-k^2-(A''/A)$ as $M\to\infty$.

Unless the mean speed of sound changes abruptly within the shear zone (which is unlikely, because of the mixing effect of the turbulence) the term A''/A in this coefficient is small compared with k^2 for the wave-numbers greater than unity with which we are concerned. The principal influence of the variation in the speed of sound in the shear zone has been accounted for by the change of variable (3.8), and even in an extreme case where A changes by a factor of two across the shear zone, the influence of the term A''/A will be felt only by the pressure fluctuations of the largest scale, for which k is of order unity. In general, then, it is sufficient to approximate the coefficient of the second term on the left-hand side of (5.1) by

$$M^2q^2(y)-k^2.$$

† It is clear that there will exist such frequencies in the sound field, since these correspond to the frequencies in the turbulence.

The details of finding the asymptotic solution as $M \to \infty$ to (5.1) are given in the Appendix, but a brief indication of the procedure followed might be in order. Equation (5.1) is transformed so that its left-hand side resembles that of (5.4). One's first inclination would be to seek an asymptotic solution for $-\infty < y < \infty$ in powers of M^{-1}, but it transpires that the first term in this series diverges. If, instead, the domain is divided into the regions $-\infty < y \leqslant Y$ and $Y \leqslant y < \infty$, a convergent asymptotic solution can be found if the large parameter corresponding to b above is taken as

$$\left.\begin{aligned} \lambda &= \left\{M^2 - \frac{k^2}{Q_-^2}\right\}^{\frac{1}{2}} \quad \text{for} \quad -\infty < y \leqslant Y, \\ \mu &= \left\{M^2 - \frac{k^2}{Q_+^2}\right\}^{\frac{1}{2}} \quad \text{for} \quad Y \leqslant y < \infty, \end{aligned}\right\} \tag{5.5}$$

where

$$Q_+ = \lim_{y \to \infty} q(y) = n + k_1,$$

$$Q_- = \lim_{y \to -\infty} q(y) = \frac{n - k_1}{A(-\infty)}.$$

The asymptotic solutions are found in these two domains by a Green's function technique, and the arbitrary constants are determined by applying radiation conditions outside the shear zone and matching conditions at $y = Y$.

In the region outside the shear zone, $y > 1$, the asymptotic expression for the Fourier transform $\varpi(y, \mathbf{k}, n)$ is given from (A. 31), (A. 40), (A. 54) and (A. 57) as

$$\varpi(y, \mathbf{k}, n) \sim \frac{(-\frac{3}{4})! \exp(\frac{3}{8}\pi i)}{4\mu^{\frac{5}{4}} Q_+^{\frac{1}{4}}} \left\{\left(\frac{\mu}{\lambda}\right)^{\frac{1}{2}} + i\right\} h(0) \exp\left\{-i\mu \int_Y^y q(y)\, dy\right\}, \tag{5.6}$$

for large λ and μ where

$$\left.\begin{aligned} h(0) &= -\frac{M^2 \Gamma(Y, \mathbf{k}, n)}{A^2(Y)\, \Omega^{\frac{3}{4}}}, \\ \Omega &= \left(\frac{dV}{dy}\right)_Y, \end{aligned}\right\} \tag{5.7}$$

from (A. 16) and (A. 34). On the other side of the shear zone, $y < -1$, the corresponding expression is

$$\varpi(y, \mathbf{k}, n) \sim \frac{-i(-\frac{3}{4})! \exp(-3\pi i/8)}{4\lambda^{\frac{5}{4}} Q_-^{\frac{1}{4}}} \left\{\left(\frac{\lambda}{\mu}\right)^{\frac{1}{2}} - i\right\} h(0) \exp\left\{i\lambda \int_Y^y q(y)\, dy\right\}. \tag{5.8}$$

Several properties of these solutions are of interest at this stage. The y-dependence, which appears in the term

$$\exp\left\{-i\mu \int_Y^y q(y)\, dy\right\}$$

in (5.6), and the corresponding term in (5.8) indicates that the solution is of the form of pressure waves, as we would expect, and since $q(y)$ is constant outside the shear layer, the wavelength in the y-direction is $2\pi(\mu Q_+)^{-1}$ for $y > 1$ and $2\pi(\lambda Q_-)^{-1}$ for $y < -1$. Secondly, the radiated pressure fluctuations for a given wave-number and frequency are dependent only on the properties of the turbulence at the critical layer Y appropriate to this $\mathbf{k}$ and n. This provides an

analytical confirmation of the intuitive remarks of the previous section. Thirdly, if λ and μ are comparable, that is, if $M^2 \gg k^2/Q_+^2$, k^2/Q_-^2 the ratio of the amplitudes of the pressure waves above and below the shear layer is approximately $(Q_-/Q_+)^{\frac{1}{2}}$. If for a particular pair $(\mathbf{k}, n)$, the critical layer is towards the upper side of the shear zone, then it can be shown simply that $Q_+ < Q_-$, and the amplitude of the pressure wave above the shear zone is greater than the amplitude below for the same $(\mathbf{k}, n)$.

These expressions simplify considerably if $M^2 \gg k^2/Q_-^2$, k^2/Q_-^2, that is if the wave-number of the disturbance lies well within the fan of figure 2. When M is very large, this requirement is satisfied by almost all wave-numbers of the pressure field except those for which k_1 is very small. Then

$$\lambda \simeq \mu \simeq M, \tag{5.9}$$

the errors being of order $\{M \cos^2\theta[1 - V(Y)]^2\}^{-1}$, and (5.6) and (5.8) become

$$\left.\begin{aligned} &\varpi(y, \mathbf{k}, n) \sim -(-\tfrac{3}{4})!\,(1+i)\exp(3\pi i/8)\,\frac{M^{\frac{3}{4}}\Gamma(Y)}{4Q_+^{\frac{1}{2}}A^2(Y)\,\Omega^{\frac{3}{4}}}\exp\left\{-i\mu\int_Y^y q\,dy\right\}, \\ &\text{for } y > 1, \text{ and} \\ &\varpi(y, \mathbf{k}, n) \sim (-\tfrac{3}{4})!\,(1+i)\exp(-3\pi i/8)\,\frac{M^{\frac{3}{4}}\Gamma(Y)}{4Q_-^{\frac{1}{2}}A^2(Y)\,\Omega^{\frac{3}{4}}}\exp\left\{i\lambda\int_Y^y q\,dy\right\}, \end{aligned}\right\} \tag{5.10}$$

for $y < -1$, where Y is defined by

$$n + k_1 V(Y) = 0.$$

It is convenient now to use the approximation (3.4) for the generation term in the equations and to replace the term G in (3.9) by

$$2\gamma A(y)\frac{\partial V}{\partial y}\frac{\partial v_3}{\partial y_1} = 2\gamma A(y)\,\Omega(y)\frac{\partial v_3}{\partial y_1}.$$

The Fourier transform $\Gamma(y, \mathbf{k}, n)$ is thus

$$\Gamma(y, \mathbf{k}, n) = -2i\gamma A(y)\,\Omega(y)\,k_1 Z(y, \mathbf{k}, n), \tag{5.11}$$

where $Z(y, \mathbf{k}, n)$ is the generalized Fourier transform of v_3, the dimensionless velocity fluctuation in the direction normal to the shear zone. From these relations we can synthesize expressions for the spectrum and mean square amplitude of the pressure fluctuation function $\zeta = A(y)\log(p/p_0)$ in terms of the properties of the shear zone. From the theory of generalized functions (Lighthill, 1958) it can be shown that

$$\overline{\varpi(y, \mathbf{k}, n)\,\varpi^*(y, \mathbf{k}-\mathbf{k}', n-n')} = \Pi(y, \mathbf{k}, n)\,\delta(k_1')\,\delta(k_2')\,\delta(n'),$$

where the bar denotes an ensemble average, the asterisk the complex conjugate, $\delta(k_1')$, etc., the Dirac delta functions and

$$\Pi(y, \mathbf{k}, n) = (2\pi)^{-3}\iint \overline{\zeta(y, y_1, y_2, \tau)\,\zeta(y, y_1+r_1, y_2+r_2, \tau+\tau')} \times \exp\{-i(\mathbf{k}.\mathbf{r} + n\tau')\}\,d\mathbf{r}\,d\tau'$$

the wave-number-frequency spectrum of the pressure function. Thus

$$\Pi(y,\mathbf{k},n)=\iint\overline{\varpi(y,\mathbf{k},n)\,\varpi^*(y,\mathbf{k}-\mathbf{k}',n-n')}\,d\mathbf{k}'\,dn', \tag{5.12}$$

the integral being over a small range containing $k_1'=k_2'=n'=0$. Similarly,

$$\begin{aligned}\Psi(Y,\mathbf{k},n)&=\iint\overline{Z(Y,\mathbf{k},n)\,Z^*(Y,\mathbf{k}-\mathbf{k}',n-n')}\,d\mathbf{k}'\,dn'\\&=(2\pi)^{-3}\iint\overline{v_3(Y,y_1,y_2,\tau)\,v_3(Y,y_1+r_1,y_2+r_2,\tau+\tau')}\\&\qquad\times\exp\{-i(\mathbf{k}.\mathbf{r}+n\tau')\}\,d\mathbf{r}\,d\tau',\end{aligned} \tag{5.13}$$

for the spectrum of the v_3-velocity fluctuations.

For definiteness, we will consider the region $y>1$ above the shear zone, and constructing $\Pi(y,\mathbf{k},n)$ from these last two expressions, (5.10) and (5.7), it is found that

$$\Pi(\mathbf{k},n)\sim\tfrac{1}{2}[(-\tfrac{3}{4})!]^2\frac{\gamma^2M^{\frac{3}{2}}\Omega^{\frac{1}{2}}(Y)\,k_1^2\Psi(Y,\mathbf{k},n)}{A^2(Y)\qquad|k_1+n|}. \tag{5.14}$$

The dependence on y of the right-hand side has disappeared, reflecting the fact that, in the present theory, the statistical properties of the pressure fluctuations in the free stream are independent of the distance from the shear zone of the plane in which they are observed. This theory has neglected the self-convection of the sound waves which leads to the development of shock waves as y increases if $\overline{\zeta^2}$ is sufficiently large, and as we have stated, can be expected to be accurate only near the shear zone before this process has distorted the pressure waves appreciably.

The instantaneous wave-number spectrum is obtained by integrating (5.14) over all frequencies n:

$$\begin{aligned}\Pi(\mathbf{k})&=\int_{-\infty}^{\infty}\Pi(\mathbf{k},n)\,dn\\&=(2\pi)^{-2}\int\overline{\zeta(y,y_1,y_2,\tau)\,\zeta(y,y_1+r_1,y_2+r_2,\tau)}\,e^{-i\mathbf{k}.\mathbf{r}}\,d\mathbf{r}.\end{aligned} \tag{5.15}$$

Since $n+k_1V(Y)=0$,

$$dn=-k_1\Omega(Y)\,dY, \tag{5.16}$$

and integration over all frequencies n with fixed $\mathbf{k}$ corresponds to integration over the position Y of the critical layer across the shear zone. Thus

$$\Pi(\mathbf{k})\sim\tfrac{1}{2}[(-\tfrac{3}{4})!]^2\gamma^2M^{\frac{3}{2}}k_1^2\int_{-\infty}^{\infty}\frac{\Omega^{\frac{3}{2}}(Y)\,\Psi(Y,\mathbf{k},n)}{A^2(Y)\,[1-V(Y)]}\,dY, \tag{5.17}$$

where $n=-k_1V(Y)$.

It should be pointed out that this expression is likely to provide a slight numerical overestimate of the pressure spectrum, since the integral includes layers near the outside edges of the shear zone, where the approximation (5.10) is not appropriate and, indeed, where the eddy wave mechanism may not be operative, since the difference between the free-stream velocity and the eddy convection velocity is subsonic. However, if M is large, these regions constitute

only a small part of the total shear zone, and the error in integrating (5.14) over the whole zone instead of over the supersonic region only should be relatively small. The relative contributions to $\Pi(\mathbf{k})$ from critical layers symmetrically spaced above and below the centre-line $y = 0$ is demonstrated clearly in this expression, since $V(Y)$ is positive in the former case and negative in the latter ($|V| \leqslant 1$). We might anticipate that a possible divergence of the integral at the upper limit, where $1 - V(Y) \to 0$, is avoided by the fact that $\Omega(Y) \to 0$ also.

The integral in (5.17) can be simplified further by making use of a plausible approximation on the nature of the turbulence in the shear zone. It will be supposed that the spectrum of the v_3-velocity covariance with time delay is independent of Y provided the observations are made in a frame of reference moving with the local mean velocity. It is shown below that this statement really involves two approximations, the first being that the mean square value of these velocity fluctuations is independent of the position in the shear layer $|y| < 1$ at which they are measured. Our experience with subsonic free turbulent flows suggests that this is a good approximation for the fully turbulent regions; Townsend (1956) quotes a considerable body of experimental support. It is difficult to see why this general property should not also be true in the supersonic shear zone. The second requirement is that the integral time scale of the velocity fluctuations, *measured in a frame of reference moving with the local convective mean velocity*, is also independent of Y. This also is strongly suggested by the observed near-homogeneity of such flows for $M < 1$.

It can be shown simply (Phillips 1957, § 4.1) that if $\Psi(Y, \mathbf{k}, \tau)$ represents the two-dimensional wave-number spectrum with time delay τ measured in a frame of reference at rest, then the corresponding quantity observed in a frame of reference moving with velocity $\mathbf{V}$ is

$$e^{i(\mathbf{k}.\mathbf{V})\tau}\,\Psi(Y, \mathbf{k}, \tau), \tag{5.18}$$

and this quantity we suppose to be independent of Y. Our wave-number-frequency spectra of this problem are all measured in a frame at rest, and are given by

$$\begin{aligned}\Psi(Y, \mathbf{k}, n) &= (2\pi)^{-1} \int_{-\infty}^{\infty} \Psi(Y, \mathbf{k}, \tau)\, e^{-in\tau}\, d\tau \\ &= (2\pi)^{-1} \int_{-\infty}^{\infty} \Psi(Y, \mathbf{k}, \tau) \exp\{ik_1 V(Y)\tau\}\, d\tau, \end{aligned} \tag{5.19}$$

since $n = -k_1 V(Y)$. In our problem, $\mathbf{V} = (V, 0, 0)$, so that, under our assumption, the integrand is independent of Y and equal to, in particular, its value at $Y = 0$. Thus

$$\begin{aligned}\Psi(Y, \mathbf{k}, n) &= (2\pi)^{-1} \int_{-\infty}^{\infty} \Psi(0, \mathbf{k}, \tau)\, d\tau \\ &= \pi^{-1} \Psi(0, \mathbf{k})\, \theta(\mathbf{k}), \quad \text{say}, \end{aligned} \tag{5.20}$$

where $\Psi(0, \mathbf{k})$ represents the usual two-dimensional wave-number spectrum with zero time delay at $Y = 0$ and $\theta(\mathbf{k})$ the integral time scale of the spectrum of the v_3-fluctuations measured at the centre-line where $V(Y) = 0$. If, in addition the mean density is approximately constant across the shear zone, the variation

in $A(Y)$ can be neglected. We might note in passing the inference that if the shear zone is hot, so that $A(Y)$ is significantly less than unity, then the pressure radiation outside the shear zone will be increased by a factor proportional to the inverse square of the sonic speed ratio.

With these simplifications, (5.17) becomes

$$\Pi(\mathbf{k}) \sim (2\pi)^{-1}[(-\tfrac{3}{4})!]^2\gamma^2 M^{\frac{3}{2}}k_1^2\Psi(0,\mathbf{k})\,\theta(\mathbf{k})\int_{-\infty}^{\infty}\frac{\Omega^{\frac{3}{2}}(Y)\,dY}{1-V(Y)}. \tag{5.21}$$

The integrand in this last expression gives the relative contributions to $\Pi(\mathbf{k})$ (or to $\overline{\zeta^2}$) from the various layers Y within the shear zone. Clearly the greater contributions to the disturbance above the layer originate from the region $Y > 0$ where $V(Y)$ is positive. The magnitude of the integral depends only on the mean velocity profile in the shear zone, and is fairly insensitive to the details of its shape. $V(Y)$ increases from approximately -1 to 1 as Y increases from -1 to 1. If we approximate $V(Y)$ by

$$|V(Y)| = 1-\exp(-2|Y|),$$

the integral has the value 3·08 approximately of which the region $0 < Y < \infty$ contributes about 90 %. If we take $V(Y)$ as the error function $\operatorname{erfc}(2Y)$, then the integral is approximately 5·13, of which 82 % is contributed by the upper half of the shear zone. It seems likely then, that the value of the integral will, under ordinary circumstances, be about 4, the probable error lying well within a factor of two. Thus

$$\Pi(\mathbf{k}) \sim \frac{2}{\pi}[(-\tfrac{3}{4})!]^2\gamma^2 M^{\frac{3}{2}}k_1^2\Psi(\mathbf{k})\,\theta(\mathbf{k}), \tag{5.22}$$

where $\Psi(\mathbf{k}) \equiv \Psi(0,\mathbf{k})$.

Equation (5.22) expresses the basic result of this part of the paper. It emphasizes the dependence of the pressure spectrum on the spectrum of $(\partial v_3/\partial y_1)$, which is in accord with our conception of the mechanism of generation in terms of Mach waves arising from the Fourier components of the fluctuations in velocity normal to the shear zone. The time scale $\theta(\mathbf{k})$ enters the problem because of the statistical nature of the process; the greater the time scale $\theta(\mathbf{k})$ (or the longer the eddy lifetime) the greater is the coherence in the contributions to the pressure field and the sum of all contributions is increased.

If the fluctuations in pressure outside the shear zone are not a large fraction of the mean pressure at infinity, p_0, then the spectrum (5.22) can be interpreted directly as the spectrum of the pressure fluctuation level. For

$$\begin{aligned}\zeta &= A(y)\log\left(\frac{p}{p_0}\right)\\ &\simeq \frac{p-p_0}{p_0}\end{aligned}$$

outside the shear layer, where $A(y) = 1$, if $(p-p_0) \ll p_0$. This requirement is equivalent to restricting our considerations to situations in which only weak shocks are generated by the turbulence, and this is consistent with our earlier approximations. At extremely high Mach numbers, $p-p_0$ may be comparable in root

mean square to p_0, but the whole theory may become unreliable, since dissociation and other phenomena may become important.

To form an estimate of $\overline{(p-p_0)^2}$ outside the shear zone, some information is needed concerning $\theta(\mathbf{k})$. If the lifetime of the eddies is determined by the straining process, as is quite conceivable in supersonic shear flow where the turbulence level is considerably smaller than in a corresponding subsonic flow, the characteristic (dimensional) time is of order $(|\partial U/\partial x_3|_{\max})^{-1}$ (Townsend 1956, p. 96), so that the dimensionless $\theta(\mathbf{k})$ is of order unity. On the other hand, if the process determining the life-time is the turbulent rate of strain due to the energy containing eddies, or some more complicated process involving compressibility effects, the time scale may be different, and in view of our lack of information in supersonic turbulence, it is difficult at this stage to evaluate the possible alternatives. It seems that to take $\theta(\mathbf{k}) = 1$ is probably the best course open; it is certainly the simplest.

Equation (5.22) can then be integrated over all wave-numbers $\mathbf{k}$ (including those outside the fan of figure 2: the spurious contribution from these will be small because of the k_1^2 factor in (5.22)) and we obtain

$$\frac{\overline{(p-p_0)^2}}{p_0^2} \sim \frac{2}{\pi}[(-\tfrac{3}{4})!]^2 \gamma^2 M^3 \overline{\left(\frac{\partial v_3}{\partial y_1}\right)^2}$$

$$\simeq 8\gamma^2 M^3 \overline{\left(\frac{\partial v_3}{\partial y_1}\right)^2} \tag{5.23}$$

in the notation of (3.5). Restoring the dimensional quantities of § 3,

$$\frac{\overline{(p-p_0)^2}}{p_0^2} \sim 8\gamma^2 U^3 a_0^{-3} \overline{\left(\frac{\partial u_3}{\partial x_1}\right)^2} \frac{L^2}{U^2}, \tag{5.24}$$

$$= 8\gamma^2 U^3 a_0^{-3} \left(\frac{\overline{u_3^2}}{U^2}\right) \frac{L^2}{l^2}, \tag{5.25}$$

where l is the differential length scale in the streaming direction of the velocity fluctuations normal to the shear zone.†

It is interesting to contrast the behaviour predicted by (5.25) for large M with the U^8 law found by Lighthill when $M \ll 1$. If $\overline{u_3^2}/U^2$ is only weakly dependent on U when the Mach number is large,‡ the mean-square-pressure fluctuations increase only as the $\frac{3}{2}$ power of the velocity for $M \gg 1$. A decrease in the steepness of the curve $\overline{(p-p_0)^2}/p_0^2$ *vs* U is very evident from the little experimental data that is available, of which perhaps the best is provided by the recent measurements of Laufer (1959). These were made inside a supersonic wind-tunnel and the major source of the sound field appeared to be the turbulent boundary layers along the walls. Laufer found that the over-all variation of $\overline{(p-p_0)^2}$ was as M^4, approximately, but that the boundary-layer thickness also increased with Mach number, a little faster than linearly. The radiation from a supersonic turbulent

† The result (5.24) is applicable also (possibly with a modified $\theta(\mathbf{k})$) to the pressure fluctuations generated by the instability of a supersonic laminar shear zone.

‡ It seems likely that $\overline{u_3^2}/U^2$ will vary only slowly with M, if at all, in view of the remarks in § 6 concerning radiation damping.

boundary layer could be considered by the methods of this paper, replacing the radiation condition at $y = -\infty$ by the appropriate wall boundary condition. It is very likely that the result would be similar to (5.25) except for a difference in the numerical constant since the basic mechanism of the sound generation is the same. This suggests that, for the boundary layer also

$$\frac{\overline{(p-p_0)^2}}{p_0^2} \propto M^{\frac{3}{2}} \frac{\delta^2}{l^2} \frac{\overline{u_3^2}}{U^2},$$

where δ is the boundary-layer thickness, and if l and $\overline{u_3^2}/U^2$ are approximately independent of Mach number (see footnote on previous page), then

$$\frac{\overline{(p-p_0)^2}}{p_0^2 M^{\frac{3}{2}} \delta^2} = \text{constant}. \tag{5.26}$$

Laufer's data are plotted in figure 3 and, although there is some scatter, there is no evident trend with Mach number of the quantity on the left-hand side of (5.26). It therefore appears that Laufer's M^4 variation represents the combined

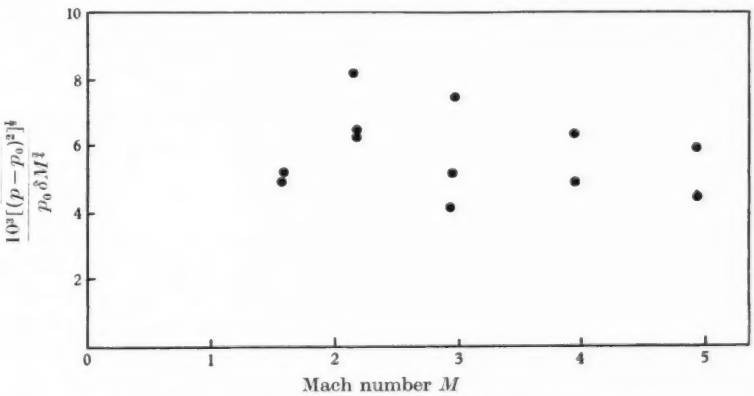

FIGURE 3. Pressure fluctuations from a supersonic turbulent boundary layer (after Laufer 1959).

effects of the $M^{\frac{3}{2}}$ factor given by the present theory and a variation of the boundary-layer thickness δ, as $M^{\frac{1}{2}}$ approximately. The present theory also indicates that the pressure field external to the shear flow is being swept past a point fixed in the external fluid with speed of order U. In the boundary layer, this convection speed would be lower, of order $\frac{1}{2}U$ corresponding to the speed of the flow outside the viscous and buffer layers. This also is in rough agreement with Laufer's results. It appears that these measurements give promising, but tentative support to the theory, though more measurements are required, both on the sound field and on the boundary-layer structure before firm conclusions can be drawn.

6. The directional distribution

The directional distribution of the radiation above the shear zone is found most readily from (5.21). Relative to the fluid in $y > 1$, the critical layer at Y is being convected with speed $U[1 - V(Y)]$, and from simple geometrical considerations, if $U[1 - V(Y)] > a_0$, the direction of propagation relative to the outside stream of waves originating at the layer Y is given by

$$\alpha = \cos^{-1} \frac{a_0}{U[1 - V(Y)]} = \cos^{-1}\{M[1 - V(Y)]\}^{-1}. \tag{6.1}$$

The relative contributions to $\overline{(p-p_0)^2}$ from the layers between Y, $Y + dY$ are given by (5.21) as

$$\frac{\Omega^{\frac{1}{2}} dY}{1 - V(Y)}, \tag{6.2}$$

and each layer Y is associated with an angle of propagation α specified by (6.1). By differentiation of (6.1)

$$\Omega(Y)\, dY = -\frac{\sin\alpha}{M\cos^2\alpha}\, d\alpha, \tag{6.3}$$

so that the directional distribution function is given by (6.1), (6.2) and (6.3) as

$$f(\alpha) = \Omega^{\frac{1}{2}}(Y)\tan\alpha, \tag{6.4}$$

where $Y = Y(\alpha)$ is given by (6.1). The approximate shape of the directional distribution can be found by assuming a shape of the velocity profile, a convenient form being given by

$$|V(Y)| = 1 - e^{-2|Y|},$$

and the directional distribution function $f(\alpha)$ is illustrated in figure 4 for this profile for Mach numbers of 2, 4 and 6 corresponding to Mach numbers based on the velocity *difference* of 4, 8 and 12. As the Mach number increases, the maximum of the directional distribution moves towards 90° and becomes sharper, since most of the Mach lines from the shear zone are inclined at quite a small angle to the direction of the free stream.

The cut-off in figure 4, which occurs when $\cos\alpha = (2M)^{-1}$ will be modified in practice by the presence of scattering phenomena introduced by the turbulence, and by pressure wave interactions, both of which have been neglected in the present theory, and which would result in the radiation of some sound in the backwards direction, at angles greater than 90°.

Figure 4 indicates that the direction of radiation observed at rest relative to the mean stream above the shear layer is for large M concentrated in directions near but less than 90°. This property makes possible a simple estimate of the acoustic energy flux N per unit area from the shear zone, using expressions derived by Ribner (1958). If $\alpha_{\max}$ is the direction in which most of the energy travels

$$N = \frac{\overline{(p-p_0)^2}}{\rho_0 a_0}\sin\alpha_{\max} \doteq \frac{\overline{(p-p_0)^2}}{\rho_0 a_0} \sim 8\rho_0 U^{\frac{3}{2}}\alpha_0^{\frac{3}{2}}\left(\frac{\overline{u_3^2}}{U^2}\right)\frac{L^2}{l^2}, \tag{6.5}$$

from (5.15), and the acoustic efficiency η is

$$\eta = \frac{\text{acoustic energy flux}}{\rho_0 U^3}$$

$$\propto M^{-\frac{3}{2}} \frac{\overline{u_3^2}}{U^2} \frac{L^2}{l^2}. \tag{6.6}$$

This decreasing acoustic efficiency with increasing M for large Mach number contrasts with an increase as M^5 when M is small shown by Lighthill (1952). This implies that at some Mach number of order one or two the acoustic efficiency

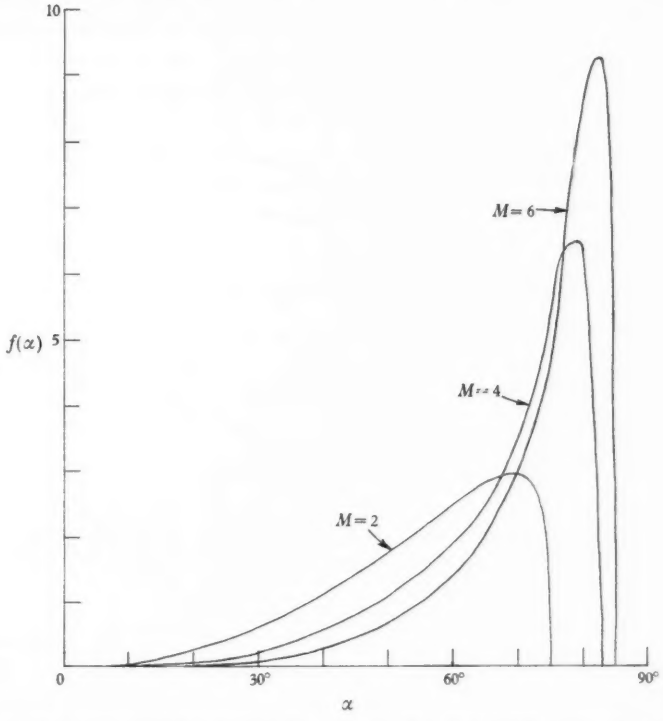

FIGURE 4. The directional distribution function for $M = 2$, 4 and 6, corresponding to Mach numbers for the velocity difference across the shear zone of 4, 8 and 12, respectively.

is a maximum, decreasing rapidly as $M \to 0$ and more slowly as $M \to \infty$. It also implies that the loss of energy from the turbulence by acoustic radiation is always small compared with the energy supply from the mean flow, and the effects of radiation damping are likely to be small.

These inferences are supported by the little data that is available. Lilley (1958), in discussing the measurements of Lassiter & Heitkotter (1954), suggests that a qualitative behaviour of this kind is indicated since the measured acoustic efficiency of a round jet at $M = 5$ is approximately the same as found at $M = 1{\cdot}8$

by Sanders & Callaghan (1956) below which it drops off rapidly. Lassiter & Heitkotter also measured the directional distribution of the radiation from a round jet whose exit Mach number was 3·16. Since most of their sound originated in the shear layer near the exit, one might hope to compare their measurements with the results of this paper. Their directional maximum occurred at about 50°, compared with the 57° predicted by this theory for the corresponding Mach number. These angles are significantly larger than those found for the maximum intensity in subsonic jets (about 30°). As α increased beyond 60°, the observed intensity dropped rapidly to a level about 60 db below the maximum, in good qualitative accord with the shapes of the curves shown in figure 4.

Although these preliminary indications are again quite promising, a great deal more data will have to be obtained before more detailed comparisons are possible. There still remains the question of the interaction of the random pattern of weak shock waves outside the shear layer, but that is another story.

I am greatly indebted to Dr L. S. G. Kovasznay, Dr M. Morkovin and Dr S. Corrsin for the stimulation of discussing this work with them. It was supported by the Office of Naval Research under Contract Nonr 248 (38).

Appendix. Asymptotic solution for large M

Equation (3.8) can be expressed as

$$\frac{d^2\varpi(y)}{dy^2} + \{M^2q^2(y) - k^2\}\,\varpi(y) = -\frac{M^2}{A^2(y)}\,\Gamma(y), \tag{A.1}$$

where $k^2 \gg |A''/A|$ and

$$q(y) = \pm\frac{n + k_1 V(y)}{A(y)}, \tag{A.2}$$

the positive or negative sign being taken according as k_1 is positive or negative. If $|k_1| > |n|$, $q(y)$ has a single zero at $y = Y$, say, and $q(y) > 0$ for $y > Y$ and $q(y) < 0$ for $y < Y$. Let

$$\xi = \chi(y), \quad \eta = \varpi(y)\,\psi(y), \tag{A.3}$$

and on substitution into (A. 1), we find

$$\frac{d^2\eta}{d\xi^2} + \frac{1}{\chi'}\left\{\frac{\chi''}{\chi'} - \frac{2\psi'}{\psi}\right\}\frac{d\eta}{d\xi} + \left\{\frac{M^2q^2 - k^2}{(\chi')^2} + \frac{\psi}{(\chi')^2}\frac{d^2}{dy^2}\psi^{-1}\right\}\eta = -\frac{\psi}{(\chi')^2}\frac{M^2}{A^2(y)}\,\Gamma(y). \tag{A.4}$$

Now choose ψ so that

$$\frac{\chi''}{\chi'} = \frac{2\chi'}{\psi},$$

or

$$\psi = (\chi')^{\frac{1}{2}}, \tag{A.5}$$

and determine χ so that

$$\frac{q^2(y)}{(\chi')^2} = \chi^2 = \xi^2. \tag{A.6}$$

Thus

$$\xi = \chi(y) = \left\{2\int_Y^y q(y)\,dy\right\}^{\frac{1}{2}}. \tag{A.7}$$

The positive values of the fractional indices are to be taken and the lower limit of the integral is chosen as Y so that ξ is real for all y. Clearly $0 \leqslant \xi < \infty$ and the transformation $y = y(\xi)$ is double valued with branch I corresponding to $Y \leqslant y < \infty$ and branch II to $-\infty < y \leqslant Y$. From (A. 5) and (A. 7)

$$\eta = \varpi(y)\,\psi(y) = q^{\frac{1}{2}}\{2\int q\,dy\}^{-\frac{1}{4}}\varpi(y), \tag{A. 8}$$

where the limits of integration are understood to be as specified above. With the transformation (A. 7) and (A. 8), (A. 4) becomes

$$\frac{d^2\eta}{d\xi^2} + M^2\xi^2\eta = \left\{k^2 + \frac{\chi'''}{2\chi'} - \frac{3}{4}\left[\frac{\chi''}{\chi'}\right]^2\right\}\frac{\eta}{(\chi')^2} - \frac{M^2\Gamma(y)}{(\chi')^{\frac{3}{2}}A^2(y)}. \tag{A. 9}$$

Now

$$\frac{d\xi}{dy} = \chi' = \frac{q(y)}{\xi}, \tag{A. 10}$$

and $|q(y)|$ is very nearly constant outside the shear zone, i.e. for $|y| > 1$. It follows by differentiation of (A. 10) that

$$\left\{k^2 + \frac{\chi'''}{2\chi'} - \frac{3}{4}\left[\frac{\chi''}{\chi'}\right]^2\right\}(\chi')^{-2} = \frac{k^2\xi^2}{Q^2} + O(\xi^{-2}), \tag{A. 11}$$

as $\xi \to \infty$, where

$$\left.\begin{aligned} Q = Q_+ &= \lim_{y\to\infty} q(y) \quad \text{for branch I,} \\ Q = Q_- &= \lim_{y\to-\infty} q(y) \quad \text{for branch II.} \end{aligned}\right\} \tag{A. 12}$$

From (A. 2), clearly

$$\left.\begin{aligned} Q_+ &= n + k_1, \\ Q_- &= \frac{n - k_1}{A(-\infty)}, \end{aligned}\right\} \tag{A. 13}$$

since $A(\infty) = V(\infty) = 1$, $V(-\infty) = -1$. The behaviour (A. 11) suggests that we incorporate the term $k^2\xi^2/Q^2$ into the left-hand side of (A. 9), giving

$$\frac{d^2\eta}{d\xi^2} + \mu^2\xi^2\eta = g(\xi)\,\eta + h(\xi), \tag{A. 14}$$

where, for branch I,

$$\mu = \left\{M^2 - \frac{k^2}{Q_+^2}\right\}^{\frac{1}{2}}, \tag{A. 15}$$

$$\left.\begin{aligned} g(\xi) &= \left\{k^2 + \frac{\chi'''}{2\chi'} - \frac{3}{4}\left[\frac{\chi''}{\chi'}\right]^2\right\}(\chi')^{-2} - \frac{k^2\xi^2}{Q_+^2}, \\ h(\xi) &= -\frac{M^2\Gamma(y)}{(\chi')^{\frac{3}{2}}A^2(y)}. \end{aligned}\right\} \tag{A. 16}$$

From (A. 10), $(\chi')^{-1}$ is bounded near $\xi = 0$, and from (A. 11) $g(\xi)$ is $O(\xi^{-2})$ as $\xi \to \infty$, so that $g(\xi)$ is integrable over $(0, \infty)$. Furthermore, $\Gamma(y) = 0$ outside the shear zone, so that $h(\xi)$ also is integrable over $(0, \infty)$. The governing equation for branch II ($-\infty < y \leqslant Y$) is the same as (A. 14) except that Q_+ is replaced by Q_-. We seek an asymptotic solution to (A. 14) which is to be matched to the corresponding solution for branch II at $\xi = 0$.

The following theorem will be used. If $K(\xi, t)$ is the solution to

$$\frac{d^2K}{d\xi^2} + \mu^2\xi^2 K = 0 \tag{A. 17}$$

satisfying the conditions

$$K(\xi, t) = 0, \quad \frac{d}{d\xi}K(\xi, t) = 1 \quad \text{when} \quad \xi = t \tag{A. 18}$$

and $H(\xi)$ is *any* solution to (A. 17), then the Volterra integral equation

$$\eta(\xi) = H(\xi) + \int_0^\xi K(\xi, t)\,[g(t)\,\eta(t) + h(t)]\,dt \tag{A. 19}$$

satisfies (A. 14). The proof is given by Erdélyi (1956, p. 99). Note that $\eta(\xi)$ and $H(\xi)$ have the same value and the same derivative at $\xi = 0$.

The fundamental solutions to (A. 17) are

$$(\mu\xi^2)^{\frac{1}{4}}\,J_{\frac{1}{4}}(\tfrac{1}{2}\mu\xi^2), \quad (\mu\xi^2)^{\frac{1}{4}}\,J_{-\frac{1}{4}}(\tfrac{1}{2}\mu\xi^2),$$

and the kernel K satisfying the conditions (A. 18) is

$$K(\xi, t) = \frac{\pi}{2\sqrt{2}\,\mu^{\frac{1}{2}}}\{(\mu\xi^2)^{\frac{1}{4}}\,J_{\frac{1}{4}}(\tfrac{1}{2}\mu\xi^2)\,(\mu t^2)^{\frac{1}{4}}\,J_{-\frac{1}{4}}(\tfrac{1}{2}\mu t^2) - (\mu\xi^2)^{\frac{1}{4}}\,J_{-\frac{1}{4}}(\tfrac{1}{2}\mu\xi^2)\,(\mu t^2)^{\frac{1}{4}}\,J_{\frac{1}{4}}(\tfrac{1}{2}\mu t^2)\}. \tag{A. 20}$$

To find the asymptotic solution to (A. 19) let

$$\eta_0(\xi) = H(\xi) + \int_0^\xi K(\xi, t)\,h(t)\,dt. \tag{A. 21}$$

If

$$\left.\begin{aligned} \Phi_1(\tfrac{1}{2}\mu\xi^2) &= \int_{\frac{1}{2}\mu\xi^2}^\infty u^{-\frac{1}{4}}J_{-\frac{1}{4}}(u)\,du, \\ \Phi_2(\tfrac{1}{2}\mu\xi^2) &= \int_{\frac{1}{2}\mu\xi^2}^\infty u^{-\frac{1}{4}}J_{\frac{1}{4}}(u)\,du, \end{aligned}\right\} \tag{A. 22}$$

then

$$(\mu t^2)^{\frac{1}{4}}\,J_{-\frac{1}{4}}(\tfrac{1}{2}\mu t^2) = -\,2^{-\frac{1}{4}}\mu^{-\frac{1}{2}}\frac{d}{dt}\,\Phi_1(\tfrac{1}{2}\mu t^2),$$

$$(\mu t^2)^{\frac{1}{4}}\,J_{\frac{1}{4}}(\tfrac{1}{2}\mu t^2) = -\,2^{-\frac{1}{4}}\mu^{-\frac{1}{2}}\frac{d}{dt}\,\Phi_2(\tfrac{1}{2}\mu t^2),$$

so that substituting (A. 20) into (A. 21), we have

$$\begin{aligned} \eta_0(\xi) &= H(\xi) - \frac{\pi}{2\sqrt{2}\,\mu}\left\{(\tfrac{1}{2}\mu\xi^2)^{\frac{1}{4}}\,J_{\frac{1}{4}}(\tfrac{1}{2}\mu\xi^2)\int_0^\xi h(t)\frac{d}{dt}\,\Phi_1(\tfrac{1}{2}\mu t^2)\,dt\right. \\ &\quad \left. - (\tfrac{1}{2}\mu\xi^2)^{\frac{1}{4}}\,J_{-\frac{1}{4}}(\tfrac{1}{2}\mu\xi^2)\int_0^\xi h(t)\frac{d}{dt}\,\Phi_2(\tfrac{1}{2}\mu t^2)\,dt\right\}, \\ &= H(\xi) + \frac{\pi}{2\sqrt{2}\,\mu}\{(\tfrac{1}{2}\mu\xi^2)^{\frac{1}{4}}\,J_{\frac{1}{4}}(\tfrac{1}{2}\mu\xi^2)\,[h(+0)\,\Phi_1(0) - h(\xi)\,\Phi_1(\tfrac{1}{2}\mu\xi^2)] \\ &\quad - (\tfrac{1}{2}\mu\xi^2)^{\frac{1}{4}}\,J_{-\frac{1}{4}}(\tfrac{1}{2}\mu\xi^2)\,[h(+0)\,\Phi_2(0) - h(\xi)\,\Phi_2(\tfrac{1}{2}\mu\xi^2)] + O(\mu^{-\frac{1}{2}})\}, \end{aligned} \tag{A. 23}$$

on integration by parts, where

$$h(+0) = \lim_{y \to Y+0}\left\{-\frac{M^2\Gamma(y)}{(\chi')^{\frac{3}{2}}\,A^2(y)}\right\}.$$

The next approximation, $\eta_0+\eta_1$, is obtained by substituting η_0 into the integral of (A. 19) (Erdélyi 1956). Equation (A. 23) is of the form

$$\eta_0(\xi) = H(\xi)+\mu^{-1}G(\xi,\mu),$$

so that

$$\int_0^\xi K(\xi,t)\,\eta_0(t)\,g(t)\,dt = \int_0^\xi K(\xi,t)\,H(t)\,g(t)\,dt+\mu^{-1}\int_0^\xi K(\xi,t)\,G(t,\mu)\,g(t)\,dt,$$

and integration by parts again shows that

$$\left|\int_0^\xi K(\xi,t)\,\eta_0(t)\,g(t)\,dt\right| \leqslant \mu^{-1}H(0)\,\Lambda,$$

where Λ is a finite constant. Thus

$$\eta_1(\xi) = H(\xi)\left[1+\mu^{-1}\frac{H(0)\,\Lambda}{H(\xi)}\right]+O(\mu^{-1}). \tag{A. 24}$$

If only the leading term in the asymptotic expansion is required, it is clear that the second term in the square bracket is negligible except near the zeros of $H(\xi)$. However, if we can take $H(\xi)$ as

$$H(\xi) = A(\tfrac{1}{2}\mu\xi^2)^{\frac{1}{4}}J_{\frac{1}{4}}(\tfrac{1}{2}\mu\xi^2)+B(\tfrac{1}{2}\mu\xi^2)^{\frac{1}{4}}J_{-\frac{1}{4}}(\tfrac{1}{2}\mu\xi^2), \tag{A. 25}$$

where the ratio of the constants A/B is complex, then $H(\xi)$ has no zeros and (A. 23) is a uniformly valid asymptotic solution as $\mu\to\infty$. It will be shown below that such constants can be found for which the radiation and matching conditions in the present problem are satisfied.

Outside the shear zone, $h(\xi) = 0$, and

$$\begin{aligned}\eta(\xi) &= (\tfrac{1}{2}\mu\xi^2)^{\frac{1}{4}}J_{\frac{1}{4}}(\tfrac{1}{2}\mu\xi^2)\left[A+\frac{\pi}{2\sqrt{2}\,\mu}h(+0)\,\Phi_1(0)\right]\\ &\quad+(\tfrac{1}{2}\mu\xi^2)^{\frac{1}{4}}J_{-\frac{1}{4}}(\tfrac{1}{2}\mu\xi^2)\left[B-\frac{\pi}{2\sqrt{2}\,\mu}h(+0)\,\Phi_2(0)\right]\\ &= \alpha(\tfrac{1}{2}\mu\xi^2)^{\frac{1}{4}}J_{\frac{1}{4}}(\tfrac{1}{2}\mu\xi^2)+\beta(\tfrac{1}{2}\mu\xi^2)^{\frac{1}{4}}J_{-\frac{1}{4}}(\tfrac{1}{2}\mu\xi^2), \quad \text{say,}\end{aligned} \tag{A. 26}$$

where

$$\left.\begin{aligned}\alpha &= A+\frac{\pi}{2\sqrt{2}\,\mu}h(+0)\,\Phi_1(0),\\ \beta &= B-\frac{\pi}{2\sqrt{2}\,\mu}h(+0)\,\Phi_2(0).\end{aligned}\right\} \tag{A. 27}$$

From (A. 8), $$\varpi(y) = q^{-\frac{1}{2}}\{2\textstyle\int q\,dy\}^{\frac{1}{4}}\,\eta = 2^{\frac{1}{4}}\mu^{-\frac{1}{4}}q^{-\frac{1}{2}}(\tfrac{1}{2}\mu\xi^2)^{\frac{1}{4}}\,\eta, \tag{A. 28}$$

so that outside the shear zone, as $\mu\to\infty$,

$$\varpi(y) \sim 2^{\frac{3}{4}}\pi^{-\frac{1}{2}}\mu^{-\frac{1}{4}}Q_+^{-\frac{1}{2}}[\alpha\cos(\tfrac{1}{2}\mu\xi^2-\tfrac{3}{8}\pi)+\beta\cos(\tfrac{1}{2}\mu\xi^2-\tfrac{1}{8}\pi)], \tag{A. 29}$$

where we have used the asymptotic relations

$$\left.\begin{aligned}x^{\frac{1}{2}}J_{\frac{1}{4}}(x) &\sim \left(\frac{2}{\pi}\right)^{\frac{1}{2}}\cos(x-\tfrac{3}{8}\pi),\\ x^{\frac{1}{2}}J_{-\frac{1}{4}}(x) &\sim \left(\frac{2}{\pi}\right)^{\frac{1}{2}}\cos(x-\tfrac{1}{8}\pi),\end{aligned}\right\} \tag{A. 30}$$

as $x \to \infty$. Equation (A. 29) can be written alternatively as

$$\varpi(y) \sim (8\pi^2\mu Q_+^2)^{-\frac{1}{4}}\{[\sqrt{2}\,\alpha+(1+i)\,\beta]\exp i(\mu\int q\,dy-\tfrac{3}{8}\pi) + [\sqrt{2}\,\alpha+(1-i)\,\beta]\exp -i(\mu\int q\,dy-\tfrac{3}{8}\pi)\}. \quad \text{(A. 31)}$$

The solution and its asymptotic form for branch II corresponding to $-\infty < y \leqslant Y$ can be expressed similarly.

$$\eta(\xi) = (\tfrac{1}{2}\lambda\xi^2)^{\frac{1}{4}}J_{\frac{1}{4}}(\tfrac{1}{2}\lambda\xi^2)\left\{C+\frac{\pi}{2\sqrt{2}\,\lambda}[h(-0)\,\Phi_1(0)-h(\xi)\,\Phi_1(\tfrac{1}{2}\lambda\xi^2)]\right\} + (\tfrac{1}{2}\lambda\xi^2)^{\frac{1}{4}}J_{-\frac{1}{4}}(\tfrac{1}{2}\lambda\xi^2)\left\{D-\frac{\pi}{2\sqrt{2}\,\lambda}[h(-0)\,\Phi_2(0)-h(\xi)\,\Phi_2(\tfrac{1}{2}\lambda\xi^2)]\right\}+O(\lambda^{-\frac{3}{2}}), \quad \text{(A. 32)}$$

where

$$\left.\begin{aligned}\lambda &= \left\{M^2-\frac{k^2}{Q_-^2}\right\}^{\frac{1}{2}},\\ h(-0) &= \lim_{y\to Y-0}\left\{\frac{-M^2\Gamma(y)}{(\chi')^{\frac{3}{2}}A^2(y)}\right\},\\ &= -ih(+0),\end{aligned}\right\} \quad \text{(A. 33)}$$

since

$$\left.\begin{aligned}\chi' &= q(y)/\xi \quad \text{from (A. 10)}\\ &= \frac{\Omega(y-Y)}{\Omega^{\frac{1}{2}}|y-Y|} \quad \text{near} \quad y=Y,\\ &\to \Omega^{\frac{1}{2}} \quad \text{as} \quad y\to Y+0,\\ &\to -\Omega^{\frac{1}{2}} \quad \text{as} \quad y\to Y-0,\end{aligned}\right\} \quad \text{(A. 34)}$$

and C and D are further constants. Outside the shear zone, as $\lambda \to \infty$,

$$\varpi(y) \sim (8\pi^2\lambda Q_-^2)^{-\frac{1}{4}}\{[\sqrt{2}\,\gamma+(1+i)\,\delta]\exp i(\lambda\int q\,dy-\tfrac{3}{8}\pi) + [\sqrt{2}\,\gamma+(1-i)\,\delta]\exp -i(\lambda\int q\,dy-\tfrac{3}{8}\pi)\}, \quad \text{(A. 35)}$$

where

$$\left.\begin{aligned}\gamma &= C-\frac{i\pi}{2\sqrt{2}\,\lambda}h(+0)\,\Phi_1(0),\\ \delta &= D+\frac{i\pi}{2\sqrt{2}\,\lambda}h(+0)\,\Phi_2(0).\end{aligned}\right\} \quad \text{(A. 36)}$$

Determination of the constants

We seek to determine the constants A, B, C, D by applying radiation conditions outside the shear zone and matching conditions between the two branches at $\xi = 0$. If W represents the component of the velocity of the convected wave outside the shear zone, observed in the direction of y increasing, then

$$\frac{\partial\zeta}{\partial t}+W\frac{\partial\zeta}{\partial y}=0,$$

or in terms of our Fourier transforms

$$in\varpi(y)+W\frac{\partial\varpi(y)}{\partial y}=0.$$

Thus

$$in\varpi(y)\Big/\left(\frac{\partial\varpi(y)}{\partial y}\right)=-W.$$

The two parts of the solution (A. 31) are of the form $\exp(\pm i\mu\int q\,dy)$; let us consider the particular wave motion represented by

$$\varpi(y) \propto \exp(-i\mu\int q\,dy). \tag{A. 37}$$

For such waves
$$W = -in\varpi\Big/\frac{\partial\varpi}{\partial y} = \frac{n}{\mu q(y)},$$
$$= \frac{n}{\mu(n+k_1)}, \tag{A. 38}$$

for $y > 1$, from (A. 13). But from (4.3), $n = -k_1 V_c$ approximately, where V_c is the convection velocity at the critical layer Y, so that from (A. 42)

$$W = \{\mu(1 - V_c^{-1})\}^{-1}. \tag{A. 39}$$

Since $|V_c| \leqslant 1$, W is positive or negative according as $V_c < 0$ or $V_c > 0$.

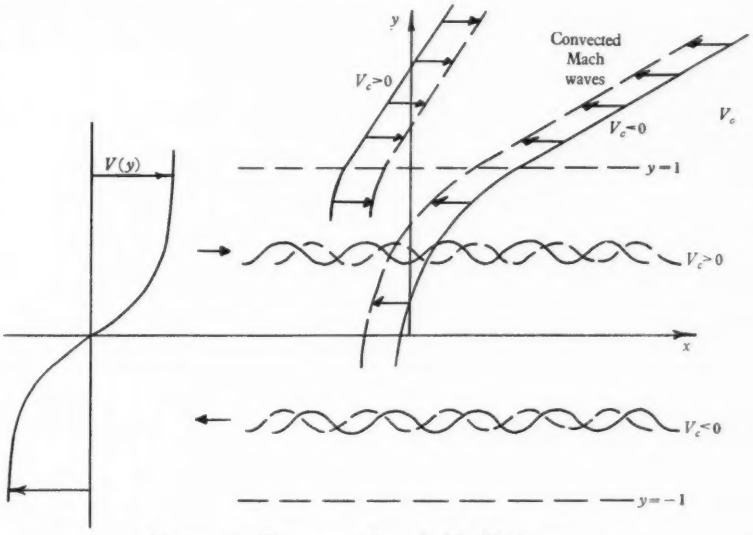

FIGURE 5. The convection of eddy Mach waves.

Figure 5 shows the nature of the solution desired for the Mach waves associated with the layers of the shear zone. If $V_c < 0$, the Mach waves move to the left and when observed in the y-direction in $y > 1$, they appear to move outwards, so that we require $W > 0$. If $V_c > 0$ the waves are convected to the right and they appear to move inwards in $y > 1$, so that $W < 0$. Equation (A. 39) shows that these properties are associated with waves of the type (A. 37); the other possibility represents waves moving in the opposite directions (incident on the shear layer). Our solution must therefore be of the form (A. 37) in $y > 1$, so that from (A. 31)

$$\sqrt{2}\,\alpha + (1+i)\beta = 0. \tag{A. 40}$$

In the region $y < -1$, for waves of the type

$$\varpi(y) \propto \exp(i\lambda\int q\,dy), \tag{A. 41}$$

equation (A. 38) is replaced by

$$W = \frac{nA(-\infty)}{\lambda(n-k_1)}, \tag{A. 42}$$

using (A. 13) for $y < -1$. Thus

$$W = \frac{-A(-\infty)}{(1+V_c^{-1})}, \tag{A. 43}$$

where $A(-\infty)$ is the dimensionless speed of sound far below the layer and is positive. When $V_c > 0$, reference to figure 5 shows that in $y < -1$ the Mach waves that we seek move outward so that $W < 0$, and when $V_c < 0$, $W > 0$; both statements being in accord with (A. 43). Thus, when $y < -1$, the waves generated by the shear zone are of the type (A. 41) and so from (A. 34),

$$\sqrt{2}\,\gamma + (1-i)\,\delta = 0. \tag{A. 44}$$

We now perform the matching of the solutions at $\xi = 0$. It will be recalled that $\eta(\xi)$ and $H(\xi)$ have the same value and the same derivative at $\xi = 0$, so that from (A. 8),

$$\varpi(y) = \frac{\{2\int q\,dy\}^{\frac{1}{4}}}{q^{\frac{1}{2}}} H(\xi) \tag{A. 45}$$

near $y = Y$. Thus

$$\left.\begin{aligned} \varpi(y) &\to \Omega^{-\frac{1}{4}} H(0) \quad \text{as} \quad y \to Y+0, \\ &\to -i\Omega^{-\frac{1}{4}} H(0) \quad \text{as} \quad y \to Y-0. \end{aligned}\right\} \tag{A. 46}$$

Now

$$H(\xi) = \frac{(-\tfrac{3}{4})!\,B}{2^{\frac{1}{4}}\pi} + \frac{\mu^{\frac{1}{4}}A}{2^{\frac{1}{2}}(\frac{1}{4})!}\,\xi + O(\tfrac{1}{2}\mu\xi^2)^{\frac{5}{4}} \tag{A. 47}$$

near $\xi = 0$ for branch I, and

$$H(\xi) = \frac{(-\tfrac{3}{4})!\,D}{2^{\frac{1}{4}}\pi} + \frac{\lambda^{\frac{1}{4}}C}{2^{\frac{1}{2}}(\frac{1}{4})!}\,\xi + O(\tfrac{1}{2}\lambda\xi^2)^{\frac{5}{4}}, \tag{A. 48}$$

for branch II. From (A. 46), then

$$B = -iD. \tag{A. 49}$$

Furthermore,

$$\frac{d\varpi}{dy} = H\frac{d}{dy}\{[2\int q\,dy]^{\frac{1}{4}} q^{-\frac{1}{2}}\} + [2\int q\,dy]^{-\frac{1}{4}} q^{\frac{1}{2}} \frac{dH}{d\xi}, \tag{A. 50}$$

from (A. 10), so that

$$\left.\begin{aligned} \frac{d\varpi}{dy} &\to \frac{\Omega^{\frac{1}{4}}\mu^{\frac{1}{2}}}{2^{\frac{1}{2}}(\frac{1}{4})!} A \quad \text{as} \quad y \to Y+0, \\ &\to \frac{i\Omega^{\frac{1}{4}}\lambda^{\frac{1}{2}}}{2^{\frac{1}{2}}(\frac{1}{4}\ !} C \quad \text{as} \quad y \to Y-0, \end{aligned}\right\} \tag{A. 51}$$

so that

$$\mu^{\frac{1}{2}} A = i\lambda^{\frac{1}{2}} C. \tag{A. 52}$$

Using (A. 27) and (A. 35) to replace $\alpha, \ldots, \delta$ in (A. 40) and (A. 44), the equations to be solved are

$$\left.\begin{aligned} \sqrt{2}\,A + (1+i)\,B &= \frac{\pi h(+0)}{2\sqrt{2}\,\mu}\{(1+i)\,\Phi_2(0) - \sqrt{2}\,\Phi_1(0)\}, \\ \sqrt{2}\,C + (1-i)\,D &= -\frac{i\pi h(+0)}{2\sqrt{2}\,\lambda}\{(1-i)\,\Phi_2(0) - \sqrt{2}\,\Phi_1(0)\}, \end{aligned}\right\} \tag{A. 53}$$

together with (A. 49) and (A. 52). But from (A. 22),

$$\Phi_1(0) = \int_0^\infty u^{-\frac{1}{4}} J_{-\frac{1}{4}}(u)\,du = \frac{(-\frac{3}{4})!}{2^{\frac{1}{4}}\pi^{\frac{1}{2}}},$$

$$\Phi_2(0) = \int_0^\infty u^{-\frac{1}{4}} J_{\frac{1}{4}}(u)\,du = \frac{\pi^{\frac{1}{2}}}{2^{\frac{1}{4}}(-\frac{1}{4})!},$$

so that

$$\frac{\Phi_2}{\Phi_1} = \frac{\pi}{(-\frac{1}{4})!\,(-\frac{3}{4})!} = 2^{-\frac{1}{2}}.$$

If, therefore, for brevity, we write

$$\begin{aligned} L &= (\tfrac{1}{4}\pi)\,\Phi_1(0)\,h(+0) \\ &= 2^{-\frac{9}{4}}\pi^{\frac{1}{2}}(-\tfrac{3}{4})!\,h(+0), \end{aligned} \tag{A. 54}$$

the equations (A. 53) become

$$\left.\begin{aligned} \sqrt{2}\,A + (1+i)\,B &= -(1-i)\,\mu^{-1}L, \\ \sqrt{2}\,C + (1-i)\,D &= -(1-i)\,\lambda^{-1}L. \end{aligned}\right\} \tag{A. 55}$$

The solution to (A. 49), (A. 52) and (A. 55) is

$$\left.\begin{aligned} A &= -\frac{L}{\mu}\frac{1-i}{\sqrt{2}}\frac{\lambda-\mu}{\lambda+\mu}\left\{1-i\left(\frac{\mu}{\lambda}\right)^{\frac{1}{2}}\right\}, \\ B &= \frac{iL}{(\lambda\mu)^{\frac{1}{2}}}, \\ C &= \frac{L}{\lambda}\frac{1-i}{\sqrt{2}}\frac{\lambda-\mu}{\lambda+\mu}\left\{1-i\left(\frac{\lambda}{\mu}\right)^{\frac{1}{2}}\right\}, \\ D &= -\frac{L}{(\lambda\mu)^{\frac{1}{2}}}, \end{aligned}\right\} \tag{A. 56}$$

and the combination of constants appearing in the asymptotic expression (A. 31) is

$$\begin{aligned} \sqrt{2}\,\alpha + (1-i)\,\beta &= -2i\beta \\ &= \frac{2L}{\mu}\left\{\left(\frac{\mu}{\lambda}\right)^2 + i\right\}. \end{aligned} \tag{A. 57}$$

If $M^2 \gg (k^2/Q_+^2)$, (k^2/Q_-^2) (for wave-numbers well inside the fan of figure 2), these expressions take the simpler forms

$$\left.\begin{aligned} A &= 0, \\ B &= \frac{iL}{M}, \\ C &= 0, \\ D &= -\frac{L}{M}, \\ \sqrt{2}\,\alpha + (1-i)\,\beta &= \frac{2L}{M}(1+i), \end{aligned}\right\} \tag{A. 58}$$

correct to $O(M^{-1})$.

REFERENCES

Chu, B. T. & Kovasznay, L. S. G. 1958 *J. Fluid Mech.* **3**, 494.

Erdélyi, A. 1956 *Asymptotic Expansions.* New York: Dover.

Howarth, L. 1953 Ed. *Modern Developments in Fluid Dynamics—High Speed Flow.* Oxford University Press.

Kramer, H. P. 1955 *J. Acoust. Soc. Amer.* **27**, 789.

Lassiter, L. W. & Heitkotter, R. H. 1954 *Nat. Adv. Comm. Aero.* (*Wash.*) *Tech. Note*, no. 3316.

Laufer, J. 1959 *Progr. Rep.* no. 20–378. J.P.L.: Calif. Inst. Tech.

Lighthill, M. J. 1952 *Proc. Roy. Soc.* A, **211**, 564.

Lighthill, M. J. 1954 *Proc. Roy. Soc.* A, **222**, 1.

Lighthill, M. J. 1956 Article in *Surveys in Mechanics.* Ed. G. K. Batchelor & R. M. Davies. Cambridge University Press.

Lighthill, M. J. 1958 *Fourier Analysis and Generalized Functions.* Cambridge University Press.

Lilley, G. M. 1958 *Aero. Res. Coun.* (*Lond.*), *Rep.* no. 20,376; F.M. 2724.

Phillips, O. M. 1957 *J. Fluid Mech.* **2**, 417.

Ribner, H. S. 1958 *Univ. Toronto Inst. Aerophys. Tech. Note*, no. 21.

Sanders, N. D. & Callaghan, E. E. 1956 *Proc. 2nd Int. Congr. Acoust.* Cambridge, Mass.

Townsend, A. A. 1956 *The Structure of Turbulent Shear Flow.* Cambridge University Press.

The propagation of sound in relaxing gases in tubes at low frequencies

By D. H. SMITH AND H. J. WINTLE*
Physics Department, Woolwich Polytechnic, London, S.E. 18

(Received 4 February 1960)

The frequency dependence of the velocity and attenuation of sound waves in a gas which undergoes vibrational relaxation have been investigated theoretically. At low audible frequencies the attenuations due to viscosity, thermal conduction and relaxation in the gas, add linearly, while the velocity is the relaxation velocity diminished by the Helmholtz–Kirchhoff factor. The relations have been confirmed experimentally, and the free gas velocities of sound at zero frequency, one atmosphere pressure and 30 °C, found for carbon dioxide, air and oxygen, are $270{\cdot}57 \pm 0{\cdot}04$ m sec^{-1}, $349{\cdot}18 \pm 0{\cdot}02$ m sec^{-1} and $331{\cdot}33 \pm 0{\cdot}03$ m sec^{-1}, respectively. The corresponding specific heats are $C_p/R = 4{\cdot}537 \pm 0{\cdot}008$ for carbon dioxide and $C_p/R = 3{\cdot}547 \pm 0{\cdot}003$ for oxygen.

Introduction

Accurate measurements of the velocity of sound in a gas combined with an accurate equation of state can yield precise values for the specific heats of the gas. For gases other than air, a container such as a cylindrical tube must be used. The speed then found is less than that in the free gas and is given by the Helmholtz–Kirchhoff equation. The limits within which the approximation given by Rayleigh (1894) applies have been investigated by Weston (1953) and it appears that almost all the work carried out to date at low frequencies falls within these limits. A considerable amount of work has been done in the ultrasonic region on gases in which vibrational relaxation occurs, and the practice has been to neglect the possibility that the velocity may at these frequencies be modified by the viscous and thermal interaction with the walls of the container, and to subtract from the measured attenuation the theoretical values of the small contributions from the bulk viscous (Stokes's) absorption and the tube absorption to obtain the relaxation absorption.

Recently some very accurate low-frequency determinations of the velocity of sound in non-relaxing gases have been made (Harlow 1954). When the work was extended to include relaxing gases (Wintle 1959*a*, *b*) it was clear that the absorptions due to the relaxation effect and to the presence of the tube were of the same order of magnitude, and that since the Helmholtz–Kirchhoff absorption and the relaxation absorption both depend on the transport properties of the gas, an interaction might well take place.

* Present address: Physics Branch, Royal Military College of Science, Shrivenham, Swindon, Wilts.

Theory

The sound pressures involved in the present work are about 2×10^{-6} atmospheres, and the non-linear terms in the hydrodynamical differential equations are therefore omitted. The classical equations governing the propagation in a tube are given to the required degree of approximation by Rayleigh (1894, sect. 348). They are:

continuity
$$\operatorname{div} \mathbf{V} = -\frac{\partial s}{\partial t}, \tag{1}$$

state
$$p = p_0(s + T/T_0), \tag{2}$$

motion
$$\frac{\partial u}{\partial t} + \frac{1}{\rho_0}\frac{\partial p}{\partial x} = -\nabla^2 u - \frac{1}{3}\frac{\eta}{\rho_0}\frac{\partial^2 s}{\partial x\,\partial t}, \tag{3}$$

where $\mathbf{V}$ = particle velocity, s = condensation, u = x-component of $\mathbf{V}$, p = pressure, η = viscosity, ρ = density, t = time, T = temperature, and the subscript 0 indicates the ambient value.

The thermal equation will be modified as follows. It will be assumed that the energy stored in the vibrational degrees of freedom is exchanged only with the translational and rotational degrees of freedom, so that if there were no other form of heat exchange, we would have

$$C_v^\infty \frac{\partial T}{\partial t} = -C_i \frac{\partial \theta}{\partial t},$$

where C_v^∞ is the translational and rotational specific heat, C_i is the vibrational specific heat, and T, θ are the corresponding temperature amplitudes. If we specify that $T = 0$ on the bounding wall, then this equation holds up to the boundary. This condition is in fact employed in the later working. The full equation, including the effects of compression and of thermal conduction, becomes

$$\frac{\partial T}{\partial t} = (\gamma_\infty - 1)\, T_0 \frac{\partial s}{\partial t} + (\gamma_\infty - 1)\, T_0 \nabla^2 T - b\frac{\partial \theta}{\partial t}, \tag{4}$$

where $b = C_i/C_v^\infty$ and $\gamma_\infty = C_p^\infty/C_v^\infty$. Following Henry's (1932) method the relaxation will be specified by the equation.

$$\frac{\partial \theta}{\partial t} = \frac{1}{\tau}(T - \theta), \tag{5}$$

where τ is the relaxation time.

It follows from the diagram given by Weston (1953, fig. 1) that most low-frequency experimental systems lie in the 'wide tube' region, and that terms beyond the leading ones in the expansions for the velocity of sound c and the amplitude attentuation α are negligible. From equations (1) to (5) above one can eliminate T and then follow the calculation given by Rayleigh (1894). The propagation coefficient q is given by

$$q^2 = \pm\left(\frac{iw}{c_\infty}\right)\frac{(1 + iw\tau + b)}{(1 + iw\tau + b/\gamma_\infty)}\left(1 + \frac{(1-i)}{r(2w)^{\frac{1}{2}}}(\mu^{\frac{1}{2}} + \nu^{\frac{1}{2}}G)\right),$$

where $q = \alpha + iw/c$,

$$G = \left(\frac{1+iw\tau}{\gamma_\infty + iw\tau\gamma_\infty + b}\right)^{\frac{1}{2}} \left(\frac{1+iw\tau}{1+iw\tau+b}\right)(\gamma_\infty - 1),$$

c_∞ = high-frequency limit of the velocity of sound in the free gas,

$\mu = \eta/\rho_0$,

$\nu = k/\rho_0 C_v$ is the thermal diffusivity, and

w = angular frequency.

So long as $\arg G$ is small, the effect of the imaginary part of $(\mu^{\frac{1}{2}} + \nu^{\frac{1}{2}}G)$ on q is negligible. This is true for the cases of subsequent interest, for which the values of b are $< 0{\cdot}01$ and $0{\cdot}4$, and the values of $w\tau$ in the present experiments are $< 0{\cdot}35$ and $< 0{\cdot}04$ for oxygen and carbon dioxide, respectively. After simplification, we obtain

$$c = c(w\tau)\left(1 - \frac{\alpha_{HK}c}{w}\right),$$

$$c(w\tau) = c_0\left(\frac{1+b}{1+b/\gamma_\infty}\right)^{\frac{1}{2}} \left(\frac{(1+b/\gamma_\infty)^2 + (w\tau)^2}{(1+b)^2 + (w\tau)^2}\right),$$

$$\alpha = \alpha_{HK} + \alpha_r,$$

$$\alpha_{HK} = \frac{1}{rc}\left(\frac{w}{2}\right)^{\frac{1}{2}} (\mu^{\frac{1}{2}} + (\nu/\gamma)^{\frac{1}{2}}(\gamma - 1)) = gf^{\frac{1}{2}},$$

$$\alpha_r = \left(\frac{b(1-1/\gamma_\infty)}{c\tau}\right)\left(\frac{(w\tau)^2}{(1+b)(1+b/\gamma_\infty) + (w\tau)^2}\right),$$

where f is the frequency of oscillation.

At low frequencies we may neglect $(w\tau)^2$ in the denominator of the last equation and so obtain

$$\alpha_r = H\tau f^2,$$

where

$$H = \frac{4b(1-1/\gamma_\infty)\pi^2}{c(1+b)(1+b/\gamma_\infty)}.$$

So far, no attention has been paid to the effect either of viscosity in the body of the gas, or of the direct radiation of heat from the gas to the walls of the container. The former Stokes's absorption is given (see Rayleigh 1894) by

$$\alpha_c = \frac{8\pi^2\mu f^2}{3\rho_0 c_0^3},$$

while the latter, according to Bhatia (1957), is such that

$$\alpha_{\text{radiation}}/\alpha_{HK} \simeq f^{-\frac{1}{2}},$$

when f is expressed in cycles per second. There is no indication that either of these gives rise to a measurable effect in the present apparatus (Harlow 1954).

At the low frequencies used, $c(w\tau)$ is practically constant, so the above equations reduce to:

$$1/c = 1/c_0 + g/2\pi f^{\frac{1}{2}},$$

$$\alpha = gf^{\frac{1}{2}} + H\tau f^2.$$

Plots of $1/c$ against $1/f^{\frac{1}{2}}$ and of $\alpha/f^{\frac{1}{2}}$ against $f^{\frac{3}{2}}$ should both give straight lines yielding values of c_0 and g, and of g and $H\tau$ respectively.

Apparatus

The apparatus used was an acoustic interferometer 175 cm long with an internal diameter of 3·78 cm, enclosed in a thermostat. Plane waves were excited at constant amplitude from an electromagnetic loudspeaker with a flat diaphragm at one end of the sound tube, and reflected from a flush-fitting steel plate at the other end. A detailed description is given by Harlow (1954) and the later modifications described by Wintle (1959*a*). The results were obtained in the form of the current $\mathscr{I}$ required to operate the loudspeaker at constant amplitude at various frequencies in the neighbourhood of a natural resonance frequency of the tube. The quantity $\mathscr{I}/f$ is of the nature of a transfer impedance and changes rapidly from a maximum to a minimum in passing through a natural resonance frequency of the acoustic system. It can be plotted on a circle diagram. From the diagram the true resonance frequency and the corresponding attenuation can be determined. The velocity in the tube c which is obtained from the resonance frequency f_n is given by

$$\frac{4\pi f_n l}{c} = 2n\pi - \alpha \frac{lc}{\pi} \frac{\partial \alpha}{\partial f},$$

where l is the length of the tube, and n is an integer. (This relation will be derived in a further publication.)

The velocities found are individually correct to about 0·01 % and the attenuations to 10 % when relaxing gases are used. The variation of the attenuation with frequency is such that the last term in the above equation corrects the velocity by about 0·5 cm sec^{-1} in the present work, and can be neglected.

If the loudspeaker employed is of the electromagnetic type, the difference between extreme values of $\mathscr{I}/f$ in the neighbourhood of a resonance frequency is given by

$$\Delta(\mathscr{I}/f) = A\rho_0 c \frac{\operatorname{sh} 2\alpha l}{\operatorname{ch} 2\alpha l - 1} \frac{2\pi a_0}{BL},$$

so that $f/\alpha\Delta\mathscr{I} \simeq BLl/2\pi a_0 A\rho_0 c$, where A is the cross-sectional area of the sound tube, a_0 the amplitude of oscillation of the loudspeaker diaphragm, L the length of the coil winding, and B the field in the magnet gap. The amplitude a_0 is determined by the disappearance of a set of interference fringes in the manner described by D. H. Smith (1945). Using the first disappearance of fringes formed by mercury green light, the amplitude a_0 is about 1000 Å and the quantity $f/\alpha\Delta\mathscr{I}$ was found to be constant to about 10 %, the limit being set by the uncertainty in the measured values of α. This provides a valuable check that the effects found at different frequencies are not due to defects in the apparatus.

Preparation of the gases

Carbon dioxide

The gas was prepared in a Kipp's apparatus. The crude gas was washed with distilled water and saturated sodium hydrogen carbonate solution and passed through a solid carbon dioxide trap and over phosphorus pentoxide. It was then condensed in a liquid-air trap and the system pumped down to a pressure of 1 μ Hg for 15 min. The gas was then sublimed into the evacuated sound tube and the pressure brought up to 1 atm.

The conditions of preparation were such that the likely impurities, methane, ethane, carbon monoxide, sulphur dioxide, hydrogen chloride and water were removed in the carbon dioxide trap or pumped off the solid. Each sample prepared was discarded after a fortnight.

Air

Air taken from the laboratory was passed through a saturated potassium hydroxide solution, up a calcium chloride tower and then over phosphorous pentoxide before entering the sound tube.

Oxygen

The gas was prepared from 'Analar' grade potassium permanganate by heating. A similar preparation by Hoge (1950) showed that the impurity to be expected is about 2 parts in 10^7.

Results

Determinations of velocity and attenuation were made on each gas at frequencies between 80 cyc sec^{-1} and 1500 cyc sec^{-1}. The measured values of velocity were reduced to the standard values of 1 atm pressure and 30 °C by assuming that over the experimental range of temperatures (less than two degrees) the

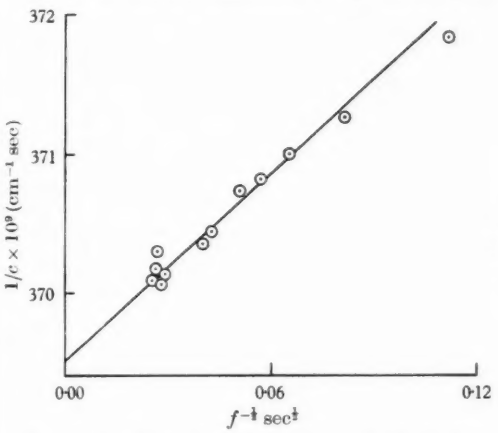

FIGURE 1. The reciprocal of the sound velocity in carbon dioxide as a function of frequency.

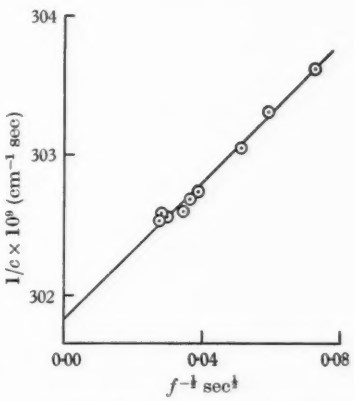

FIGURE 2. The reciprocal of the sound velocity in oxygen as a function of frequency.

velocity is proportional to the square root of the absolute temperature. The pressure correction, due to the imperfection of the gas, amounts to only 0·2 cm sec^{-1} (cm Hg)$^{-1}$ for CO_2 and is less for air and oxygen. The attenuations were reduced to the standard conditions by assuming that α is proportional to $p^{-\frac{1}{2}}$. This is a good approximation since the relaxation absorption is proportional to p^{-1} in the region of interest. The results of the velocity determinations are plotted in figures 1 and 2, and the results of the attenuation determinations in figures 3

and 4, and the details summarized in table 1. The velocities in air were found by the direct application of the Helmholtz–Kirchhoff relation to the measured values of tube velocity and attenuation.

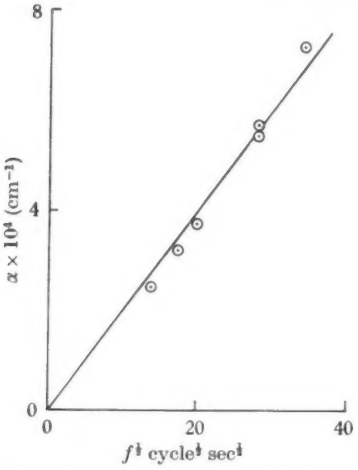

FIGURE 3. The attenuation in air as a function of frequency.

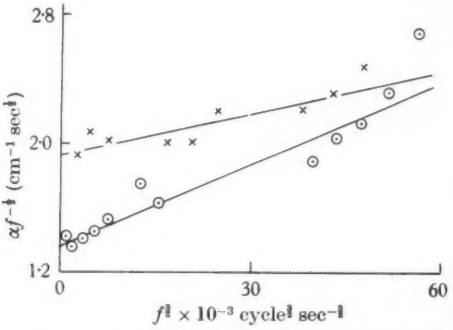

FIGURE 4. The total attenuation in carbon dioxide and oxygen as a function of frequency. ⊙, CO_2; ×, O_2.

Gas	CO_2	O_2	Air
No. of determinations	41	18	6
No. of frequencies	12	9	5
c_0 (m sec^{-1})	270·57 ± 0·03	331·33 ± 0·04	349·18 ± 0·02
g (deduced from velocity) (cm^{-1} sec$^{\frac{1}{2}}$)	$1{\cdot}42 \times 10^{-5}$	$1{\cdot}54 \times 10^{-5}$	—
Correlation coeff.	0·96	0·99	—
g (deduced from absorption) (cm^{-1} sec$^{\frac{1}{2}}$)	$1{\cdot}36 \times 10^{-5}$	$1{\cdot}93 \times 10^{-5}$	$1{\cdot}90 \times 10^{-5}$
$H\tau$ (cm^{-1} sec^2)	$1{\cdot}70 \times 10^{-10}$	$0{\cdot}87 \times 10^{-10}$	—
Correlation coeff.	0·92	0·80	—
g (theoretical) (cm^{-1} sec$^{\frac{1}{2}}$)	$1{\cdot}20 \times 10^{-5}$	$1{\cdot}58 \times 10^{-5}$	$1{\cdot}60 \times 10^{-5}$
H (expected) (cm^{-1} sec)	$9{\cdot}3 \times 10^{-5}$	$2{\cdot}1 \times 10^{-6}$	—
τ (sec)	$1{\cdot}8 \times 10^{-6}$	4×10^{-5}	—

TABLE 1

The expected values of g were determined by calculating the viscosity and thermal conductivity from the data given by Keyes (1952), and using four-figure approximations for the density and ratio of specific heats.

The uncertainty in the velocity quoted is obtained for carbon dioxide and oxygen as the sum of the uncertainty due to the intercept of the graph plus the standard deviation obtained by correcting the individual velocity measurements by the Helmholtz–Kirchhoff formula, assuming these values to have a Gaussian distribution. Only the second term is considered for air.

The expected values for H are obtained from the formula above, assuming that for carbon dioxide $C_v^0 = 5R/2, C_v = 3{\cdot}515R$, and for oxygen that C_i is given by a single Einstein function with $\theta = 2260\,°\mathrm{K}$.

The specific heats

The velocity of sound in a free body of gas is given by

$$c_0^2 = \gamma(\partial p/\partial \rho)_T,$$

where γ is the ratio of the principal specific heats.

Gas	CO_2	O_2
	Beattie–Bridgman equations	
$\left(\frac{\partial p}{\partial \rho}\right)_T \frac{M}{RT}$	0·990 359	0·998 767
$\frac{C_p - C_v}{R}$	1·021 89	1·005 234
$\frac{(C_v - C_v^0)}{R}$	$5{\cdot}713 \times 10^{-3}$	$1{\cdot}653 \times 10^{-4}$
	Virial equations	
$\left(\frac{\partial p}{\partial \rho}\right)_T \frac{M}{RT}$	0·900 506	0·998 859
$\frac{C_p - C_v}{R}$	1·023	1·005 020
	Uncertainties	
$\frac{(C_p - C_v)}{R}$	0·001	0·0001
$\left(\frac{\partial p}{\partial \rho}\right)_T \frac{M}{RT}$	0·0001	0·0001

TABLE 2

Gas ...	...	CO_2	O_2
30 °C, 1 atm	γ	1·2907 ± 0·0004	1·3954 ± 0·0003
	C_v/R	3·515 ± 0·006	2·542 ± 0·002
	C_p/R	4·537 ± 0·008	3·547 ± 0·003
30 °C, zero pressure	γ^0	1·2849 ± 0·0004	1·3934 ± 0·0003
	C_v^0/R	3·509 ± 0·006	2·542 ± 0·002
	C_p^0/R	4·509 ± 0·008	3·542 ± 0·003

TABLE 3

The most accurate closed equation of state for carbon dioxide is that of Beattie and Bridgman (see Beattie & Stockmayer 1940). A virial expansion for oxygen has been given by Meyers (1948) and for carbon dioxide, using new data, by Michels & Michels (1937). The relevant thermodynamic functions are given in table 2. By adopting the numerical values given by the Beattie–Bridgman equation, together with the values $R = 8{\cdot}31436$ joule deg^{-1} mole^{-1} (Birge 1941), $M = 44{\cdot}011$ for CO_2 (Wichers 1954) and $M = 32{\cdot}00$ for O_2, the experimental values of the velocity of sound have been used to find the specific heats and specific heat ratios given in table 3.

Discussion

Most recent work on the velocity of sound in carbon dioxide has been carried out at ultrasonic frequencies, and the extrapolation to zero frequency does not have the precision required for the present purpose. The most accurate low-frequency determinations are listed in table 4. A correction suggested by Woolley (1953) has been applied to the work of Katz, Leverton & Woods (1949).

	Date	Frequency (cycle sec^{-1})	velocity (m sec^{-1})
	Carbon dioxide		
Abbey & Barlow	1948	1000	271·2 ± 0·2
Katz, Leverton & Woods	1949	Low	270·67 ± 0·05
Koehler	1950	Low	270·87 ± 0·05
This work	1959	100–1500	270·57 ± 0·04
	Oxygen		
Abbey & Barlow	1948	1000	331·8 ± 0·2
Knötzel & Knötzel	1948	Audible	331·30 ± 0·08
Koehler	1950	Low	331·70 ± 0·13
This work	1959	200–1300	331·33 ± 0·04

TABLE 4. Velocity of sound determinations at 30 °C and 1 atm pressure.

	Date	Method	C_p^0/R
	Carbon dioxide		
Kistiakowsky & Rice	1939	Expansion	4·501 ± 0·008
Lapshina & Khomyakov	1951	Flow comparison	4·487 ± 0·009
Masi & Petkof	1952	Constant flow	4·495 ± 0·007
Woolley	1954	Spectroscopic	4·493
This work	1959	Velocity of sound	4·510 ± 0·008
	Oxygen		
Wacker, Cheney & Scott	1947	Constant flow	3·536 ± 0·005
Woolley	1948	Spectroscopic	3·536 ± 0·003
Masi & Petkof	1952	Constant flow	3·537 ± 0·005
This work	1959	Velocity of sound	3·542 ± 0·003

TABLE 5. Specific heat determinations at 30 °C

The best determinations in oxygen at low frequencies are also given in table 4. The values quoted by Knötzel & Knötzel (1948) were based on a value for the velocity of sound in air of 342·94 m sec^{-1} at 19 °C and 1 atm pressure. The value quoted in the table has been corrected in the light of more recent determinations. Recent specific heat determinations for both gases are compared in table 5.

With the exception of the work by Katz *et al.*, Koehler and the present authors, no account has been taken in the velocity investigations of the impedance effect pointed out by P. W. Smith (1952). He showed that the apparent wavelength measured in a tube is not independent of the transfer impedance between the acoustic and detecting systems. The analysis was carried out specifically for a

two pole network, but there seems no bar to extending the argument to a system in which the exciting and detecting elements are separate. The frequency change brought about by allowing for the detector impedance is about 1 part in 500 in the present instance, so that the uncorrected velocity results from similar systems are suspect to about the same extent.

From the data given by Sette & Hubbard (1953), the apparent concentration of water vapour in the samples of carbon dioxide and oxygen was about 0·05 and 0·4 % respectively. However, the drying agents should have reduced the water-vapour content to about 1 part in 10^8. It is possible that the diffusion of excited molecules from the body of the gas to the walls of the tube, which takes place in a time of the order of 10^{-4} sec, plays a considerable part in the relaxation characteristics. Support for this assumption is given by the lack of relaxation effects in the results of Harlow (1954) and Lee (1957) on air.

Conclusion

The velocities of sound and specific heats found by the authors are in excellent agreement with other determinations. The velocities quoted by Koehler (1950) appear in both cases to be somewhat high.

It is seen from figures 1 and 2 that the form of the Helmholtz–Kirchhoff relation is obeyed by relaxing gases at low frequencies. The theoretical prediction that at these frequencies the tube and relaxation absorptions add linearly is confirmed from figure 4. The experimental Helmholtz–Kirchhoff coefficients are about 15 % in excess of the theoretical values, in agreement with the majority of work in this field (for a bibliography, see Lee 1957).

The measurement of the specific heats of gases by the velocity-of-sound method cannot be further improved until a more detailed knowledge of the equation of state is available.

The authors wish to express their thanks to the Governing Body of the Woolwich Polytechnic for providing facilities for the research. The junior author (H. J. W.) also wishes to thank the London County Council for awarding him a Research Assistantship.

REFERENCES

Abbey, R. L. & Barlow, G. E. 1948 *Aust. J. Sci. Res.* A **1**, 175.
Beattie, J. A. & Stockmayer, W. H. 1940 *Rep. Progr. Phys.* **7**, 195.
Bhatia, A. B. 1957 *J. Acoust. Soc. Amer.* **29**, 823.
Birge, R. T. 1941 *Rev. Mod. Phys.* **13**, 233.
Harlow, R. G. 1954 Ph.D. Thesis, London.
Henry, P. S. H. 1932 *Proc. Camb. Phil. Soc.* **28**, 249.
Hoge, H. J. 1950 *J. Res. Nat. Bur. Stand.* **44**, 321.
Katz, L., Leverton, W. F. & Woods, S. B. 1949 *Canad. J. Phys.* **27** A. 39.
Keyes, F. G. 1952 *Trans. Amer. Soc. Mech. Engrs*, **73**, 589.
Kistiakowsky, G. B. & Rice, W. W. 1939 *J. Chem. Phys.* **7**, 281.
Knötzel, H. & Knötzel, L. 1948 *Ann. Phys.* (6) **2**, 393.
Koehler, W. F. 1950 *J. Chem. Phys.* **18**, 465.
Lapshina, M. I. & Khomyakov, K. G. 1951 *Dokl. Akad. Nauk SSSR*, **2**, 35.

Lee, T. A. 1957 Ph.D. Thesis, London.
Masi, J. F. & Petkof, B. 1952 *J. Res. Nat. Bur. Stand.* **48**, 179.
Meyers, C. H. 1948 *J. Res. Nat. Bur. Stand.* **40**, 457.
Michels, A. & Michels, C. 1937 *Proc. Roy. Soc.* A, **160**, 348.
Rayleigh, Lord 1894 *Theory of Sound.* London: Macmillan.
Sette, D. & Hubbard, J. C. 1953 *J. Acoust. Soc. Amer.* **25**, 994.
Smith, D. H. 1945 *Proc. Phys. Soc.* **57**, 534.
Smith, P. W. 1952 *J. Acoust. Soc. Amer.* **24**, 687.
Wacker, P. F., Cheney, R. K. & Scott, R. B. 1947 *J. Res. Nat. Bur. Stand.* **38**, 651.
Weston, D. E. 1953 *Proc. Phys. Soc.* B, **66**, 695.
Wichers, E. 1954 *J. Amer. Chem. Soc.* **76**, 2033.
Wintle, H. J. 1959*a* M.Sc. Thesis, London.
Wintle, H. J. 1959*b* *Nature, Lond.*, **184**, 2007.
Woolley, H. W. 1948 *J. Res. Nat. Bur. Stand.* **40**, 163.
Woolley, H. W. 1953 *Canad. J. Phys.* **31**, 604.
Woolley, H. W. 1954 *J. Res. Nat. Bur. Stand.* **52**, 289.

Observations on bubble growths in various superheated liquids

By PAUL DERGARABEDIAN*
U.S. Naval Ordnance Test Station, Underwater Ordnance Department, Pasadena, California

(Received 11 January 1960)

Experimental data are presented for the growth of vapour bubbles in various superheated liquids, such as carbon tetrachloride, benzene, ethyl alcohol, and methyl alcohol. These data are compared with the theoretical results obtained by Plesset & Zwick (1953) who derived these results by taking into account the heat diffusion across the bubble boundary. The agreement in all cases between experiment and theory is found to be good.

The growth of vapour bubbles in slightly superheated water is also presented in the form of experimental data for bubbles just beginning to grow from a point of equilibrium which is presumed to be dynamically unstable. The radii corresponding to the points of equilibrium are of the same order of magnitude as those predicted by theoretical considerations.

1. Introduction

The importance of the cavitation phenomenon in the field of hydrodynamics is well recognized by both the theoretical physicist and the design engineer. In particular, the engineer in the field of underwater ordnance is constantly confronted with problems having to do with performance degradation of propulsion systems and missiles. An intelligent application of the present knowledge in cavitating flow requires some insight into the basic mechanism of cavitation. The present paper is an attempt to add to this knowledge of the mechanism of cavitation rather than to furnish some tools to the design engineer for direct application to design problems.

The analogy between producing bubbles by a reduction of the external pressure and by increasing the vapour pressure of a liquid by heating is used in the present study, and hence all the experiments are conducted by superheating liquids with the use of infra-red lamps. The experimental procedures are the same as those described in a previous paper by the author (1953). In the case of carbon tetrachloride and benzene, the work was carried out in a ventilated hood. Since carbon tetrachloride is a very poor absorber of infra-red radiation, the container for the carbon tetrachloride was placed inside a larger beaker containing water. Thus the infra-red lamps heated the water which in turn increased the temperature of the carbon tetrachloride. By the use of Eastman Tri-X film, it was also possible to obtain larger magnifications with smaller lens openings. This film, together with

* Now at the Space Technology Laboratories, Inc., Los Angeles, California.

the Edgerton lamps, made it possible to obtain useful data for bubble radii of the order of 10^{-3} cm.

The experimental part of this paper is an analysis of high-speed photographs of the growth of vapour bubbles in water, carbon tetrachloride, benzene, ethyl alcohol, and methyl alcohol, at superheat temperatures, in order to obtain a detailed check with the Plesset–Zwick (1953) theory for bubble growth. Previous work by the author (1953) had shown that the experimental data obtained for the growth of bubbles in superheated water indicated good agreement with theory. All of the data in this previous work were obtained in an observable range of radii considerably larger than the equilibrium bubble size predicted by the theory in the report by the author (1953). Thus, in the case of water, the present experiments are an attempt to measure bubble growth from the equilibrium point, whereas the data for the other liquids are intended to show a comparison with water for rate of growth using the same amount of superheat in each case.

The theoretical part of this paper is a detailed presentation of the analysis for calculating the range of bubble radii that are unstable and those that are stable for any given set of conditions.

2. Growth rates for various liquids

The Plesset–Zwick (1953) theory, which includes the effect of heat diffusion across the bubble wall, predicts a growth rate which has the following behaviour:

$$R \sim 2\frac{\rho c}{\rho' L}\sqrt{\left(\frac{3}{\pi}Dt\right)}(T-T_0) \quad (t\to\infty), \tag{1}$$

where $T-T_0$ indicates the amount of superheat in °C, ρ and ρ' are the liquid and vapour densities, respectively, c is the specific heat for the liquid, L is the latent heat of vaporization, and D is the thermal diffusivity for the superheated liquid. This formula for R, the radius as a function of the time t, indicates that, for a given amount of superheat $T-T_0$, together with vapour-pressure curves having similar slopes, the growth of bubbles in different liquids should be proportional to the quantity

$$\frac{\rho c}{\rho' L}\sqrt{D}. \tag{2}$$

For the liquids used, the values of this parameter and the variations of pressure with temperature near the pressure of 760 mm of mercury are shown in the following table:

	$\frac{\rho c}{\rho' L}\sqrt{D}$ (cm/°C sec$^{\frac{1}{2}}$)	Temp. (°C)	Variation (°C/cm)
water	0·121	100·0	0·37
carbon tet.	0·034	76·7	0·41
benzene	0·046	80·1	0·43
methyl alc.	0·046	64·6	0·35
ethyl alc.	0·044	78·3	0·34

Since the pressure variations with temperature are nearly the same, the parameter (2) predicts a growth rate for bubbles in water of approximately 3·5 times that for carbon tetrachloride, 2·6 times that for benzene and methyl alcohol,

and 2·8 times that for ethyl alcohol. All of the liquids used in the experiment were chemically of reagent grade. Figure 1 shows a comparison of the growth rates. The amounts of superheat are: 5·3 °C for water, 6·3 °C for ethyl alcohol, 5·4 °C for methyl alcohol, 5·4 °C for benzene, and 5·4 °C for carbon tetrachloride. The Plesset–Zwick (1953) theory shows good agreement with the data for water, and the agreement is seen to be good for the other liquids, which all show a smaller rate

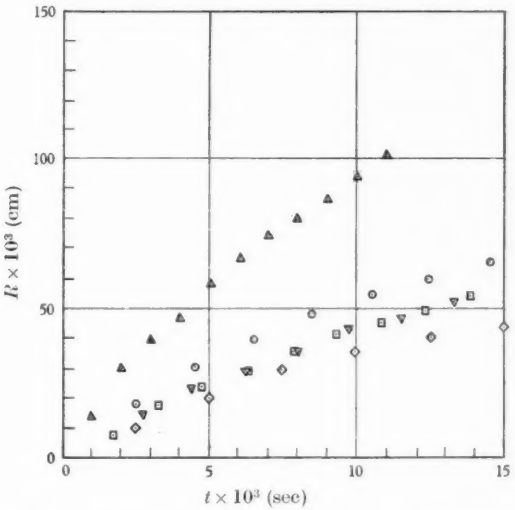

FIGURE 1. Radius as a function of time in various superheated liquids. R is shown as a function of t for vapour bubbles growing in superheated water, ethyl alcohol, methyl alcohol, benzene, and carbon tetrachloride. △, H_2O, 105·3 °C, B.P. (760 mm), 100 °C; ⊙, CH_3CH_2OH, 84·6 °C, B.P. (760 mm), 78·3 °C; ▽, CH_3OH, 70·0 °C, B.P. (760 mm), 64·6 °C; □, C_6H_6, 85·5 °C, B.P. (760 mm), 80·1 °C; ◇, CCl_4, 82·1 °C, B.P. (760 mm), 76·7 °C.

of growth as predicted by the theory. The temperature measurements are presumed to be accurate within ± 0·2 °C. In addition, the true boiling points for all the liquids with the exception of water are not known within ± 0·1 °C. Because of these inaccuracies, the comparison with theory is of a qualitative nature. However, the trend is seen to be the one predicted by the theory in every case.

3. Growth rate near equilibrium

All of the data used in the previous discussion were obtained in an observable range of radii considerably larger than the equilibrium bubble size predicted by theory (see Appendix). The mechanism for bubble growth, as described in the Appendix, is that for growth from a radius corresponding to a dynamically unstable equilibrium. The subsequent growth from this equilibrium is then predicted by the Plesset–Zwick theory. To clarify this model, consider the equation of motion for the bubble

$$R\ddot{R} + \tfrac{3}{2}\dot{R}^2 = \frac{p_v - p_\infty + p_a - (2\sigma/R)}{\rho},$$

where ρ is the density of the liquid, R is the radius of the bubble at time t, p_v is the vapour pressure of the water at the appropriate temperature, p_a is the partial pressure of air which may be present in the bubble, p_∞ is the atmospheric pressure, and σ is the surface-tension constant for water. With the assumptions of the Appendix, it turns out that the range of bubble radii in terms of the amount of superheat, external pressure, and initial air content, for which a condition of dynamic instability exists is given by

$$\frac{4\sigma}{3\delta p} \leqslant R_0 \leqslant \frac{2\sigma}{\delta p}, \quad \text{with} \quad \delta p \equiv p_v - p_\infty \geqslant 2p_{a0} \geqslant 0.$$

Thus, for superheats of 3 °C and 1 °C for water,

$$R_0 \simeq 10^{-3}\,\text{cm} \quad \text{and} \quad R_0 \simeq 3{\cdot}1 \times 10^{-3}\,\text{cm},$$

respectively. It is evident that to obtain data for R of the order of 10^{-3} cm, it is necessary to have relatively large magnifications. This requirement is reflected in the need for faster film and a more intense light source. With the use of Edgerton

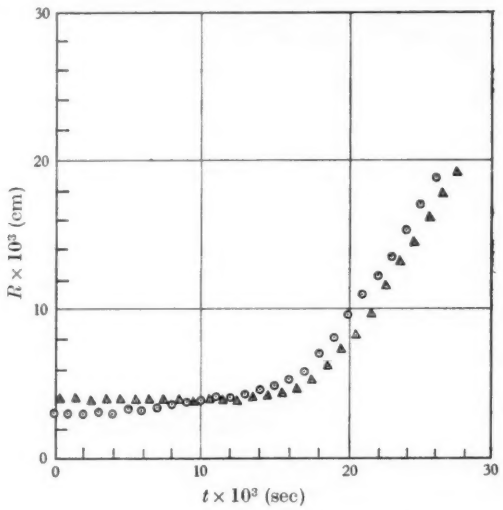

FIGURE 2. Radius as a function of time in slightly superheated water. R is shown as a function of t for two vapour bubbles growing in slightly superheated water. The growth in this case is from a radius near the equilibrium size for the given temperature. ⊙, 101·0 °C; △, 100·8 °C.

lamps and Eastman Tri-X film, the possibility of obtaining useful data for bubble radii of the order of 10^{-3} cm was investigated and found to yield satisfactory results. Figure 2 shows the results for two bubbles, one for 1 °C superheat and the other for 0·8 °C superheat. The bubbles are seen to grow very slowly from a radius between 3×10^{-3} and 4×10^{-3} cm until a point near 0·013 sec, at which time the growth rate is markedly increased. Actually, the bubbles remain nearly constant in size for a time corresponding to 0·1 sec. The value $t = 0$ was chosen arbitrarily for the graph. The bubble radii compare favourably with the predicted value of

$R_0 \simeq 3{\cdot}1 \times 10^{-3}$ cm for $T = 101$ °C. However, for these low values of superheat the growth rate is sufficiently slow for translational effects of the bubble to modify its growth rate, and a comparison with the Plesset–Zwick theory is made difficult. However, the growth from an equilibrium size seems to be indicated from the data. Higher superheats would furnish better data for a comparison with theory, but the difficulty in obtaining such data is greatly increased because of the greater growth rates and smaller initial radii involved.

Appendix

Equilibrium radii for bubble growth

(1) *Equation of motion for the growth of a cavitation bubble*

Frequent reference is made in the literature on cavitation to Rayleigh's (1917) solution for the collapse of a spherical cavity in a liquid. Rayleigh's theory can be extended to the case of growth of a bubble. Rayleigh considered the situation in which the pressure at a great distance from the bubble is constant. With this assumption, and the assumption of an incompressible fluid, the variation of the bubble radius with time is obtained from the energy integral of the motion. For the present problem of the growth of a bubble, the extension of the Rayleigh theory as carried out by Plesset (1949) can be used to obtain the equation of motion. The equation is obtained by considering a spherical bubble in a perfect incompressible fluid of infinite extent. Neglecting the effects of gravity, the origin is chosen at the bubble centre which is at rest. The radius of the bubble for any time t is R, and r is the radius to any point in the liquid. Thus the velocity potential for the liquid is expressed by

$$\phi = \frac{R^2\dot{R}}{r}, \tag{1}$$

and the Bernoulli integral of the motion is

$$-\frac{\partial\phi}{\partial t} + \tfrac{1}{2}(\nabla\phi)^2 + \frac{p(r)}{\rho} = \frac{P(t)}{\rho}, \tag{2}$$

where ρ is the constant density of the liquid, $\dot{R} = dR/dt$, $p(r)$ is the static pressure at r, and $P(t)$ is the static pressure at a large distance from the bubble. From (1),

$$(\nabla\phi)^2 = \frac{R^4\dot{R}^2}{r^4}, \tag{3}$$

$$\frac{\partial\phi}{\partial t} = \frac{1}{r}(2R\dot{R}^2 + R^2\ddot{R}), \tag{4}$$

and applying (2) at $r = R$, we then obtain the equation of motion for the bubble radius. Thus, with

$$\left(\frac{\partial\phi}{\partial t}\right)_{r=R} = 2\dot{R}^2 + R\ddot{R},$$

$$(\nabla\phi)^2_{r=R} = \dot{R}^2,$$

(2) becomes

$$R\ddot{R} + \tfrac{3}{2}\dot{R}^2 = \frac{p(R) - P(t)}{\rho}. \tag{5}$$

Equation (5) is the general equation of motion for a spherical bubble in a liquid with given external pressure $P(t)$, and with the pressure at the bubble boundary $p(R)$. Rayleigh's equation is obtained as a special case if

$$P(t)-p(R)=P_0 \text{ (a constant)}.$$

Equation (5) is adapted to the present problem with the assumption that

$$p(R)=p_v+p_a-\frac{2\sigma}{R},$$

where p_v is the vapour pressure of the water at the appropriate temperature, p_a is the pressure of any air which may be in the bubble of radius R, and σ is the surface-tension constant for water. Letting

$$P(t)=p_\infty \text{ (a constant)},$$

where p_∞ is the atmospheric pressure, the equation of motion for the bubble radius becomes

$$R\ddot{R}+\tfrac{3}{2}\dot{R}^2=\frac{p_v-p_\infty+p_a-(2\sigma/R)}{\rho}. \tag{6}$$

(2) *Solution of* (6) *with* p_v = *constant*

If the assumption is made that the vapour pressure p_v remains constant throughout the growth of the bubble, then the bubble growth is isothermal, so that

$$p_a=p_{a0}\frac{R_0^3}{R^3}, \tag{7}$$

where p_{a0} is the initial pressure of the air in a bubble of radius R_0. Equation (7) implies the assumption that no air diffuses across the bubble boundary as it grows. Plesset & Epstein (1950) have shown that the diffusion process for gas bubbles is so slow compared with the rate of growth of the bubble that it does not affect the air content of the bubble. Thus (7) is a reasonable expression for the air pressure p_a as a function of the bubble radius.

From (6) it can be seen that the bubble is in dynamic equilibrium with the liquid if

$$f(R)=p_v-p_\infty+p_{a0}\frac{R_0^3}{R^3}-\frac{2\sigma}{R}=0 \quad (\dot{R}=0). \tag{8}$$

One obvious root of (8) is $R=R_0$, where

$$R_0=\frac{2\sigma}{p_v+p_{a0}-p_\infty}.$$

The remaining roots of (8) are then found to be

$$R=\frac{p_{a0}\sigma}{\delta p(\delta p+p_{a0})}\left\{1\pm\sqrt{\left(1+4\frac{\delta p}{p_{a0}}\right)}\right\},$$

where $\delta p=p_v-p_\infty$. If $\delta p>0$, then the two positive roots of (8) that correspond to actual bubble radii are

$$R=\frac{2\sigma}{\delta p+p_{a0}}$$

and

$$R=\frac{p_{a0}\sigma}{\delta p(\delta p+p_{a0})}\left\{1+\sqrt{\left(1+4\frac{\delta p}{p_{a0}}\right)}\right\}.$$

The case $\delta p > 0$ corresponds to the condition that the vapour pressure p_v is greater than the atmospheric pressure p_∞, so that the liquid can boil. If $\delta p \leqslant 0$, then there is only one positive root of (8), namely

$$R = \frac{2\sigma}{\delta p + p_{a0}},$$

provided that $p_{a0} > |\delta p|$.

The effect of varying the value of the initial air pressure p_{a0} on the equilibrium radii will be considered next.

For the case $\delta p > 0$, it should be noted that

$$p_{a0} R_0^3 = p_{a0}\left(\frac{2\sigma}{\delta p + p_{a0}}\right)^3$$

has the value zero for $p_{a0} = 0$, increases to a maximum value of

$$\tfrac{1}{2}\delta p(4\sigma/3\delta p)^3 \quad \text{at} \quad p_{a0} = \tfrac{1}{2}\delta p$$

and then approaches zero as $p_{a0} \to \infty$. Thus the entire range of values of $p_{a0} R_0^3$ is covered in the range $0 \leqslant p_{a0} \leqslant \frac{1}{2}\delta p$. For the case of a vapour bubble, $p_{a0} = 0$, and there is only one positive root of (8), its value being $R = 2\sigma/\delta p$. When $p_{a0} = \frac{1}{2}\delta p$, the two positive roots coincide with a value of $R = 4\sigma/3\delta p$. If any values of $p_{a0} > \frac{1}{2}\delta p$ are considered, the two roots merely interchange roles. Thus for the case $\frac{1}{2}\delta p > 0$, it is sufficient to consider the two roots

$$R = R_0 = \frac{2\sigma}{\delta p + p_{a0}}$$

for $0 \leqslant p_{a0} \leqslant \frac{1}{2}\delta p$, and

$$R = R_1 = \frac{p_{a0}\sigma}{\delta p(\delta p + p_{a0})}\left\{1 + \sqrt{\left(1 + 4\frac{\delta p}{p_{a0}}\right)}\right\}$$

$$= \frac{2\sigma}{\delta p + p_{a1}},$$

$$p_{a1} = \frac{2\delta p(\delta p + p_{a0})}{p_{a0}\left\{1 + \sqrt{\left(1 + 4\dfrac{\delta p}{p_{a0}}\right)}\right\}} - \delta p$$

for $p_{a1} > \frac{1}{2}\delta p$. Thus the entire range of possible values for the initial air pressure in the bubble is covered. For the case $\delta p \leqslant 0$, the only root is

$$R = R_0 = \frac{2\sigma}{\delta p + p_{a0}}$$

with $p_{a0} > |\delta p|$.

To determine whether the equilibrium of a bubble is dynamically stable or unstable, one may consider

$$\frac{df(R)}{dR} = \frac{2\sigma}{R^2} - 3p_{a0}\frac{R_0^3}{R^3} \tag{9}$$

for the given radius. Thus for dynamic stability $df(R)/dR < 0$, and for dynamic instability $df(R)/dR > 0$. For the case $\delta p > 0$ and radius

$$R = R_0 = \frac{2\sigma}{\delta p + p_{a0}},$$

(9) becomes $$\left[\frac{df(R)}{dR}\right]_{R=R_0} = \frac{\delta p + p_{a0}}{2\sigma}(\delta p - 2p_{a0})$$

or $$\left[\frac{df(R)}{dR}\right]_{R=R_0} \geqslant 0,$$

if $0 \leqslant p_{a0} \leqslant \frac{1}{2}\delta p$. This means that the equilibrium of a bubble of radius $R_0 = 2\sigma/\delta p + p_{a0}$, with $\delta p > 0$, is dynamically unstable if $0 \leqslant p_{a0} < \frac{1}{2}\delta p$. For the case $p_{a0} = \frac{1}{2}\delta p$, $df(R)/dR = 0$, the bubble is dynamically unstable if the radius is increased beyond R_0, but is dynamically stable if the radius is decreased below R_0. In terms of the growth of the bubble, the range of equilibrium radii are

$$\frac{4\sigma}{3\delta p} \leqslant R_0 \leqslant \frac{2\sigma}{\delta p} \quad \text{with} \quad \tfrac{1}{2}\delta p \geqslant p_{a0} \geqslant 0.$$

For the radius

$$R = R_1 = \frac{2\sigma}{\delta p + p_{a1}} \quad (p_{a1} > \tfrac{1}{2}\delta p),$$

(9) becomes $$\left[\frac{df(R)}{dR}\right]_{R=R_1} = -3p_{a0}\frac{R_0^3}{R_1^4} + \frac{2\sigma}{R_1^2}.$$

Since $R_1 < R_0$ and $\left[\frac{df(R)}{dR}\right]_{R=R_0} = 0$ for $p_{a0} = \frac{1}{2}\delta p$,

one obtains $$\left[\frac{df(R)}{dR}\right]_{R=R_1} < 0$$

for all $p_{a1} > \frac{1}{2}\delta p$. This means that all bubbles of radius $R_1 < 4\sigma/3\delta p$, with $\delta p > 0$, are dynamically stable. However, these bubbles soon dissolve through diffusion of air out of the bubble (Plesset & Epstein 1950).

For the case $\delta p \leqslant 0$, with $p_{a0} > |\delta p|$, the equilibrium radius is

$$R_0 = \frac{2\sigma}{\delta p + p_{a0}},$$

and (9) becomes $$\left[\frac{df(R)}{dR}\right]_{R=R_0} = \frac{\delta p + p_{a0}}{2\sigma}(\delta p - 2p_{a0}).$$

Since $p_{a0} > |\delta p|$, one obtains $\left[\frac{df(R)}{dR}\right]_{R=R_0} < 0.$

This means that if the vapour pressure, p_v, is less than the atmospheric pressure, p_∞, then any air bubble existing in the liquid of radius R_0, with $R_0 = 0$, is dynamically stable. However, these bubbles also slowly dissolve through diffusion of air out of the bubble. Evidence for the existence of these bubbles can be found in observing water as it is slowly heated. Near the temperature of 80 °C,

where the vapour pressure, p_v, is still less than the atmospheric pressure, p_∞, corresponding to the condition $\delta p < 0$, these bubbles can be seen floating within the body of the liquid or clinging to the container walls. Their duration, although limited by diffusion, is still long enough for visual observation.

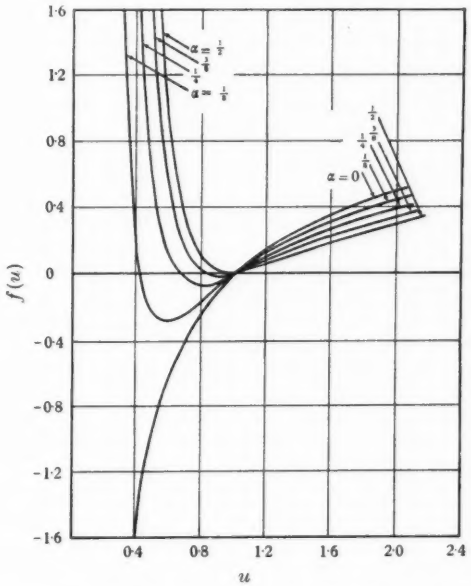

FIGURE 3. The function $f(u)$, the dimensionless form for the total pressure $f(R)$ acting on the bubble wall (see (10)), for various values of α. The case $\alpha = 0$ corresponds to a vapour bubble.

A convenient way to plot $f(R)$ as a function of R for various initial values of p_{a0} is to write $p_{a0} = \alpha\delta p$ and then change $f(R)$ to dimensionless form by dividing through by $\delta p + p_{a0}$. Thus

$$\frac{f(R)}{\delta p + p_{a0}} = \frac{\delta p}{\delta p + p_{a0}} + \frac{p_{a0}}{\delta p + p_{a0}} \frac{R_0^3}{R^3} - \frac{2\sigma}{(\delta p + p_{a0})\, R};$$

and, with $u = R/R_0$ and $\qquad (1+\alpha)\dfrac{f(R)}{\delta p + p_{a0}} = f(u),$

one gets

$$f(u) = 1 - \frac{1+\alpha}{u} + \frac{\alpha}{u^3}. \tag{10}$$

Figure 3 shows $f(u)$ as a function of u for various values of α. The case $\alpha = 0$ corresponds to the growth of a vapour bubble.

The preceding analysis has shown that for the growth of a bubble as governed by the equation of motion

$$R\ddot{R} + \tfrac{3}{2}\dot{R}^2 = \frac{\delta p + p_{a0}(R_0/R)^3 - (2\sigma/R)}{\rho}, \tag{11}$$

with initial conditions R_0 and $\dot{R}_0$, the range of equilibrium bubble radii which are dynamically unstable is

$$\frac{4\sigma}{3\delta p} \leqslant R_0 \leqslant \frac{2\sigma}{\delta p},$$

where

$$\tfrac{1}{2}\delta p \geqslant p_{a0} \geqslant 0.$$

This investigation was carried on at the Hydrodynamics Laboratory of the California Institute of Technology by the U.S. Naval Ordnance Test Station.

The work was performed during 1955 under NOTS Contract No. N123s 91875.

The author wishes to thank Dr Milton S. Plesset of the California Institute of Technology, and G. V. Schliestett of the U.S. Naval Ordnance Test Station (presently at Space Technology Laboratories, Inc.) for suggesting this investigation and for the time devoted to many helpful discussions. The author is also indebted to Dr Albert T. Ellis of the California Institute of Technology for his help in the experimental phase of the work.

REFERENCES

Dergarabedian, P. 1953 The rate of growth of vapor bubbles in superheated water. *J. Appl. Mech.* **20**, p. 537.

Plesset, M. S. 1949 The dynamics of cavitation bubbles. *J. Appl. Mech.* **71**, 277.

Plesset, M. S. & Epstein, P. S. 1950 On the stability of gas bubbles in liquid-gas solutions. *J. Chem. Phys.* **18**, 1505.

Plesset, M. S. & Zwick, S. A. 1953 The growth of vapor bubbles in superheated liquids. *California Institute of Technology, Hydrodynamics Laboratory Report*, no. 26-6.

Rayleigh, Lord 1917 On the pressure developed in a liquid during the collapse of a spherical cavity. *Phil. Mag.* **34**, 94.

A study of the structure of the magnetohydrodynamic switch-on shock in steady plane motion

By Z. O. BLEVISS†
Douglas Aircraft Co., Inc., Santa Monica, California

(Received 3 November 1959 and in revised form 10 March 1960)

The structure of the steady magnetohydrodynamic switch-on shock wave is investigated for several orderings of the four diffusivities involved in the problem. The various orderings are approximated to by allowing one or more of the appropriate diffusivities to approach zero, and approximate solutions that are uniformly valid to order unity are sought. In general, singular perturbation problems are encountered, the number occurring (from zero to a maximum of three) depending upon the ordering of the diffusivities and the magnitude of the downstream velocity normal to the shock relative to certain critical velocities downstream of the shock. Where necessary, the approximate solutions are rendered uniformly valid to first order by the insertion of boundary layers, for which the approximate equations are determined to first order. For most of the cases considered, the limiting forms of the integral curves are determined and they are sketched in appropriate three-dimensional phase spaces.

1. Introduction

The study of the structure of steady magnetohydrodynamic shock waves in plane motion using continuum theory was initiated by Marshall (1956). He studied the 'parallel' shock, i.e. a case where the flow is normal and the magnetic field is parallel to the shock. He obtained explicit results for the shock structure for two limiting cases: (i) magnetic diffusivity large (low electrical conductivity), and (ii) magnetic diffusivity small (high electrical conductivity) compared with the other diffusivities. The parallel shock for the case of low electrical conductivity was also studied by Burgers (1957) and Whitham (1959). Recently, Ludford (1959) studied, in addition to the parallel shock, some general features of switch-on, switch-off, and transverse magnetohydrodynamic shocks, as defined by Friedrichs (1957). His treatment is essentially restricted to moderate to low electrical conductivity. Independently, Bleviss (1959) investigated in detail the structure of the switch-on shock for the case of low electrical conductivity.

This paper presents a more general investigation of the structure of the switch-on shock. The switch-on shock is a shock that has the velocity and magnetic field vectors normal to it on the upstream side and oblique to it on the downstream side (see figure 1). The name derives from the fact that tangential components of velocity and magnetic field are 'switched-on'. This turning of the normal flow, which is not possible with hydrodynamic shocks, is accomplished here by Maxwell

† Now at Space Technology Laboratories, Inc., Los Angeles, California.

stresses that are parallel to the shock front. This shock is of interest because of its peculiar properties and because it is generally more complex than the parallel shock.

The equations that govern the shock structure can be reduced to a system of four first-order non-linear ordinary differential equations. In this system of equations, each of the four different derivatives is multiplied by a different one of the four diffusivities. In general, this system of equations must be solved

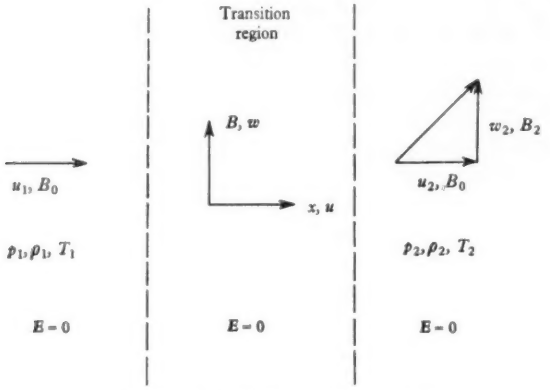

FIGURE 1. Switch-on shock wave.

numerically. When order-of-magnitude differences occur among the diffusivities, the system of equations can be approximated to by allowing the appropriate diffusivities to approach zero. These limiting cases are, of course, simpler and many of them can be solved analytically. A few of the many possible order-of-magnitude orderings of the diffusivities represent physically realistic cases, the other cases being only of mathematical interest.

In this paper, several such limiting cases are investigated and approximate solutions that are uniformly valid to order unity are sought. In general, 'singular perturbation' or 'boundary-layer type' problems are encountered and they are investigated by studying the limiting forms of the integral curves in phase space. The conditions for the appearance and location of the boundary layers and the boundary-layer equations to first order are determined.

A discussion of the validity of some of the main assumptions and of the necessary (but not sufficient) conditions for the existence of a switch-on shock has been given by Bleviss (1959) and is not repeated here. The sufficiency conditions, which must depend upon the boundary conditions, are not known and will not be discussed, but a paper by Cole (1959) sheds some light on this subject.

2. Discussion of equations of motion

The steady, plane, continuum flow of a compressible, viscous, heat conducting, electrically conducting, electrically neutral, perfect gas is considered. The electrical conductivity is assumed to be a scalar. The equations of motion for the

switch-on shock will not be derived here since they have already been given by Bleviss (1959), or can be readily deduced from a convenient form of the general equations of steady magnetohydrodynamics as given by Bleviss (1958). A system of four first-order non-linear ordinary differential equations in the four dependent variables B, w, u and T is obtained by eliminating the variables p, ρ and h through the use of the continuity equation $\rho u = m =$ constant and the perfect gas relations $p = \rho RT$ and $h = C_p T$, where B is the magnetic field component parallel to the shock, w and u are the velocity components parallel and normal, respectively, and h is specific enthalpy. It is readily deduced from the general equations that the x-component of the magnetic field is a constant (denoted here by B_0) and that the electric field is zero.

Using the notation and co-ordinate system shown in figure 1 and the rationalized M.K.S.Q. system of units, the equations of motion can be written in the following convenient form:

$$\lambda \frac{dB}{dx} = uB - wB_0 = (u-u_2)B + (B-B_2)u_2 - (w-w_2)B_0 = J(B,w,u), \quad (1a)$$

$$\eta \frac{dw}{dx} = mw - \frac{BB_0}{\mu} = m(w-w_2) - (B-B_2)\frac{B_0}{\mu} = L(B,w), \quad (1b)$$

$$\eta'' u \frac{du}{dx} = mR(T-T_2) + m\left(u - \frac{RT_2}{u_2}\right)(u-u_2) + \frac{B^2-B_2^2}{2\mu}u = M(B,u,T), \quad (1c)$$

$$k\frac{dT}{dx} = mC_v(T-T_2) + \frac{mRT_2}{u_2}(u-u_2) - \frac{m}{2}(u-u_2)^2 - \frac{m}{2}(w-w_2)^2 - \frac{B^2-B_2^2}{2\mu}u + \frac{B_0}{\mu}(B-B_2)w = N(B,w,u,T). \quad (1d)$$

The coefficients describing physical properties of the fluid are shear coefficient of viscosity η, longitudinal coefficient of viscosity η'', coefficient of thermal conduction k, magnetic permeability μ, electrical conductivity σ, magnetic diffusivity $\lambda = 1/\mu\sigma$, and specific heat at constant volume C_v. Equation (1*a*) is a combination of Ohm's law and Maxwell's current equation; (1*b*) is the once-integrated tangential momentum equation with the constant of integration equal to zero since $w = B = 0$ at 1 (the uniform flow region upstream of the shock, i.e. $x = -\infty$). Equations (1*c*) and (1*d*) are the longitudinal momentum and the energy equations, respectively, integrated once and with constants of integration evaluated at 2, the uniform flow region downstream of the shock ($x = +\infty$). It should be noted that it has been implicitly assumed in these equations (and in the shock relations) that the current is free to flow in closed circles. Thus, the present one-dimensional problem must be viewed as an approximation to an axisymmetrical problem at a large distance from the axis of symmetry.

To avoid unnecessary complications in notation and equations, system (1) will be retained throughout this paper in its dimensional form, as written above. In addition, it is convenient to refer to all of the parameters λ, η, η'', and k as diffusivities in the various order-of-magnitude statements, even though the actual diffusivities are λ, η/ρ, η''/ρ, and $k/\rho C_p$. Thus, $\eta, \eta'', k \ll \lambda$ should be interpreted as an order-of-magnitude statement about the corresponding diffusivities.

The switch-on shock relations are obtained by setting the left-hand side of system (1) equal to zero at 1 and/or 2. The following simple shock relations obtained from (1*a*) and (1*b*) are listed here for future reference:

$$u_2 B_2 = w_2 B_0, \tag{2a}$$

$$mw_2 = \frac{B_0 B_2}{\mu}, \tag{2b}$$

$$u_2 = \frac{B_0^2}{\mu m}, \tag{2c}$$

$$w_2^2 = \frac{B_2^2}{\mu \rho_2} \equiv b_2^2. \tag{2d}$$

Equations (2*a*) and (2*b*) were used to obtain the second forms of the right-hand sides of (1*a*) and (1*b*).

Solutions of system (1) may be represented as integral curves between the singularities at 1 and 2 in the (B, w, u, T) phase space with x as a parameter along the curves. In general, this system of equations must be solved numerically using methods similar to those of Gilbarg & Paolucci (1953) and Marshall (1956).

When order-of-magnitude differences occur among the diffusivities, the system of equations and, hence, the solution can be approximated to by allowing the appropriate diffusivities to approach zero. Such limiting cases are simpler and many of them can be solved analytically. For example, if $\eta, \eta'', k \ll \lambda$ one can set the left-hand sides of (1*b*), (1*c*) and (1*d*) equal to zero (i.e. $\eta = \eta'' = k = 0$) and the resulting system of equations is readily solved analytically, the approximate solution being uniformly valid to order unity for a certain range of conditions. Of the many possible order-of-magnitude orderings of the four diffusivities, a few represent physically realistic cases, the others being primarily of mathematical interest for the system (1). In general, 'singular perturbation' or 'boundary-layer type' problems arise in such limiting cases, these problems being heralded by double-valued shock profiles.

The limiting cases corresponding to several order-of-magnitude orderings will be investigated in detail in this paper. Approximate solutions that are uniformly valid to first order will be sought. A very convenient non-standard method for handling the singular perturbation problems for any limiting case will be presented. The method is based upon a study of the limiting forms of the integral curves in the phase space.

Order-of-magnitude orderings that correspond to physically realistic possibilities will now be discussed. Within the assumptions of this paper, the diffusivities η and η'' should be of the same order of magnitude.† A natural ordering arises in highly ionized gases because the Prandtl number becomes small, i.e. $\eta, \eta'' \ll k$. The magnetic diffusivity will be large compared with the others over a large range of hypersonic flow conditions. This leads to the physically realistic cases $\eta, \eta'', k \ll \lambda$ and $\eta, \eta'' \ll k \ll \lambda$. At high enough temperatures, λ can be of the

† If the gas were highly ionized, the density were low enough, and the magnetic field were strong enough, η and η'' could differ considerably but, under such conditions, k and σ would have to be tensors.

same order or much less than the other diffusivities. This leads to the possibilities $\eta, \eta'' \ll k, \lambda$; $\eta, \eta'' \ll \lambda \ll k$; $\eta, \eta'', \lambda \ll k$; and $\lambda \ll \eta, \eta'' \ll k$.

It is useful to write out two reduced systems of equations obtained from system (1) by, first, setting $\eta = 0$ and eliminating w from the other equations and, secondly, setting $\lambda = 0$ and eliminating B from the other equations. The notation $\eta = 0$ (or $\lambda = 0$) is just a convenient way of making the mathematical statement that the left-hand side of (1*b*) [or (1*a*)] is set equal to zero. For $\eta = 0$, the reduced system is

$$\lambda \frac{dB}{dx} = (u - u_2)\, B, \tag{3a}$$

$$\eta'' u \frac{du}{dx} = mR(T - T_2) + m\left(u - \frac{RT_2}{u_2}\right)(u - u_2) + \frac{B^2 - B_2^2}{2\mu} u, \tag{3b}$$

$$k \frac{dT}{dx} = mC_v(T - T_2) - (u - u_2)\left[\frac{B^2 - B_2^2}{2\mu} + \frac{m}{2}(u - u_2) - \frac{mRT_2}{u_2}\right], \tag{3c}$$

with w given by

$$w = u_2 \frac{B}{B_0}. \tag{3d}$$

For $\lambda = 0$, the reduced system is

$$\eta \frac{u}{m} \frac{dw}{dx} = (u - u_2)\, w, \tag{4a}$$

$$\eta'' \frac{u^2}{m} \frac{du}{dx} = R(T - T_2)\, u + u\left(u - \frac{RT_2}{u_2}\right)(u - u_2) + \frac{u_2}{2}\left(w^2 - \frac{u^2}{u_2^2} w_2^2\right), \tag{4b}$$

$$k \frac{u}{m} \frac{dT}{dx} = C_v(T - T_2)\, u - \frac{u - u_2}{2}\left[w^2 - \frac{u}{u_2} w_2^2 + u(u - u_2) - \frac{2RT_2 u}{u_2}\right], \tag{4c}$$

with B given by

$$B = \frac{w}{u} B_0. \tag{4d}$$

Equations (2) have been used to obtain these forms. The limiting integral curves in these three-dimensional phase spaces will be shown later. For the moment, these reduced systems are useful to illustrate in a simple way the occurrence of discontinuities or boundary layers.

To illustrate the difficulties encountered, consider the case $\eta, \lambda \ll \eta'', k$. The standard procedure for obtaining the lowest order or first approximation is to set $\eta = \lambda = 0$ in system (1) and study the consequences. This also corresponds to setting $\lambda = 0$ in system (3) or $\eta = 0$ in (4). Consider system (3). When $\lambda = 0$, at least one of the quantities B and $u - u_2$ is zero. Since the boundary condition at 1 ($x = -\infty$) is $B = B_1 = 0$ (i.e. no tangential component of magnetic field), the integral curve from 1 to 2 must leave 1 in the plane $B = 0$ and must lie in that plane until $u = u_2$ and then the curve must lie in the plane $u = u_2$ until 2 ($x = +\infty$) is reached, unless difficulties arise. Equations (3*b*) and (3*c*) with $B = 0$ are the equations for a hydrodynamic shock between the upstream end-point 1 and a downstream end-point 3 that is different from 2 (it can be shown that $T_3 \geqslant T_2$ and $u_3 \leqslant u_2$). Hence, the integral curve leaves 1 along *some* integral curve of a hydro-

dynamic shock. In the plane $u = u_2$, the integral curve would have to satisfy the equations [(3*b*) and (3*c*) with $u = u_2$]

$$mR(T - T_2) + \frac{B^2 - B_2^2}{2\mu} u_2 = 0,$$

$$k\frac{dT}{dx} = mC_v(T - T_2).$$

The second equation shows that T reaches its downstream value T_2 at $x = -\infty$. Since the upstream value T_1 also occurs at $x = -\infty$, this would mean that the temperature profile is double valued. The other quantities of interest will also exhibit double-valued profiles [cf. figure *D* 5*d* in Hayes (1958) and figure 4 in Bleviss (1959)]. In order to recover single-valued profiles and satisfy the boundary conditions at $x = +\infty$ one needs to insert a discontinuity for $\eta = \lambda = 0$. To obtain a uniformly valid approximation for η and λ near zero this discontinuity must be replaced by a thin transition layer (referred to hereinafter as a boundary layer).

Once it has been determined that a discontinuity or boundary layer is necessary, a standard method can be followed for determining the location of the boundary layer and the first-order approximate equations that determine its structure. Roughly and briefly, the method is as follows. One assumes a location for the boundary layer and writes the variables in appropriate form relative to this location. Then one divides each of the variables, dependent and independent, by a different unknown scale factor, each factor being the parameter that goes to zero to some, as yet undetermined, positive exponent. A scale factor describes how the corresponding variable behaves in the boundary layer as the parameter goes to zero. Therefore, the variable divided by the scale factor is an $O(1)$ quantity in the boundary layer. One then substitutes these $O(1)$ variables into the full set of equations, makes assumptions about the exponents, obtains reduced sets of equations to first order as the parameter goes to zero, and sees if any of the solutions to these sets of equations is sensible and consistent with the boundary conditions for the discontinuity. If proper equations cannot be found a different location is assumed and the procedure is repeated. In the process, both the equations and the scale factors are determined. If, as in the present case, there are several variables, it is clear that the method can be tedious. Often, the procedure can be considerably shortened by judicious guessing as to the location of the boundary layer and which terms in the equations should be retained.

In the present problem there is a much more convenient and direct method for determining the boundary-layer equations. It turns out that the discontinuity or boundary layer is always located at the downstream side of the switch-on shock. This result was assumed from previous experience and then proved by its success in all cases studied. This is the reason why all of the equations have been written in terms of the end-point 2. By studying the behaviour of the integral curves in the neighbourhood of 2 and requiring that these curves approach 2 as $x \to +\infty$, the conditions for the appearance of the boundary layers, the scale factors, and, hence, the boundary-layer equations to first order are readily determined. With this information, the remaining portions of the integral curves are easily deduced.

3. Behaviour of the intergral curve near 2

Following the usual procedure for studying the behaviour of the integral curve in the neighbourhood of a point, the system (1) is linearized near 2 by writing $B = B_2 + \Delta B$, etc., and dropping higher-order terms. The solution of this system is assumed to be of the form

$$B - B_2 \equiv \Delta B = Ce^{\kappa x},$$
$$w - w_2 \equiv \Delta w = C' e^{\kappa x},$$
$$\text{etc.}$$

A solution is possible only if κ satisfies the quartic

$$[L_B J_w - (J_B - \lambda\kappa)(L_w - \eta\kappa)][(N_T - k\kappa)(M_u - \eta'' u_2 \kappa) - N_u M_T] + J_u M_B (N_T - k\kappa)(L_w - \eta\kappa) = 0, \quad (5)$$

where

$$\left.\begin{aligned} &J_B = \left(\frac{\partial J}{\partial B}\right)_2 = u_2, && J_w = -B_0, && J_u = B_2, && J_T = 0; \\ &L_B = \left(\frac{\partial L}{\partial B}\right)_2 = -\frac{B_0}{\mu}, && L_w = m, && L_u = 0, && L_T = 0; \\ &M_B = \frac{u_2 B_2}{\mu}, && M_w = 0, && M_u = \frac{m}{u_2}\left(u_2^2 - \frac{a_2^2}{\gamma}\right), && M_T = mR; \\ &N_B = \frac{B_0 w_2}{\mu} - \frac{u_2 B_2}{\mu} = 0, && N_w = 0, && N_u = \frac{m a_2^2}{\gamma u_2}, && N_T = mC_v. \end{aligned}\right\} \quad (6)$$

Other relations of interest are

$$\left.\begin{aligned} &L_B J_w - J_B L_w = \frac{B_0^2}{\mu} - m u_2 = 0, \\ &N_T M_u - N_u M_T = \frac{m^2 C_v}{u_2}(u_2^2 - a_2^2), \\ &J_B(N_T M_u - N_u M_T) - J_u M_B N_T = m^2 C_v (u_2^2 - a_2^2 - b_2^2), \\ &J_B M_u - J_u M_B = m\left(u_2^2 - \frac{a_2^2}{\gamma} - b_2^2\right). \end{aligned}\right\} \quad (7)$$

In these equations γ is the ratio of heats, a_2 is the hydrodynamic sound speed downstream of the shock, and b_2, defined in (2*d*), is a magnetohydrodynamic sound speed downstream of the shock. It is important to note that all of the quantities (6) have fixed sign except M_u and that the last three quantities (7) can also change sign.

The slope of the integral curve at 2 is then given by

$$\left.\begin{aligned} &\frac{T - T_2}{u - u_2} = \frac{\Delta T}{\Delta u} = \frac{N_u}{k\kappa - N_T}, \quad \frac{B - B_2}{w - w_2} = \frac{\Delta B}{\Delta w} = \frac{\eta\kappa - L_w}{L_B}, \\ &\frac{\Delta w}{\Delta u} = \frac{L_B J_u}{(J_B - \lambda\kappa)(L_w - \eta\kappa) - L_B J_w}, \\ &\frac{\Delta B}{\Delta u} = \frac{J_u(L_w - \eta\kappa)}{L_B J_w - (J_B - \lambda\kappa)(L_w - \eta\kappa)} = \frac{M_T N_u - (N_T - k\kappa)(M_u - \eta'' u_2 \kappa)}{M_B(N_T - k\kappa)}. \end{aligned}\right\} \quad (8)$$

κ is required to be negative in order that $x \to +\infty$ as point 2 is approached. (It is easy to show that the integral curves leave 1 at $x = -\infty$.) In the limiting cases to be studied, this requirement on κ indicates immediately the conditions for the existence of a boundary layer. Furthermore, the form of κ together with (8) indicates the scale factors for the various quantities.

In the previous section, where the case $\eta, \lambda \ll \eta'', k$ was briefly considered, it was found that if η and λ were simultaneously set equal to zero a discontinuity must occur. This conclusion is readily checked here by setting $\eta = \lambda = 0$ in (5). Using the first equation of (7), the result is $\kappa \doteq N_T/k = mC_v/k$. Since κ is positive the integral curve will not approach 2 as $x \to +\infty$ and a discontinuity must be inserted.

4. Solutions for some limiting cases

The simplified equations for several limiting cases will now be derived. In nearly all cases the solution of these equations involves simple quadrature and the solutions are not carried out explicitly since their general nature is clear.

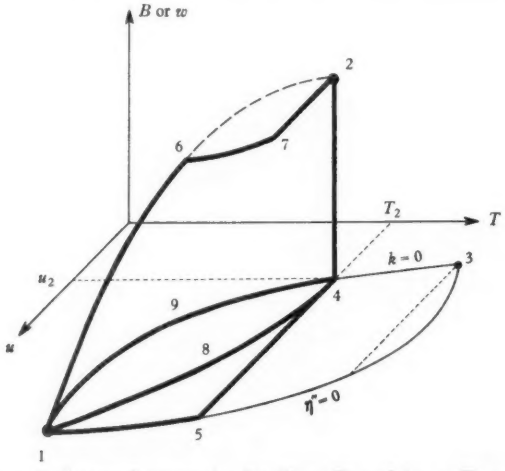

FIGURE 2. Integral curves in the (B, u, T) and (w, u, T) spaces.

The integral curves for many of these limiting cases are readily sketched in one or the other of the three-dimensional phase spaces corresponding to the reduced systems (3) and (4). This will become clear when some limiting cases are actually considered. For the moment, it is useful to examine the surfaces in the (B, u, T) space obtained by setting λ, η'', and k equal to zero in system (3) and the surfaces in the (w, u, T) space obtained by setting η, η'', and k equal to zero in system (4). Because of the similarity between systems (3) and (4), the following discussion applies to either but, for discussion purposes, only the (B, u, T) space corresponding to system (3) will be considered.

Some of the features to be discussed now are shown in figures 2 and 3. Points 1 and 2 are the singular points corresponding to the initial and final conditions, respectively. From equation (3a) it is clear that the surface corresponding to

$\lambda = 0$ consists of the two planes $B = 0$ and $u = u_2$. The curves in the $B = 0$ plane labelled $\eta'' = 0$ (1–5–3) and $k = 0$ (1–4–3) are the intersections of the $B = 0$ plane with the $\eta'' = 0$ and $k = 0$ surfaces, respectively. These curves correspond to the so-called 'non-viscous' and 'non-conducting' curves in hydrodynamic shock theory [see, for example, figure $D\,5a$ in Hayes (1958)]; points 1 and 3 are the initial and final end-points, respectively, for a hydrodynamic shock. The intersection of the $\eta'' = 0$ and $k = 0$ surfaces is shown schematically as the dashed curve

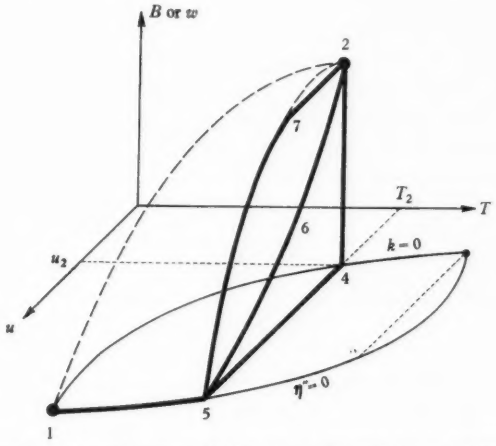

FIGURE 3. Integral curves in the (B, u, T) and (w, u, T) spaces.

from 1 to 2 in figure 3 (1–6–2 in figure 2). There is, of course, a continuation of this curve from 2 to 3. An important property of the $k = 0$ surface that should be noted is that the straight line $u = u_2$, $T = T_2$ (4–2) lies in this surface; only B and w vary along this line. These surfaces play important roles in many of the limiting cases to be studied.

(A) $\eta, \eta'', k \ll \lambda$ (*low electrical conductivity*)

Although this limiting case was treated in detail by Bleviss (1959), it is repeated here to illustrate the present method. Setting $\eta = \eta'' = k = 0$ in (5), the result for κ is

$$\kappa \doteqdot -\frac{J_u M_B N_T}{\lambda(N_T M_u - N_u M_T)} = -\frac{b_2^2 u_2}{\lambda(u_2^2 - a_2^2)} = O\left(\frac{1}{\lambda}\right), \tag{9}$$

where (2*d*) and the first two equations of (7) have been used. Since κ is negative only when $u_2 > a_2$, the procedure of setting $\eta = \eta'' = k = 0$ leads to a uniformly valid limiting solution only when $u_2 > a_2$.

The above equation will now be used to illustrate several additional important conclusions that can always be drawn from the result for κ. The dissipation mechanism is always clear from the diffusivity contained in the result. In the present case λ is the diffusivity and Joule heating is the dissipation mechanism. Since the thickness of a one-dimensional shock wave is always proportional to the diffusivities involved, the scale factor for x is immediately apparent. Note that

this is consistent with the fact that κ has the dimensions of reciprocal length and is always essentially proportional to the reciprocal of a diffusivity.

Using the fact that $\kappa = O(1/\lambda)$, the following conclusions can be drawn from (8)

$$\left.\begin{aligned} &\frac{T-T_2}{u-u_2} = \frac{\Delta T}{\Delta u} = O(1), \quad \frac{\Delta w}{\Delta u} = O(1), \\ &\frac{\Delta B}{\Delta w} = O(1), \qquad\qquad \frac{\Delta B}{\Delta u} = O(1). \end{aligned}\right\} \tag{10}$$

With ΔB, Δw, Δu and ΔT all $O(1)$ and with the x-range over which these variables change appreciably (i.e. the shock thickness) also $O(1)$ since $\lambda = O(1)$, the approximate equations for this limiting case are obtained from (1) by simply setting $\eta = \eta'' = k = 0$. This corresponds to setting $\eta'' = k = 0$ in (3). This simplified system of equations can be reduced to a single first-order ordinary differential equation that is readily solved.

The integral curve in the (B, u, T) space is the curve 1–6–2 (figure 2), i.e. the intersection of the $\eta'' = 0$ and $k = 0$ surfaces. The requirement $u_2 > a_2$ restricts the results to those curves for which B increases monotonically, i.e. curves for which B is single-valued between 1 and 2.

$u_2 < a_2$

When $u_2 < a_2$, κ cannot vary as $1/\lambda$ but must instead be a function of one or more of the diffusivities η, η'' and k. This means that the solution obtained by setting $\eta = \eta'' = k = 0$ must be discontinuously adjusted through a boundary layer to the final conditions at 2. The nature and location of this boundary layer will now be determined.

Using the fact that $\lambda\kappa \gg 1$, (5) reduces to

$$(L_w - \eta\kappa)\,[(N_T - k\kappa)\,(M_u - \eta'' u_2 \kappa) - N_u M_T] \doteq 0.$$

The first factor cannot be zero since then κ would not be negative. Therefore, κ is given by the quadratic equation

$$(N_T - k\kappa)\,(M_u - \eta'' u_2 \kappa) - N_u M_T \doteq 0. \tag{11}$$

With $N_T M_u - N_u M_T < 0$, this equation yields negative values for κ. Note that since η is not contained in the result for κ the dissipation in this boundary layer must be due to viscosity (η'') and heat conduction (k) only, just as in the case of the hydrodynamic shock. Then the essential results for this boundary layer will be independent of how η is related to η'' and k. Some minor results are affected by this relationship and, to avoid writing out all the cases, the realistic assumption $\eta = O(\eta'')$ is made.

Assuming η'' and k to be of the same order and writing $k = \alpha\eta''$ [with $\alpha = O(1)$] in (11), it is clear that $\kappa = O(1/\eta'')$. Using this result, (8) becomes

$$\left.\begin{aligned} &\frac{\Delta T}{\Delta u} = O(1), \quad \frac{\Delta w}{\Delta u} = O\left(\frac{\eta''}{\lambda}\right), \\ &\frac{\Delta B}{\Delta w} = O(1), \quad \frac{\Delta B}{\Delta u} = O\left(\frac{\eta''}{\lambda}\right). \end{aligned}\right\} \tag{12}$$

This shows that to first order w and B are constant through this boundary layer, having their downstream values w_2 and B_2.

With the scale factors known from the result for κ and (12), the following $O(1)$ quantities for this boundary layer can now be defined

$$T^* = T - T_2 = \Delta T, \quad u^* = u - u_2 = \Delta u, \quad w^* = \frac{\lambda}{\eta''}\Delta w, \quad B^* = \frac{\lambda}{\eta''}\Delta B, \quad x^* = \frac{x}{\eta''}.$$

Subsituting these new variables into (1) and carrying only the largest terms in each equation, the first-order equations for the boundary layer are

$$\frac{dB^*}{dx^*} = u^* B_2, \tag{13a}$$

$$\frac{dw^*}{dx^*} = mw^* - \frac{B_0 B^*}{\mu}, \tag{13b}$$

$$u\frac{du^*}{dx^*} = mRT^* + m\left(u - \frac{RT_2}{u_2}\right)u^*, \tag{13c}$$

$$\alpha\frac{dT^*}{dx^*} = mC_v T^* + \frac{mRT_2}{u_2}u^* - \frac{m}{2}u^{*2}. \tag{13d}$$

Note that (13c) and (13d) can be obtained from (1c) and (1d) by setting $w = w_2$ and $B = B_2$. Then (13c) and (13d) are the equations for a hydrodynamic shock and must be solved simultaneously for $u^*(x^*)$ and $T^*(x^*)$. Knowing $u^*(x^*)$, $B^*(x^*)$ can be obtained from (13a) and then $w^*(x^*)$ can be obtained from (13b). With $B^*(x^*)$ a known function, it is easy to show that the solution of (13b) is

$$mw^* = \frac{B_0 B^*}{\mu}. \tag{13b'}$$

(13a) and (13b') arise because $B^*(x^*)$ and $w^*(x^*)$ have slope discontinuities across the boundary layer.

The x position of the boundary layer is determined by the criterion already discussed by Bleviss (1959). Briefly, this can be described by examination of the typical shock profiles $u(x)$ and $B(x)$ shown in figure 4. The curves *abcd* are the profiles obtained by setting $\eta = \eta'' = k = 0$ in (1). The boundary layer occurs at b, where $B = B_2$, and the solid curves show the correct single-valued profiles.

The integral curve in the (B, u, T) space is indicated in figure 2. The curve 1–6–2 intersects the plane $B = B_2$ at 6 and at 2. The correct integral curve is then the solid curve from 1 to 6 followed by a curve from 6 to 2 that lies in the plane $B = B_2$. The portion of the curve from 6 to 2 is the integral curve for a hydrodynamic shock between 6 and 2 and the properties of this curve are well known. Note that x is constant along the curve from 6 to 2. The solid curve 6–7–2 corresponds to the special case treated below.

(B) $\eta, \eta'' \ll k \ll \lambda$

This is a special case of (A) in which $\eta = O(\eta'')$ but the Prandtl number is small. It is clear that the foregoing results are altered only for the case $u_2 < a_2$ and that only the portion of the integral curve from 6 to 2 is affected. Since this is a hydrodynamic shock for zero Prandtl number the results are well known.

Assuming $\kappa = O(1/k)$ and using the fact that $\eta''\kappa \ll 1$, (11) reduces to

$$\kappa \doteq \frac{N_T M_u - N_u M_T}{k M_u} = \frac{mC_v(u_2^2 - a_2^2)}{k(u_2^2 - a_2^2/\gamma)}. \tag{14}$$

This is negative for $a_2^2/\gamma < u_2^2 < a_2^2$. For this case it is easily shown that the resulting equations for u and T are those for a hydrodynamic shock with $\eta'' = 0$, i.e.

$$R(T - T_2) + \left(u - \frac{RT_2}{u_2}\right)(u - u_2) = 0, \tag{15a}$$

$$k\frac{dT}{dx} = mC_v(T - T_2) + \frac{mRT_2}{u_2}(u - u_2) - \frac{m}{2}(u - u_2)^2. \tag{15b}$$

In figure 2 the integral curve from 6 to 2 is the intersection of the plane $B = B_2$ with the surface $\eta'' = 0$. The condition $a_2^2/\gamma < u_2^2 < a_2^2$ restricts this case to those curves for which T increases monotonically from 6 to 2. Then, along the integral curve the dissipation mechanisms are Joule heating between 1 and 6 and heat conduction between 6 and 2. The case shown in figure 2 is discussed below.

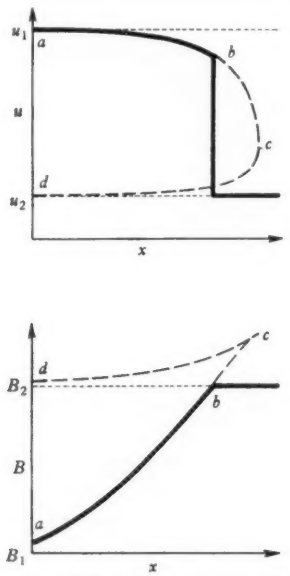

FIGURE 4. Shock profiles $u(x)$ and $B(x)$ and location of boundary layer for $u_2 < a_2$.

$u_2^2 < a_2^2/\gamma$

To obtain a negative value for κ, it is necessary to take $\kappa = O(1/\eta'')$ in (11). The result is

$$\kappa \doteq \frac{M_u}{\eta'' u_2} = \frac{m(u_2^2 - a_2^2/\gamma)}{\eta'' u_2^2}. \tag{16}$$

There is now a second boundary layer within the first that discontinuously adjusts the solution for the first boundary layer to the final conditions at 2. This case

corresponds to that described by Bleviss (1959) as a 'shock within a shock within a shock'. Using (8), the slope of the integral curve at 2 is given by

$$\left.\begin{aligned} \frac{\Delta T}{\Delta u} &= O\left(\frac{\eta''}{k}\right), \quad \frac{\Delta w}{\Delta u} = O\left(\frac{\eta''}{\lambda}\right), \\ \frac{\Delta B}{\Delta w} &= O(1), \qquad \frac{\Delta B}{\Delta u} = O\left(\frac{\eta''}{\lambda}\right), \end{aligned}\right\} \tag{17}$$

For this second boundary layer only u changes, the other quantities being constant at their final values. Defining the $O(1)$ quantities

$$u^* = \Delta u, \quad T^* = \frac{k}{\eta''}\Delta T, \quad w^* = \frac{\lambda}{\eta''}\Delta w, \quad B^* = \frac{\lambda}{\eta''}\Delta B, \quad x^* = \frac{x}{\eta''},$$

the equations for the second boundary layer are

$$\frac{dB^*}{dx^*} = u^* B_2, \tag{18a}$$

$$\frac{dw^*}{dx^*} = mw^* - \frac{B_0 B^*}{\mu}, \tag{18b}$$

$$u\frac{du^*}{dx^*} = m\left(u - \frac{RT_2}{u_2}\right)u^*, \tag{18c}$$

$$\frac{dT^*}{dx^*} = \frac{mRT_2}{u_2}u^* - \frac{m}{2}u^{*2}, \tag{18d}$$

where (18*b*) simplifies in the same way as (13*b*). u is the only quantity that is varying and it is determined by (18*c*), which is readily solved. (18*c*) is obtained from (1*c*) by setting $T = T_2$ and $B = B_2$. The integral curve is shown in figure 2 as 1–6–7–2. The curve from 6 to 7 is the same as that discussed just above but in this case the curve does not increase monotonically to 2; it intersects the plane $T = T_2$ at 7. The portion of the curve from 7 to 2 is parallel to the u-axis. Along the integral curve the dissipation mechanisms are Joule heating between 1 and 6, heat conduction between 6 and 7, and viscosity (η'') between 7 and 2.

(C) $\lambda \ll \eta'' \ll k \ll \eta$ (*high electrical conductivity*)

When λ is much less than the other diffusivities the case will be referred to as one of high electrical conductivity. This case is essentially case (B) with η and λ interchanged, and it is being presented to show the similarities of and the differences between the two cases. Only the main results will be given. It will be found that there are comparable integral curves in the (B, u, T) and (w, u, T) spaces for the two cases, but that the conditions for the appearances of the boundary layers and the equations governing the shock structure are quite different.

$u_2^2 > a_2^2 + b_2^2$

When $u_2^2 > a_2^2 + b_2^2$, $\kappa = O(1/\eta)$ and the governing equations are obtained from (1) by setting $\lambda = \eta'' = k = 0$. The integral curve in the (w, u, T) space is 1–6–2 in figure 2 with w increasing monotonically from 1 to 2. The dissipation is due to viscosity (η).

$a_2^2/\gamma + b_2^2 < u_2^2 < a_2^2 + b_2^2$

When $u_2^2 < a_2^2 + b_2^2$ a boundary layer arises regardless of the relative magnitudes of λ, η'' and k. This boundary layer is not a hydrodynamic shock but is, instead, the parallel shock studied by Marshall, i.e. a shock through which the flow is not turned but the magnetic field parallel to the shock front varies. For this shock, B_0 does not interact with the flowing gas. The integral curve goes from 1 to 6 and then from 6 to 2 in the plane $w = w_2$. Note that B varies from 6 to 2.

With $\eta'' \ll k$, a single boundary layer arises if $a_2^2/\gamma + b_2^2 < u_2^2$. The integral curve from 6 to 2 is the intersection of the $w = w_2$ plane and the $\eta'' = 0$ surface with T increasing monotonically. The dissipation mechanism is heat conduction. The equations governing the changes in B, u and T are (1a), (1c) and (1d) with $\lambda = \eta'' = 0$ and $w = w_2$.

$u_2^2 < a_2^2/\gamma + b_2^2$

A second boundary layer now arises in which the dissipation is due to viscosity (η'') and through which $T = T_2$. The integral curve is 1–6–7–2. The equations for B and u are (1a) and (1c) with $\lambda = 0$, $w = w_2$ and $T = T_2$.

(D) $\eta \ll \lambda \ll \eta'', k$

Although unrealistic, all cases where η and λ are small compared with the other diffusivities have a number of interesting features. Since η and λ cannot be simultaneously set equal to zero, this case will always involve at least one boundary layer. As previously discussed, the integral curve leaves 1 in the plane $B = 0$ along *some* integral curve for the hydrodynamic shock and this part of the integral curve must terminate in the $u = u_2$ plane. The exact terminus is determined by a study of the boundary layer which adjusts the solution to the conditions at 2.

If η is set equal to zero and it is assumed that $\kappa = O(1/\lambda)$ in (5), a negative result cannot be obtained for κ. However, if $\eta = 0$ and it is assumed only that κ contains λ in such a way that $\eta''\kappa \gg 1$, (5) reduces to

$$(N_T - k\kappa)(u_2\lambda\eta''\kappa^2 - J_u M_B) \doteq 0.$$

Only the second parenthesis leads to $\kappa < 0$, with the result

$$\kappa \doteq -\sqrt{\frac{J_u M_B}{\lambda\eta'' u_2}} = -\frac{B_2}{\sqrt{\lambda\eta''\mu}}. \tag{19}$$

This result is independent of the order of magnitude of $k\kappa$ and of the relative orders of magnitude of k and η''. Note that $k\kappa$ can be $\ll 1$, $O(1)$, or $\gg 1$ when $k \ll \eta''$ and that $k\kappa \gg 1$ when $k = O(\eta'')$ or $k \gg \eta''$. The essential results are the same for all of these cases and, to avoid writing them all out, it will be assumed that $k\kappa \gg 1$. Then, from (8),

$$\begin{aligned} &\frac{\Delta T}{\Delta u} = O\left(\frac{1}{k\kappa}\right) = O\left(\sqrt{\frac{\lambda\eta''}{k^2}}\right), \quad \frac{\Delta w}{\Delta u} = O\left(\frac{1}{\lambda\kappa}\right) = O\left(\sqrt{\frac{\eta''}{\lambda}}\right), \\ &\frac{\Delta B}{\Delta w} = O(1), \qquad\qquad \frac{\Delta T}{\Delta w} = O\left(\frac{\lambda}{k}\right). \end{aligned} \tag{20}$$

The integral curve in the (B, u, T) space (figure 2) is now clear. $u = u_2$ and $T = T_2$ through the boundary layer. Then this portion of the integral curve is 4–2, the intersection of the $u = u_2$ and $T = T_2$ planes, and only B (and w) varies along this portion. The portion of the integral curve that lies in the $B = 0$ plane must extend from 1 to 4. For $\eta'' = O(k)$, a typical integral curve is 1–8–4–2. The curve 1–8–4 is parallel to the u-axis at 4, i.e. $\partial T/\partial u = 0$.

The curve 1–8–4 is obtained by solving (1*c*) and (1*d*) with $w = B = 0$. When $k \ll \eta''$ the integral curve is 1–9–4–2 and the equations for 1–9–4 are the same as for 1–8–4 but with $k = 0$. When $\eta'' \ll k$ the integral curve is 1–5–4–2. Now, two boundary layers occur, the first from 5 to 4 and the second from 4 to 2. The equations for the portion 1–5 are (1*c*) and (1*d*) with $\eta'' = w = B = 0$. The equation for the portion 5–4 is (1*c*) with $T = T_2$ and $B = 0$.

The detailed characteristics of the boundary layer 4–2 will now be studied. The following $O(1)$ quantities are defined:

$$B^* = \Delta B, \quad w^* = \Delta w, \quad u^* = \sqrt{\frac{\eta''}{\lambda}}\,\Delta u, \quad T^* = \frac{k}{\lambda}\Delta T, \quad x^* = \frac{x}{\sqrt{(\lambda\eta'')}}. \tag{21}$$

The orders of magnitude of the time rate of energy dissipation per unit volume for the four dissipation mechanisms are

$$\eta''\left(\frac{du}{dx}\right)^2 = \frac{1}{\eta''}\left(\frac{du^*}{dx^*}\right)^2 = O\left(\frac{1}{\eta''}\right), \quad \frac{\lambda}{\mu}\left(\frac{dB}{dx}\right)^2 = O\left(\frac{1}{\eta''}\right),$$

$$\eta\left(\frac{dw}{dx}\right)^2 = O\left(\frac{\eta}{\lambda\eta''}\right), \quad \frac{k}{T}\left(\frac{dT}{dx}\right)^2 = O\left(\frac{\lambda}{k\eta''}\right).$$

This shows that the dissipation is due to Joule heating and viscosity (η'').

The order of magnitude of the entropy increase across the boundary layer can be obtained by integrating the time rate of entropy production per unit volume across the boundary layer

$$\int \frac{\eta''}{T}\left(\frac{du}{dx}\right)^2 dx = \int \sqrt{\frac{\lambda}{\eta''}}\left(\frac{du^*}{dx^*}\right)^2 \frac{dx^*}{T} = O\left(\sqrt{\frac{\lambda}{\eta''}}\right).$$

This means that there is no entropy increase across this boundary layer to first order! This result can also be derived from the fact that u and T and, hence, ρ and p are constant through the boundary layer.

Using (21), the system (1) reduces to

$$\frac{dB^*}{dx^*} = u^* B, \tag{22a}$$

$$mw^* - \frac{B_0 B^*}{\mu} = mw - \frac{B_0 B}{\mu} = 0, \tag{22b}$$

$$\frac{du^*}{dx^*} = \frac{B^2 - B_2^2}{2\mu}, \tag{22c}$$

$$\frac{dT^*}{dx^*} = u^*\left(\frac{mRT_2}{u_2} - \frac{B^2 - B_2^2}{2\mu}\right). \tag{22d}$$

Even though $u = u_2$, essentially, in the boundary layer, u is still coupled to B through the pair of equations (22a) and (22c). Once this pair of equations is solved for $u^*(x^*)$ and $B^*(x^*)$, $w^*(x^*)$ and $T^*(x^*)$ are obtained from (22b) and (22d).

The solution of (22a) and (22c) can be reduced to a single quadrature in the following way. It is convenient to work with the variable B^2 instead of B^*. Dividing one equation by the other and integrating leads to the result

$$u^* = \frac{1}{\sqrt{2\mu}} \sqrt{\left[B_2^2 \ln\left(\frac{B_2^2}{B^2}\right) + B^2 - B_2^2 \right]}.$$

If this is substituted into (22a), $B(x^*)$ is given implicitly by

$$x^* = \sqrt{\frac{\mu}{2}} \int \frac{dB^2}{B^2 \sqrt{\left[B_2^2 \ln\left(\frac{B_2^2}{B^2}\right) + B^2 - B_2^2 \right]}} + \text{const.},$$

where the constant determines the arbitrary origin of x^*.

If η and λ are interchanged the results are essentially the same, the roles of B and w being interchanged.

(E) $\lambda \ll \eta,\ \eta'' \ll k$

This is the physically realistic case of high electrical conductivity. Again, since λ and η cannot both be set equal to zero, a boundary layer will always occur. Then it is expected that κ will contain both η and η''.

Setting $\lambda = 0$ and letting $\eta\kappa = O(1)$, $\eta''\kappa = O(1)$, and $k\kappa \gg 1$, (5) reduces to

$$\eta\kappa J_B(M_u - \eta'' u_2 \kappa) + J_u M_B(L_w - \eta\kappa) \doteq 0. \tag{23}$$

This quadratic equation yields negative values for κ without further restrictions.

Writing $\eta'' = \alpha\eta$ [with $\alpha = O(1)$] in (23), it is clear that $\kappa = O(1/\eta)$. Then (8) becomes

$$\left.\begin{aligned} &\frac{\Delta T}{\Delta u} = O\left(\frac{1}{k\kappa}\right) = O\left(\frac{\eta}{k}\right), \quad && \frac{\Delta w}{\Delta u} = O(1), \\ &\frac{\Delta B}{\Delta w} = O(1), && \frac{\Delta B}{\Delta u} = O(1). \end{aligned}\right\} \tag{24}$$

The temperature is constant through this boundary layer at its final value T_2.

Carrying through the analysis, it is easy to show that the equations governing the variations of B, w and u are (1a), (1b) and (1c) with $\lambda = 0$ and $T = T_2$. Using system (4), the equations for w and u can be written

$$\eta \frac{u}{m} \frac{dw}{dx} = (u - u_2) w, \tag{25a}$$

$$\eta'' \frac{u^2}{m} \frac{du}{dx} = u\left(u - \frac{RT_2}{u_2}\right)(u - u_2) + \frac{u_2}{2}\left(w^2 - \frac{u^2}{u_2^2} w_2^2\right), \tag{25b}$$

with B given by

$$B = \frac{w}{u} B_0. \tag{25c}$$

From (25a) and (25b) it is readily deduced that the upstream and downstream end-points in the (w, u, T) space (figure 3) are 5 and 2, respectively. A typical

integral curve for this boundary layer is 5–6–2, where the curve lies in the $T = T_2$ plane. Since $\eta'' \ll k$, the portion of the integral curve from 1 to 5 lies along the intersection of the $w = 0$ plane and the $\eta'' = 0$ surface. Along the integral curve the dissipation mechanisms are heat conduction between 1 and 5 and viscosity (η and η'') between 5 and 2.

(F) $\lambda \ll \eta \ll \eta'' \ll k$

This is a subcase of (E) in which $\eta \ll \eta''$. Using (23) the result for κ is

$$\kappa \doteq -\sqrt{\frac{J_u M_B L_w}{\eta\eta'' u_2 J_B}} = -B_2\sqrt{\frac{m}{\eta\eta''\mu u_2}},$$

and it is clear that this is just case (D) with $\eta'' \ll k$ and η and λ interchanged. Then the integral curve in the (w, u, T) space of figure 3 is 1–5–4–2 with the dissipation due to heat conduction between 1 and 5, viscosity (η'') between 5 and 4, and viscosity (η and η'') between 4 and 2. As before, there is no entropy increase between 4 and 2.

(G) $\lambda \ll \eta'' \ll \eta \ll k$

This is a subcase of (E) in which $\eta'' \ll \eta$. Assuming $\kappa = O(1/\eta)$ and setting $\eta'' = 0$, (23) reduces to

$$\kappa \doteq -\frac{J_u M_B L_w}{\eta(J_B M_u - J_u M_B)} = -\frac{mb_2^2}{\eta(u_2^2 - a_2^2/\gamma - b_2^2)}. \tag{26}$$

This is negative for $u_2^2 > a_2^2/\gamma + b_2^2$. The equations for this case are given by the system (25) with $\eta'' = 0$. The integral curve is 1–5–7–2 following the dashed curve from 7 to 2. The portion 5–7–2 is the intersection of the $T = T_2$ plane and the $\eta'' = 0$ surface. The condition $u_2^2 > a_2^2/\gamma + b_2^2$ restricts the portion 5–7–2 to curves for which w increases monotonically from 5 to 2. The dissipation along 5–7–2 is due to viscosity (η).

$u_2^2 < a_2^2/\gamma + b_2^2$

Assuming $\kappa = O(1/\eta'')$, (23) reduces to

$$\kappa \doteq \frac{J_B M_u - J_u M_B}{\eta'' u_2 J_B} = \frac{m(u_2^2 - a_2^2/\gamma - b_2^2)}{\eta'' u_2^2}. \tag{27}$$

A second boundary layer is now obtained. The integral curve is the heavy curve 1–5–7–2, with 7–2 along the intersection of the $w = w_2$ and $T = T_2$ planes. The equation for u along the portion 7–2 is (25*b*) with $w = w_2$ and the dissipation is due to viscosity (η'').

(H) $\eta, \eta'' \ll \lambda \ll k$

This is a physically realistic case with intermediate electrical conductivity. It can be shown that this case is very similar to that of (G) but with η and λ interchanged. For $u_2^2 > a_2^2/\gamma$ the integral curve in the (B, u, T) space of figure 3 is again 1–5–7–2, following the dashed curve from 7 to 2. For $u_2^2 < a_2^2/\gamma$ the integral curve is the heavy curve 1–5–7–2 and the dissipation mechanisms are heat conduction between 1 and 5, Joule heating between 5 and 7, and viscosity (η'') between 7 and 2.

(I) $\eta'' \ll k \ll \lambda \ll \eta$

In all the cases that have been studied, there have been at most two boundary layers. With four diffusivity parameters, it would be expected that for some order-of-magnitude orderings there would be three boundary layers, the maximum number possible. The present physically unrealistic case is being presented to illustrate one such case. Only a brief summary of the results will be given.

$u_2^2 > a_2^2 + b_2^2$

The results here are the same as for case (C) when $u_2^2 > a_2^2 + b_2^2$.

$a_2^2 < u_2^2 < a_2^2 + b_2^2$

For this condition the first boundary layer occurs. w is constant and equal to w_2 through this boundary layer. A plot of $w(x)$, using the equations for $u_2^2 > a_2^2 + b_2^2$, would be similar to that shown for $B(x)$ in figure 4 and, similarly, the location of the boundary layer is determined by the condition $w = w_2$. The dissipation in this boundary layer is due to Joule heating and the equations governing the variations in B, u and T are (1*a*), (1*c*) and (1*d*) with $w = w_2$ and $k = \eta'' = 0$.

$a_2^2/\gamma < u_2^2 < a_2^2$

Now, a second boundary layer arises. In general, when $u_2 < a_2$ this boundary layer is simply a hydrodynamic shock, regardless of the relative magnitudes of η'' and k. With $\eta'' \ll k$, the condition $u_2^2 > a_2^2/\gamma$ guarantees that T increases monotonically through the boundary layer. $B = B_2$ (and $w = w_2$) through this boundary layer and the location of the second boundary layer within the first is determined by this condition. The dissipation is due to heat conduction and the equations for u and T are obtained from (1*c*) and (1*d*) by setting $w = w_2$, $B = B_2$ and $\eta'' = 0$.

$u_2^2 < a_2^2/\gamma$

For this condition, a third boundary layer occurs. Only the velocity u varies through this boundary layer and the dissipation is due to viscosity (η''). The equation for u is (1*c*) with $B = B_2$ and $T = T_2$.

(J) $\eta, \eta'' \ll k, \lambda$

This case and the following one complete the list of physically realistic cases given in § 2. The results will be summarized very briefly.

The integral curve in the (B, u, T) space is a curve between 1 and 2 that lies in the $\eta'' = 0$ surface and is bracketed by the curves 1–6–2 (figure 2) and 1–5–7–2 (figure 3). This case reduces to (B) when $k \ll \lambda$ and reduces to (H) when $\lambda \ll k$. The system of equations for this case is (1) with $\eta = \eta'' = 0$ or the reduced system (3) with $\eta'' = 0$. The conditions for the appearance of boundary layers are more complicated than for cases (B) and (H) and will depend upon the relative magnitudes of k and λ. These conditions are determined from the quadratic equation for κ obtained by setting $\eta = \eta'' = 0$ in (5).

(K) $\lambda, \eta, \eta'' \ll k$

Since λ and η cannot be set equal to zero simultaneously, a boundary layer must occur. Upstream of the boundary layer the integral curve is 1–5 in either the (B, u, T) or (w, u, T) space. This curve is a portion of an integral curve for a hydrodynamic shock and the equations that govern the variations of u and T along this curve are (1*c*) and (1*d*) with $\eta'' = w = B = 0$, the dissipation mechanism being heat conduction. The boundary layer occurs between 5 and 2, the temperature being constant at its final value T_2. The integral curve for the boundary layer cannot be sketched in the (B, u, T) or (w, u, T) space since λ and η are of the same order of magnitude. The equations that govern the variations of B, w and u through the boundary layer are (1*a*), (1*b*) and (1*c*) with $T = T_2$.

The author would like to express his deep appreciation to Prof. H. W. Liepmann, of the California Institute of Technology, for his continual interest and encouragement and for many stimulating and helpful discussions. Thanks are also due to Prof. J. D. Cole and P. A. Lagerstrom for several clarifying discussions.

REFERENCES

Bleviss, Z. O. 1958 Magnetogasdynamics of hypersonic Couette flow. *J. Aero./Space Sci.* **25**, 601–15.

Bleviss, Z. O. 1959 The structure of a steady magnetohydrodynamic switch-on shock wave. 1959 *Heat Transfer and Fluid Mechanics Institute Preprint of Papers.*

Burgers, J. M. 1957 Penetration of a shock wave into a magnetic field. *Magnetohydrodynamics* (ed. R. K. M. Landshoff), pp. 36–56. Stanford University Press.

Cole, J. D. 1959 Magnetohydrodynamic waves. *AFOSR-TN-59-13.*

Friedrichs, K. O. 1957 Nonlinear wave motion in magnetohydrodynamics. *Los Alamos Rep.* no. 2105.

Gilbarg, D. & Paolucci, D. 1953 The structure of shock waves in the continuum theory of fluids. *J. Rat. Mech. Anal.* **2**, 617–42.

Hayes, W. D. 1958 The basic theory of gasdynamic discontinuities. *High Speed Aerodynamics and Jet Propulsion*, Vol. III (ed. H. W. Emmons), pp. 416–81. Princeton University Press.

Ludford, G. S. S. 1959 The structure of a hydromagnetic shock in steady plane motion. *J. Fluid Mech.* **5**, 67–80.

Marshall, W. 1956 The structure of magneto-hydrodynamic shock waves. *Proc. Roy. Soc.* A, **233**, 367–76.

Whitham, G. B. 1959 Some comments on wave propagation and shock wave structure with application to magnetohydrodynamics. *Comm. Pure Appl. Math.* **12**, 113–58.

A transformation for non-homentropic flows, with an application to large-amplitude motion in the atmosphere

By CHIA-SHUN YIH

Department of Engineering Mechanics, University of Michigan*

(Received 23 March 1960)

A transformation has been found which reduces steady non-homentropic flows of a compressible fluid to homentropic flows, provided diffusive and gravity effects are negligible. With this transformation, the equation governing steady two-dimensional flows of a compressible fluid with variable entropy in a gravitational field is derived, which is then applied to the study of atmospheric waves in the lee of mountains. The corresponding equation governing swirling axisymmetric flows is also given.

1. Introduction

It is well known that the flow of gas behind a curved shock is non-homentropic. In the atmosphere, waves are sometimes formed in the lee of mountains as a result of the non-homentropy of air and of the action of gravity. But the equations governing non-homentropic flows are so complicated that no non-trivial exact solution exists. Therefore in existing literature on the formation of lee waves, the theory has always been based on perturbation methods, and is thus only valid if the amplitude of wave motion (i.e. the vertical displacement) is small.

In this paper a transformation will be presented which will render unnecessary the consideration of non-homentropy in steady flows of ideal gases, provided the effects of viscosity and of gravity are neglected, in the sense that every steady non-homentropic flow can be reduced thereby to a steady homentropic flow. Gravity effects can certainly be neglected in the aerodynamics of aircraft or flying objects, though it is of primary importance in the study of waves in the atmosphere. Viscous effects can, as usual, be neglected outside of the boundary layer, and are certainly of secondary importance in atmospheric flows. Thus the transformation to be presented here is not without practical value.

In the study of lee waves in the atmosphere, the presence of gravity, which is now of paramount importance, prevents the above-mentioned transformation from absorbing the effects of non-homentropy altogether. Nevertheless, the use of this transformation leads to the derivation of a much simplified equation for steady two-dimensional flows, which, for an atmosphere slightly stratified in entropy and in specific energy, possesses four essentially different classes of

* At Department of Applied Mathematics and Theoretical Physics, University of Cambridge, during 1959–60.

solutions, provided the Mach number is everywhere small, so that the effect of *dynamic* compressibility on density variation can be neglected. (In the first 10 or 15 km of the atmosphere, where lee waves can conceivably be expected to occur, the Mach number of atmospheric flows is certainly everywhere small.) The solutions are exact in the sense that the displacements are not assumed to be small, but can have any arbitrary values of the same magnitude as the scale of the motion.

An equation governing steady axisymmetric flows with swirl has also been obtained, which may be helpful for the study of the Hirsch-tube phenomenon and of tornadoes.

2. The transformation

To bring out the full significance for ordinary aerodynamics of the transformation mentioned in the Introduction, body forces will be ignored for the time being. The equations of motion for steady flows are then

$$u_j \frac{\partial u_i}{\partial x_j} = -\frac{1}{\rho}\frac{\partial p}{\partial x_i}, \tag{1}$$

in which u_i is the velocity component in the direction of the Cartesian coordinate x_i ($i = 1, 2, 3$), ρ is the density, p is the pressure, and the summation convention has been adopted. The equation of continuity is, exactly,

$$\frac{\partial u_j}{\partial x_j} + \frac{1}{\rho} u_j \frac{\partial \rho}{\partial x_j} = 0. \tag{2}$$

If the flow is homentropic, and the fluid is a perfect gas,

$$p/\rho^\gamma = \text{constant}, \tag{3}$$

in which γ is the ratio of the specific heat* at constant pressure (c_p) to that at constant volume (c_v), and the flow is governed by equations (1) to (3). If the flow is not homentropic but diffusion is neglected, the entropy along a path line is constant. For steady flows this means that

$$u_j \frac{\partial}{\partial x_j}\left(\frac{p}{\rho^\gamma}\right) = 0, \tag{4}$$

which replaces equation (3), and states the constancy of entropy along a streamline in steady flows.

One of the great difficulties encountered in dealing with non-homentropic flows is that, since the gas is no longer barotropic (which is another way of saying that a single relationship between p and ρ does not exist), ρ cannot be absorbed into the pressure term in (1), and the motion, even started from rest, will not continue to be irrotational. The system consisting of equations (1), (2), and (4) is so complicated that at present no non-trivial solutions exist. However, the situation is not as bad as it appears at first sight, as the transformation now to be given will show.

* Both c_p and c_v are assumed to be constant.

In virtue of (4),

$$u_j \frac{\partial F(\lambda)}{\partial x_j} = 0, \tag{5}$$

in which $F(\lambda)$ is any arbitrary function of λ, defined by

$$\lambda = \frac{\rho}{\rho_0}\left(\frac{p_0}{p}\right)^{1/\gamma}, \tag{6}$$

with p_0 denoting a reference pressure and ρ_0 a reference density. Since the entropy S is connected with p, ρ, and c_v by

$$p/\rho^\gamma = \text{constant} \times e^{S/c_v}, \tag{7}$$

the quantity λ is connected with the entropy by

$$\lambda = \text{constant} \times e^{-S/c_p}, \tag{8}$$

and is to be determined *for each streamline* from the upstream conditions, by virtue of its constancy along a streamline in steady flows, as stated in (5). With the transformation

$$u_i' = \sqrt{\lambda}\, u_i, \quad \rho' = \rho/\lambda, \quad \text{and} \quad p' = p, \tag{9}$$

equations (1) and (2) become, in virtue of (5),

$$u_j' \frac{\partial u_i'}{\partial x_j} = -\frac{1}{\rho'}\frac{\partial p'}{\partial x_i} \tag{10}$$

and

$$\frac{\partial u_j'}{\partial x_j} + \frac{1}{\rho'} u_j' \frac{\partial \rho'}{\partial x_j} = 0. \tag{11}$$

Furthermore, the last two of equations (9) and equation (6) can be combined to give

$$\frac{p'}{\rho'^\gamma} = \frac{p}{\rho'^\gamma} = \frac{p_0}{\rho_0^\gamma} = \text{constant}. \tag{12}$$

Now equations (10), (11), and (12) are identical in form to (1), (2), and (3), and hence govern homentropic flows in terms of the primed quantities. But this means that to any solution of equations (10) to (12) representing a homentropic flow in terms of u_i', ρ', and p', there corresponds a non-homentropic flow in terms of u_i, ρ, and p, which are obtained from equations (9), and vice versa. Consideration of boundary conditions does not affect this conclusion. For convenience the flow in terms of the primed quantities will be called the associated flow.

The *associated* flow may not be irrotational. But if it originates from a big reservoir, where the fluid is at rest and therefore possesses no vorticity, irrotationality (in the u_i'-field) will persist downstream. This can be seen by eliminating p' from (10) by cross-differentiation, producing

$$u_j' \frac{\partial \xi_i'}{\partial x_j} = \xi_j' \frac{\partial u_i'}{\partial x_j} + \frac{\xi_i'}{\rho'} u_j' \frac{\partial \rho'}{\partial x_j}. \tag{13}$$

in which ξ_i' is the ith component of the vorticity in the u_i'-field. Equation (13) clearly indicates the persistence of irrotationality (or of the vanishing of ξ_i').

If $\xi_i' = 0$, integration of equations (10) in the usual way produces (with q' as the speed in the associated flow)

$$\tfrac{1}{2}q'^2 + \frac{\gamma}{\gamma-1}\frac{p'}{\rho'} = \tfrac{1}{2}q'^2_{\max} = \text{constant}, \tag{14}$$

which is valid for the whole field of flow. This equation can also be written

$$\tfrac{1}{2}q^2 + \frac{\gamma}{\gamma-1}\frac{p}{\rho} = \frac{1}{2\lambda}q'^2_{\max} = \text{constant} \times \frac{p^{1/\gamma}}{\rho}, \tag{15}$$

in which q is the speed of the actual flow. If $\xi_i' \neq 0$,

$$\tfrac{1}{2}q^2 + \frac{\gamma}{\gamma-1}\frac{p}{\rho} = f(S), \tag{16}$$

in which $f(S)$ is an arbitrary function of the entropy S.

Equation (14) is simply the ordinary Bernoulli equation. In fact, if gravity is not neglected the complete equation is (with z measured vertically upward)

$$\tfrac{1}{2}q^2 + gz + \frac{\gamma}{\gamma-1}\frac{p}{\rho} = f(S), \tag{17}$$

which is well known.

Since the transformation presented in this section may suggest a similarity in its underlying idea with Crocco's stream function, it is desirable to point out the essential differences between the two inventions. Crocco dealt with the homenergic (constant specific energy, or constant $f(S)$ in (17)) but non-homentropic flows behind a shock, and, utilizing the constancy of entropy along a streamline in steady flows, obtained the equation of continuity for two-dimensional flow* (in the usual notation)

$$\frac{\partial}{\partial x}[u(q^2_{\max} - q^2)^{1/(\gamma-1)}] + \frac{\partial}{\partial y}[v(q^2_{\max} - q^2)^{1/(\gamma-1)}] = 0, \tag{18}$$

which permits the use of a stream function ψ (Crocco's stream function), in terms of which the velocity components can be expressed

$$u = (q^2_{\max} - q^2)^{-1/(\gamma-1)}\frac{\partial \psi}{\partial y}, \quad v = -(q^2_{\max} - q^2)^{-1/(\gamma-1)}\frac{\partial \psi}{\partial x}. \tag{19}$$

Close examination of the factor

$$(q^2_{\max} - q^2)^{1/(\gamma-1)}$$

shows that it is really just the density ρ multiplied by a function of the entropy. To this extent there is some similarity between the present transformation and Crocco's invention. But the similarity stops here. The important differences are: (*a*) Crocco's development is only for homenergic flows, whereas the present transformation deals with non-homenergic and non-homentropic flows; (*b*) Crocco's development is only for two-dimensional or axisymmetric flows, whereas the present transformation deals with general three-dimensional flows; (*c*) Crocco invented a new stream function but left the velocity unchanged, hence did not arrive at the transformation embodied in (9).

* The development for axisymmetric flows is similar.

We shall now take stock and see what conclusions can be drawn from the transformation embodied in (9). As is evident, the associated flow has the same *pattern* as the actual flow. It (the associated flow) is irrotational if the actual flow originates from a large reservoir where the gas is at rest, or, more generally, if the associated flow is irrotational far upstream. Whether the associated flow is irrotational or not, the third of equations (9) ensures that the drag and lift on any body placed in the gas stream will be the same as that calculated from the associated flow. If far upstream the actual flow* is unidirectional, with constant velocity but variable entropy, the associated flow will be rotational, and there will in general be lift on a body placed in the stream. This is an example illustrating how entropy stratification upstream can give rise to lift on a body moving with constant velocity in a quiescent but stratified gas.

The above conclusions, and indeed the transformation embodied in (9), are based on the conservation of entropy along each streamline. Therefore flows with shocks must be considered anew, if they are to be considered *as a whole* and not as a collection of separate regions. Looking at such flows in their entirety, we can draw some interesting conclusions in spite of the entropy change across the shock. Since three-dimensional shocks differ from two-dimensional ones only in complexity, not in principle, only two-dimensional shocks will be considered here. The pre-shock flow is assumed to be parallel to the x-axis, with velocity u_1 (which may vary with y), with the subscript 1 now referring to pre-shock flow and 2 to post-shock flow. The shock wave is in general curved and the post-shock flow in general non-parallel. With u and v denoting velocity components in the x- and y-directions, and β denoting the local angle of inclination of the shock wave, continuity demands (Liepmann & Puckett 1947, p. 51) that along the shock wave

$$\rho_1 u_1 \sin\beta = \rho_2(u_2 \sin\beta - v_2 \cos\beta), \tag{20}$$

in which ρ is the density. The conservation of momentum normal to the shock wave demands that, along the shock wave,

$$p_1 + \rho_1 u_1^2 \sin^2\beta = p_2 + \rho_2(u_2 \sin\beta - v_2 \cos\beta)^2, \tag{21}$$

in which p is the pressure. The conservation of momentum parallel to the shock wave demands

$$p_1 u_1^2 \sin\beta \cos\beta = \rho_2(u_2 \sin\beta - v_2 \cos\beta)(u_2 \cos\beta + v_2 \sin\beta), \tag{22}$$

and the energy equation remains

$$\tfrac{1}{2}u_1^2 + \frac{\gamma}{\gamma-1}\frac{p_1}{\rho_1} = \tfrac{1}{2}(u_2^2 + v_2^2) + \frac{\gamma}{\gamma-1}\frac{p_2}{\rho_2}. \tag{23}$$

Equations (20) to (23) contain five unknowns: u_2, v_2, ρ_2, p_2, and β. The variation of β from place to place along the shock wave can only be determined by the equations governing the flow before the shock, those governing post-shock flow, equations (20) to (23), and the conditions at the solid boundaries and at infinity, by a trial-and-error process.

* The flow is the steady flow equivalent to the flow caused by a body moving with constant velocity in a quiescent but stratified gas.

Whereas the transformation embodied in (9) does not obviate this tedious process, it does throw some light on shock waves ahead of which the fluid is already non-homentropic. With λ defined by (6) and determined for each streamline (even after it pierces through the shock wave) by the upstream or pre-shock condition, we insist on making the transformation represented by (9), in spite of the abrupt increase of entropy along each streamline as it crosses the shock wave. The associated flow is parallel and homentropic upstream, and is irrotational if λu_1^2 is constant throughout. Behind the shock even the associated flow is not homentropic, but is governed by the equations

$$\left(u'\frac{\partial}{\partial x}+v'\frac{\partial}{\partial y}\right)(u',v')=-\frac{1}{\rho'}\left(\frac{\partial}{\partial x},\frac{\partial}{\partial y}\right)p',$$

$$\frac{\partial u'}{\partial x}+\frac{\partial v'}{\partial y}+\frac{1}{\rho'}\left(u'\frac{\partial}{\partial x}+v'\frac{\partial}{\partial y}\right)\rho'=0,$$

$$\left(u'\frac{\partial}{\partial x}+v'\frac{\partial}{\partial y}\right)\left(\frac{p'}{\rho'^{\gamma}}\right)=0,$$

because λ is constant on each streamline by imposition. These equations, with the primes dropped, are identical with the equations governing post-shock flow. The transformation (9) achieves homentropy in the pre-shock region, but otherwise leaves the governing equations unchanged in form. At the shock wave, (20) to (23) are still valid if all the quantities (except, of course, β and γ) are primed. Thus, even when shock waves are present, to every flow with entropy stratification before the shock corresponds an associated flow of the *same pattern for the entire field of flow*, with homentropy (though not necessarily irrotationality) before the shock. The actual lift and drag on a body placed in the gas stream are the same as those calculated from the associated flow.

Although gravity has been neglected in this section, equations (9) are still helpful when gravity is taken into account, because they simplify the governing equations a great deal, as will be shown in the following sections.

3. Equation governing two-dimensional flows in a gravitational field

If (x_1, x_3) and (u_1, u_3) are now written as (x, z) and (u, w), the equations of motion for steady two-dimensional flows are, with the gravity included,

$$\rho\left(u\frac{\partial u}{\partial x}+w\frac{\partial u}{\partial z}\right)=-\frac{\partial p}{\partial x},$$

$$\rho\left(u\frac{\partial w}{\partial x}+w\frac{\partial w}{\partial z}\right)=-\frac{\partial \rho}{\partial z}-g\rho,$$

in which z is measured in a direction opposite to that of the gravitational acceleration g. With the transformation embodied in (7), the equations of motion become

$$u'\frac{\partial u'}{\partial x}+w'\frac{\partial u'}{\partial z}=-\frac{1}{\rho'}\frac{\partial p'}{\partial x}, \tag{24}$$

$$u'\frac{\partial w'}{\partial x}+w'\frac{\partial w'}{\partial z}=-\frac{1}{\rho'}\frac{\partial p'}{\partial z}-g\lambda. \tag{25}$$

The equation of continuity $$\frac{\partial(\rho u)}{\partial x}+\frac{\partial(\rho w)}{\partial z}=0$$

now has the form $$\frac{\partial(\rho' u')}{\partial x}+\frac{\partial(\rho' w')}{\partial z}=0,$$

which permits the use of the stream function ψ' such that

$$u'=\frac{1}{\rho'}\frac{\partial\psi'}{\partial z},\quad w'=-\frac{1}{\rho'}\frac{\partial\psi'}{\partial x}.$$

With $$q'^2=u'^2+w'^2,\quad I'=\frac{q'^2}{2}+\int\frac{dp'}{\rho'},$$

$$H'=\frac{q'^2}{2}+gz\lambda+\int\frac{dp'}{\rho'}\quad\text{and}\quad\eta'=\frac{\partial u'}{\partial z}-\frac{\partial w'}{\partial x},\tag{26}$$

the equations of motion can be written

$$\frac{\eta'}{\rho'}\frac{\partial\psi'}{\partial x}=\frac{\partial I'}{\partial x},\tag{27}$$

$$\frac{\eta'}{\rho'}\frac{\partial\psi'}{\partial z}=\frac{\partial I'}{\partial z}+g\lambda.\tag{28}$$

Multiplication of (27) by dx and (28) by dz and addition of the resulting equations produces

$$\frac{\eta'}{\rho'}d\psi'=dI'+g\lambda\,dz=dH'-gz\,d\lambda.$$

But since H and λ are functions of ψ' alone,

$$\frac{\eta'}{\rho'}+gz\frac{\partial\lambda}{\partial\psi'}=\frac{dH'}{d\psi'}=h(\psi'),\tag{29}$$

or, from equation (25) and the last of equations (26),

$$V^2\psi'-\frac{1}{\rho'}\left(\frac{\partial\rho'}{\partial x}\frac{\partial\psi'}{\partial x}+\frac{\partial\rho'}{\partial z}\frac{\partial\psi'}{\partial z}\right)+gz\rho'^2\frac{d\lambda}{d\psi'}=\rho'^2h(\psi'),\tag{30}$$

which is the desired equation. The density ρ' has to be evaluated from the third of equations (26), in which $H'(\psi')$ and $\lambda(\psi')$ are determined from upstream conditions.

4. Swirling axisymmetric flows in a gravitational field

Cylindrical co-ordinates (r,θ,z) will be used. In these co-ordinates, the velocity components will be denoted by u,v, and w, respectively. The equations of motion for steady axisymmetric flows are, with viscosity neglected,

$$u\frac{\partial u}{\partial r}+w\frac{\partial u}{\partial z}-\frac{v^2}{r}=-\frac{1}{\rho}\frac{\partial p}{\partial r},\tag{31}$$

$$u\frac{\partial v}{\partial r}+w\frac{\partial v}{\partial z}+\frac{uv}{r}=0,\tag{32}$$

$$u\frac{\partial w}{\partial r}+w\frac{\partial w}{\partial z}=-\frac{1}{\rho}\frac{\partial p}{\partial z}-g,\tag{33}$$

in which z is again measured in the direction opposite to that of the gravitational acceleration. The equation of continuity is

$$\frac{\partial(r\rho u)}{\partial r}+\frac{\partial(r\rho w)}{\partial z}=0.$$

By the transformation indicated by equations (7), equations (31) to (33) become

$$u'\frac{\partial u'}{\partial r}+w'\frac{\partial u'}{\partial z}-\frac{v'^2}{r}=-\frac{1}{\rho'}\frac{\partial p'}{\partial r}, \tag{34}$$

$$u'\frac{\partial v'}{\partial r}+w'\frac{\partial v'}{\partial z}+\frac{u'v'}{r}=0, \tag{35}$$

$$u'\frac{\partial w'}{\partial r}+w'\frac{\partial w'}{\partial z}=-\frac{1}{\rho'}\frac{\partial p'}{\partial z}-g\lambda, \tag{36}$$

and the equation of continuity becomes

$$\frac{\partial(r\rho' u')}{\partial r}+\frac{\partial(r\rho' w')}{\partial z}=0. \tag{37}$$

Equation (37) permits the use of a stream function ψ' in terms of which the velocity components can be expressed:

$$u'=-\frac{1}{r\rho'}\frac{\partial\psi'}{\partial z},\quad w'=\frac{1}{r\rho'}\frac{\partial\psi'}{\partial r}. \tag{38}$$

Equation (35) expresses the conservation of angular momentum for the same particle, because it can be written as

$$u'\frac{\partial(rv')}{\partial r}+w'\frac{\partial(rv')}{\partial z}=0.$$

Consequently rv' is a function of ψ' alone. For convenience, we take

$$(rv')^2=f(\psi'). \tag{39}$$

With $\quad q'^2=u'^2+v'^2+w'^2,\quad J'=\dfrac{u'^2+w'^2}{2}+\displaystyle\int\frac{dp'}{\rho'},\quad I'=\frac{q'^2}{2}+\int\frac{dp'}{\rho'},$

$$H'=\frac{q'^2}{2}+gz\lambda+\int\frac{dp'}{\rho'},\quad \eta'=\frac{\partial u'}{\partial z}-\frac{\partial w'}{\partial r}, \tag{40}$$

equations (34) and (36) can be written, with the aid of (38) and (39)

$$\frac{\eta'}{r\rho'}\frac{\partial\psi'}{\partial r}-\frac{f(\psi')}{r^3}=-\frac{\partial J'}{\partial r},$$

$$\frac{\eta'}{r\rho'}\frac{\partial\psi'}{\partial z}=-\frac{\partial J'}{\partial z}-g\lambda,$$

or

$$\frac{\eta'}{r\rho'}\frac{\partial\psi'}{\partial r}-\frac{1}{2r^2}\frac{\partial}{\partial r}f(\psi')=-\frac{\partial I'}{\partial r}, \tag{41}$$

$$\frac{\eta'}{r\rho'}\frac{\partial\psi'}{\partial z}-\frac{1}{2r^2}\frac{\partial}{\partial z}f(\psi')=-\frac{\partial I'}{\partial z}-g\lambda. \tag{42}$$

Multiplication of (41) by $-dr$ and (42) by $-dz$ and addition of the results gives

$$-\frac{\eta'}{r\rho'}+\frac{1}{2r^2}\frac{df}{d\psi'}=\frac{dH'}{d\psi'}-gz\frac{d\lambda}{d\psi'}, \tag{43}$$

or, with the aid of (38) and the last of equations (40),

$$\left(\frac{\partial^2}{\partial r^2}-\frac{1}{r}\frac{\partial}{\partial r}+\frac{\partial^2}{\partial z^2}\right)\psi'-\frac{1}{\rho'}\left(\frac{\partial\rho'}{\partial r}\frac{\partial\psi'}{\partial r}+\frac{\partial\rho'}{\partial z}\frac{\partial\psi'}{\partial z}\right)+\frac{\rho'^2}{2}\frac{df}{d\psi'}+g\rho'^2zr^2\frac{d\lambda}{d\psi'}=r^2\rho'^2\frac{dH'}{d\psi'}, \tag{44}$$

which is the equation governing swirling axisymmetric motion in a gravitational field. In many engineering applications (such as to the Hirsch tube), the term involving g can be neglected. Again, ρ' is to be calculated from the equation involving H' in (40), in which the functions $H'(\psi')$ and $\lambda(\psi')$ are again to be determined from upstream conditions. Equation (44) could serve as a starting point for the study of tornadoes.

5. Lee waves of large amplitude

The phenomenon of gravity waves in air (considered as a compressible fluid) in the lee of mountain ridges has been studied by Lyra, Queney, Corby, Scorer, and others, and recently by Crapper (1949). (For references, see Crapper's work.) Perturbation methods have been used by all of these authors, so that their results do not apply to large vertical displacements. Batchelor (1953) gave an equation governing homentropic flows in the atmosphere, obtained on the assumption of irrotationality (which is a consequence of homentropy if the motion has been started from rest) and small Mach number in the entire flow field. The effect of gravity is retained in Batchelor's equation, so that it applies to large vertical displacements under the assumptions stated. However, since wave motions in the atmosphere are essentially due to non-homentropy or non-homenergy, Batchelor's equation cannot be applied to a study of lee waves.

The exact equation governing steady two-dimensional non-homentropic flows is equation (30), which can be used to study lee waves. However, the equation is so very complicated that no solution can be obtained without some simplifying assumptions. With Batchelor, we shall assume that the Mach number is everywhere small, so that, *a fortiori*, the *variation* of the square of the speed is small compared with the square of the sound speed. Therefore the density variation due to the variation of speed is negligible, and any change in the density along the same streamline is due to change of elevation alone. Since isentropy along a streamline is the most important assumption underlying the derivation of (29), it might appear that the simplifying assumption on ρ (hence on ρ') implies that the pressure is a function of elevation alone for any streamline. Such an implication must not be inferred from the assumption on the density, because the pressure must be calculated from the equation containing H' in (26), with the term $\frac{1}{2}q'^2$ included. Indeed, if the pressure were only dependent on z on any one streamline, scarcely any non-trivial motion would be possible. The situation is not unlike that encountered in the study of free-convection problems, in which the fluid is assumed incompressible as far as continuity and the inertia of the

fluid is concerned, but is considered to have a variable density as far as the important term representing body force is concerned. Another similar situation is encountered in the study of incompressible fluids. If entropy is assumed constant along a path line, surely there is some relation connecting the density to the pressure on such a line. But the assumption of constant density does not imply constant pressure, because the pressure can change a great deal for an infinitesimal change in the density of what is normally considered to be an incompressible fluid. In the present case, the assumption concerning ρ' affects only the first term in (29) or the first two groups of terms in (30), and is an assumption concerning essentially the continuity equation only. The inertia effect of density change has been absorbed once and for all in the transformation represented by equation (9). Gravity force is exactly represented by $gz(d\lambda/d\psi')$ and the force resulting from pressure gradient is represented by $dH'/d\psi'$ in (29), with H' given by the *full* expression in (26). The factor ρ'^2 in the last two terms of (30) appears from a common multiplication by that factor, and does not affect the physical reasoning given above.

If the variation of H' or of λ with ψ' is large, equation (30) is still too difficult to solve. Therefore we shall assume the variation of H' and λ to be small. As far as the calculation of ρ' is concerned, we shall ignore the variation of H' and λ altogether and justify the procedure by the same arguments as those presented in the last paragraph. For ρ', then, calculation from the third of (26), with the term $\frac{1}{2}q'^2$ neglected and λ equal to 1 (if the reference density and pressure are those at some point in the atmosphere under discussion), yields

$$\frac{\gamma}{\gamma-1}\frac{p_0}{\rho_0^\gamma}\rho'^{\gamma-1} = H' - gz, \tag{45}$$

or

$$\rho'^{\gamma-1} = \frac{H'-gz}{K}, \quad K = \frac{\gamma}{\gamma-1}\frac{p_0}{\rho_0^\gamma}. \tag{46}$$

With (46), equation (30) becomes

$$\nabla^2\psi' + \frac{1}{\gamma-1}\frac{g}{H'-gz}\frac{\partial\psi'}{\partial z} + gz\left(\frac{H'-gz}{K}\right)^{2/(\gamma-1)}\frac{d\lambda}{d\psi'} = \left(\frac{H'-gz}{K}\right)^{2/(\gamma-1)}h(\psi'), \tag{47}$$

in which, as in (45) and (46), H' is considered to be a constant except in connexion with $h(\psi')$. It must be remembered that whatever assumptions have been made on ρ', H', and λ, they do not limit the amplitude of the vertical displacement of the motion in any way, or the slope of the streamlines. Freedom from such limitations is the chief merit of the present theory. The functions $\lambda(\psi')$ and $h(\psi')$ are to be determined from upstream conditions.

Equation (47) is exactly linear if

$$\frac{d\lambda}{d\psi'} = a\psi' + b, \quad h(\psi') = m\psi' + n.$$

Since ψ' can be changed by a constant, there are seven different cases:

(1) $a \neq 0, b = 0, m = n = 0,$
(2) $a \neq 0, b = 0, m = 0, n \neq 0,$
(3) $a \neq 0, b = 0, m \neq 0, n = 0,$
(4) $a \neq 0, b = 0, m \neq 0, n \neq 0,$
(5) $a = 0, b \neq 0, m = n = 0,$
(6) $a = 0, b \neq 0, m = 0, n \neq 0,$
(7) $a = 0, b \neq 0, m \neq 0, n = 0.$

We have not included the cases in which $a = b = 0$, because they correspond to homentropic flows. If in addition $m = n = 0$, the flow is in fact irrotational. But if $m \neq 0$, wave motion is possible. This wave motion is not due to non-homentropy because the entropy is constant for $a = b = 0$, but is due to non-homenergy.

Since z can be changed by a constant, the seven cases can be reduced to four essentially different cases. Thus cases (3), (4), and (6) are not essentially different from cases (1), (2), and (5), respectively. The four essentially different cases, are therefore, (1), (2), (5), and (7).

If

$$\Psi = \psi'/\psi_0, \quad \xi = x/d, \quad \eta = z/d, \tag{48}$$

in which d is a reference length which can be taken either to be the depth of the troposphere or the depth below some very stable layer, and ψ_0 is a reference stream function, the linear cases are represented by

$$\left(\frac{\partial^2}{\partial\xi^2}+\frac{\partial^2}{\partial\eta^2}\right)\Psi+\frac{1}{\gamma-1}\frac{1}{\alpha-\eta}\frac{\partial\Psi}{\partial\eta}+\eta(\alpha-\eta)^{2/(\gamma-1)}(A\Psi+B)=(\alpha-\eta)^{2/(\gamma-1)}(C\Psi+D), \tag{49}$$

in which

$$\alpha = H'/gd \tag{50}$$

is the ratio of the *equivalent* depth of the atmosphere, assumed completely homentropic (for defining this depth only), to the reference depth d. The value of α may vary over a range, but if d is taken to be 10 km (average depth for the troposphere) a representative value for α is 3·5.

In all the linear cases the solution can be put in the form

$$\Psi = \Psi_1(\eta) + \Psi_2(\xi, \eta), \tag{51}$$

in which both parts on the right-hand side satisfy (49). If we suppose that from $\eta = 1$ (or $z = d$) upwards the atmosphere is much more stable than the layer below, so that the vertical displacement at $\eta = 1$ is small compared with that prevailing in the layer $0 \leqslant \eta < 1$ (see Yih 1960*a*), a rigid plane may be imagined to be situated at $\eta = 1$. The boundary conditions for Ψ are then

$$\Psi_1(0) = 0, \quad \Psi_1(1) = E \text{ (a constant)}. \tag{52}$$

Solution of the differential equation (49), with Ψ_1 replacing Ψ therein, together with (52) then yield a $\Psi_1(\eta)$ corresponding to an upstream condition which makes (47) linear. Although the actual upstream condition may not give rise to the linearity of (47), suitable choices of the constants A, B, C, D, and E can produce infinitely many upstream conditions one of which may approximate the actual upstream condition rather closely, while the linearity of (47) is maintained throughout. The method of approach is therefore an inverse one, as is often the case in classical aerodynamics.

As to Ψ_2, the boundary conditions are, with the gas flowing from $\xi = -\infty$ to $\xi = +\infty$,

$$\Psi_2 \to 0 \quad \text{as} \quad \xi = -\infty, \tag{53a}$$

$$\Psi_2(\xi, 1) = 0, \tag{53b}$$

$$\Psi = \Psi_1 + \Psi_2 = 0 \quad \text{on the lower boundary (ground)}. \tag{53c}$$

No boundary condition is imposed at $\xi = +\infty$, because waves may exist in the lee of a barrier, and when they do not exist the condition far downstream is automatically the same as that far upstream. The condition (53*a*) is imposed on the assumption that the existence of a barrier, the effect of which is represented by Ψ_2, does not influence the condition far upstream. The (assumed) rigidity of the boundary at $\eta = 1$ demands (53*b*). The satisfaction of (53*c*) on the surface of a ground of given profile is difficult. But the inverse method given in another paper (Yih 1960*b*) can again be used. As described in that paper, the auxillary condition

$$\Psi_2(\xi, 0) = 0 \tag{53d}$$

is imposed to guarantee good behaviour of the solution far downstream, where the ground is assumed level and where the lee-wave components contained in Ψ_2 do not die out exponentially. The streamline $\Psi = 0$ therefore consists of two branches: the line $\eta = 0$ and the surface of the ground. As in the case of lee-wave formation in an incompressible fluid (Yih 1960*b*), the amplitudes of the lee-wave components depend only on certain integral properties of the barrier, and not on its detailed shape.

Although the calculation for the details of lee-waves governed by (49) involves the detailed calculations for the eigenfunctions, in case (7) at least, the number of lee-wave components can be predicted from the value of C without detailed calculations. Thus, the function Ψ_1 satisfies the equation (with $A = D = 0$ in case (7))

$$\Psi_1'' + \frac{1}{\gamma-1}\frac{1}{\alpha-\eta}\Psi_1' + \eta(\alpha-\eta)^{2/(\gamma-1)}B = (\alpha-\eta)^{2/(\gamma-1)}C\Psi_1,$$

in which the primes indicate ordinary differentiation. The other part of the solution consists of terms of the form

$$\Psi_2 = \begin{Bmatrix}\sin k\xi \\ \cos k\xi\end{Bmatrix} f(\eta),$$

in which k may be imaginary, and f satisfies the equation

$$f'' + \frac{1}{\gamma-1}\frac{1}{\alpha-\eta}f' - [C(\alpha-\eta)^{2/(\gamma-1)} + k^2]f = 0. \tag{54}$$

With

$$\zeta = \frac{\gamma-1}{\gamma}(\alpha-\eta)^{\gamma/(\gamma-1)}, \tag{55}$$

equation (54) becomes

$$\frac{d^2f}{d\zeta^2} - \left[C + k^2\left(\frac{\gamma}{\gamma-1}\zeta\right)^{-2/\gamma}\right]f = 0. \tag{56}$$

The interval $0 \leqslant \eta \leqslant 1$ is now transformed to

$$\frac{\gamma-1}{\gamma}(\alpha-1)^{\gamma/(\gamma-1)} \leqslant \zeta \leqslant \frac{\gamma-1}{\gamma}\alpha^{\gamma/(\gamma-1)}.$$

Let

$$l = \frac{\gamma-1}{\gamma}[\alpha^{\gamma/(\gamma-1)} - (\alpha-1)^{\gamma/(\gamma-1)}]. \tag{57}$$

By equating k to zero and computing the values for C which will enable f to satisfy the boundary conditions corresponding to (53*b*) and (53*d*), i.e.

$$f(0) = 0, \quad f(1) = 0,$$

we have $$C_n = -(n\pi/l)^2.$$

If $$(n\pi/l)^2 \leqslant -C < \{[(n+1)\pi]/l\}^2,$$

there are n non-negative eigenvalues for k^2, and hence n lee-wave components.

This work has been done during the tenure of a Senior Post-doctoral Fellowship granted by the National Science Foundation.

REFERENCES

BATCHELOR, G. K. 1953 The conditions for dynamic similarity of motions of a frictionless perfect-gas atmosphere. *Quant. J. Roy. Soc. Met.* **79**, 224–35.

CRAPPER, G. D. 1959 A three-dimensional solution for waves in the lee of mountains. *J. Fluid Mech.* **6**, 51–76.

LEIPMANN, H. W. & PUCKETT, A. E. 1947 *Introduction to Aerodynamics of a Compressible Fluid.* New York: Wiley and Sons.

YIH, C.-S. 1960*a* Gravity waves in a stratified fluid. *J. Fluid Mech.* **8**, 481–508.

YIH, C.-S. 1960*b* Exact solutions for steady two-dimensional flows of a stratified fluid. *J. Fluid Mech.* **9**, 161–174.

Transonic rotational flow over a convex corner

By ROBERTO VAGLIO-LAURIN
Polytechnic Institute of Brooklyn, New York

(Received 12 October 1959 and in revised form 12 February 1960)

A singularity is encountered in the flow field about two-dimensional and axisymmetric bodies characterized by a sharp corner, where the fluid velocity becomes sonic. Investigation shows that the problem in question belongs, as do many other discontinuity problems, to the family of asymptotic or 'boundary-layer' phenomena of mathematical physics. The solution of a first approximation to the flow equations is given by a series in powers of a variable measuring the distance from the corner, with coefficients depending on an appropriate similarity variable. The leading coefficient of the series is independent of three-dimensional and rotationality effects, in complete analogy to the well-known solution of the corner problem in supersonic flow. Detailed results are presented for the leading singularity and for the first two corrections due to rotationality and axial symmetry of the flow.

1. Introduction

The uses of blunt wings and bodies for hypersonic flight has presented the aerodynamicist again with problems of the transonic type, wherein regions of subsonic and supersonic flow are encountered simultaneously. Among the many possible configurations, there is particular practical interest in those characterized by a sharp corner, which determines the location of the sonic point. This point of view is prompted by the experimental results of Ferri (1958) who showed that, by suitable location of the shoulder, one may reduce the heat transfer at the stagnation point on a blunt profile having a prescribed radius of curvature of the nose. From a theoretical point of view it is of interest to obtain information which, when combined with available methods such as those of Vaglio-Laurin & Ferri (1958), and Van Dyke (1958), permits the analysis of the flow field about general blunt-body shapes.

The investigation of the transonic portion of two-dimensional and axisymmetric rotational flows with a sonic singularity cannot take advantage of the hodograph transformation which has been the main tool of the aerodynamicist interested in classical two-dimensional irrotational transonic flow. For the present problem, however, analysis in the physical plane does not present excessive complications; in fact it has the advantage that one gains an immediate physical appreciation of the phenomenon which would be lost in the hodograph plane. The subsonic and supersonic portions of the flow are joined by a 'boundary layer' with a behaviour typical of the classical discontinuity phenomena common to many branches of physics (see, for example, von Kármán (1940), Carrier (1953), and Friedrichs (1955)). The leading term of the solution describing the flow in the 'boundary

layer' predicts the same pressure distribution on the wall and the same sonic line shape as the leading singularity of Guderley's (1948) hodograph solution for the transonic corner problem in two-dimensional irrotational flow; the boundary-layer feature, and its bearing on the numerical analysis of complicated flow fields, could hardly be detected in the hodograph plane.

Transonic rotational flow around a sharp corner on an axisymmetric body has been investigated by Ho & Holt (1956), who used series expansions in powers of the distance from the shoulder with coefficients depending on the angular co-ordinate based on the shoulder. They found that the lowest-order terms correspond to a Prandtl–Meyer expansion; and they gave formal solutions for the first-order perturbations in the subsonic and in the supersonic regions of the flow. However, they did not investigate in detail the problem of matching the two regions. It is shown in §2 that direct matching cannot be carried out. This impossibility of matching together with the classical symptoms of (*a*) different analytic laws obtained to zero order in the subsonic and in the supersonic region, and (*b*) an infinite value of one velocity component at the boundary between the two regions, strongly suggest the occurrence of a boundary layer. Just to quote a few examples, the symptoms are the same as those encountered in the study of classical viscous boundary-layer theory, in the study of transonic flows by small-perturbation theory, and in the asymptotic theory of the wave equation at a caustic surface.

In general, boundary-layer analyses connected with solutions of non-linear partial differential equations are employed heuristically. In the present case one obtains *a posteriori* proof of validity from the following findings:

(*a*) As should be expected on physical grounds (see Vaglio-Laurin & Ferri (1958)), the leading term of the solution coincides with that pertaining to plane potential flow.

(*b*) The behaviour on the supersonic side is exactly that predicted by perturbation of a Prandtl–Meyer flow; however, the infinity in the perturbation velocities is eliminated.

Further heuristic substantiation of the approach may be found in the fact that the prevailing equations are the classical ones of transonic flow.

The details of the subject analysis are presented in the following sequence. The boundary-layer approach, the pertaining equations, their solution by means of a series of functions of an appropriate similarity variable, and the requirements thereon are first discussed (§2). A detailed study of the non-linear ordinary differential equation governing the leading singularity and the solution of this equation are the subject of §3. The linear equations governing the subsequent coefficients of the series solution and detailed results for the leading axisymmetric and rotational effects are then given (§4). Finally, the application of the results to the numerical analysis of the supersonic flow about blunt nosed bodies with a sonic shoulder is discussed in §5.

2. The governing equations

The difficulty associated with a straightforward analysis of the corner singularity is apparent when one particularizes the results of Ho & Holt (1956) to plane

potential flow. With the notation of these authors shown in figure 1, one obtains for the first-order coefficients in the subsonic region

$$U_1(\theta) = A_s[1+\cos 2(\theta+\alpha)], \tag{1a}$$

$$V_1(\theta) = -A_s \sin 2(\theta+\alpha), \tag{1b}$$

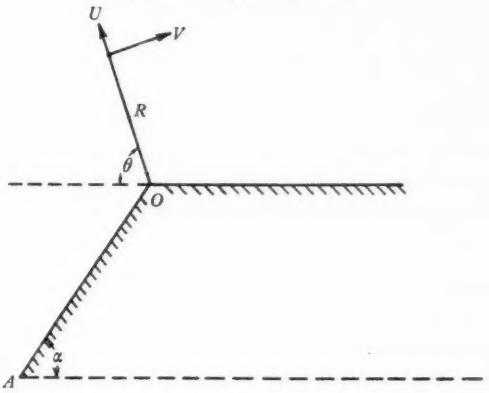

FIGURE 1. Schematic diagram and notation for preliminary considerations.

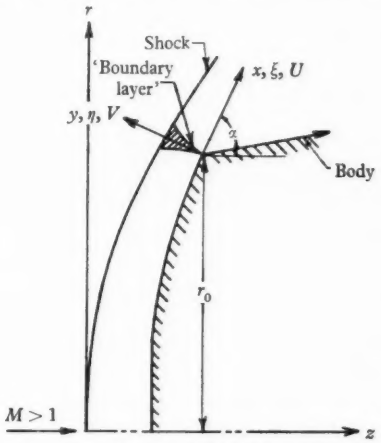

FIGURE 2. Schematic diagram of typical sonic shoulder and reference co-ordinate system.

and in the supersonic region

$$U_1(\theta) = \text{const.}\,[\cos(\lambda\phi)]^{(2\lambda^2+1)/2\lambda^2}[\sin(\lambda\phi)]^{\frac{1}{2}}, \tag{2a}$$

$$V_1(\theta) = \tfrac{1}{2}U_1'(\theta), \tag{2b}$$

with $$\lambda^2 = \frac{\gamma-1}{\gamma+1}, \quad \phi = \theta+\alpha-\tfrac{1}{2}\pi.$$

Matching at the sonic line requires

$$(V_1)_{\phi=0} = 0,$$

or, in view of (2*a*, *b*) zero perturbation in the flow field. The different behaviour with ϕ of the subsonic and of the supersonic perturbations suggests the same

conclusion; yet the perturbations in question are certainly valid outside of the sonic region. The situation is then typical of an asymptotic phenomenon; a boundary-layer approach is suggested.

As in many classical problems, the parameter of the asymptotic expansion does not occur in the differential equations governing the flow considered here. This parameter must then be related to one of the characteristic quantities in the problem, say the departure of the local velocity from the sonic value, by the requirement that the approximate boundary-layer equations have all the qualitative features necessary to describe the phenomenon on hand, namely, a transonic flow. With the notation of figure 2 (x-co-ordinate across the boundary layer), the asymptotic expansion is easily carried out along the following lines:

(*a*) New independent variables are introduced

$$\bar{\xi} = x/\delta, \quad \bar{\eta} = y, \tag{3}$$

where δ is a quantity which may represent the thickness of the boundary layer, and which tends to zero as the magnitude of the velocity perturbation from sonic at the edges of the layer tends to zero.

(*b*) The velocity field is described by small perturbations superposed on a parallel sonic stream in the x-direction. However, the orders of magnitude of the perturbations in the $\bar{\xi}$ and $\bar{\eta}$ directions can be different; we denote them by ϵ_i and ν_i, respectively, to get

$$\frac{U}{a_*} = 1 + \epsilon_1 U_1(\bar{\xi}, \bar{\eta}) + \epsilon_2 U_2(\bar{\xi}, \bar{\eta}) + \ldots, \tag{4a}$$

$$\frac{V}{a_*} = \nu_1 V_1(\bar{\xi}, \bar{\eta}) + \nu_2 V_2(\bar{\xi}, \bar{\eta}) + \ldots. \tag{4b}$$

(*c*) In view of the asymptotic Prandtl–Meyer expansion behaviour to be matched on the supersonic side, we set $\nu_1^2 = \epsilon_1^3$.

(*d*) In the axisymmetric case we assume $\delta \ll r$, that is, the thickness δ of the boundary layer at any point is much smaller than the radial distance of the point from the axis. Under these conditions, which are met by all present practical configurations, the effect of transverse curvature is negligible, and one can set within the boundary layer

$$r = r(\eta) = r_0 + \eta \cos \alpha. \tag{5}$$

The analogy with the classical problem of the viscous boundary layer on a body of revolution is quite evident.

On this basis one can proceed to the expansion of the equations of motion for homoenergetic flow written in the form

$$a^2 \operatorname{div} \mathbf{q} = \mathbf{q} \cdot \nabla(\tfrac{1}{2} q^2), \tag{6a}$$

$$a^2 = \frac{\gamma + 1}{2} a_*^2 - \frac{\gamma - 1}{2} q^2, \tag{6b}$$

$$\boldsymbol{\omega} \times \mathbf{q} = \frac{\rho^{\gamma - 1}}{\gamma - 1} \nabla(p_\infty \rho_\infty^{-\gamma} \pi^{1-\gamma}), \tag{6c}$$

$$\pi = \exp\left(\frac{S_\infty - S}{R}\right), \tag{6d}$$

where $\mathbf{q}$ denotes the local velocity vector, a the local speed of sound, $\boldsymbol{\omega}$ the vorticity vector, p the pressure, ρ the density, S the entropy, and R the gas constant. The subscript ∞ refers to free-stream conditions.

It is of interest to notice that, since we are concerned with a local boundary-layer phenomenon, the ideal gas analysis to be developed here can be applied also to problems involving flows of real gases in thermodynamic equilibrium. When $(6a, c)$ are expanded along the lines stipulated in (a) to (d) above, one obtains the following leading equations

$$\epsilon_1^{\frac{3}{2}}\left(V_{1\bar{\eta}} + j\frac{\cos\alpha}{r_0+\bar{\eta}\cos\alpha}V_1\right) - \epsilon_1^2\delta^{-1}(\gamma+1)U_1U_{1\bar{\xi}} = 0, \tag{7a}$$

$$\epsilon_1 U_{1\bar{\eta}} - \epsilon_1^{\frac{3}{2}}\delta^{-1}V_{1\bar{\xi}} = \mu_1 D\left(\frac{2}{\gamma+1}\right)^{1/(\gamma-1)}\frac{\rho_{0\infty}}{\rho_r}\frac{a_*}{\gamma}\frac{d\pi}{d\psi}, \tag{7b}$$

where the quantities j and D are defined by

$$\left.\begin{aligned} &j = 0, \quad D = 1 && \text{for two-dimensional flow,}\\ &j = 1, \quad D = \left(1+\frac{\bar{\eta}\cos\alpha}{r_0}\right)r_0 && \text{for axisymmetric flow,}\end{aligned}\right\} \tag{8a}$$

the stream function ψ is defined by

$$\frac{\partial\psi}{\partial x} = -\frac{\rho}{\rho_r}VD, \quad \frac{\partial\psi}{\partial y} = \frac{\rho}{\rho_r}UD, \tag{8b}$$

and the factor μ_1 denotes the order of magnitude of the local entropy level. Physically significant results are obtained from $(7a, b)$ only for

$$\delta = \epsilon_1^{\frac{1}{2}}, \quad \mu_1 = \epsilon_1. \tag{9}$$

Thus, we find that the thickness of the boundary layer is proportional to the square root of the perturbation velocity in the $\bar{\xi}$-direction; upon completion of the solution we shall give a quantitative definition of the thickness δ. The second relation in (9), namely, the identity of the orders of magnitude of velocity perturbations and entropy gradients, could have been stipulated *a priori*.

Equations $(7a, b)$ can be simplified further. First, we notice that for $\alpha = \frac{1}{2}\pi$ the axisymmetric problem degenerates into the strictly two-dimensional problem; with this understanding we introduce new independent variables ξ, η defined by

$$\left.\begin{aligned} &\xi = \bar{\xi}, \quad \eta = \bar{\eta} && \text{for two-dimensional flow,}\\ &\xi = \frac{\cos\alpha}{r_0}\bar{\xi}, \quad \eta = \frac{\cos\alpha}{r_0}\bar{\eta} && \text{for axisymmetric flow.}\end{aligned}\right\} \tag{10}$$

Secondly, we observe that, within the boundary-layer approximation, the entropy gradients can be expressed by

$$\frac{d\pi}{d\psi} = \sum_{i=0}^{\infty} c_i\eta^i. \tag{11}$$

Then $(7a, b)$ can be rearranged in the final form

$$V_{1\eta} + j\left[1 + \sum_{i=1}^{\infty} (-1)^i \eta^i\right] V_1 - (\gamma+1) U_1 U_{1\xi} = 0, \tag{12a}$$

$$U_{1\eta} - V_{1\xi} = \sum_{i=0}^{\infty} K_i \eta^i, \tag{12b}$$

where

$$\left.\begin{aligned} K_i &= \left(\frac{2}{\gamma+1}\right)^{1/(\gamma-1)} \frac{\rho_{0\infty}}{\rho_r} \frac{a_*}{\gamma} c_i \qquad \text{for two-dimensional flow,} \\ K_i &= \left(\frac{2}{\gamma+1}\right)^{1/(\gamma-1)} \frac{r_0^2}{\cos\alpha} \frac{\rho_{0\infty}}{\rho_r} \frac{a_*}{\gamma} (c_{i-1} + c_i) \quad \text{for axisymmetric flow } (i \geqslant 1). \end{aligned}\right\} \tag{13}$$

The final form of the equations is, from a mathematical point of view, the same as that obtained in the analysis of transonic flow. The essential non-linearity that permits the description of mixed flows is retained.

The solution of $(12a, b)$ by means of series expansions in powers of the distance from the shoulder, with coefficients depending on an appropriate similarity variable, will now be sought. To this effect we let

$$\left.\begin{aligned} U_1 &= (\gamma+1)^{-\frac{1}{3}} \sum_{m=0}^{\infty} \eta^{d_m} u_m(\zeta), \\ V_1 &= \sum_{m=0}^{\infty} \eta^{e_m} v_m(\zeta), \\ \zeta &= (\gamma+1)^{-\frac{1}{3}} \xi \eta^{-p}. \end{aligned}\right\} \tag{14}$$

Substitution of (14) into (12) yields

$$d_0 = 2p-2, \quad d_1 = 1, \quad d_2 = 2p-1, \quad d_3 = 2,$$

$$e_0 = 3p-3, \quad e_1 = p, \quad e_2 = 3p-2, \quad e_3 = 1+p, \text{etc.}$$

One can easily prove that the exponent p in the equation for the similarity variable ζ must satisfy the requirement $1 \leqslant p < 1{\cdot}5$. The changes of flow properties along the body surface in the supersonic region must satisfy the compatibility condition for a characteristic line, namely (cf. Ferri 1954)

$$\cot\mu \frac{dq}{q} - d\theta + \sin\mu\cos\mu \frac{dS}{\gamma R} - \frac{\sin\mu\sin\theta}{\cos(\theta+\mu)} \frac{dz}{r} = 0. \tag{15}$$

Since the boundary layer extends into the supersonic region, the solution must comply with (15); effects of either three-dimensionality or rotationality of the flow must vanish at $\eta = 0$. Hence, one requires $d_1 > d_0$ and $p < 1{\cdot}5$. Also, if one combines the equation expressing the slope of the sonic line

$$\left(\frac{d\eta}{d\xi}\right)_{\text{sonic}} = \frac{1}{q}\left(\frac{\partial q}{\partial\theta}\right)_{S=\text{const.}}$$

with (15), one obtains $(d\eta/d\xi)_{\text{sonic}} = \infty$ and, therefore, $p \geqslant 1$. The equations to be satisfied by the leading terms $(n = m = 0)$ in the series (14) follow immediately

$$(3p-3) v_0 - p\zeta v_0' - u_0 u_0' = 0, \tag{16a}$$

$$(2p-2) u_0 - p\zeta u_0' - v_0' = 0. \tag{16b}$$

Upon solution of (16a, b) (see § 3 for details), one finds $p = 1{\cdot}25$. The difference between subsequent powers of η in the series (14) is then equal to $\frac{1}{2}$; the linear equations to be satisfied by the pertaining coefficients can be written in the following general form

$$(d_m + p - 1)\, v_m - p\zeta v'_m - (u_0 u'_m + u'_0 u_m) = \sum_{i=1}^{m-1} u_i u'_{m-i} - j \sum_{i=1}^{\frac{1}{2}m} (-1)^{-1} v_{(m-2i)}, \quad (17a)$$

$$d_m u_m - p\zeta u'_m - v'_m = K_{\frac{1}{2}(m-1)}\, (\gamma+1)^{\frac{1}{2}}. \quad (17b)$$

As $\zeta \to +\infty$ (supersonic side), the solutions of the systems (16) and (17) are required to behave like a Prandtl–Meyer expansion and perturbations thereof. A second set of boundary conditions consistent with the given body profile is imposed on the subsonic side. The detailed solutions of the systems (16) and (17) are reviewed in the following two sections. Several relevant considerations are similar to those made by Guderley & Yoshihara (1949) in their study of axisymmetric transonic flows.

3. The leading singularity

The flow described by (16a, b) is irrotational; and so a potential can be introduced

$$\Phi = \eta^{3p-2} g(\zeta), \quad (18)$$

such that

$$u_0 = g', \quad v_0 = (3p-2)\, g - p\zeta g'. \quad (19)$$

Equation (16b) is then identically satisfied, while (16a) becomes

$$(g' - p^2\zeta^2)\, g'' + 5p(p-1)\, \zeta g' - (3p-3)\,(3p-2)\, g = 0. \quad (20)$$

The non-linear ordinary differential equation (20) has a group property; namely, if $g = G(\zeta)$ is a solution then other solutions are given by $g = k^{-3} G(k\zeta)$, where k is an arbitrary constant. When an equation has such a property, its order can be lowered by one through an appropriate change of variables. In the present case one introduces new variables s and t

$$s = \zeta^{-3} g, \quad t = \zeta^{-2} g', \quad (21)$$

to obtain the first-order equation

$$\frac{dt}{ds} = \frac{(3p-2)\,(3p-3)\, s - p(3p-5)\, t - 2t^2}{(t-3s)\,(t-p^2)}, \quad (22)$$

and the inverse transformation law

$$\log \zeta = \int \frac{ds}{t-3s}. \quad (23)$$

Actually the change of variables is advantageous only in as far as (22) lends itself more readily to a qualitative study of the integral curves; on this basis one can proceed directly to the numerical integration of (20).

Investigation of (22) must provide the following information: (a) location of the singular points; (b) physical significance of these points; (c) structure of the integral curves in their neighbourhood; (d) general trend of the integral curves. The singular points in the finite portion of the (s, t)-plane are

$$s = 0,\ \tfrac{1}{3},\ \tfrac{5}{3}p^3(3p-2)^{-1}, \quad t = 0,\ 1,\ p^2. \quad (24)$$

The behaviour at infinity in the (s, t)-plane is studied by the conical transformation

$$s = x_1/x_0, \quad t = x_2/x_0 \tag{25}$$

and by subsequent intersection of the conical surfaces representing the integral curves with a selected plane, say $x_1 = 1$. With this choice of the plane of intersection, the integral curves of (22) are projected into those of the equation

$$\frac{dx_2}{dx_0} = \frac{x_2(x_2-3)(x_2-p^2x_0)+2x_2^2+p(3p-5)x_2x_0-(3p-2)(3p-3)x_0}{x_0(x_2-3)(x_2-p^2x_0)}, \tag{26}$$

with singular points at

$$x_0 = 0,\ 0, \quad x_1 = 1,\ 1, \quad x_2 = 0,\ 1. \tag{27}$$

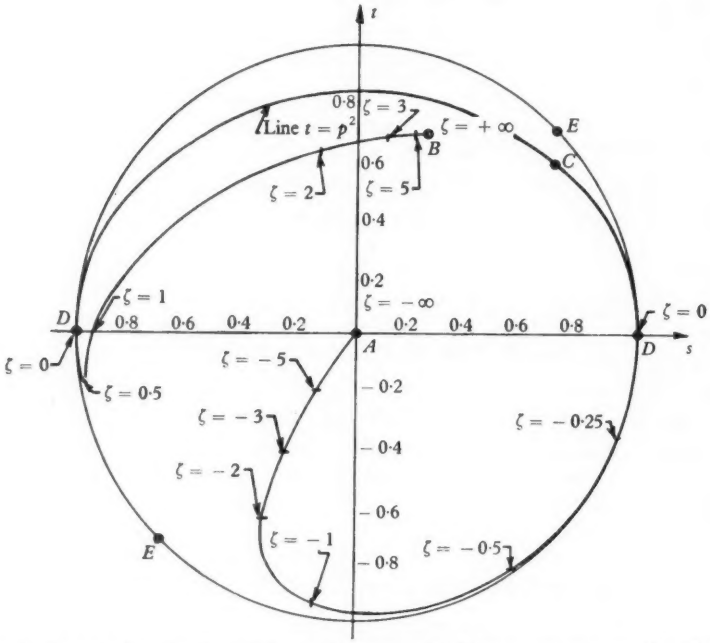

FIGURE 3. Spherical projection of the (s, t)-plane and of the curve representing the coefficient of the leading singularity. (The indicated scale of ζ is that for sonic velocity at $\zeta = 1$.)

If one selected $x_2 = 1$ as projection plane, no other singularity would appear. Hence, we conclude that all the singular points of (22) are those listed in (24) and (27). In the following we shall examine them in detail. The schematic diagram of the (s, t)-plane shown in figure 3 will be of some assistance in these considerations.

Point $s = 0, t = 0$

In the neighbourhood of this point the differential equation can be simplified to the form

$$\frac{dt}{ds} = \frac{(3p-2)(3p-3)s-p(3p-5)t}{p^2(3s-t)}. \tag{28}$$

The integral curves are then given by

$$(t-\alpha s)^{\mu}(t-\beta s)^{\nu} = C_1, \tag{29}$$

where

$$\alpha = \frac{1}{p}(3p-2), \quad \beta = \frac{1}{p}(3p-3),$$

$$\mu = -2, \quad \nu = 3.$$

The point in question is a node. In the neighbourhood of the same,

$$\zeta = C_2\left[t-\frac{1}{p}(3p-2)s\right]^{-\frac{1}{2}p}, \tag{30a}$$

$$\Phi_\xi = (\gamma+1)^{(\frac{2}{3}-p)/p}\,\xi^{2(p-1)/p}\,tC_2^{\frac{3}{2}}\left[t-\frac{1}{p}(3p-3)s\right]^{-\frac{2}{3}}, \tag{30b}$$

$$\Phi_\eta = -(\gamma+1)^{(1-p)/p}\frac{C_2^{3/p}}{p}\xi^{3(p-1)/p}. \tag{30c}$$

Since $\zeta \to \infty$, the point represents one of the edges of the boundary layer. The velocity components (30*b*, *c*) do not match the desired behaviour on the supersonic side; hence, the edge in question must be the subsonic one ($\zeta \to -\infty$). For a regular body shape on the subsonic side the velocity component Φ_η must have a non-singular asymptotic behaviour as $\zeta \to -\infty$; therefore, the solution (30*c*) is not acceptable in general. This condition leads to selecting among the solutions (29) that characterized by $C_1 = \infty$ and by

$$\left.\begin{aligned} t &= \frac{1}{p}(3p-2)s, \quad \zeta = C_3 s^{-\frac{1}{2}p}, \\ \Phi_\xi &= (\gamma+1)^{(\frac{2}{3}-p)/p}\frac{3p-2}{p}C_3^{2/p}\,|\xi|^{2(p-1)/p}, \quad \Phi_\eta = 0. \end{aligned}\right\} \tag{31}$$

Correspondingly, one finds for the function g the asymptotic expansion

$$g = (-\zeta)^{3-2/p}\sum_{i=0}^{\infty} A_i(-\zeta)^{-2i/p}, \tag{32}$$

with A_0 arbitrary ($A_0 = -C_3^{2/p}$) and

$$A_1 = \left(3-\frac{2}{p}\right)^2\left(\frac{1}{p}-1\right)A_0^2, \tag{33a}$$

$$A_2 = \frac{1}{6p^3}(2-3p)(3-2p)(4-3p)A_0A_1, \tag{33b}$$

$$A_3 = \frac{1}{15p^3}[6(2-p)^2(2-3p)A_0A_2 + (2-p)(4-3p)^2A_1^2], \tag{33c}$$

$$A_4 = \frac{1}{28p^3}[(2-3p)(5-2p)(8-3p)A_0A_3 + 3(2-p)(4-3p)(5-2p)A_1A_2], \tag{33d}$$

$$\begin{aligned} A_5 = \frac{1}{45p^3}[&2(2-3p)(3-p)(10-3p)A_0A_4 \\ &+ 2(3-p)(4-3p)(8-3p)A_1A_3 + 9(2-p)^2(3-p)A_2^2]. \end{aligned} \tag{33e}$$

The sign of A_0 (>0) is determined by the condition that $\Phi_\xi < 0$ (subsonic flow) as $\zeta \to -\infty$. Correspondingly, one moves along the integral curve in the (s,t)-plane in the direction of negative t. The magnitude of A_0 (i.e. the scale of ζ) remains arbitrary in accordance with the group property mentioned above; we shall select it so as to obtain sonic velocity ($g' = 0$) at $\zeta = 1$.

Point $s = \frac{1}{3}$, $t = 1$

In the neighbourhood of this point equation (22) is simplified by introducing variables

$$\sigma = s - \tfrac{1}{3}, \quad \tau = t - 1$$

to get

$$\frac{d\tau}{d\sigma} = \frac{(3p-2)(3p-3)\sigma - (3p^2-5p+4)\tau}{(1-p^2)(\tau-3\sigma)}. \tag{34}$$

The integral curves are then given by

$$(\tau - \alpha\sigma)^\mu (\tau - \beta\sigma)^\nu = C_1, \tag{35}$$

where

$$\alpha = (3p-2)(p-1)^{-1}, \quad \beta = 3(p-1)(p+1)^{-1},$$
$$\mu = (p+1)(7p-5)^{-1}, \quad \nu = 6(p-1)(7p-5)^{-1}.$$

For the range of interest $1 \leqslant p < 1{\cdot}5$, it is $1 \geqslant \mu > 0$ and $0 \leqslant \nu < 1$; hence, the point in question is a saddle of the integral surface (35). Along the principal directions $\tau = k\sigma$ ($k = \alpha, \beta$) through the saddle-point (these are the only two integral curves through the point), one obtains

$$\zeta = C_2 \sigma^{1/(k-3)}, \tag{36a}$$

$$\Phi_\xi = (\gamma+1)^{-\frac{1}{2}} \eta^{2p-2} \zeta^2 = (\gamma+1)^{-1} \frac{\xi^2}{\eta^2}, \tag{36b}$$

$$\Phi_\eta = -\tfrac{2}{3}\eta^{3p-3}\zeta^3 = -\tfrac{2}{3}(\gamma+1)^{-1}\frac{\xi^3}{\eta^3}. \tag{36c}$$

If $k = \alpha$, ζ tends to zero and the point $s = \frac{1}{3}$, $t = 1$ represents the η-axis. The sonic line ($\Phi_\xi = 0$) coincides with the η-axis; however, the flow is supersonic on either side of this line. Hence, the solution represented by the α integral curve must be rejected. If $k = \beta$, ζ tends to infinity, and the point in question represents either edge of the boundary layer, depending on the sign of the constant C_2. The appropriate choice is $\zeta \to +\infty$ since the velocity components (36*b*, *c*) exhibit the desired asymptotic behaviour of a Pradtl–Meyer expansion. Thus, we find that the solution for the leading singularity must be represented by the integral curve entering the singular point in the β-direction. Correspondingly, we obtain for the function g the asymptotic expansion

$$g = \zeta^3 \left[\frac{1}{3} + \sum_{i=0}^{\infty} B_i \zeta^{(\beta-3)(i+1)}\right], \tag{37}$$

with B_0 arbitrary and

$$B_1 = \beta^2(1-\beta) B_0^2 \{(3-2\beta)[2(1-\beta)(1-p^2) - p(7p-5)] - (3p-2)(3p-3)\}^{-1}, \tag{38a}$$

$$B_2 = -\beta(3-2\beta)(5-3\beta) B_0 B_1 \times \{(6-3\beta)[(5-3\beta)(1-p^2) - p(7p-5)] - (3p-2)(3p-3)\}^{-1}, \tag{38b}$$

$$B_3 = -2(2-\beta)[6\beta(2-\beta)B_0B_2-(3-2\beta)B_1^2] \times\{(9-4\beta)[4(2-\beta)(1-p^2)-p(7p-5)]-(3p-2)(3p-3)\}^{-1}, \quad (38c)$$

$$B_4 = -(11-5\beta)[\beta(9-4\beta)B_0B_3-3(3-2\beta)(2-\beta)B_1B_2] \times\{(12-5\beta)[(11-5\beta)(1-p^2)-p(7p-5)]-(3p-2)(3p-3)\}^{-1}, \quad (38d)$$

$$B_5 = -(7-3\beta)[2\beta(12-5\beta)B_0B_4-2(3-2\beta)(9-4\beta)B_1B_3-9(2-\beta)^2B_2^2] \times\{3(5-2\beta)[2(7-3\beta)(1-p^2)-p(7p-5)]-(3p-2)(3p-3)\}^{-1}. \quad (38e)$$

The sign of $B_0\,(<0)$ is determined by the condition that the velocity component Φ_ξ be decreasing as one moves inside the boundary layer from the supersonic edge; in the (s,t)-plane one is then limited to move along the β-direction in the sense of decreasing t. Again the magnitude of B_0 (scale of ζ) can be fixed arbitrarily in view of the group property of (20).

Point $s = \frac{5}{3}p^3[3p-2]^{-1}$, $t = p^2$

In the neighbourhood of this point the differential equation (22) is simplified by introducing variables

$$\sigma = s-\tfrac{5}{3}p^3(3p-2)^{-1}, \quad \tau = t-p^2$$

to get

$$\frac{d\tau}{d\sigma} = \frac{p(7p-5)(3p-2)\tau-(3p-2)^2(3p-3)\sigma}{2p^2(p+1)\tau}. \quad (39)$$

As for the previous singular point considered, the integral curves are formally given by (35) with

$$\alpha = \frac{3p-2}{2p}, \quad \beta = 3(3p-2)\frac{p-1}{p(p+1)},$$

$$\mu = 6(1-p)(7-5p), \quad \nu = (1+p)(7-5p)^{-1}.$$

For the range of interest ($1 \leqslant p < 1{\cdot}5$), μ and ν are of opposite sign; hence, the point in question is a node.

Several comments are warranted at this stage. First, we observe that any integral curve intersecting the line $t = p^2$ at $s \neq \frac{5}{3}p^3(3p-2)^{-1}$ represents a solution with a limiting line. Indeed, at the point of intersection one finds an extremum of ζ, since

$$\frac{ds}{dt} = 0 \quad \text{and, therefore,} \quad d(\log\zeta) = 0,$$

Any such solution must be rejected. Secondly, we note that any point on the line $t = p^2$ represents a first family (positive slope) characteristic line of the system (16a, b) in the physical plane since, for $t = p^2$, the two quantities

$$\left(\frac{d\eta}{d\xi}\right)_{\zeta=\text{const.}} = (\gamma+1)^{-\frac{1}{2}}(p\eta^{p-1}\zeta)^{-1},$$

$$\left(\frac{d\eta}{d\xi}\right)_{\text{charact.}} = (\gamma+1)^{-\frac{1}{2}}\Phi_\xi^{-\frac{1}{2}}$$

become identical; however, consistent with the aforementioned occurrence of limiting lines, the compatibility conditions along the characteristic, namely

$$d(\Phi_\eta)-\tfrac{2}{3}(\gamma+1)^{\frac{1}{2}}d(\Phi_\xi^{\frac{3}{2}}) = 0,$$

is identically satisfied only when the representative point is at $s = \frac{5}{3}p^3(3p-2)^{-1}$. Solutions represented by integral curves passing through the latter point must also be rejected on the following grounds: When $p > 1$ the quantities α and β are positive while the quantity $(t-3s)$ is negative; then

$$\frac{d}{dt}(\log \zeta) = (t-3s)^{-1}\frac{ds}{dt}$$

is smaller than zero. An observer proceeding in the sense of increasing ζ across the boundary layer described by such a solution, would encounter a compression in the neighbourhood of the characteristic that maps at the singular point; this situation is impossible in the subject expansion flow.

Thus, we conclude that the integral curve of interest must lie all below the line $t = p^2$.

Point $x_0 = 0, x_2 = 0$

In the neighbourhood of this point equation (26) can be simplified to the form

$$\frac{dx_2}{dx_0} = \frac{p(6p-5)x_0x_2 - x_2^2 - (3p-2)(3p-3)x_0}{3x_0(p^2x_0 - x_2)}, \tag{40}$$

which is not reducible to the standard type encountered in the previous cases. We introduce then an additional assumption; namely, $x_2 \gg x_0$, and reduce (40) to

$$\frac{dx_2}{dx_0} = \frac{x_2}{3x_0} + (p-1)(3p-2)\frac{1}{x_2},$$

which can immediately be integrated to obtain

$$x_2 = x_0^{\frac{1}{3}}[C_1 + 6(3p-2)(p-1)x_0^{\frac{1}{3}}]^{\frac{1}{2}} \tag{41}$$

consistent with the assumption. If we assumed $x_0 \gg x_2$, we could also integrate the equation readily; however, the result would not be consistent with the simplifying hypothesis. We conclude that (41) represents the integral curves of (40) within the neighbourhood in question. A plot of these integral curves is shown in figure 4. From (23), (25) and (41) one obtains

$$\zeta = C_2 s^{-\frac{1}{2}}. \tag{42}$$

Thus, as one proceeds along an integral curve through the point in question, the variable ζ goes through zero and changes of sign. It may then be conjectured that such will be the case for the integral curve of interest.

Point $x_0 = 0, x_2 = 1$

In the neighbourhood of this point (26) is simplified by introducing the variable $\sigma = (x_2 - 1)$ to obtain

$$\frac{d\sigma}{dx_0} = -\frac{\sigma}{2x_0} + (2p^2 - 5p + 3)$$

with the integral curves

$$x_2 - 1 = C_1 x_0^{-\frac{1}{2}} + \tfrac{2}{3}(2p^2 - 5p + 3)x_0. \tag{43}$$

From (23), (25) and (43) one obtains

$$\zeta = C_2 \exp(s^{-\frac{1}{2}}).$$

For s and t tending to either $+\infty$ or $-\infty$, ζ remains finite; hence, g and g' must tend to infinity, given infinite velocity. The integral curves passing in the vicinity (or through) this point must be rejected.

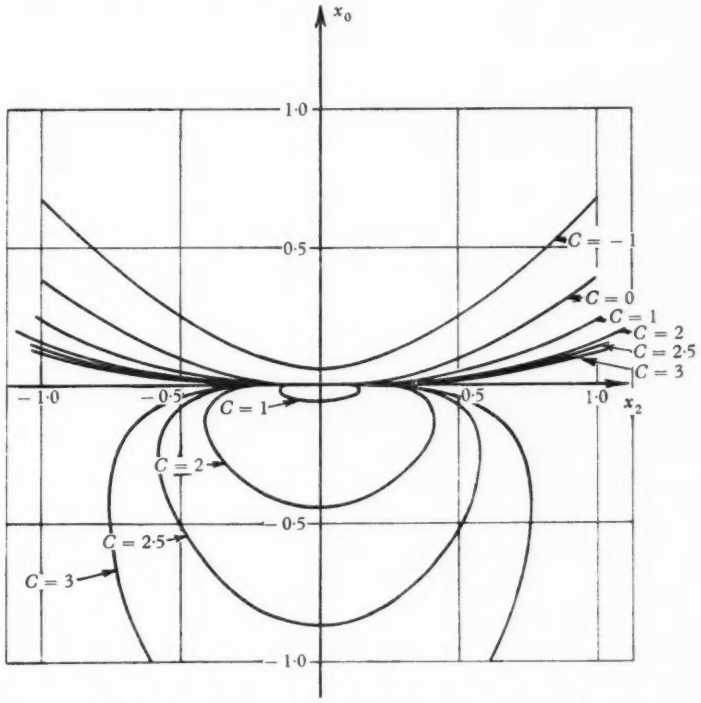

FIGURE 4. Integral curves in the neighbourhood of the singular point $x_0 = 0$, $x_2 = 0$.

From the above investigation of the singular points of (22), we conclude that the desired integral curve should have the trend shown in figure 3. The value of the exponent p, which defines the similarity variable ζ, is determined by the condition that the integral curves through the points $s = 0, t = 0$ and $s = \frac{1}{3}, t = 1$ are described by the same asymptotic law (41) as $s \to \infty$ and $t \to \infty$ ($\zeta \to 0$).

The numerical work is expedited if one operates directly on (20) along the following lines: (*a*) Two numerical integrations, both proceeding toward $\zeta = 0$, are carried out for several values of p; one integration proceeds from large negative ζ with initial values given by the series (32), and one from large positive ζ with initial values given by the series (37). (*b*) The quantities s and t are computed in the neighbourhood of $\zeta = 0$ (on both sides) from the definitions (21), and are used to determine the constant C_1 in (41). (*c*) The correct p is that for which the two values of C_1, as determined for $\zeta > 0$ and for $\zeta < 0$, are identical. In this way one finds

$$p = 1{\cdot}25, \quad C_1 = 1{\cdot}4369.$$

The scale of ζ can then be chosen and matched on both sides of $\zeta = 0$. We have selected it so that the sonic line ($g' = 0$) is described by the equation

$$\zeta = (\gamma+1)^{-\frac{1}{3}} \xi \eta^{-\frac{2}{3}} = 1.$$

With this choice of scale the coefficients A_0, B_0 and C_2 in (32), (37) and (42) become, respectively,

$$A_0 = 1{\cdot}9444, \quad B_0 = -3{\cdot}2636, \quad C_2 = -1{\cdot}2489.$$

Corresponding values of the functions g, g', g'', and $v_0 = [(3p-2)g - p\zeta g']$ are plotted in figure 5 for the range $-3 \leqslant \zeta \leqslant 3$. Outside of this range all the aforementioned functions are accurately described by the series (32) and (37).

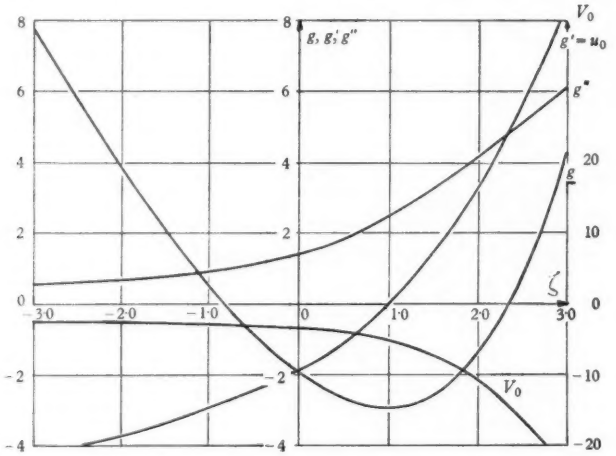

FIGURE 5. The function $g(\zeta)$ and its derivatives.

Several aspects of the solution just obtained warrant some comment. We emphasize again that the coefficient of the leading term in the series (14), which describes the flow in the boundary layer, is independent of axial symmetry and rotationality, and that it exhibits the behaviour of a Prandtl–Meyer expansion on the supersonic side. From the asymptotic behaviour of Φ_η for $\zeta \to -\infty$ [equation (31)], we find that this leading term is consistent with a flat wall on the subsonic side; we shall see in the following section that the effect of wall shape is manifested in subsequent terms of the series.

We can then compare some results of the present analysis with those obtained by Guderley's (1948) hodograph solution for two-dimensional irrotational flow over a corner with a flat wall on the subsonic side. From (31) we obtain on the subsonic side

$$\Delta p \sim \Phi_\xi \sim |\xi|^{0{\cdot}4}.$$

From the definitions of the variable ζ and of the velocity component $\Phi_\eta \sim \theta$ ($\theta \equiv$ flow direction measured from the ξ-axis), we obtain on the sonic line ($\zeta = 1$, $g' = 0$)

$$\theta \sim \eta^{\frac{1}{3}} \sim \xi^{\frac{1}{5}}.$$

Both results coincide with those given by Guderley. It can also be shown that the present solution degenerates into the well-known Prandtl–Meyer expansion when the subsonic flow is uniform (see Vaglio-Laurin 1959).

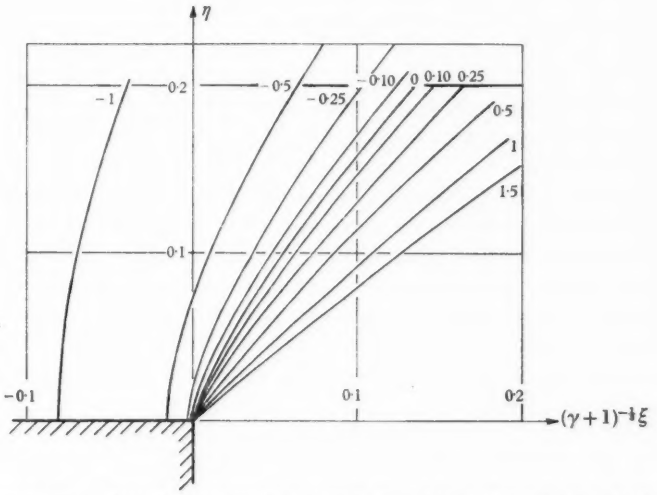

FIGURE 6. Flow described by leading singularity. Lines of constant velocity $(\gamma+1)^{\frac{1}{2}}\,\Phi_\xi = \text{const.}$

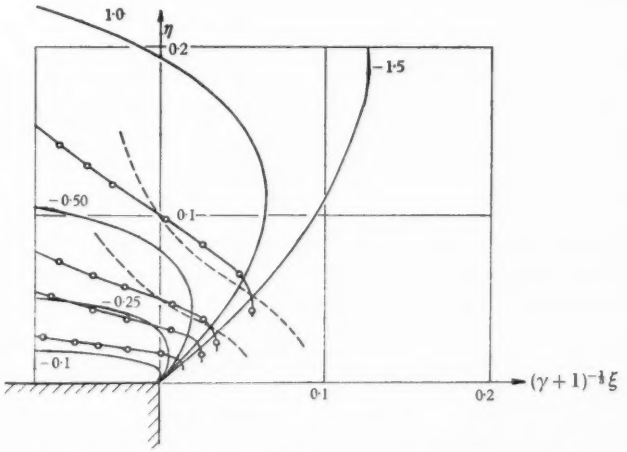

FIGURE 7. Flow described by basic singularity: ———Lines of constant flow deflexion $\theta = \Phi_\eta = \text{const.}$; —○— approximate streamlines $(\gamma+1)^{\frac{1}{2}}\,(d\eta/d\xi) = \Phi_\eta$; ---- actual streamlines $(\gamma+1)^{\frac{1}{2}}\,(d\eta/d\xi) = \Phi_\eta(1+\Phi_\xi)^{-1}$.

Some features of the flow field described by the leading singularity are shown in figures 6 and 7, where isobars, isoclines, and streamlines are plotted for the case with sonic line at $\zeta = 1$.

4. The coefficients of higher-order terms

Subsequent terms in the series (14) must be determined when the analysis of an actual flow field (either plane or axisymmetric), with given velocity and entropy distributions at infinity, is required. Upon determination of the coefficients of the higher-order terms, the behaviour of the subsonic flow in the neighbourhood of the sonic velocity can be prescribed; these boundary conditions, together with conditions at infinity and on the surface of the body, are sufficient to determine the subsonic flow field and, in particular, the magnitude of the aforementioned coefficients at the subsonic edge of the boundary layer ($\zeta \to -\infty$). Corresponding velocity distributions at the supersonic edge of the layer are provided readily by the subject solutions; thus, initial values for classical perturbations superposed on a Prandtl–Meyer flow are obtained, while the matching difficulty attached to a straightforward perturbation procedure is overcome.

The coefficients of subsequent terms in the series (14) are given by the solution of systems of linear equations written in general form at (17). Since the equations are linear, the pertaining solutions can be divided into a complementary function and a particular integral, which we shall denote by $u_m^{(0)}$, $v_m^{(0)}$ and $u_m^{(p)}$, $v_m^{(p)}$, respectively. Here we shall discuss the determination of the complementary functions, and give the particular integrals for the coefficients representing the leading effects of rotationality and axial symmetry, namely, the coefficients of η^{d_1} and η^{d_2} ($d_1 = 1$, $d_2 = 1{\cdot}5$).

In connexion with the analysis of the complementary solutions we can introduce potential functions

$$\phi_m = \eta^{d_m+p} f_m(\zeta), \tag{44}$$

such that

$$u_m^{(0)} = f_m', \quad v_m^{(0)} = (d_m+p) f_m - p\zeta f_m'. \tag{45}$$

The homogeneous equation associated with (17b) is then identically satisfied, while the homogeneous equation associated with (17a) becomes

$$(g'-p^2\zeta^2) f_m'' + [g'' + (2d_m+p-1)\, p\zeta] f_m' - (d_m+p)(d_m+p-1) f_m = 0. \tag{46}$$

Since the quantity $(g'-p^2\zeta^2)$ is never equal to zero (negative for all values of ζ), (46) has only two singular points at $\zeta = \pm\infty$. By standard methods two independent solutions for $\zeta \to -\infty$ are found:

$$f_{m1} = (-\zeta)^{(d_m/p)+1} \sum_{i=0}^{\infty} a_{mi}^{(1)} (-\zeta)^{-2i/p}, \tag{47a}$$

$$f_{m2} = (-\zeta)^{[(d_m-1)/p]+1} \sum_{i=0}^{\infty} a_{mi}^{(2)} (-\zeta)^{-2i/p} \tag{47b}$$

with $a_{m0}^{(1)}$, $a_{m0}^{(2)}$ arbitrary and, for $i \geqslant 1$,

$$a_{mi}^{(1)} = \frac{d_m+2p-2i}{p^3 i(2i-1)} \sum_{j=0}^{i-1} (d_m+p-2j)(i-j-\tfrac{3}{2}p) A_{i-j-1} a_{mj}^{(1)}, \tag{48a}$$

$$a_{mi}^{(2)} = \frac{d_m+2p-(2i+1)}{p^3 i(2i+1)} \sum_{j=0}^{i-1} (d_m+p-1-2j)(i-j-\tfrac{3}{2}p) A_{i-j-1} a_{mj}^{(2)}. \tag{48b}$$

For $\zeta \to +\infty$, two independent solutions are given by

$$\bar{f}_{m1} = \zeta^{(d_m+p)/(p-1)} \sum_{i=0}^{\infty} b_{mi}^{(2)} \zeta^{-6i/(p+1)}, \tag{49a}$$

$$\bar{f}_{m2} = \zeta^{(d_m+p-1)/(p+1)} \sum_{i=0}^{\infty} b_{mi}^{(2)} \zeta^{-6i/(p+1)}, \tag{49b}$$

with $b_{m0}^{(1)}$, $b_{m0}^{(2)}$ arbitrary and, for $i \geqslant 1$,

$$b_{mi}^{(1)} = -\frac{1}{2i}\left[\frac{d_m+p}{p-1} - \frac{6i}{p+1} + 1\right][(6i-1)(1-p) + 2(d_m+p)]^{-1} \times \sum_{j=0}^{i-1} [p-1-2(i-j-1)]\left[\frac{d_m+p}{p-1} - \frac{6j}{p+1}\right] B_{i-j-1} b_{mj}^{(1)}, \tag{50a}$$

$$b_{mi}^{(2)} = -\frac{1}{2i(p+1)^2}[d_m+2p-6i][(6i-1)(1-p) - 2(d_m+p)]^{-1} \times \sum_{j=0}^{i-1} [p-1-2(i-j-1)][d_m+p-1-6j] B_{i-j-1} b_{mj}^{(2)}. \tag{50b}$$

The solutions (47*a*, *b*) give the following asymptotic behaviour of the velocity components at the subsonic edge of the boundary layer ($\zeta \to -\infty$):

$$(\gamma+1)^{-\frac{1}{3}} \eta^{d_m} u_{m1}^{(0)} = -(\gamma+1)^{-(d_m+p)/3p}\left(\frac{d_m}{p}+1\right)|\xi|^{d_m/p}, \tag{51a}$$

$$\eta^{e_m} v_{m1}^{(0)} = 0, \tag{51b}$$

$$(\gamma+1)^{-\frac{1}{3}} \eta^{d_m} u_{m2}^{(0)} = -(\gamma+1)^{-(d_m+p-1)/3p}\left(\frac{d_m-1}{p}+1\right)\eta\,|\xi|^{(d_m-1)/p}, \tag{52a}$$

$$\eta^{e_m} v_{m2}^{(0)} = (\gamma+1)^{-(d_m+p-1)/3p}\,|\xi|^{(d_m+p-1)/p}. \tag{52b}$$

The solutions (49*a*, *b*) give the following asymptotic behaviours at the supersonic edge ($\zeta \to +\infty$):

$$(\gamma+1)^{-\frac{1}{3}} \eta^{d_m} u_{m1}^{(0)} = (\gamma+1)^{-(d_m+p)/3(p-1)} \frac{d_m+p}{p-1} \eta^{-1}\left(\frac{\xi}{\eta}\right)^{(d_m+1)/(p-1)}, \tag{53a}$$

$$\eta^{e_m} v_{m1}^{(0)} = (\gamma+1)^{-(d_m+p)/3(p-1)} \eta^{-1}\left(\frac{\xi}{\eta}\right)^{(d_m+p)/(p-1)}, \tag{53b}$$

$$(\gamma+1)^{-\frac{1}{3}} \eta^{d_m} u_{m2}^{(0)} = (\gamma+1)^{-(d_m+p-1)/3(p+1)} \frac{d_m+p-1}{p+1} \eta^{2(d_m+p-1)/(p+1)}\left(\frac{\xi}{\eta}\right)^{(d_m-2)/(p+1)}, \tag{54a}$$

$$\eta^{e_m} v_{m2}^{(0)} = (\gamma+1)^{-(d_m+p-1)/3(p+1)} \frac{d_m+2p}{p+1} \eta^{2(d_m+p-1)/(p+1)}\left(\frac{\xi}{\eta}\right)^{(d_m+p-1)/(p+1)}. \tag{54b}$$

One can immediately verify that, as $\zeta \to +\infty$, the solution $u_{m2}^{(0)}$, $v_{m2}^{(0)}$, described by (54*a*, *b*), exhibits the behaviour appropriate to perturbations superposed on a Prandtl–Meyer flow; hence, such a solution merges smoothly with that proposed by Ho & Holt (1956) at the supersonic edge of the boundary layer. Vice versa, it can be seen from (53*a*, *b*) that the second solution [cf. (49*a*)] for $\zeta \to +\infty$ must be rejected; indeed, infinite velocities at the corner would be obtained, in contrast with the physical boundary condition that the flow exactly on the body exhibit the behaviour of a Prandtl–Meyer expansion, as described by the leading singularity.

Thus, one boundary condition is obtained for the second-order equation (46) and, therefore, for the general system (17). The second condition is imposed at the subsonic edge of the boundary layer by requiring that the asymptotic behaviour of the η-component of velocity $[\eta^{e_m}(v_{m2}^{(0)} + v_m^{(p)})]$ be such as to satisfy tangency at the surface of the given body. The solution is then completely determined.

The complementary functions pertaining to (46) must be evaluated numerically. Initial conditions at large positive values of ζ are obtained (except for one arbitrary multiplying constant) from the series (49b): the solution is then continued by numerical integration toward large negative values of ζ, where it is matched with a linear combination of the series (47a, b). Upon evaluation of the particular integral, the arbitrary constant is finally determined by imposing the tangency condition on the subsonic side.

Inspection of the asymptotic behaviour of the velocity components described by the complementary functions [see (51a, b), (52a, b), and (54a, b)] leads to the

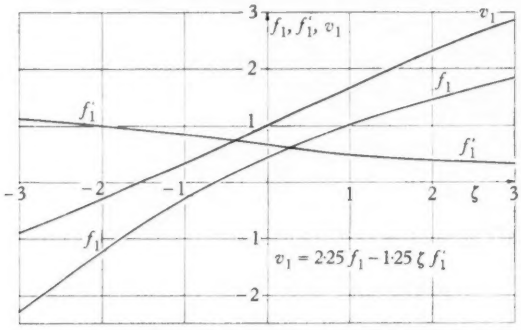

FIGURE 8. The functions $f_1(\zeta)$, $f_1'(\zeta)$ and $v_1(\zeta)$ associated with the effect of rotationality.

interesting conclusion that the subsonic and the supersonic flow are described by series involving different powers of η. Under these conditions neither straightforward expansion procedures nor gross numerical schemes can be used to analyse the flow around the sonic shoulder on a body.

Having in mind the application of the present results to the analysis of the hypersonic flow field about blunt-nosed bodies characterized by a sonic shoulder, we have determined in detail the solutions pertaining to the second and third terms in the series (14); the leading effects of entropy gradient at the wall and of axial symmetry of the flow are found thereby. It is felt that such information may be sufficient to describe the flow field within a reasonably large neighbourhood of the corner; outside of this neighbourhood the calculations could be continued by a suitable numerical scheme without requiring an extremely refined network. In this connexion, one must not overlook the fact that the present results have been obtained on the basis of a transonic small-perturbation theory and are applicable to regions of the flow field within which this approximation is valid.

The complementary functions for $d_1 = 1$ and $d_2 = 1{\cdot}5$ (satisfying the boundary conditions on the supersonic side) are plotted in figures 8 and 9 for the range

$-3 \leqslant \zeta \leqslant 3$. The solution f_1 contributes to the terms representing the effect of a uniform vorticity; the solution f_2 gives the analogous contribution for the effect of axial symmetry. Outside of the range $-3 \leqslant \zeta \leqslant 3$ the functions are accurately predicted by the series (47*a*, *b*) and (49*b*). The particular integrals to be used in

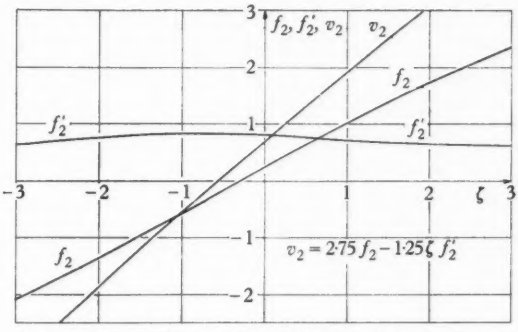

FIGURE 9. The functions $f_2(\zeta)$, $f_2'(\zeta)$ and $v_2(\zeta)$ associated with the effect of axial symmetry.

connexion with these complementary functions are easily found by inspection of the pertaining systems of equations. From the general form (17) one obtains

$$\left.\begin{aligned} pv_1 - p\zeta v_1' - (u_0 u_1' + u_0' u_1) &= 0, \\ (p+1)\,u_1 - p\zeta u_1' - v_1' &= (\gamma+1)^{\frac{1}{3}} K_0, \end{aligned}\right\} \tag{55}$$

$$\left.\begin{aligned} (p+\tfrac{1}{2})\,v_2 - p\zeta v_2' - (u_0 u_2' + u_0' u_2) &= u_1 u_1' - j v_0, \\ \tfrac{3}{2} u_2 - p\zeta u_2' - v_2' &= 0, \end{aligned}\right\} \tag{56}$$

for $d_1 = 1$ and $d_2 = 1{\cdot}5$, respectively. A particular integral of the system (55) is given by

$$u_1^{(p)} = 0, \quad v_1^{(p)} = -(\gamma+1)^{\frac{1}{3}} K_0 \zeta, \tag{57}$$

with the asymptotic behaviour

$$\zeta \to \pm\infty, \quad \eta^p v_1^{(p)} = \mp K_0 |\xi|.$$

A particular integral of the system (56), accounting only for the axisymmetric contribution (term jv_0), is given by

$$u_2^{(p)} = \tfrac{1}{10}[p\zeta g'' - 2(p+1)\,g'], \tag{58a}$$

$$v_2^{(p)} = -\tfrac{1}{10}[p^2\zeta^2 g'' - (5p+1)\,p\zeta g' + (3p-1)\,(3p+2)\,g], \tag{58b}$$

with the following asymptotic behaviour. For $\zeta \to -\infty$,

$$(\gamma+1)^{-\frac{1}{3}}\,\eta^{1{\cdot}5} u_2^{(p)} = \tfrac{1}{25}(\gamma+1)^{-\frac{7}{15}} A_0\,\eta\,|\xi|^{\frac{3}{5}}, \tag{59a}$$

$$\eta^{1{\cdot}75} v_2^{(p)} = -\tfrac{2}{5}(\gamma+1)^{-\frac{7}{15}} A_0 |\xi|^{\frac{7}{5}}, \tag{59b}$$

while for $\zeta \to +\infty$,

$$(\gamma+1)^{-\frac{1}{3}}\,\eta^{1{\cdot}5} u_2^{(p)} = -\tfrac{1}{5}(\gamma+1)^{-1}\,\eta\left(\frac{\xi}{\eta}\right)^2, \tag{60a}$$

$$\eta^{1{\cdot}75}\, v_2^{(p)} = \tfrac{1}{15}(\gamma+1)^{-1}\,\eta\left(\frac{\xi}{\eta}\right)^3. \tag{60b}$$

It will be noticed that identical asymptotic expressions of the η-component of velocity at the subsonic edge of the boundary layer are obtained from the complementary functions and from the particular integrals in the two cases considered. Hence, the tangency condition at the wall in the subsonic region can be satisfied. It should also be noticed that at the supersonic edge of the boundary layer the particular integrals depend on lower powers of η as compared to the complementary functions; thus, the contribution of the former is predominant in the immediate neighbourhood of the corner.

Finally, it should be recognized that the higher-order terms under consideration predict a finite ξ-component of velocity on the η-axis (line $\zeta = 0$). The asymptotic solutions ($54a, b$) are valid for large ζ and $\xi/\eta > 0$; therefore, no difficulty is associated with the cases characterized by $d_m < 2$.

With the information obtained thus far one may, for example, set up a procedure for the numerical determination of hypersonic flow fields about blunt bodies with a sonic shoulder. This problem is discussed in the following section.

5. Outline for application

A representative configuration of a blunt body with a sonic shoulder is shown in figure 10. The problem of determining in detail the flow field about blunt bodies of general shape can only be attacked by numerical methods. Two approaches can be followed to this effect, namely: (*a*) the 'integral method' as applied, for example, by Belotserkovskii (1958); (*b*) the 'forward integration method' as proposed, for example, by Vaglio-Laurin & Ferri (1958).

For the particular category of bodies considered here, an extension of the integral method is required to obtain the appropriate behaviour at the sonic velocity. Several difficulties are encountered in connexion with the choice of an appropriate co-ordinate system for the region adjacent to the corner, and with the determination of the number of terms required for a reasonably accurate description of the flow at a general station.

No procedural difficulty arises when the forward integration method is used. Between the alternatives of proceeding either from a prescribed shock shape or from an estimated pressure distribution on the body, the latter is preferable on the grounds of numerical work involved and of available rules for carrying out initial estimates. This point of view is corroborated by a study of Kendall's (1959) experiments; observed pressure distributions upstream of the shoulder are in agreement with the present results and with the Mach number independence principle over a range extending to low supersonic flight conditions ($M_\infty \geqslant 2$), while correlations of observed shock shapes remain uncertain.

If the forward integration analysis of the subsonic region is to proceed from the body toward the shock, one prescribes a pressure distribution consistent with the singularity at the shoulder and then analyses simultaneously the elliptic and the transonic regions up to the limiting characteristic; the final solution is obtained by iteration. When the pressure distribution in the neighbourhood of the shoulder is given, the scale of the subject singularity can readily be determined in accord with the transonic similarity rule appropriate to the simplified governing equa-

tions of §2;* thus, consistent initial conditions can be prescribed on a contour enclosing the shoulder point and extending into the supersonic region. The procedure and the transformation suggested by Vaglio-Laurin & Ferri (1958) appear to be useful for the numerical calculations. The transformation in question stretches the region adjacent to the shoulder and, therefore, requires a relatively less refined network in this neighbourhood; also, *a priori* knowledge of the

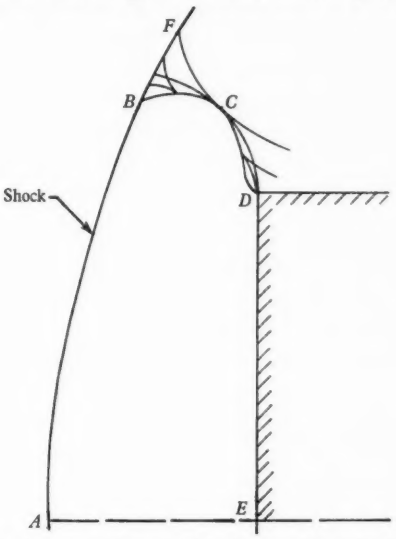

FIGURE 10. Schematic diagram of flow field about a blunt body with sonic shoulder. $ABCDEA$ = subsonic region; $DCFBCD$ = transonic region.

location of streamlines and shock in the transformed plane facilitates the estimate of a consistent entropy distribution and the application of boundary conditions at the shock front. Determination of complete flow fields using initial data based on the present solution, and subsequent comparison of theoretically determined shapes of sonic line and shock against experiments, will be of interest. Such an investigation will establish the domain of validity of the present results for practical configurations and flight conditions.

6. Concluding remarks

A critical review of the difficulties associated with a straightforward series-expansion approach to the present problem has led to the introduction of a boundary layer joining subsonic and supersonic regions. The pertaining equations have been given; a series solution therefor has been indicated. Upon determination of the leading terms in the series, the validity of the boundary layer concept has been established on the basis of: (*a*) physical criteria, such as the predicted behaviour on the solid boundary; (*b*) comparison with the known hodograph solution for two-dimensional irrotational flow; (*c*) consideration of the 'boundary-

* This similarity rule also manifested itself in the analysis of the leading singularity through arbitrariness of scale for the similarity variable ζ.

layer' flow at the supersonic edge, where the behaviour of a Prandtl–Meyer expansion and superposed perturbations is attained.

Detailed results have been presented for the leading singularity and for the first two corrections due to rotationality and axial symmetry of the flow. It has been shown that the boundary conditions at the supersonic edge essentially determine the behaviour of the coefficients in the series solution, while the conditions at infinity and the body profile in the subsonic region determine the thickness of the boundary layer, the nature of the series describing the flow in the layer, and the magnitude of the velocity components encountered therein.

As an example, the application of the present results in the analysis of the hypersonic flow about blunt bodies characterized by a sonic shoulder has been discussed. Bodies within this category are of practical interest, since, by suitable location of the shoulder, one may reduce the heat transfer at the stagnation point.

This research was supported by the United States Air Force through the Air Force Office of Scientific Research, Air Research and Development Command, under Contract No. AF 49(638)-217. The author wishes also to express his appreciation to Professor Antonio Ferri for many stimulating discussions.

Appendix

Numerical values of the leading coefficients for the series about the various singular points discussed in the analysis are compiled here. The reader interested in results outside of the asymptotic range can find detailed tabulations of the functions g, f_1 and f_2 in a report by Vaglio-Laurin (1959).

Leading singularity. When the scale of ζ is selected so that the sonic line coincides with $\zeta = 1$, the coefficients of the series (32), relative to the singularity $\zeta = -\infty$, are

$$A_0 = \ 1{\cdot}9444, \qquad A_1 = -1{\cdot}4821, \qquad A_2 = \ 0{\cdot}053795,$$
$$A_3 = -0{\cdot}017573, \qquad A_4 = \ 0{\cdot}0095676, \qquad A_5 = -0{\cdot}0067092.$$

The coefficients of the series (37), relative to the singularity $\zeta = +\infty$, are

$$B_0 = -3{\cdot}2636, \qquad B_1 = -0{\cdot}056356, \qquad B_2 = \ 0{\cdot}015895,$$
$$B_3 = -0{\cdot}0096063, \qquad B_4 = 0{\cdot}0081281, \qquad B_5 = -0{\cdot}0083370.$$

Higher-order terms. Numerical values are provided for the leading terms, respectively characterized by $d_1 = 1$ and $d_2 = 1{\cdot}5$. With the selected scale of ζ, the coefficients of the series (47 a, b), relative to the singularity at $\zeta = -\infty$, are

	$d_1 = 1$		$d_2 = \frac{3}{2}$	
i	$a_{1i}^{(1)}$	$a_{1i}^{(2)}$	$a_{2i}^{(1)}$	$a_{2i}^{(2)}$
0	1	1	1	1
1	−2·9394	−0·18144	−4·7901	−0·50804
2	−0·035555	0·035555	0	0·027654
3	−0·014193	−0·018493	−0·056770	−0·013763
4	0·018962	0·013276	0·046353	0·010353
5	−0·020263	−0·011346	−0·040683	−0·0093181

The coefficients of the series (49*b*), relative to the singularity $\zeta = +\infty$, are

	$d_1 = 1$	$d_2 = 1{\cdot}5$
i	$b_{1i}^{(2)}$	$b_{2i}^{(2)}$
0	1	1
1	0·040292	0·038902
2	−0·015134	−0·013883
3	0·011670	0·010644
4	−0·012053	−0·010998
5	0·014615	0·013356

The complementary functions f_m satisfying the boundary condition at $\zeta \to +\infty$ are linearly related to the solutions f_{m1}, f_{m2} about $\zeta \to -\infty$

$$d_1 = 1, \quad f_1 = -0{\cdot}11918 f_{11} - 0{\cdot}65264 f_{12};$$
$$d_2 = 1{\cdot}5, \quad f_2 = \quad 0{\cdot}080053 f_{21} - 0{\cdot}52709 f_{22}.$$

REFERENCES

Belotserkovskii, O. M. 1958 Flow with detached shock wave about a symmetrical profile. *Prikladnaia Matematika i Mekhanika*, **22**, 206–19.

Carrier, G. F. 1953 Boundary layer problems in applied mechanics. *Advances in Applied Mechanics*, Vol. III, pp. 1–19. New York: Academic Press.

Ferri, A. 1954 The method of characteristics. *High Speed Aerodynamics and Jet Propulsion*, Vol. VI, Section G. Princeton University Press.

Ferri, A. 1958 A review of some recent developments in hypersonic flow. *Advances in Aeronautical Sciences*, Vol. II, pp. 723–70. London: Pergamon Press.

Friedrichs, K. O. 1955 Asymptotic phenomena in mathematical physics. *Bull. Amer. Math. Soc.* **61**, 485–504.

Guderley, K. G. 1948 Singularities at the sonic velocity. *Wright-Patterson AFB Report F-TR-1171-ND.*

Guderley, K. G. & Yoshihara, H. 1949 Axial-symmetric transonic flow patterns. *Wright-Patterson AFB Report* 5797.

Ho, H. T. & Holt, M. 1956 Supersonic rotational flow around a sharp corner on a body of revolution. *WADC TN* 56-394.

Kendall, J. M. Jr. 1959 Experiments on supersonic blunt-body flows. *Jet Propulsion Laboratory, California Inst. of Technology, Rep.* 20–372.

Vaglio-Laurin, R. & Ferri, A. 1958 Theoretical investigation of the flow field about blunt-nosed bodies in supersonic flight. *J. Aero/Space Sci.* **25**, 761–70.

Vaglio-Laurin, R. 1959 *Polytechnic Institute of Brooklyn Aerodynamics Lab. Rep.* 431.

Van Dyke, M. D. 1958 The supersonic blunt-body problem—review and extension. *J. Aero. Sci.* **25**, 485–96.

von Kármán, T. 1940 The engineer grapples with non-linear problems. *Bull. Amer. Math. Soc.* **46**, 615–83.

An approximate equation for the spectrum of a conserved scalar quantity in a turbulent fluid

By I. D. HOWELLS
Trinity College, Cambridge

(Received 6 February 1960)

The formula for transfer of $\overline{\theta}^2$-stuff across the θ-spectrum, which was obtained by Batchelor, Howells & Townsend (1959) for wave-numbers at which molecular conduction is important, is extended here to smaller wave-numbers by means of a simplified general picture of the mechanism involved. The interaction of velocity and temperature fields is represented by a combination of eddy conductivity due to the smaller eddies, and a straining action due to the larger eddies, and this leads to an approximate equation for the θ-spectrum, for a fluid of arbitrary Prandtl number, over at least the equilibrium range of wave-numbers.

An earlier paper (Batchelor *et al.* 1959) on the spectrum function of a conserved scalar quantity θ (such as temperature) in a turbulent fluid was concerned with the case of small Prandtl number, and gave a formula for an effective eddy conductivity due to low Péclet number components of the flow. This eddy conductivity κ_e due to velocity Fourier components having wave-numbers greater than n is such that the rate of transfer of $\overline{\theta}^2$-stuff to wave-numbers greater than n is $2\kappa_e$ times the mean square gradient of θ associated with wave-numbers less than n, and was found to be

$$\kappa_e(n) = \frac{2}{3}\int_n^\infty \frac{E(n)}{\kappa n^2}\,dn \quad \text{provided} \quad n \gg \epsilon^{\frac{1}{4}}\kappa^{-\frac{3}{4}}, \tag{1}$$

where κ is the molecular conductivity, ϵ and $E(n)$ are the rate of dissipation, and spectrum function, of kinetic energy.

We notice that the eddy conductivity is inversely proportional to the molecular conductivity—in other words the effectiveness of the Fourier components in convecting heat down a gradient, or in transferring $\overline{\theta}^2$-stuff from lower wave-numbers, is limited by molecular conduction. The reason for this can be seen from an adaptation of the usual 'mixing-length' argument. A blob of hot fluid of size l, convected into colder fluid, loses its excess heat by conduction, in a *time* $l^2\kappa^{-1}$, whereas in a high Péclet number flow, where conduction is not important, the excess heat is lost in a *distance* l. In the latter case the eddy conductivity due to wave-numbers greater than $n(\ll \epsilon^{\frac{1}{4}}\kappa^{-\frac{3}{4}})$ is given by a formula such as

$$\int_n^\infty \left\{\frac{E(n)}{n^3}\right\}^{\frac{1}{2}} dn. \tag{2}$$

Now it is of interest to obtain one formula which includes both expressions (1) and (2). To do this we start from (1), which is asymptotically exact, and consider how it is to be extended to Péclet numbers which are not small. Here the transfer of $\overline{\theta^2}$-stuff from lower wave-numbers by velocity Fourier components is limited not only by molecular conduction but by the interference of other Fourier components, and, to make use of (1), we represent this interference as the effect of an eddy conductivity due to larger wave-numbers. That is, we replace κ in the integrand of (1) by $\kappa+\kappa_e(n)$

$$\kappa_e(n) = \frac{2}{3}\int_n^\infty \frac{E(n)}{n^2\{\kappa+\kappa_e(n)\}}\,dn,$$

which leads to

$$\kappa_e(n) = \left[\kappa^2+\frac{4}{3}\int_n^\infty \frac{E(n)}{n^2}\,dn\right]^{\frac{1}{2}} - \kappa. \tag{3}$$

At low Péclet numbers, equation (3) is equivalent to (1), and at high Péclet numbers it agrees sufficiently well with (2). However, in (2) the square-root comes inside the integral, because of the supposition that each small element of the range of wave-numbers from n to ∞ should make a separate and similar contribution to the eddy conductivity (carrying over by analogy the argument for eddy viscosity summarized in Batchelor 1953, §6.6). But this supposition implies that (2) should hold for all wave-numbers, in contradiction to (1), and when it is applied to the calculation of spectra the asymptotic forms obtained for $n\to\infty$ are negative powers of n, which are difficult to accept because they are inconsistent with the existence of all derivatives of the scalar field. In the argument leading to (3), the effect of each Fourier component involves the others, and this feature appears in the result, where the integral is inside the square root. The one general picture of the mechanism (although it is simplified) leads to a formula which includes the two limiting expressions, each in its range of validity.

The eddy conductivity mechanism is not adequate to describe the entire transfer of $\overline{\theta^2}$-stuff, since it neglects the straining action of the larger eddies, which is responsible for the transfer beyond the viscous cut-off in the case of large Prandtl number (Batchelor 1959). The additional quantity which must be introduced is a rate of strain due to wave-numbers less than n, say $\zeta(n)$. Then using the results of the above reference, and making the same sorts of approximation as are involved in the eddy conductivity arguments, we write the contribution from this mechanism to the rate of transfer of $\overline{\theta^2}$-stuff across wave-number n as $n\zeta(n)\Gamma(n)$, where $\Gamma(n)$ is the spectrum function of θ. $\zeta(n)$ should be proportional to

$$\left[\int_0^n n^2 E(n)\,dn\right]^{\frac{1}{2}},$$

and the constant of proportionality must be chosen to be about $1/\sqrt{2}$, in order to make $\zeta(\infty)$ agree with the value $\frac{1}{2}\sqrt{(\epsilon/\nu)}$ used in the paper quoted for the quantity denoted there by $-\gamma$.

Combining these effects, we can write an equation for $\Gamma(n)$ which should be valid in the same approximate way for all wave-numbers in the equilibrium

range (and possibly for part of the energy-containing range) and for all Prandtl numbers:

$$\frac{\partial}{\partial t}\int_0^n \Gamma(n)\,dn+\left[\frac{1}{2}\int_0^n n^2E(n)\,dn\right]^{\frac{1}{2}} n\Gamma(n)+2\left[\kappa^2+\frac{4}{3}\int_n^\infty \frac{E(n)}{n^2}\,dn\right]^{\frac{1}{2}}\int_0^n n^2\Gamma(n)\,dn = 0. \tag{4}$$

It might be expected that something similar could be done for kinetic energy spectrum of turbulence—certainly the simple eddy viscosity approach is in error beyond the viscous cut-off. But there are two differences, one arising from the vector nature of the velocity field, and the other from the fact that it is interacting with itself. The problem of the magnetic field in a turbulent conducting fluid (when magnetic forces are not important) also differs from that of the scalar field in the first way, but not in the second; it is possible that its study may help elucidate some of the difficulties of the kinetic energy transfer in turbulence.

REFERENCES

Batchelor, G. K. 1953 *The Theory of Homogeneous Turbulence*. Cambridge University Press.

Batchelor, G. K. 1959 *J. Fluid Mech.* **5**, 113.

Batchelor, G. K., Howells, I. D. & Townsend, A. A. 1959 *J. Fluid Mech.* **5**, 134.

Weak thermal vortex rings

By B. R. MORTON
Department of Mathematics, University of Manchester

(Received 28 February 1960)

A similarity solution is obtained up to the first order in an effective Rayleigh number for the behaviour of very weak thermal vortex rings produced by the rapid release of heat at one point of a large region of fluid.

The laminar pattern of flow is similar to that in ordinary vortex rings, but the temperature decreases outwards from the centre in all directions with some asymmetry about the horizontal plane through the centre, and there is no accumulation of heat into the vortex ring. The vortex propagates slowly in relation to its rate of growth, and the process is dominated by viscous and thermal diffusion.

Introduction

The rapid release of a quantity of heat from a compact isolated source into a large region of fluid at rest will set in motion a small volume of heated fluid. As it rises, this buoyant fluid will grow in volume through conduction of heat and viscous diffusion of momentum outwards. Since the heated fluid is displaced upwards by ambient fluid from approximately its own level and in turn displaces ambient fluid from its path, the flow must have the general pattern of a vortex ring, although this may sometimes be obscured from the observer by an opaque envelope of marked fluid or by turbulence in and around the core.

The behaviour of buoyant vortices formed by the release of buoyant fluid from rest can be characterized by a non-dimensional parameter which is proportional to the initial release of buoyancy and which plays a part corresponding to that of the Rayleigh number in problems where a length and a temperature difference are specified; it will be convenient to refer to it in this case also as a Rayleigh number. By analogy with the buoyant plumes that rise from steady sources of heat or other sources of pure positive buoyancy (positive in the sense that upwards motion is induced) it may be expected that for small over-all Rayleigh numbers the flow will be laminar in and around the corresponding vortex rings while for large Rayleigh numbers it will be turbulent. But in fact there is an additional strong source of stability in buoyant vortex rings which have light cores because the reduced density of fluid in the ring produces a stable stratification in the field of centrifugal force due to rotation about the core. Thus thermal vortex rings of normal type should have a stable pattern of laminar flow over an appreciable range of Rayleigh numbers, which will certainly include the range of small values that is to be considered here. Indeed there is evidence to show that, when sufficient time is available, initially turbulent regions of rising buoyant fluid will form into relatively well-ordered vortex rings (see, for example, Turner 1957).

When the Rayleigh number is negative, vortex rings have a heavy core and their behaviour shows a marked contrast. The rotating core is now inherently unstable to disturbances and will break up unless the Rayleigh number is small; moreover, vortex rings will not so readily grow from less ordered motions, at any rate until density differences have been reduced to a low level. This type of behaviour may be illustrated by releasing drops of dyed salt solution just below the surface of a beaker of water.

It may be noted that this difference in behaviour according as the Rayleigh number is positive or negative must be borne in mind when model experiments are designed, unless all density variations are kept very small. A further factor is that the behaviour of the accelerating surface of a volume of buoyant fluid will be different according as the fluid moving forwards is heavier or lighter than its surroundings (cf. Taylor 1950).

The analysis of buoyant vortex rings which follows will be valid only for small values of the Rayleigh number, in which case a similarity solution can be found as a power series in the Rayleigh number for the momentum and energy equations including the effects of viscosity and thermal conductivity. Under these circumstances the motion may be expected to remain laminar for a considerable time in the absence of grave disturbances in the ambient fluid, and provided that the Rayleigh number is positive. Hence the solution will represent, for suitable initial conditions, the behaviour of weak thermal vortex rings generated from rest by the rapid release of a small quantity of heat in the close neighbourhood of one point of an extensive region of fluid. The discharge of a thermal vortex ring with given initial circulation can be investigated by using appropriately modified initial conditions, but will not be included here. The results given below may be regarded as providing an asymptotic solution for weak buoyant vortex rings; an approximate treatment has already been given by Turner (1957) for stronger buoyant vortices.

Formulation

The idealized problem is the ascent, through a uniform environment of incompressible fluid, of the vortex ring generated from an instantaneous point source of heat. The flow will start impulsively from the virtual source, and for small values of the Rayleigh number will remain laminar over an appreciable distance so that it is appropriate to seek a similarity type solution.

The motion is symmetrical about a vertical axis and it seems natural to use cylindrical polar co-ordinates for reference; in fact it is more convenient to use spherical polar co-ordinates (r, θ, ϕ) with origin at the point of release of heat and the axis $\theta = 0$ directed vertically upwards, because the analysis is concerned with finding patterns of velocity and temperature which in the similarity solution do not vary with time. The velocity components can be taken as $(u, v, 0)$ since the system is independent of ϕ; the time t will be measured from the instant of release. If it is now assumed: (i) that variations in density due to temperature changes are so small that they need only be taken into account in the buoyancy term; (ii) that the effects of dissipation and the pressure term in the energy equation are negligible; and (iii) that the kinematic viscosity ν and the thermometric con-

ductivity κ may be taken as constants; then the equations that represent the convective flow are

$$\frac{\partial u}{\partial t}+u\frac{\partial u}{\partial r}+\frac{v}{r}\frac{\partial u}{\partial \theta}-\frac{v^2}{r}=-\frac{1}{\rho}\frac{\partial p}{\partial r}+\nu\left(\nabla_1^2 u-\frac{2u}{r^2}-\frac{2v\cot\theta}{r^2}-\frac{2}{r^2}\frac{\partial v}{\partial \theta}\right)+\beta g(T-T_0)\cos\theta, \tag{1}$$

$$\frac{\partial v}{\partial t}+u\frac{\partial v}{\partial r}+\frac{v}{r}\frac{\partial v}{\partial \theta}+\frac{uv}{r}=-\frac{1}{\rho r}\frac{\partial p}{\partial \theta}+\nu\left(\nabla_1^2 v-\frac{v}{r^2\sin^2\theta}+\frac{2}{r^2}\frac{\partial u}{\partial \theta}\right)-\beta g(T-T_0)\sin\theta, \tag{2}$$

$$\frac{\partial}{\partial r}(r^2 u\sin\theta)+\frac{\partial}{\partial \theta}(rv\sin\theta)=0, \tag{3}$$

$$\frac{\partial T}{\partial t}+u\frac{\partial T}{\partial r}+\frac{v}{r}\frac{\partial T}{\partial \theta}=\kappa\nabla_1^2 T, \tag{4}$$

where ρ is the fluid density, p the pressure excess over hydrostatic, T the temperature in the vortex ring and T_0 the uniform temperature of the ambient fluid, β the coefficient of expansion, and

$$\nabla_1^2\equiv\frac{1}{r^2}\frac{\partial}{\partial r}r^2\frac{\partial}{\partial r}+\frac{1}{r^2\sin\theta}\frac{\partial}{\partial \theta}\sin\theta\frac{\partial}{\partial \theta}.$$

A stream function ψ can be introduced, with

$$u=\frac{1}{r^2\sin\theta}\frac{\partial\psi}{\partial\theta},\quad v=-\frac{1}{r\sin\theta}\frac{\partial\psi}{\partial r}.$$

If p is now eliminated between (1) and (2), and (4) is rewritten in terms of the stream function,

$$\frac{\partial Z}{\partial t}+\frac{\partial(Z/r^2\sin\theta,\psi)}{\partial(r,\theta)}=\nu\left(\nabla_1^2 Z-\frac{2}{r}\frac{\partial Z}{\partial r}-\frac{Z}{r^2\sin^2\theta}\right)+\beta g\left(\frac{\partial T}{\partial\theta}\cos\theta+\frac{\partial T}{\partial r}r\sin\theta\right), \tag{5}$$

$$\frac{\partial T}{\partial t}+\frac{1}{r^2\sin\theta}\frac{\partial(T,\psi)}{\partial(r,\theta)}=\kappa\nabla_1^2 T, \tag{6}$$

where the vorticity has components $(0, 0, -Z/r)$, and

$$Z=\frac{\partial u}{\partial\theta}-\frac{\partial(rv)}{\partial r}=\operatorname{cosec}\theta\left(\frac{\partial^2\psi}{\partial r^2}+\frac{1}{r^2}\frac{\partial^2\psi}{\partial\theta^2}-\frac{\cot\theta}{r^2}\frac{\partial\psi}{\partial\theta}\right).$$

The initial conditions are that u and v are zero and $T=T_0$ at $t=0$ for all points of the field except $r=0$, where there is a singular point; for $t>0$ the field is free from singularities. The boundary conditions for $t>0$ are

$$\left.\begin{aligned} &u, v=0 \quad\text{and}\quad T=T_0 \quad\text{at}\quad r=\infty;\\ &\frac{1}{r}\frac{\partial u}{\partial\theta},\ v, \quad\text{and}\quad \frac{1}{r}\frac{\partial T}{\partial\theta}=0 \quad\text{at}\quad \theta=0,\pi.\end{aligned}\right\} \tag{7}$$

The excess of heat in the vortex ring over that in the same volume of ambient fluid remains constant and is equal to the amount Q of heat released initially,

$$2\pi\int_0^\infty\int_0^\pi(T-T_0)r^2\sin\theta\,d\theta\,dr=\frac{Q}{\rho c}=\frac{F}{\beta g},$$

where ρF is the total initial release of buoyancy.

If a similarity solution of (5) and (6) exists it must be such as to relate r and t in the group $rt^{-\frac{1}{2}}$ if t is not to appear explicitly in the transformed equations. Using the same criterion, it may be shown that (5) and (6) are reduced to non-dimensional form by the transformations

$$\eta = r/(2\kappa t)^{\frac{1}{2}},$$

$$\psi = \kappa(2\kappa t)^{\frac{1}{2}} f(\eta, \theta),$$

$$\beta(T - T_0) = \frac{1}{g} F(2\kappa t)^{-\frac{3}{2}} h(\eta, \theta).$$

Also put $$\zeta = (2t/\kappa)^{\frac{1}{2}} Z = \operatorname{cosec}\theta\left(\frac{\partial^2 f}{\partial \eta^2} + \frac{1}{\eta^2}\frac{\partial^2 f}{\partial \theta^2} - \frac{\cot\theta}{\eta^2}\frac{\partial f}{\partial \theta}\right).$$

The reduced equations are

$$-\left(\zeta + \eta\frac{\partial \zeta}{\partial \eta}\right) + \frac{\partial(\zeta/\eta^2 \sin\theta, f)}{\partial(\eta, \theta)} = \sigma\left(\nabla^2_{\eta,\theta} - \frac{2}{\eta}\frac{\partial}{\partial \eta} - \frac{1}{\eta^2 \sin^2\theta}\right)\zeta + \sigma A\left(\frac{\partial h}{\partial \theta}\cos\theta + \frac{\partial h}{\partial \eta}\eta\sin\theta\right), \tag{8}$$

$$-\left(3h + \eta\frac{\partial h}{\partial \eta}\right) + \frac{1}{\eta^2 \sin\theta}\frac{\partial(h, f)}{\partial(\eta, \theta)} = \nabla^2_{\eta,\theta} h. \tag{9}$$

The transformed boundary conditions are:

$$\left.\begin{aligned} &\frac{1}{\eta^2 \sin\theta}\frac{\partial f}{\partial \theta} = 0, \quad \frac{1}{\eta \sin\theta}\frac{\partial f}{\partial \eta} = 0, \quad h = 0, \quad \text{at} \quad \eta = \infty; \\ &\frac{1}{\eta}\frac{\partial}{\partial \theta}\frac{1}{\eta^2 \sin\theta}\frac{\partial f}{\partial \theta} = 0, \quad \frac{1}{\eta \sin\theta}\frac{\partial f}{\partial \eta} = 0, \quad \frac{1}{\eta}\frac{\partial h}{\partial \theta} = 0, \quad \text{at} \quad \theta = 0, \pi; \end{aligned}\right\} \tag{10}$$

and the integral condition reduces to

$$2\pi \int_0^\infty \int_0^\pi \eta^2 \sin\theta\, h(\eta, \theta)\, d\theta\, d\eta = 1. \tag{11}$$

The non-dimensional parameter $A = \beta g Q/\rho c \kappa \nu = F/\kappa\nu$ plays the same part in this problem as that of the Rayleigh number for cases in which a length and a temperature difference are specified, and it will also be referred to as a Rayleigh number here. For small values of A the flow in the thermal vortex ring should certainly remain laminar for a considerable time, and as the exact solution of (5) and (6) will be difficult, this suggests that a solution should be obtained as a power series expansion in the Rayleigh number A. Hence assume the expansions

$$f = Af_1 + A^2 f_2 + \ldots, \tag{12}$$

$$h = h_0 + Ah_1 + A^2 h_2 + \ldots, \tag{13}$$

where $f_i = f_i(\eta, \theta)$ and $h_i = h_i(\eta, \theta)$. The term $f_0(\eta, \theta)$ is constant, since there is no motion when $A = 0$ (i.e. $\partial f/\partial \eta = 0$, $\partial f/\partial \theta = 0$ then), and this constant can be absorbed into f. Further, the value of $h_0(\eta, \theta)$ can be found immediately from the theory of conduction of heat in solids; for when $A = 0$ (provided that κ is finite and $Q \neq 0$) the heat spreads as by conduction in a uniform solid from an instan-

taneous point source. For such a case the solution given by Carslaw & Jaeger (1947) can be written in the present notation as

$$h_0(\eta,\theta) = (2\pi)^{-\frac{3}{2}} e^{-\frac{1}{2}\eta^2}. \tag{14}$$

The other coefficient functions $f_i(\eta,\theta)$ and $h_i(\eta,\theta)$ can be found by substituting the expansions (12) and (13) into equations (8) and (9) and equating to zero the coefficients of powers of A in the two relations to give two sets of linear partial differential equations:

$$-\left(\zeta_1+\eta\frac{\partial\zeta_1}{\partial\eta}\right) = \sigma\left(\nabla_1^2-\frac{2}{\eta}\frac{\partial}{\partial\eta}-\frac{1}{\eta^2\sin^2\theta}\right)\zeta_1+\sigma\left(\cos\theta\frac{\partial h_0}{\partial\theta}+\eta\sin\theta\frac{\partial h_0}{\partial\eta}\right), \tag{15a}$$

$$-\left(\zeta_2+\eta\frac{\partial\zeta_2}{\partial\eta}\right)+\frac{\partial(\zeta_1/\eta^2\sin\theta, f_1)}{\partial(\eta,\theta)} = \sigma\left(\nabla_1^2-\frac{2}{\eta}\frac{\partial}{\partial\eta}-\frac{1}{\eta^2\sin^2\theta}\right)\zeta_2 + \sigma\left(\cos\theta\frac{\partial h_1}{\partial\theta}+\eta\sin\theta\frac{\partial h_1}{\partial\eta}\right), \tag{15b}$$

... ...;

and

$$-\left(3h_0+\eta\frac{\partial h_0}{\partial\eta}\right) = \nabla_1^2 h_0, \tag{16a}$$

$$-\left(3h_1+\eta\frac{\partial h_1}{\partial\eta}\right)+\frac{1}{\eta^2\sin\theta}\frac{\partial(h_0,f_1)}{\partial(\eta,\theta)} = \nabla_1^2 h_1, \tag{16b}$$

$$-\left(3h_2+\eta\frac{\partial h_2}{\partial\eta}\right)+\frac{1}{\eta^2\sin\theta}\left\{\frac{\partial(h_0,f_2)}{\partial(\eta,\theta)}+\frac{\partial(h_1,f_1)}{\partial(\eta,\theta)}\right\} = \nabla_1^2 h_2, \tag{16c}$$

... ...;

where in equations (15) and (16) ζ has been taken in the form

$$\zeta = A\zeta_1(\eta,\theta)+A^2\zeta_2(\eta,\theta)+\ldots,$$

so that

$$\zeta_i(\eta,\theta) = \operatorname{cosec}\theta\left(\frac{\partial^2}{\partial\eta^2}+\frac{1}{\eta^2}\frac{\partial^2}{\partial\theta^2}-\frac{\cot\theta}{\eta^2}\frac{\partial}{\partial\theta}\right)f_i,$$

and ∇_1^2 has been written in place of $\nabla^2_{\eta,\theta}$. The solution to equation (16a) satisfying the appropriate boundary conditions is known already; hence a solution of (15a) and (16b) will provide a first approximation to the behaviour of thermal vortex rings, that is a solution to the first order in the Rayleigh number.

The analysis simplifies a good deal for the particular case $\sigma = 1$, and as this is sufficient to give a good idea of the behaviour of thermal vortex rings in gases and to demonstrate the important properties of these rings, only this case will be pursued.

As a result of the boundary conditions (10), which do not depend on A, the following conditions are imposed on the f_i and h_i:

$$\left.\begin{aligned} &\frac{1}{\eta^2}\frac{\partial f_i}{\partial\theta} = 0, \quad \frac{1}{\eta}\frac{\partial f_i}{\partial\eta} = 0, \quad h_i = 0 \quad \text{at} \quad \eta = \infty; \\ &\frac{1}{\eta}\frac{\partial}{\partial\theta}\frac{1}{\eta^2\sin\theta}\frac{\partial f_i}{\partial\theta} = 0, \quad \frac{1}{\eta\sin\theta}\frac{\partial f_i}{\partial\eta} = 0, \quad \frac{1}{\eta}\frac{\partial h_i}{\partial\theta} = 0 \quad \text{at} \quad \theta = 0,\pi; \end{aligned}\right\} \tag{17}$$

and from the integral condition (11),

$$2\pi \int_0^\infty \int_0^\pi \eta^2 \sin\theta\, h_0(\eta,\theta)\, d\theta\, d\eta = 1,$$

and

$$\int_0^\infty \int_0^\pi \eta^2 \sin\theta\, h_i(\eta,\theta)\, d\theta\, d\eta = 0 \quad \text{for} \quad i \geqslant 1.$$

Solution

The first approximation to the flow field. The vorticity variable ζ_1 satisfies the differentiai equation

$$-\left(\zeta_1 + \eta \frac{\partial \zeta_1}{\partial \eta}\right) = \left(\frac{1}{\eta^2}\frac{\partial}{\partial \eta}\eta^2 \frac{\partial}{\partial \eta} + \frac{1}{\eta^2 \sin\theta}\frac{\partial}{\partial \theta}\sin\theta \frac{\partial}{\partial \theta} - \frac{2}{\eta}\frac{\partial}{\partial \eta} - \frac{1}{\eta^2 \sin^2\theta}\right)\zeta_1$$

$$+ (2\pi)^{-\frac{3}{2}}\, \eta \sin\theta \frac{\partial}{\partial \eta}(e^{-\frac{1}{2}\eta^2}), \quad (18)$$

where the Prandtl number has been given the value $\sigma = 1$. No boundary conditions for ζ_1 have been stated, but those on the related stream function variable $f_1(\eta,\theta)$ are given in (17).

If ζ_1 is assumed to be of form $\zeta_1 = z(\eta)\sin\theta$, by substitution in (18) the dependent variable $z(\eta)$ must satisfy the ordinary differential equation

$$\frac{d^2 z}{d\eta^2} + \eta \frac{dz}{d\eta} + \left(1 - \frac{2}{\eta^2}\right) z = (2\pi)^{-\frac{3}{2}}\, \eta^2 e^{-\frac{1}{2}\eta^2}. \quad (19)$$

This has the general solution

$$z = \frac{1}{\eta}\left\{c_1 \int_0^\eta t^2 e^{-\frac{1}{2}t^2}\, dt + c_2\right\} - \tfrac{1}{2}(2\pi)^{-\frac{3}{2}}\, \eta^2 e^{-\frac{1}{2}\eta^2},$$

involving two arbitrary constants c_1 and c_2. Although boundary conditions on ζ_1 have not been stated, it is clear that $c_2 = 0$ since, as $\eta \to 0$, z cannot diverge; however, it seems probable that at great distances from the point of release of heat ζ will decrease exponentially, whereas the term in c_1 behaves as η^{-1} and hence $c_1 = 0$. It will be shown at the next stage that as a result of taking

$$\zeta_1 = -\tfrac{1}{2}(2\pi)^{-\frac{3}{2}}\, \eta^2 e^{-\frac{1}{2}\eta^2} \sin\theta, \quad (20)$$

the resultant solution for f_1 satisfies all the appropriate boundary conditions from set (17), and this confirms the value $c_1 = 0$.

The stream function $f_1(\eta,\theta)$ satisfies the equation

$$\frac{\partial^2 f_1}{\partial \eta^2} + \frac{1}{\eta^2}\frac{\partial^2 f_1}{\partial \theta^2} - \frac{\cot\theta}{\eta^2}\frac{\partial f_1}{\partial \theta} = \zeta_1 \sin\theta = -\tfrac{1}{2}(2\pi)^{-\frac{3}{2}}\, \eta^2 \sin^2\theta\, e^{-\frac{1}{2}\eta^2}. \quad (21)$$

In this case the independent variable can be separated if $f_1(\eta,\theta)$ is supposed to be of form $f_1(\eta,\theta) = y(\eta)\sin^2\theta$, where

$$\frac{d^2 y}{d\eta^2} - \frac{2}{\eta^2} y = -\tfrac{1}{2}(2\pi)^{-\frac{3}{2}}\, \eta^2 e^{-\frac{1}{2}\eta^2}. \quad (22)$$

Equation (22) has the general solution

$$y = \tfrac{1}{2}(2\pi)^{-\frac{3}{2}}\left\{c_3\eta^2 + \frac{c_4}{\eta} - e^{-\frac{1}{2}\eta^2} + \frac{1}{\eta}\int_0^\eta e^{-\frac{1}{2}t^2}\,dt\right\},$$

where the arbitrary constants c_3 and c_4 can here be found from boundary conditions (17) as $c_3 = 0$ and $c_4 = 0$. It follows that the stream function variable

$$\left.\begin{aligned} f_1 &= \tfrac{1}{2}(2\pi)^{-\frac{3}{2}}\left\{\frac{1}{\eta}\int_0^\eta e^{-\frac{1}{2}t^2}\,dt - e^{-\frac{1}{2}\eta^2}\right\}\sin^2\theta, \\ &= \tfrac{1}{2}(2\pi)^{-\frac{3}{2}}\left\{\sqrt{\frac{\pi}{2}}\frac{\operatorname{erf}(\eta/\sqrt{2})}{\eta} - e^{-\frac{1}{2}\eta^2}\right\}\sin^2\theta, \end{aligned}\right\} \tag{23}$$

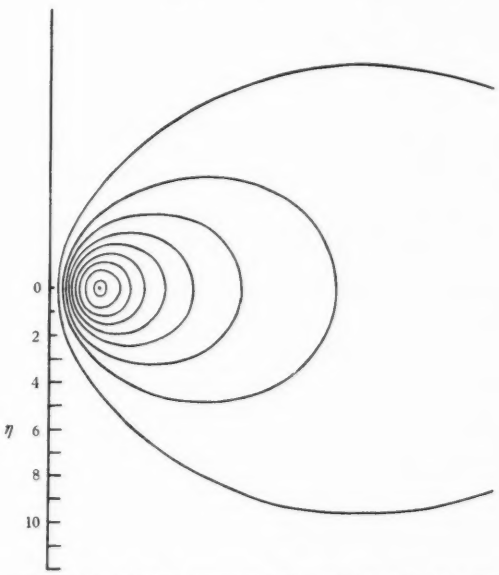

FIGURE 1. The streamlines for the first approximation to the flow in a weak thermal vortex ring. Curves are shown for equal increments of the stream function. Only the right-hand half of the field of flow is shown, and the scale for the non-dimensional length η is shown on the dividing streamline.

satisfies equation (18) written fully in terms of f_1, and also satisfies appropriate boundary conditions from the set (17), so that it gives the first approximation to the flow field. The corresponding contributions to the components of the velocity field are

$$\frac{A}{8\pi}\sqrt{\frac{\kappa}{\pi t}}\left\{\frac{2\cos\theta}{\eta^3}\left[\int_0^\eta e^{-\frac{1}{2}t^2}\,dt - \eta\,e^{-\frac{1}{2}\eta^2}\right],\quad \frac{\sin\theta}{\eta^3}\left[\int_0^\eta e^{-\frac{1}{2}t^2}\,dt - (\eta^2+1)\,\eta\,e^{-\frac{1}{2}\eta^2}\right],\quad 0\right\}.$$

Figure 1 shows a set of streamlines for the section of the vortex ring by the half plane $\phi = 0$ calculated from the first approximation $f_1(\eta, \theta)$ given by (23) and drawn at equal increments of the stream function. The vortex ring character of the flow is brought out clearly, but the pattern differs from that of an ordinary

vortex ring without buoyancy (cf. Lamb, 1932, p. 238) in that there is a larger core to the ring. This is to be expected on account of the inherently stable nature of such a light core under the forces produced by rotation about its axis.

The second approximation to the temperature field. This approximation will determine the temperature field up to the term in A, and is to be compared with the approximation to the flow field obtained above. The excess temperature variable $h_1(\eta, \theta)$ satisfies the differential equation (16*b*)

$$-\left(3h_1+\eta\frac{\partial h_1}{\partial\eta}\right)+\frac{1}{\eta^2\sin\theta}\frac{\partial(h_0,f_1)}{\partial(\eta,\theta)}=\left(\frac{1}{\eta^2}\frac{\partial}{\partial\eta}\eta^2\frac{\partial}{\partial\eta}+\frac{1}{\eta^2\sin\theta}\frac{\partial}{\partial\theta}\sin\theta\frac{\partial}{\partial\theta}\right)h_1,$$

and if the solutions for h_0 and f_1 are substituted this reduces to

$$\left\{\frac{\partial^2}{\partial\eta^2}+\left(\eta+\frac{2}{\eta}\right)\frac{\partial}{\partial\eta}+\frac{1}{\eta^2}\left(\frac{\partial^2}{\partial\theta^2}+\cot\theta\frac{\partial}{\partial\theta}\right)+3\right\}h_1$$
$$=-\frac{1}{8\pi^3\eta^2}e^{-\frac{1}{2}\eta^2}\left\{\int_0^\eta e^{-\frac{1}{2}t^2}\,dt-\eta\,e^{-\frac{1}{2}\eta^2}\right\}\cos\theta.$$

The independent variables can be separated if it is supposed that h_1 is of form $h_1(\eta,\theta)=x(\eta)\cos\theta$, where $x(\eta)$ satisfies the ordinary differential equation

$$\frac{d^2x}{d\eta^2}+\left(\eta+\frac{2}{\eta}\right)\frac{dx}{d\eta}+\left(3-\frac{2}{\eta^2}\right)x=-\frac{1}{8\pi^3\eta^2}e^{-\frac{1}{2}\eta^2}\left\{\int_0^\eta e^{-\frac{1}{2}t^2}\,dt-\eta\,e^{-\frac{1}{2}\eta^2}\right\}. \tag{24}$$

The general solution of equation (24) can be written

$$x(\eta)=-\frac{1}{8\pi^3}\frac{1+\eta^2}{\eta^2}e^{-\frac{1}{2}\eta^2}\int_0^\eta\frac{t^2e^{\frac{1}{2}t^2}}{(1+t^2)^2}\int_0^t\left\{\frac{1+s^2}{s^2}e^{-\frac{1}{2}s^2}\int_0^s e^{-\frac{1}{2}\alpha^2}\,d\alpha-\frac{1+s^2}{s}e^{-s^2}\right\}ds\,dt$$
$$+c_5\frac{1+\eta^2}{\eta^2}e^{-\frac{1}{2}\eta^2}\int_0^\eta\frac{t^2}{(1+t^2)^2}e^{\frac{1}{2}t^2}\,dt+c_6\frac{1+\eta^2}{\eta^2}e^{-\frac{1}{2}\eta^2}$$
$$=\frac{1}{32\pi^3\eta^2}e^{-\frac{1}{2}\eta^2}\{\eta\,e^{-\frac{1}{2}\eta^2}-\sqrt{(\tfrac{1}{2}\pi)}\,(1-\eta^2)\,\mathrm{erf}\,(\eta/\sqrt{2})\}$$
$$+\left(c_5-\frac{1}{16\pi^3}\right)\frac{1+\eta^2}{\eta^2}e^{-\frac{1}{2}\eta^2}\int_0^\eta\frac{t^2e^{\frac{1}{2}t^2}}{(1+t^2)^2}dt+c_6\frac{1+\eta^2}{\eta^2}e^{-\frac{1}{2}\eta^2}, \tag{25}$$

where $\sqrt{(\frac{1}{2}\pi)}\,\mathrm{erf}\,(t/\sqrt{2})=\int_0^t e^{-\frac{1}{2}\alpha^2}\,d\alpha$.

The boundary conditions on h_1, that is on $x\cos\theta$, are that $x(\eta)\cos\theta\to0$ as $\eta\to\infty$, $\eta^{-1}x(\eta)\sin\theta=0$ on $\theta=0,\ \pi$ for all η including $\eta=0$, and the integral condition

$$\int_0^\infty\int_0^\pi\eta^2x(\eta)\sin\theta\cos\theta\,d\theta\,d\eta=0.$$

For small values of η $\qquad x(\eta)=c_6/\eta^2+\frac{1}{2}c_6+O(\eta)$,

and hence $c_6=0$ since $x(0)=0$. The value of $c_5-(16\pi^3)^{-1}$ can be found using the integral condition, and the fact that this integral vanishes as the difference of two equal (but not large) parts; thus in spite of the fact that the integration over θ is zero, the integration over η must also be finite and in consequence $c_5-(16\pi^3)^{-1}=0$. Thus the excess temperature perturbation is given by

$$h_1(\eta,\theta)=\frac{1}{32\pi^3\eta^2}e^{-\frac{1}{2}\eta^2}\{\eta\,e^{-\frac{1}{2}\eta^2}-\sqrt{(\tfrac{1}{2}\pi)}\,(1-\eta^2)\,\mathrm{erf}\,(\eta/\sqrt{2})\}\cos\theta, \tag{26}$$

and the whole temperature field to the present approximation is

$$T - T_0 = \frac{\kappa\nu A}{8\beta g(\pi\kappa t)^{\frac{3}{2}}} e^{-\frac{1}{2}\eta^2}\left\{1 + \frac{A\cos\theta}{4(2\pi)^{\frac{3}{2}}}\left(\frac{1}{\eta}e^{-\frac{1}{2}\eta^2} - \sqrt{\frac{\pi}{2}}\frac{1-\eta^2}{\eta^2}\operatorname{erf}\frac{\eta}{\sqrt{2}}\right)\right\}. \tag{27}$$

This is symmetrical about the vertical ($\theta = 0, \pi$) through the origin, and the effect of the term (26) just calculated is to provide a small increase in temperature above the horizontal plane through the origin and an antisymmetrical decrease in temperature below this plane. The modification is small, and at the point where h_1 has its greatest value amounts to roughly $A/100$ times the magnitude of the initial term (relation (14)). The pattern of this modification due to the term $h_1(\eta, \theta)$ is shown by itself in figure 3 for the upper half of the thermal vortex; for

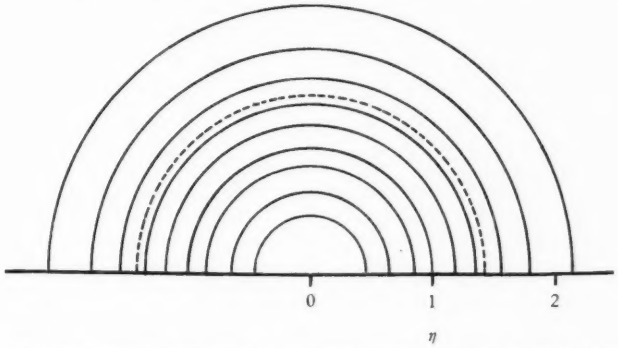

FIGURE 2. The basic approximation to the temperature field for a weak thermal vortex ring. This is the distribution produced in a solid by the instantaneous release of heat from a point. Curves are shown for equal increments of temperature (in tenths of the temperature at the centre); at the broken curve the temperature is $1/e$ of the central value, and this may be used to compare the scale of the temperature and velocity field.

purposes of comparison and so that the scale of the temperature distribution may be compared with that of motion (shown in figure 1) the first approximation to the temperature field (expression (14)) is illustrated in figure 2, again for the upper half of the thermal vortex only. Although there is a maximum value of h_1 at a distance roughly $\eta = 1$ above the origin, because of the relative smallness of this term the point of maximum temperature in the fluid will be much nearer the origin.

The point of the vortex ring at which the temperature is greatest will be vertically above the origin of release at a height which can be found by putting $\partial T/\partial r = 0$ from expression (27), and which is given by

$$\eta = \frac{A}{6(2\pi)^{\frac{3}{2}}} - \frac{13}{10}\left(\frac{A}{6(2\pi)^{\frac{3}{2}}}\right)^3 + \ldots.$$

Thus to the order of the present approximation $\eta = A/[6(2\pi)^{\frac{3}{2}}]$.

It may be noted that the distribution of heat in the thermal vortex ring is basically similar to the pattern of thermal diffusion from an instantaneous point release of heat in a solid, with the modification produced by the term $h_1(\eta, \theta)$

shown in figure 3 and resulting in a displacement upwards of the heat relative to the flow field, so that temperatures are increased in the upper parts and decreased in the lower parts of the vortex ring. There is no concentration of heat into the core of a weak thermal vortex ring.

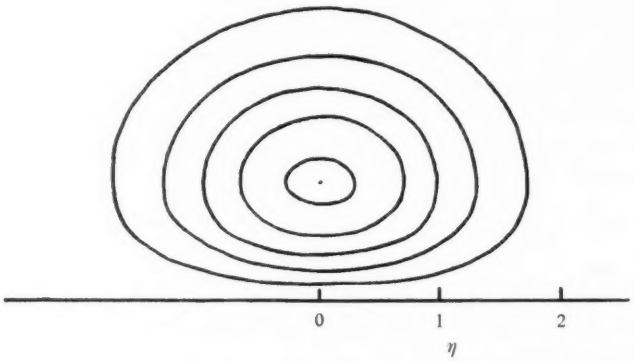

FIGURE 3. The next approximation (h_1) to the temperature field plotted separately for the upper half of the thermal vortex; the contours shown are of equal temperature increase, while a similar set of contours below the dividing horizontal will correspond with lines of equal temperature decrease relative to the basic approximation shown in figure 2. Maximum temperatures in this field are small relative to those at corresponding positions of figure 2. There is an increase of temperature corresponding to the upper half plane and a decrease for the lower.

Behaviour of weak thermal vortex rings

The next approximation to the flow field will introduce a small asymmetry which will have the effect of raising the level of the core axis above that of the origin in the similarity profile, but apart from this will introduce relatively little change in the flow pattern. Thus it will be sufficient to regard the 'centre' of the thermal vortex ring as the point at which the fluid temperature is a maximum, and this point can be identified with the information now available. According to this viewpoint, the actual height h of the vortex ring above its point of release at time t is approximately

$$h = \frac{A}{12\pi}\sqrt{\frac{\kappa t}{\pi}};$$

and the vertical velocity V of the vortex ring is

$$V = \frac{A}{24\pi}\sqrt{\frac{\kappa}{\pi t}}.$$

In addition, the radius R of the vortex ring measured from the vertical axis to the centre of the core is

$$R = 1{\cdot}512\sqrt{(2\kappa t)},$$

and the circulation K is

$$K = \frac{\kappa A}{4\pi}.$$

The energy of the system is

$$T = \frac{15}{64\pi}\rho\kappa^2 A^2 \sqrt{\frac{\kappa t}{2\pi}},$$

and the impulse is wholly upwards with magnitude

$$P = \frac{5}{4\pi}\rho\kappa^2 t A.$$

It should be noted that these have been calculated from the solution for $\sigma = 1$ (i.e. $\nu = \kappa$); they should give a good approximation for values of σ not too great or too small relative to unity, but in this case κ in the results above should be replaced by $(\kappa\nu)^{\frac{1}{2}}$ to take account of the equal importance of thermal conduction and viscous diffusion in establishing the character of convection.

It is possible now to compare these results with those of Turner (1957), although it must be borne in mind that Turner considered relatively strong vortex rings in which much of the buoyancy is concentrated into a ring core, whereas in these weak thermal vortices there is no concentration of the heat into a ring. Indeed the special features of these weak vortices is that they combine a flow field which is very much the same as that of a normal vortex ring, with a completely different distribution of temperature with a central maximum and temperature decreasing radially outwards in all directions and with a small asymmetry about the horizontal. The diameter of the ring increases linearly with height according as

$$AR = 45{\cdot}5h;$$

hence the rate of spread of a weak thermal vortex ring in terms of its rate of propagation is very much greater than for a normal buoyant vortex ring (for which $R \doteqdot 0{\cdot}2h$, say, from Turner). In fact the very weakest vortices scarcely propagate at all, although they increase in size at the same rate (depending only on $\kappa\nu$) as stronger ones. This brings out clearly the fact that the growth of weak vortices is due essentially to molecular diffusion (thermal and viscous) and not to the more familiar process of mixture with the environment produced by drawing ambient fluid into the rear of the ring. Moreover, this explains the differences found in the temperature field, for any ambient fluid which is drawn into the centre of a weak vortex enters so slowly that on the way it is heated by conduction to very nearly the previous temperature at the centre.

It may be noted that the circulation K remains constant and is proportional to the Rayleigh number A; thus the flow in the vortex ring is started impulsively at the initial instant, though the ring itself moves off from rest. The impulse, $P = 1{\cdot}094\rho K R^2$, is proportionally smaller than the value taken by Turner on account of the lower rate of propagation of weak vortices. The value of Turner's constant $c = VR/K$ is in this case 0·20; this is surprisingly close to his experimental value 0·27 found for strong buoyant rings of orthodox pattern, because the decrease in velocity is offset by the increase in radius, and it may well be that this constant varies little over a very wide range of vortex strengths.

The arguments for stability of the normal vortex ring no longer apply when the heat is concentrated towards the centre and not into the ring, and there is no

reason why weak thermal vortices should be particularly stable to disturbances. If the flow becomes unsteady there will be increased mixing with the ambient fluid in the outer sheaths and fluid drawn back towards the centre will be colder. This is probably the way in which orthodox vortex rings are produced.

As far as can be estimated from the solution to the stage it has been calculated, the results are likely to give a reasonably good picture of thermal vortices up to Rayleigh numbers of 10 or more, and in the absence of stability effects this behaviour is unlikely to change radically up to Rayleigh numbers of a few hundred, say. However, even these correspond to a release of heat in air of the order of a thousandth of a calorie, or in water of a calorie. And so the solution given above is of very little practical use, although it is interesting because it shows the existence of a different temperature distribution in weak thermal vortex rings, and because the solution in closed form can be used for a number of calculations.

REFERENCES

CARSLAW, H. S. & JAEGER, J. C. 1947 *The conduction of heat in solids.* Oxford University Press.

LAMB, H. 1932 *Hydrodynamics.* Cambridge University Press.

TAYLOR, G. I. 1950 *Proc. Roy. Soc.* A, **201**, 192.

TURNER, J. S. 1957 *Proc. Roy. Soc.* A, **239**, 61.

The propagation of waves along and through a conducting layer of gas

By G. S. S. LUDFORD
University of Maryland

(Received 10 February 1959)

Two related questions concerning the transmission of electromagnetic waves are considered:

(i) The reflexion and transmission of plane waves at a perfectly conducting layer of gas in an otherwise non-conducting atmosphere, when there is a uniform external magnetic field perpendicular to the layer. Here the main result is that a layer of finite depth h is an almost perfect filter, being transparent to waves of frequency $n\pi A_0/h$ (A_0 = Alfvén velocity, n an integer).

(ii) The existence of plane surface waves for such a finite layer. There is always one such wave and, for certain ranges of frequency, two. The first becomes 'choked' at the filter frequencies, its velocity first tending to zero and then jumping to a finite value. The second chokes at the frequencies $n\pi A_0 a_0/h\sqrt{(a_0^2+A_0^2)}$ (a_0 = acoustic velocity).

1. Introduction

At large distances from a transmitter such as a monochromatic Hertzian dipole, situated in an unbounded atmosphere, the local electromagnetic field is essentially that of a plane wave. When a layer* of different material is also present, however, the field at points on the same side as the transmitter is modified by a reflected plane wave and, for a layer of suitable composition, by a surface wave. At points sufficiently close to the layer the latter provides by far the largest contribution to the field.

In electromagnetic theory, where the emphasis is on solid materials, surface waves are associated with the names of Zenneck and Sommerfeld [though their discovery was the result of mathematical errors, see e.g. Wait (1958)]. In the theory of elasticity their counterparts are known by the names of Rayleigh and Love. The main property of plane surface waves is that they propagate along the layer without change in waveform, their amplitudes decreasing exponentially with distance from the interface(s).

Here we consider a perfectly conducting layer in an otherwise non-conducting gas when there is a uniform external magnetic field perpendicular to the layer. Plane electromagnetic waves incident on the layer are in general completely reflected,† as in the case of a conducting solid. However, a layer of finite depth h

* Here the term 'layer' is also used for a half-space, i.e. a layer of infinite depth. In the following sections a distinction is made.

† This is meant in the energy sense. There is always a refracted wave, but it transports a negligible amount of energy in general.

is completely transparent to waves of frequency $n\pi A_0/h$; here A_0 is the Alfvén velocity and n is an integer. The layer is an almost perfect filter, and this applies whatever the polarization or angle of incidence (with the exception of certain grazing incidences).*

It appears that there are two types of surface wave for a layer of finite depth, corresponding to the two types of wave which can propagate through a conducting gas. The first can be excited by a transmitter of any frequency, though as a filter frequency is approached the wave becomes 'choked', its velocity tending rapidly to zero and then jumping to the velocity of light c directly the frequency is passed. The choking also marks a transition in the symmetry of the wave. For waves of the second type, the choking takes place at other frequencies, the velocity now jumping from zero to a_0, the acoustic speed in the non-conducting part of the gas. However, there are certain ranges of frequency for which they do not exist. There are no surface waves for a layer of infinite depth.

The discussion is based on the linearized form of the continuum equations. A finite coefficient of conductivity is retained in the basic equations since this provides the link between the waves inside and outside the layer and also avoids possible error in the boundary conditions. Simplifications arise from two sources: (i) the two types of wave motion can be treated separately—this would not be the case for any other orientation of the external field with respect to the layer; (ii) the propagation velocity of the incident electromagnetic wave is much greater than that of a refracted wave inside the layer (c large compared to a_0 and A_0), which means that the refracted waves cross the layer almost normally. It is essential, however, that a_0/c and A_0/c are not neglected indiscriminately.

2. Basic equations

We consider the motion of an electrically conducting inviscid gas in the absence of body forces and heat conduction. Further we shall assume that the material coefficients μ (permeability), ϵ (dielectric constant), and σ (conductivity) are constant. Then, as has been shown in a previous paper (Ludford 1959), the equations governing small perturbations of a given uniform state

$$\mathbf{E} = 0, \quad \mathbf{H} = \mathbf{H}_0, \quad \mathbf{v} = 0, \quad p = p_0, \quad \rho = \rho_0$$

are

$$\left.\begin{aligned} \mu\frac{\partial \mathbf{H}}{\partial t} &= -\operatorname{curl}\mathbf{E}, \quad \frac{1}{\sigma}\mathbf{J} = \mathbf{E} + \mu\mathbf{v}\times\mathbf{H}_0, \\ \rho_0\frac{\partial \mathbf{v}}{\partial t} &= -\operatorname{grad} p + \mu\mathbf{J}\times\mathbf{H}_0, \\ \frac{\partial \rho}{\partial t} + \rho_0 \operatorname{div}\mathbf{v} &= 0, \quad \frac{\partial p}{\partial t} - a_0^2\frac{\partial \rho}{\partial t} = 0, \end{aligned}\right\} \tag{1}$$

where

$$\mathbf{J} = \operatorname{curl}\mathbf{H} - \epsilon\frac{\partial \mathbf{E}}{\partial t}.$$

In these equations $\mathbf{H}$, p, ρ denote deviations from $\mathbf{H}_0$, p_0, ρ_0, while $a_0^2 = (dp/d\rho)_0$, where this derivative is to be evaluated for fixed entropy.

* In some unpublished work, F. J. Fishman has found a similar result for the special case of normal incidence. This type of filtering action may have implications for propagation in the ionosphere.

The plane wave solutions may be determined as follows. Take the y-axis along $\mathbf{H}_0$ and let the x, y-plane contain the direction of propagation.* Then with all variables proportional to $\exp i(\omega t - \kappa x - \lambda y)$ and the same symbols used for factors, the equations divide into two sets, I and II, involving only E_1, E_2, H_3, v_3 for type I, and $E_3, H_1, H_2, v_1, v_2, p, \rho$, for type II. We omit the details (cf. paper cited above) and give only the results.

For waves of type I we have

$$E_1 = \frac{\kappa^2 - k^2}{\kappa\lambda} E_2 = \frac{\kappa^2 - k^2}{e\omega\lambda} H_3 = \frac{\rho_0}{H_0}(A_0^2 + i\eta\omega) v_3, \tag{2}$$

while κ, λ, and ω must satisfy the dispersion relation

$$\lambda^2 + (1-\delta)(\kappa^2 - k^2) = 0, \quad \delta = \frac{A_0^2 c^2}{(A_0^2 + i\eta\omega)(c^2 + i\eta\omega)}. \tag{3}$$

Here e is the 'complex dielectric constant' frequently used in the optics of absorbing media

$$e = \epsilon - \frac{i\sigma}{\omega} \quad \text{and} \quad k^2 = \mu e \omega^2 = \frac{\omega^2}{c^2} - \frac{i\omega}{\eta}, \tag{4}$$

while $c^2 = 1/\mu\epsilon$, $A_0^2 = \mu H_0^2/\rho_0$, and $\eta = 1/\mu\sigma$ (magnetic diffusivity).

For waves of type II we find $p = a_0^2 \rho$ and

$$E_3 = \frac{\mu\omega}{\lambda} H_1 = -\frac{\mu\omega}{\kappa} H_2 = -\frac{i\mu\omega H_0}{\eta(\kappa^2 + \lambda^2 - k^2)} v_1 = \frac{i\mu\omega H_0(\lambda^2 - \omega^2/a_0^2)}{\eta\kappa\lambda(\kappa^2 + \lambda^2 - k^2)} v_2$$
$$= \frac{iA_0^2(\lambda^2 - \omega^2/a_0^2)}{H_0\eta\kappa(\kappa^2 + \lambda^2 - k^2)} p, \tag{5}$$

while the dispersion relation becomes

$$\eta^2(\lambda^2 + \kappa^2 - k^2)(\lambda^2 + \nu\kappa^2 - \omega^2/a_0^2) = \nu A_0^2(\lambda^2 - \omega^2/a_0^2), \quad \nu = \frac{i\eta\omega}{A_0^2 + i\eta\omega}. \tag{6}$$

The corresponding results for a non-conducting fluid are obtained in the limit $\eta \to \infty$ ($\sigma \to 0$). From equations (2) and (3) we find the well-known formulas

$$E_1 = -\frac{\lambda}{\kappa} E_2 = -\frac{\lambda}{\epsilon\omega} H_3, \quad v_3 = 0, \tag{7}$$

where $\kappa^2 + \lambda^2 = \omega^2/c^2$; similarly, equations (5) and (6) yield

$$E_3 = \frac{\mu\omega}{\lambda} H_1 = -\frac{\mu\omega}{\kappa} H_2, \quad v_1 = v_2 = p = 0, \tag{8}$$

if $\kappa^2 + \lambda^2 = \omega^2/c^2$, and

$$v_1 = \frac{\kappa}{\lambda} v_2 = \frac{\kappa}{\omega\rho_0} p, \quad E_3 = H_1 = H_2, \tag{9}$$

if $\kappa^2 + \lambda^2 = \omega^2/a_0^2$. Thus the waves of type I reduce to electromagnetic waves with $\mathbf{E}$ polarized in the plane of $\mathbf{H}_0$ and the direction of propagation, while those of type II reduce either to the perpendicularly polarized waves or acoustic waves.

* This is not the same choice of axes as in the paper cited above. However, it is more convenient for the present purposes.

For future reference we also list here the first two terms in the expansions of δ and ν in ascending powers of η:

$$\left.\begin{aligned} \delta &= 1 - i\eta\omega\left(\frac{1}{A_0^2}+\frac{1}{c^2}\right)+\ldots, \\ \nu &= \frac{i\eta\omega}{A_0^2}+\frac{\eta^2\omega^2}{A_0^4}+\ldots. \end{aligned}\right\} \tag{10}$$

These will hold when the fluid is a good conductor. The detailed form of the waves in this case has also been discussed in Ludford (1959).

3. Waves of type I. Semi-infinite conducting space

Suppose that the fluid fills the whole of space, but that for $y < 0$ its conductivity is zero, while for $y > 0$ it is non-zero (but constant). All other given quantities $(\mu, \epsilon, H_0, p_0, \rho_0, a_0)$ are to remain unchanged on crossing the interface $y = 0$.

When an electromagnetic wave i (of type I) is incident on the interface from below, there will be a reflected wave r and a refracted or transmitted wave t (both of type I). The ω's and κ's of all three waves will be the same, but

$$\lambda_r = -\lambda_i, \quad \lambda_t = \sqrt{[(1-\delta)(k^2-\kappa^2)]}$$

[see equation (3)], where the root with positive real part is to be taken. Now the tangential components of the (total) electric and magnetic fields must be continuous at the interface. On expressing E_1 in terms of H_3 for each wave [see equations (2) and (7)], this leads to the conditions

$$H_i + H_r = H_t, \quad H_i - H_r = \theta H_t, \tag{11}$$

where the subscript 3 has been suppressed and

$$\theta = \frac{\epsilon(k^2-\kappa^2)}{e\lambda_i\lambda_t} = \frac{\epsilon\sqrt{(k^2-\kappa^2)}}{e\lambda_i\sqrt{(1-\delta)}}. \tag{12}$$

Thus we have

$$H_r = \frac{1-\theta}{1+\theta}H_i, \quad H_t = \frac{2}{1+\theta}H_i. \tag{13}$$

In particular, if the fluid is perfectly conducting above the interface,

$$\lambda_t = \frac{\omega}{A_0 c}\sqrt{(A_0^2+c^2)} \quad \text{and} \quad \theta = \frac{\omega A_0}{\lambda_i c\sqrt{(A_0^2+c^2)}}; \tag{14}$$

these limiting values as $\eta \to 0$ are obtained by using equations (4) and (10). The transmitted wave is an Alfvén wave which propagates in the $\mathbf{H}_0$-direction at a speed $A_0 c/\sqrt{(A_0^2+c^2)} \doteqdot A_0$, this value being independent of the incident wave. In terms of the angle of incidence ϕ_i we have

$$\theta = \frac{A_0}{\sqrt{(A_0^2+c^2)}}\sec\phi_i \doteqdot \frac{A_0}{c}\sec\phi_i, \tag{15}$$

which is an extremely small quantity except in the case of glancing incidence. Correspondingly we have

$$H_r = \tfrac{1}{2}H_t = H_i, \tag{16}$$

to a high degree of accuracy,* except for ϕ_i close to 90°. In the latter case, H_r decreases rapidly through zero to $-H_i$ and H_t decreases rapidly to zero, as $\phi_i \to 90°$. The corresponding range for the angle of refraction ϕ_t is extremely small, the largest possible value of $\tan\phi_t$ being given by

$$\max \frac{\kappa}{\lambda_t} = \frac{\omega}{c\lambda_t} = \frac{A_0}{\sqrt{(A_0^2+c^2)}} \doteq \frac{A_0}{c}.\dagger$$

For $\theta = 1$, i.e. the angle of incidence

$$\phi_i = \cos^{-1}\frac{A_0}{\sqrt{(A_0^2+c^2)}} \doteq \frac{\pi}{2} - \frac{A_0}{c}, \tag{17}$$

there is no reflected wave. The wave field is then the prototype for an alternating current in a 'fluid wire' (see, for example, Sommerfeld's treatment (1952, p. 160) of solid wires). Note the absence of a skin effect: λ_t is real and finite.

4. Waves of type I. Conducting layer

Now the conductivity of the fluid is assumed to be non-zero only within the layer $0 < y < h$. The refracted wave at $y = 0$ is also the incident wave at $y = h$ and will now be denoted by the subscript α; in addition, there will be a reflected wave β at the second interface and a transmitted wave t. The various values of λ are given by

$$\lambda_r = -\lambda_i, \quad \lambda_\alpha = -\lambda_\beta = \sqrt{[(1-\delta)(k^2-\kappa^2)]}, \quad \lambda_t = \lambda_i.$$

From the continuity of the tangential components of **E** and **H** at $y = 0$ we obtain the relations

$$H_i + H_r = H_\alpha + H_\beta, \quad H_i - H_r = \theta(H_\alpha - H_\beta), \tag{18a}$$

where θ is given by (12) (with λ_t replaced by λ_α in the first expression). Similar continuity requirements at $y = h$ yield the equations

$$\left.\begin{aligned} H_\alpha \exp(-i\lambda_\alpha h) + H_\beta \exp(-i\lambda_\beta h) &= H_t \exp(-i\lambda_t h), \\ H_\alpha \exp(-i\lambda_\alpha h) - H_\beta \exp(-i\lambda_\beta h) &= (1/\theta) H_t \exp(-i\lambda_t h). \end{aligned}\right\} \tag{18b}$$

Thus the reflected and transmitted waves are given by

$$\left.\begin{aligned} H_r &= \frac{(1/\theta - \theta)\, i \sin\lambda_\alpha h}{2\cos\lambda_\alpha h + i(1/\theta + \theta)\sin\lambda_\alpha h} H_i, \\ H_t &= \frac{2\exp(i\lambda_i h)}{2\cos\lambda_\alpha h + i(1/\theta + \theta)\sin\lambda_\alpha h} H_i. \end{aligned}\right\} \tag{19}$$

For a perfectly conducting layer, λ_α and θ are given by (14), or, in the case of θ, by (15). Since θ is very small, except for glancing incidence, it follows that the same is true of H_t, provided $\lambda_\alpha h$ is not close to a multiple of π. This last condition is violated when the frequency is near

$$\omega = \frac{A_0 c}{\sqrt{(A_0^2+c^2)}} \frac{n\pi}{h} \doteq \frac{n\pi A_0}{h} \quad \text{for some integer } n. \tag{20}$$

* This is essentially complete reflexion, since the electromagnetic waves transfer energy much faster than the Alfvén wave.

† If the incident wave were an Alfvén wave coming from above the interface, this would give the angle of incidence beyond which total reflexion occurs. Thus, effectively all such Alfvén waves are trapped.

The layer is therefore an almost perfect filter, allowing only waves with the frequencies (20) to be transmitted; to these waves it is transparent. For example, even if A_0 is as large as 10^5 cm/sec and angles of incidence up to 89° are admitted, the amplitude of H_t/H_i will have dropped from 1 to at most 1/40 by the time ω deviates by $\pi A_0/180h$ from its value (20). For normal incidence the decrease is to less than 1/2500 for the same deviation.

When $\theta = 1$ there is no reflected wave whatever the frequency. For the corresponding angle of incidence (17) the layer is transparent. For angles much closer to $\pi/2$ than (17), the filter action occurs again (θ large). Both of these last effects are almost certainly unattainable physically (for the above data ϕ_i is about $\frac{7}{10}$ of a second off 90°).

5. Waves of type II. Semi-infinite conducting space

Waves of the second type present more difficulty. For each given ω and κ there are two possible values of λ^2 satisfying (6), and hence two waves which may be excited. In the limit of zero conductivity these can be identified as electromagnetic and acoustic waves, the former carrying the variations in E_3, H_1, H_2 and the latter those in v_1, v_2, p (and ρ). In general, however, each wave bears the fluctuations of all six quantities and no distinction can be made.

Thus, when an electromagnetic wave (of type II) is incident on the single interface from below, there will be not only a reflected electromagnetic wave r but also a reflected acoustic wave a, and, in addition, two transmitted waves t and τ. All five waves will have the same ω's and κ's, while

$$\lambda_\tau = -\lambda_i, \quad \lambda_a = -\sqrt{(\omega^2/a_0^2 - \kappa^2)},$$

and λ_t, λ_τ will be the roots of (6) which have positive real part.

The continuity of the tangential component of the (total) electric field implies that of the normal component of magnetic induction, see equations (5). To these must be added the continuity of the tangential component of the magnetic field, so that in all we obtain the two relations

$$\left.\begin{aligned} H_i + H_r &= H_t + \frac{1}{C_\tau} p_\tau, \\ H_i - H_r &= \frac{\lambda_i}{\lambda_t} H_t + \frac{\lambda_i}{\lambda_\tau} \frac{1}{C_\tau} p_\tau, \end{aligned}\right\} \tag{21a}$$

when E_3 is expressed in terms of H_1 or p and the subscript 1 omitted.* Here

$$C_\tau = \frac{\rho_0 \eta \omega \kappa (\kappa^2 + \lambda_\tau^2 - k^2)}{i H_0 \lambda_\tau (\lambda_\tau^2 - \omega^2/a_0^2)}. \tag{22}$$

The remaining conditions are the continuity of pressure and of the normal component of velocity. When these two quantities are expressed in terms of H_1, for the wave t, and of p, for the waves a, and τ, we find

$$\left.\begin{aligned} p_a &= C_t H_t + p_\tau, \\ p_a &= \frac{\lambda_t}{\lambda_a} C_t H_t + \frac{\lambda_\tau}{\lambda_a} p_\tau, \end{aligned}\right\} \tag{21b}$$

where C_t is obtained from C_τ by replacing λ_τ with λ_t.

* The reason for using p instead of H_1 in the τ-wave will appear immediately.

Little is gained by writing down the solution of these four equations without first passing to the limit of infinite conductivity, and making certain approximations. In the limit we obtain

$$C = \frac{\rho_0 \omega^2 \kappa}{H_0 \lambda (\lambda^2 - \omega^2/a_0^2)}, \tag{23}$$

and the equation (6) for λ_t, λ_τ reduces, with the aid of equations (10), to

$$\left[\lambda^2 + \kappa^2 - \omega^2\left(\frac{1}{A_0^2} + \frac{1}{c^2}\right)\right]\left(\lambda^2 - \frac{\omega^2}{a_0^2}\right) = \frac{\omega^2 \kappa^2}{A_0^2}. \tag{24}$$

It is easily seen that this quadratic in λ^2 has positive roots when $\kappa \leqslant \omega/c$, so that λ_t and λ_τ are always real. We now use the fact that a_0/c and A_0/c are extremely small, which implies that κ and ω/c are small compared to ω/a_0 and ω/A_0. This yields the approximations*

$$\left.\begin{aligned} \lambda_t &= \frac{\omega}{A_0}\left[1 + \frac{A_0^2}{2\omega^2}\left(\frac{A_0^2}{a_0^2 - A_0^2}\kappa^2 + \frac{\omega^2}{c^2}\right)\right], \\ \lambda_\tau &= \frac{\omega}{a_0}\left[1 - \frac{a_0^4}{2\omega^2(a_0^2 - A_0^2)}\kappa^2\right], \end{aligned}\right\} \tag{25}$$

provided $a_0 \neq A_0$. To these may be added the approximation

$$\lambda_a = -\frac{\omega}{a_0}\left[1 - \frac{a_0^2}{2\omega^2}\kappa^2\right].$$

The expression for λ_τ shows us that the electromagnetic variables are of higher order than the dynamical in the τ-wave. From this follows the use of p_τ rather than H_τ above. In fact, the τ-wave is a modified acoustic wave and the t-wave a modified Alfvén wave [as may easily be seen from equations (5)], both of which move almost along the normal to the interface.†

With these approximations and with λ_i and κ expressed in terms of the angle of incidence ϕ_i, the solution becomes

$$\left.\begin{aligned} H_r &= \left(1 - 2\frac{A_0}{c}\cos\phi_i\right) H_i, \quad \frac{p_a}{\rho_0 a_0^2} = -\frac{A_0}{a_0 + A_0}\frac{A_0}{c}\sin\phi_i \frac{H_i}{H_0}, \\ H_t &= 2\left(1 - \frac{A_0}{c}\cos\phi_i\right) H_i, \quad \frac{p_\tau}{\rho_0 a_0^2} = -\frac{A_0}{a_0 - A_0}\frac{A_0}{c}\sin\phi_i \frac{H_i}{H_0}, \end{aligned}\right\} \tag{26}$$

where terms of the second order in a_0/c, A_0/c have been neglected. Comparison with equations (13) and (15) for waves of type I shows that $\sec\phi_i$ has been replaced by $\cos\phi_i$, as far as H_r and H_t are concerned. This means that equations (16) hold to a high degree of accuracy without qualification about the angle of incidence. The range of ϕ_t is A_0/c and that of ϕ_τ is a_0/c. There is always a reflected wave (this corresponds to the non-existence of magnetic principal waves on wires, see Sommerfeld (1952, p. 160) and the end of § 3). The acoustic waves a and τ are very weak, and in fact vanish for normal incidence.

* All we really need to know is that the second term in each bracket is of the second order. The case $a_0 = A_0$ is treated in Appendix A.

† The largest possible values of ϕ_t and ϕ_τ are A_0/c and a_0/c, respectively. If the incident wave were a t- or τ-wave coming from above the interface, the appropriate one of these would give the angle of incidence beyond which total reflexion (of electromagnetic effects) takes place. Thus, effectively all such waves are trapped.

6. Waves of type II. Conducting layer

The refracted waves at $y = 0$ are also incident waves at $y = h$ and will now be denoted by α, γ; in addition, there will be their reflexions β and δ, say, and two transmitted waves t and τ, the first electromagnetic and the second acoustic. The eight values of λ other than λ_i are determined by

$$\lambda_\tau = -\lambda_i, \quad \lambda_a = -\sqrt{[(\omega^2/a_0^2) - \kappa^2]}, \quad \lambda_\beta = -\lambda_\alpha,$$
$$\lambda_\delta = -\lambda_\gamma, \quad \lambda_t = \lambda_i, \qquad\qquad \lambda_\tau = -\lambda_a,$$

where λ_α, λ_γ are the roots of equation (6) which have positive real part.

The continuity requirements at $y = 0$ lead to the equations

$$\left.\begin{aligned} H_i + H_r &= H_\alpha + H_\beta + \frac{1}{C_\gamma}(p_\gamma - p_\delta), \\ H_t - H_r &= \frac{\lambda_i}{\lambda_\alpha}(H_\alpha - H_\beta) + \frac{\lambda_i}{\lambda_\gamma}\frac{1}{C_\gamma}(p_\gamma + p_\delta), \\ p_a &= C_\alpha(H_\alpha - H_\beta) + p_\gamma + p_\delta, \\ p_a &= \frac{\lambda_\alpha}{\lambda_a}C_\alpha(H_\alpha + H_\beta) + \frac{\lambda_\gamma}{\lambda_a}(p_\gamma - p_\delta), \end{aligned}\right\} \tag{27a}$$

while those at $y = h$ give

$$\left.\begin{aligned} e_i H_t &= e_\alpha H_\alpha + \frac{1}{e_\alpha}H_\beta + \frac{1}{C_\gamma}\left(e_\gamma p_\gamma - \frac{1}{e_\gamma}p_\delta\right), \\ e_i H_t &= \frac{\lambda_i}{\lambda_\alpha}\left(e_\alpha H_\alpha - \frac{1}{e_\alpha}H_\beta\right) + \frac{\lambda_i}{\lambda_\gamma}\frac{1}{C_\gamma}\left(e_\gamma p_\gamma + \frac{1}{e_\gamma}p_\delta\right), \\ \frac{1}{e_a}p_\tau &= C_\alpha\left(e_\alpha H_\alpha - \frac{1}{e_\alpha}H_\beta\right) + e_\gamma p_\gamma + \frac{1}{e_\gamma}p_\delta, \\ -\frac{1}{e_a}p_\tau &= \frac{\lambda_\alpha}{\lambda_a}C_\alpha\left(e_\alpha H_\alpha + \frac{1}{e_\alpha}H_\beta\right) + \frac{\lambda_\gamma}{\lambda_a}\left(e_\gamma p_\gamma - \frac{1}{e_\gamma}p_\delta\right). \end{aligned}\right\} \tag{27b}$$

Here the C's are given by (22) with λ_τ replaced by the appropriate λ. The e's stand for $\exp(-i\lambda h)$, with the suitable λ inserted, and give the changes in phase across the layer.

We pass immediately to the limit of infinite conductivity, and make the same approximations* as in the last section. The waves α, β are then seen to be modified Alfvén waves and γ, δ modified acoustic waves. The solution of the eight equations (27) for the two reflected and two transmitted waves turns out to be

$$\begin{aligned} \frac{H_r}{i\sin\lambda_\alpha h} &= \frac{(H_0 p_a/\rho_0 a_0^2)}{\{A_0[A_0\cos\lambda_\alpha h - a_0 i\sin\lambda_\alpha h - A_0\exp(-i\lambda_\gamma h)]/(a_0^2 - A_0^2)\}(A_0\sin\phi_i/c)} \\ &= \frac{(H_0 p_\tau/\rho_0 a_0^2)}{\{A_0\exp(-i\lambda_a h)[A_0 - \exp(-i\lambda_\gamma h)(A_0\cos\lambda_\alpha h + a_0 i\sin\lambda_\alpha h)]/(a_0^2 - A_0^2)\}(A_0\sin\phi_i/c)} \\ &= \frac{H_t}{2(A_0\cos\phi_i/c)\exp(i\lambda_i h)} = \frac{H_i}{i\sin\lambda_\alpha h + 2(A_0\cos\phi_i/c)\cos\lambda_\alpha h}, \end{aligned} \tag{28}$$

when terms of the second order are neglected.

* The case $a_0 = A_0$ is treated in Appendix A.

The values of H_r and H_t should be compared with equation (19) for waves of type I; $1/\theta$ has been replaced by $c/A_0 \cos\phi_i$, in accordance with what we found in the last section, and θ by zero. As a consequence the qualification about glancing incidence is absent* and the layer is an almost perfect filter for all angles of incidence, effectively transmitting only waves whose frequency satisfies $\sin \lambda_x h = 0$, i.e.

$$\omega = \frac{n\pi A_0}{h}, \quad \text{with } n \text{ an integer.} \tag{29}$$

The acoustic waves are usually very weak, and in any case vanish for normal incidence. The incident wave is, in general, essentially reflected as an electromagnetic wave.

7. Surface waves of type I

We turn now to a related but quite different question, namely, the existence of wave systems, propagating without loss parallel to the layer,† in which the amplitudes of the waves outside the layer decrease exponentially with distance from the interface(s). The importance of such natural oscillations of the conducting region is that they tend to trap the energy radiated by an electromagnetic transmitter and transport it parallel to the layer [see Wait (1958) for a discussion of solid conductors].

Note that, in the case of the semi-infinite conducting space, we are not concerned with the total reflexion of waves coming from above the interface, though these give an exponentially damped electromagnetic wave. Such wave systems are produced by a source of energy deep within the conducting fluid. In the notation of § 3, we ask for a solution of (11) in which $H_i = 0$, the only condition on λ_r being that it is positive imaginary; ω is assumed given, while κ, henceforth assumed positive for definiteness, is to be determined. It is clear on physical grounds that there is no solution; since λ_t is real in equation (14), energy would be propagated away from the interface into the conducting region. This is confirmed by showing that $\theta = -1$ has no solution of the required kind.

For the finite conducting layer the situation is different. We ask for a solution of equations (18) with $H_i = 0$, the condition on $\lambda_r = -\lambda_t$ again being that it is positive imaginary. Physically the question makes sense. The Alfvén waves can combine to form a standing wave in y-direction, the energy transport taking place in the x-direction. In fact, this is what occurs, the wave system being symmetric about $y = \frac{1}{2}h$ for some values of h and antisymmetric for the rest.

On setting the determinant of equations (18) equal to zero [i.e. the denominator in either of equations (19)], we find the condition

$$\theta = \frac{\omega A_0}{\lambda_t c \sqrt{(A_0^2 + c^2)}} = i \cot \tfrac{1}{2}\lambda_x h, \quad -i \tan \tfrac{1}{2}\lambda_x h,$$

where

$$\lambda_x = \omega \frac{\sqrt{(A_0^2 + c^2)}}{A_0 c}.$$

* In fact the filtering action improves as the angle of incidence increases, and the example for normal incidence in § 5 is now a conservative estimate for all angles of incidence.

† The conductivity is assumed infinite from now on.

Thus, remembering that $\lambda_i = \sqrt{[(\omega^2/c^2) - \kappa^2]}$, we have

$$\lambda_i = -i\frac{\omega A_0}{c\sqrt{(A_0^2+c^2)}}\tan\tfrac{1}{2}\lambda_\alpha h, \quad i\frac{\omega A_0}{c\sqrt{(A_0^2+c^2)}}\cot\tfrac{1}{2}\lambda_\alpha h,$$

$$\kappa^2 = \frac{\omega^2}{c^2}\left[1+\frac{A_0^2}{A_0^2+c^2}\tan^2\tfrac{1}{2}\lambda_\alpha h\right], \quad \frac{\omega^2}{c^2}\left[1+\frac{A_0^2}{A_0^2+c^2}\cot^2\tfrac{1}{2}\lambda_\alpha h\right].$$

The corresponding wave systems are

$$\frac{H_r}{2\cos\frac{1}{2}\lambda_\alpha h} = \frac{H_\alpha}{\exp(\frac{1}{2}i\lambda_\alpha h)} = \frac{H_\beta}{\exp(-\frac{1}{2}i\lambda_\alpha h)} = \frac{H_t}{2\cos\frac{1}{2}\lambda_\alpha h\exp(i\lambda_i h)},$$

and

$$\frac{H_r}{2i\sin\frac{1}{2}\lambda_\alpha h} = \frac{H_\alpha}{\exp(\frac{1}{2}i\lambda_\alpha h)} = -\frac{H_\beta}{\exp(-\frac{1}{2}i\lambda_\alpha h)} = -\frac{H_t}{2i\sin\frac{1}{2}\lambda_\alpha h\exp(i\lambda_i h)},$$

respectively, the first being symmetric and the second antisymmetric.

From the condition on λ_r it follows that the first system is acceptable only when $\tan\frac{1}{2}\lambda_\alpha h$ is positive and the second only when this quantity is negative. As ω increases, the change from one to the other takes place at the filter frequencies (20), the velocity ω/κ decreasing rapidly to zero and then jumping to c. Between two filter frequencies, the penetration depth $1/|\lambda_i|$ of the electromagnetic waves decreases from ∞ to 0 as ω increases.

8. Surface waves of type II

As in the case of waves of type I (and for a similar reason), there are no surface waves of type II when the conducting region is semi-infinite. This is shown formally in Appendix B.

We therefore pass to the conducting layer, and consider the determinant of the system (27) with $H_i = 0$. As before we require that $\lambda_r = -\lambda_t$ shall be positive imaginary, and, correspondingly, that λ_a shall be positive imaginary. This determinant splits into two factors, one corresponding to an antisymmetric wave-system in H and the other to a symmetric one. Thus κ satisfies one or other of the equations

$$\left.\begin{aligned}
&[(\omega^2/a_0^2)-\lambda_\alpha^2](\lambda_\alpha\sin\tfrac{1}{2}\lambda_\alpha h - i\lambda_i\cos\tfrac{1}{2}\lambda_\alpha h)(\lambda_\gamma\sin\tfrac{1}{2}\lambda_\gamma h + i\lambda_a\cos\tfrac{1}{2}\lambda_\gamma h)\\
&\quad = [(\omega^2/a_0^2)-\lambda_\gamma^2](\lambda_\gamma\sin\tfrac{1}{2}\lambda_\gamma h - i\lambda_i\cos\tfrac{1}{2}\lambda_\gamma h)(\lambda_\alpha\sin\tfrac{1}{2}\lambda_\alpha h + i\lambda_a\cos\tfrac{1}{2}\lambda_\alpha h),\\
&[(\omega^2/a_0^2)-\lambda_\alpha^2](\lambda_\alpha\cos\tfrac{1}{2}\lambda_\alpha h + i\lambda_i\sin\tfrac{1}{2}\lambda_\alpha h)(\lambda_\gamma\cos\tfrac{1}{2}\lambda_\gamma h - i\lambda_a\sin\tfrac{1}{2}\lambda_\gamma h)\\
&\quad = [(\omega^2/a_0^2)-\lambda_\gamma^2](\lambda_\gamma\cos\tfrac{1}{2}\lambda_\gamma h + i\lambda_i\sin\tfrac{1}{2}\lambda_\gamma h)(\lambda_\alpha\cos\tfrac{1}{2}\lambda_\alpha h - i\lambda_a\sin\tfrac{1}{2}\lambda_\alpha h),
\end{aligned}\right\} \tag{30}$$

where λ_α and λ_γ are determined as functions of κ by the equation (24).

The situation is not as simple as it was for waves of type I. We therefore consider two limiting cases, namely, (i) a_0 small, and (ii) A_0 small, and then (iii) the 'choking' phenomenon $\kappa = \infty$, for arbitrary a_0, A_0. The first corresponds to low temperature and the second to small applied magnetic field.

(i) When a_0 is small the roots of (24) are given by

$$\lambda_a = i\kappa, \quad \lambda_\gamma = \frac{\omega}{a_0},$$

correct to terms $O(1)$. Note that κ is no smaller than ω/a_0, since we require $\lambda_a^2 < 0$. The first of the relations (30) now reduces to

$$(\lambda_\alpha \sin \tfrac{1}{2}\lambda_\alpha h - i\lambda_i \cos \tfrac{1}{2}\lambda_\alpha h)(\lambda_\gamma \sin \tfrac{1}{2}\lambda_\gamma h + i\lambda_a \cos \tfrac{1}{2}\lambda_\gamma h) = 0,$$

where we may take $\lambda_i = -i\kappa$. Since the first factor is negative [it may be rewritten as $-\kappa(\sinh \frac{1}{2}\kappa h + \cosh \frac{1}{2}\kappa h)$], we are left with

$$i\lambda_a = -\lambda_\gamma \tan \tfrac{1}{2}\lambda_\gamma h = -\frac{\omega}{a_0} \tan \frac{1}{2}\frac{\omega h}{a_0},$$

which, because of the requirement on λ_a, can only be satisfied when $\tan \omega h/2a_0$ is positive. Then we have

$$\kappa = \frac{\omega}{a_0}\left|\sec \frac{1}{2}\frac{\omega h}{a_0}\right|, \quad \lambda_a = i\frac{\omega}{a_0} \tan \frac{1}{2}\frac{\omega h}{a_0}.$$

Similarly, the second of equations (30) can be satisfied only when $\tan \omega h/2a_0$ is negative and then

$$\kappa = \frac{\omega}{a_0}\left|\operatorname{cosec} \frac{1}{2}\frac{\omega h}{a_0}\right|, \quad \lambda_a = -i\frac{\omega}{a_0} \cot \frac{1}{2}\frac{\omega h}{a_0}.$$

As ω increases the change from one wave system to the other takes place at the values

$$\omega = \frac{n\pi a_0}{h}, \quad \text{with } n \text{ an integer}, \tag{31}$$

and not at the filter frequencies (29), as in the case of waves of type I. Between adjacent frequencies (31), the penetration depth $1/|\lambda_i|$ of the electromagnetic waves decreases from a_0/ω to zero, while that of the acoustic waves decreases from ∞ to 0.

(ii) We turn now to the case where A_0 is small, for which two possibilities for κ must be distinguished. If κ is small compared to ω/A_0, we find

$$\lambda_\alpha = i\sqrt{\left(\kappa^2 - \frac{\omega^2}{a_0^2}\right)}, \quad \lambda_\gamma = \frac{\omega}{A_0},$$

correct to terms $O(1)$, and the first of equations (30) reduces to

$$(\lambda_\gamma \sin \tfrac{1}{2}\lambda_\gamma h - i\lambda_i \cos \tfrac{1}{2}\lambda_\gamma h)(\sin \tfrac{1}{2}\lambda_\alpha h + i \cos \tfrac{1}{2}\lambda_\alpha h)\lambda_a = 0.$$

It follows that either $\lambda_a = 0$, i.e. $\kappa = \omega/a_0$, or else

$$i\lambda_i = \lambda_\gamma \tan \tfrac{1}{2}\lambda_\gamma h = \frac{\omega}{A_0} \tan \frac{1}{2}\frac{\omega h}{A_0},$$

i.e.

$$\kappa = \sqrt{\left(\frac{\omega^2}{c^2} + \frac{\omega^2}{A_0^2} \tan^2 \frac{1}{2}\frac{\omega h}{A_0}\right)}. \tag{32}$$

Since λ_i must be negative imaginary and κ larger than ω/a_0, this last result holds for

$$\tan \frac{1}{2}\frac{\omega h}{A_0} \geqslant A_0\sqrt{\left(\frac{1}{a_0^2} - \frac{1}{c^2}\right)}. \tag{33}$$

Further approximation shows that the first result is valid (in the sense that λ_a is actually a small positive imaginary) when

$$\frac{1}{1 + 2/\omega h\sqrt{(1/a_0^2 - 1/c^2)}} A_0\sqrt{\left(\frac{1}{a_0^2} - \frac{1}{c^2}\right)} \leqslant \tan \frac{1}{2}\frac{\omega h}{A_0} \leqslant A_0\sqrt{\left(\frac{1}{a_0^2} - \frac{1}{c^2}\right)}.$$

The κ, ω-curve is continuous at the right end-point of such an interval; its approximate representation changes from $\kappa = \omega/a_0$ to equation (32), however.* On the other hand, for values of κ comparable with or greater than ω/A_0, a similar analysis shows that

$$\kappa = \frac{\omega}{A_0} \tan \frac{1}{2} \frac{\omega h}{A_0},$$

where once again the tangent must be positive. Clearly this is the completion of equation (32).

Similarly, the second of equations (30) yields equation (32) and the inequality (33) with the tangent replaced by the minus cotangent. The solution corresponding to $\lambda_a = 0$ above is the exact root $\lambda_x = 0$, which must be rejected [$\kappa < \omega/a_0$, see equation (24)].

The pattern is now clear. As ω increases there is a change from one wave-system to the other at the filter frequencies (29). With the exception of the first interval, there is a portion at the lower end of each of the intervals between filter frequencies for which no wave system exists. In the intervals for which $\tan \omega h/2A_0$ is positive the penetration depth $1/|\lambda_i|$ of the electromagnetic waves decreases from $1/\omega\sqrt{(1/a_0^2 - 1/c^2)}$ to zero [at first like $1/\omega\sqrt{(1/a_0^2 - 1/c^2)}$] while that of the acoustic waves decreases from ∞ to 0 (at first remaining infinite). In the remaining intervals ($\tan \omega h/2A_0 < 0$) the total changes are the same, though the initial phases are absent.

(iii) Finally, we consider the 'choking' phenomenon $\kappa = \infty$, for arbitrary values of a_0 and A_0. When κ is large (in comparison with ω/a_0, ω/A_0), the roots of equation (24) are determined by

$$\lambda_x = i\kappa, \quad \lambda_\gamma = \omega \sqrt{\left(\frac{1}{a_0^2} + \frac{1}{A_0^2}\right)},$$

correct to terms $O(1)$. Now the two relations (30) reduce to

$$\lambda_\gamma \sin \tfrac{1}{2}\lambda_\gamma h - \kappa \cos \tfrac{1}{2}\lambda_\gamma h = 0, \quad \text{i.e. } \kappa = \lambda_\gamma \tan \tfrac{1}{2}\lambda_\gamma h,$$

$$\lambda_\gamma \cos \tfrac{1}{2}\lambda_\gamma h + \kappa \sin \tfrac{1}{2}\lambda_\gamma h = 0, \quad \text{i.e. } \kappa = -\lambda_\gamma \cot \tfrac{1}{2}\lambda_\gamma h,$$

the first being valid for $\tan \frac{1}{2}\lambda h$ positive and the second for it negative. Thus, in fact, the choking takes place for the values

$$\omega = \frac{n\pi}{h} \frac{a_0 A_0}{\sqrt{(a_0^2 + A_0^2)}}, \quad \text{with } n \text{ an integer},$$

the previous approximations being in agreement with this value. In particular we see that, in contrast to waves of type I, it is fortuitous if a choking frequency is also a filter frequency.

I am indebted to S. Goldstein for suggesting this problem and for his interest at every stage. My thanks are also due to Max Krook for improvements in the manuscript. This research was supported in part by the United States Air Force under Contract No. AF 49(638)–154, monitored by the AF Office of Scientific Research of the Air Research and Development Command, and in part by the Office of Ordnance Research, U.S. Army, under Contract DA–36–034–ORD–1486 with the University of Maryland.

* The situation is similar to that of two half-asymptotes being the limit curve of a family of half-hyperbolas.

Appendix A

For $a_0 = A_0$ and $\kappa \neq 0$,* the approximations (25) are replaced by

$$\lambda_t = \frac{\omega}{a_0}\left[1 + \frac{a_0\kappa}{2\omega} + \frac{a_0^2}{8\omega^2}\left(2\frac{\omega^2}{c^2} - 3\kappa^2\right)\right],$$

$$\lambda_\tau = \frac{\omega}{a_0}\left[1 - \frac{a_0\kappa}{2\omega} + \frac{a_0^2}{8\omega^2}\left(2\frac{\omega^2}{c^2} - 3\kappa^2\right)\right],$$

where now it is necessary to know the second-order terms explicitly in order to determine the solution of the equations (21) correct to the first order. We find, in terms of the angle of incidence ϕ_i,

$$H_r = \left(1 - 2\frac{a_0}{c}\cos\phi_i\right) H_i, \quad \frac{p_a}{\rho_0 a_0^2} = -\frac{1}{2}\frac{a_0}{c}\sin\phi_i \frac{H_i}{H_0},$$

$$H_t = \left[1 + \frac{a_0}{c}\left(\tfrac{1}{2}\operatorname{cosec}\phi_i - \cos\phi_i - \tfrac{1}{4}\sin\phi_i\right)\right] H_i,$$

$$\frac{p_\tau}{\rho_0 a_0^2} = -\left[1 + \frac{a_0}{c}\left(\tfrac{1}{4}\sin\phi_i - \cos\phi_i\right)\right]\frac{H_i}{H_0}.$$

Thus the reflected waves are the same as for $A_0 \to a_0$ [see equations (26)], but the τ-wave is no longer weak, compensatory changes occurring in the t-wave.

Similarly, the solution of the system (27) for the layer becomes

$$\frac{H_r}{\tfrac{1}{2}(\overline{e_\alpha + e_\gamma}^2 - 4) + (a_0/c)\left[\tfrac{1}{2}(e_\alpha^2 - e_\gamma^2)\operatorname{cosec}\phi_i + (\overline{e_\alpha + e_\gamma}^2 - 4)\cos\phi_i\right]}$$

$$= \frac{(H_0 p_a/\rho_0 a_0^2)}{(e_\gamma^2 - e_\alpha^2) + (a_0/c)\left[(e_\gamma^2 - e_\alpha^2)\cos\phi_i + (1 - e_\alpha e_\gamma)\sin\phi_i - \tfrac{1}{2}(e_\alpha - e_\gamma)^2\operatorname{cosec}\phi_i\right]}$$

$$= \frac{e_i H_t}{-4(a_0/c)(e_\alpha + e_\gamma)\cos\phi_i}$$

$$= \frac{(1/e_a)(H_0 p_\tau/\rho_0 a_0^2)}{2(e_\gamma - e_\alpha) + (a_0/c)\left[6(e_\gamma - e_\alpha)\cos\phi_i + \tfrac{1}{2}(e_\alpha + e_\gamma)(1 - e_\alpha e_\gamma)\sin\phi_i\right]}$$

$$= \frac{H_i}{\tfrac{1}{2}(\overline{e_\alpha + e_\gamma}^2 - 4) - (a_0/c)\left[8\cos\phi_i + \tfrac{1}{2}(e_\gamma^2 - e_\alpha^2)\operatorname{cosec}\phi_i\right]},$$

so far as the transmitted and reflected waves are concerned. When these formulas are simplified by setting $e_\gamma = e_\alpha(1 + i\omega h \sin\phi_i/c)$ the result is the formal limit of equations (28). Hence similar remarks to those at the end of §6 apply here also.

Appendix B

The vanishing of the determinant of the system (21) with $H_i = 0$ yields the condition

$$\left(\frac{\omega^2}{a_0^2} - \lambda_t^2\right)(\lambda_t + \lambda_i)(\lambda_\tau - \lambda_a) = \left(\frac{\omega^2}{a_0^2} - \lambda_\tau^2\right)(\lambda_\tau + \lambda_i)(\lambda_t - \lambda_a), \tag{34}$$

* When $\phi_i = 0$ the results (26) and (28) hold even when $a_0 = A_0$. In fact in both cases $p_a = p_\tau = 0$ without approximation.

where the value of C has been taken from equation (23). Now λ_i and λ_a are required to be pure imaginaries, while for real $\kappa > \omega/a_0$ equation (24) has two real roots ($\pm\lambda_t$, say) and two purely imaginary roots ($\pm\lambda_\tau$). Since $\lambda_i \neq -\lambda_a$ for any κ, it follows [on taking real and imaginary parts of equation (34)] that

$$\left(\frac{\omega^2}{a_0^2} - \lambda_t^2\right)(\lambda_\tau - \lambda_a) = 0, \quad \left(\frac{\omega^2}{a_0^2} - \lambda_\tau^2\right)(\lambda_\tau + \lambda_i) = 0$$

must hold simultaneously. It is now easily checked that none of the four possibilities which these last conditions offer is compatible with λ_t and λ_τ satisfying (24).

REFERENCES

LUDFORD, G. S. S. 1959 The propagation of small disturbances in hydromagnetics. *J. Fluid Mech.* **5**, 387–400.

SOMMERFELD, A. 1952 *Electrodynamics.* New York: Academic Press.

WAIT, J. R. 1958 Transmission and reflection of electromagnetic waves in the presence of stratified media. *J. Res. Nat. Bur. Standards*, **61**, 205–32.

The flow past a flat plate of finite width

By J. W. ELDER
Geophysics Division, D.S.I.R., Wellington, New Zealand

(Received 8 February 1960)

An experimental study of the incompressible flow near the side edge of a finite flat plate at zero incidence is reported for the Reynolds number range 10^4 to 10^6, but comparison with data already published shows that the conclusions are quantitatively valid for Reynolds numbers up to 10^9. The laminar velocity field is everywhere convex and does not contain any secondary flow other than that of the normal diffusive growth of the layer, but has a logarithmic singularity at the edge where the stress is controlled by the local radius of curvature. The excess skin friction due to the edge is considerably greater than that given by calculations based on the Rayleigh approximation but agrees with a recent Pohlhausen calculation by Varley (1958). Near the edge the high stress and ease of momentum diffusion makes the flow very unstable and turbulent spots occur well upstream of the normal transition zone in the middle of the plate. The spots originate from a nearly point-like region at the edge of the plate and grow linearly in time at the same rate as ordinary turbulent spots to sweep out a narrow tongue of turbulent fluid near the edge until they merge with the normal transition zone. Within this tongue a weak secondary flow of Prandtl's second kind, driven by the anisotropic Reynolds stresses, begins to develop. In fully turbulent flow when the secondary flow is largely localized to within a few boundary-layer thicknesses of the edge the secondary flow velocities are everywhere less than 0·04 of the free-stream velocity. Nevertheless, the secondary flows from each of the side edges interact, regardless of the width of the plate, to increase the total drag coefficient by an amount 0·0004 which is independent both of the Reynolds number and the width of the plate except when it is very narrow. This simple result allows apparent discrepancies between various formulations of the drag coefficient of a finite plate to be reduced to less than $\pm 1\,\%$ S.D. Of these formulations Schoenherr's (1932) empirical relation agrees best with the present data.

1. Introduction

Here is an experimental study of certain three-dimensional boundary layers directed towards a knowledge of the laminar, transitional and turbulent flow over a flat plate of finite breadth and in particular to the flow near a side edge. Consider a thin rectangular plate of breadth B and thickness $T \ll B$ in the XOZ plane of the Cartesian frame $OXYZ$ in a uniform free stream of velocity U_1 parallel to OX, as shown in figure 1. Let the side edges $z = 0, B$ be rounded to some definite form so that the typical radius of curvature of the edge cross-section a is of order T and the leading edge of sufficiently slender elliptical form to avoid separation, except during studies of the fully turbulent flow when separation

and transition is encouraged by a leading edge of square form. The flow at section x will be determined by U_1, the kinematic viscosity ν, x, a and B. (The intensity of turbulence in the free stream will also be important but its effect will not be considered here.) Suitable dimensionless parameters are the Reynolds number $R = U_1 x/\nu$, δ/a and δ/B, where $\delta(x)$ is the boundary-layer thickness. Near the leading edge for laminar, transitional and turbulent flow the flow will be dominated by R. Further downstream where the boundary-layer thickness is no longer small compared with a or B the flow will be influenced by the form of the

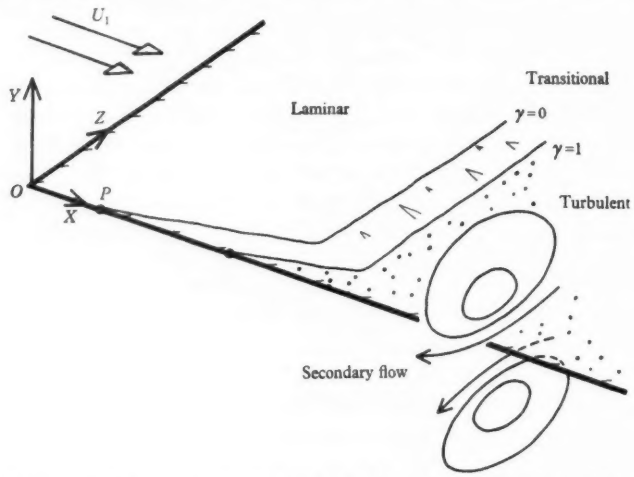

FIGURE 1. Diagram of the edge of a flat plate showing the Cartesian co-ordinate system, the laminar, transitional and turbulent flow areas and the form of the mean secondary flow streamlines.

body cross-section. Such effects arise near the side edges of the plate and will be found to be dominated by δ/a for laminar and transitional flow but by δ/B for turbulent flow. Initially the flow in the middle of the plate is unaffected by the presence of the edges, but for large values of δ/B when the boundary-layer thickness is comparable with the largest dimension of the body cross-section the entire flow field is influenced by the presence of the edges. For very large values of δ/B when the boundary-layer thickness is very much larger than B the flow is again almost everywhere independent of the form of the body cross-section. The present work is a study of the dependence of the various flow régimes on the above parameters. Briefly, as sketched in figure 1, these flow régimes, laminar, transitional and turbulent, will be found to succeed each other in the normal fashion except that near the edge (1) in the laminar zone the wall stress is very large, (2) transition to turbulence occurs very early and (3) the turbulent flow maintains a weak secondary flow. These effects are not unexpected.

In spite of a considerable amount of work in recent years on three-dimensional laminar boundary layers (Moore 1956) very little progress has been made for the present case where the boundary wall is everywhere parallel to the incident flow. The only full solution of such a flow is the calculation by Lighthill & Glauert

(1955) for the axisymmetric boundary layer on a circular cylinder. No detailed solution of the laminary boundary-layer flow near an edge has been given but two well-known approximations have been applied to the problem. The first is based on Rayleigh's (1911) method of obtaining a rough answer by assuming that momentum is convected everywhere at the speed of the free stream. Batchelor (1954) has applied the method to cylinders of arbitrary cross-section, while Howarth (1950) has given a detailed solution for the flow near the edge of a quarter-infinite plate. Lighthill & Glauert (1955) showed that the approximation is good only a long way downstream. The second approach is Varley's (1958) valuable calculation of the total drag for cylinders of arbitrary section by a Pohlhausen method.

The comparative stability of a laminar boundary layer over, say, a laminar jet is due to the restraining action of the wall. Near an edge it is to be expected that the restraint will be less than that distant from the edge so that disturbances will grow more quickly near the edge. In fact, after my experiments were completed, I found that there was already definite evidence in the literature to this effect. First, Murphy & Phinney (1951) to illustrate a paint method of indicating transition give a photograph showing the transition curve on a finite flat plate. Secondly, Tagori *et al.* (1955) have compared the position of transition as indicated by hot wires and the paint method by means of the flow over a semi-submerged plank. In both instances no particular significance was attached to the form of the transition curves. The curves show, near the edges, wedges of turbulent fluid growing downstream at an angle of 8–10° to the wall (as sketched by the lines $\gamma = 0$ and $\gamma = 1$ in figure 1) till they merge with the normal transition zone. This is similar to the so-called transverse contamination of a laminar flow studied by Charters (1943).

For practical reasons such as estimating the drag of ships it is desirable to make measurements of the frictional drag on flat plates due to the turbulent boundary layer at the largest possible Reynolds number, in which case it has been necessary to use rather narrow rectangular plates (Hughes 1954) when the drag coefficient may be influenced by the finite width of the plates. In 1954 Townsend predicted that the inequality of the normal Reynolds stresses in the turbulent layer would produce a secondary flow near the edge. The Reynolds equations for the turbulent layer on a finite flat plate for a fluid of density ρ, mean velocity (U, V, W) and fluctuating velocity (u, v, w) are

$$U\frac{\partial U}{\partial x} + V\frac{\partial U}{\partial y} + W\frac{\partial U}{\partial z} + \frac{\partial}{\partial y}\overline{uv} + \frac{\partial}{\partial z}\overline{wu} = -\frac{1}{\rho}\frac{\partial P}{\partial x} + \nu\left(\frac{\partial^2 U}{\partial y^2} + \frac{\partial^2 U}{\partial z^2}\right), \tag{1.1}$$

$$\frac{\partial}{\partial y}\overline{v^2} + \frac{\partial}{\partial z}\overline{vw} = -\frac{1}{\rho}\frac{\partial P}{\partial y}, \tag{1.2}$$

$$\frac{\partial}{\partial y}\overline{vw} + \frac{\partial}{\partial z}\overline{w^2} = -\frac{1}{\rho}\frac{\partial P}{\partial z}. \tag{1.3}$$

Consider a point (x_0, y_0, z_0) distant from the edge or by symmetry where $\overline{vw} = 0$ so that integrating (1.2) with respect to y,

$$-\rho\overline{v_0^2} = P_0 - P_1, \tag{1.4}$$

where P_1 is the pressure outside the layer and P_0, v_0 are evaluated at (x_0, y_0, z_0). Further, integrating (1.3) with respect to z,

$$\rho\int_{-\infty}^{z_0}\frac{\partial}{\partial y}\overline{vw}\,dz-\rho\overline{w_0^2}=P_0-P_1. \tag{1.5}$$

By (1.4), (1.5)
$$\int_{-\infty}^{z_0}\frac{\partial}{\partial y}\overline{vw}\,dz=\overline{w_0^2}-\overline{v_0^2}. \tag{1.6}$$

Near the wall $\overline{w_0^2}-\overline{v_0^2}\doteqdot 2\tau_0/\rho$ (Klebanoff 1954) where τ_0 is the skin friction. If $\overline{vw}$ is concentrated in a narrow strip of width b then $\partial\overline{vw}/\partial y$ will be of order $\tau_0/\rho b$. Within this strip the stress will not be parallel to the free stream and the high values of $\partial\overline{vw}/\partial y$ will induce rapid accelerations of the flow. Such a secondary flow is similar to that found in pipes of non-circular section and is a flow of Prandtl's second kind (1952). The mean streamlines of the secondary flow are sketched in figure 1.

2. The experimental method

The flow around a number of slender metal bodies was measured. The bodies were (1) flat plates of widths 2, 6, 22, 30 cm and thickness 0·16 cm and a similar plate of width 20 cm but with one edge chamfered to 10°, (2) rods of rectangular section 3·84 × 0·32 cm and 0·64 × 0·32 cm, called the 12:1 and 2:1 rods, and (3) a circular cylinder of diameter 0·59 cm. They were all 100 cm long with the leading edge shaped to the form of 8:1 ellipses or left square for turbulent flow. The corners of the side edges were rounded to a radius of 0·5 mm except for 0·15 mm on the chamfered plate. The bodies were supported from the rear so that the edge or axis of symmetry was near the tunnel centre line.

Most of the measurements were made in the 15 in. wind tunnel of the Cavendish Laboratory. The working section is 38 cm square and 200 cm long. Speeds from 30 to 1500 cm/sec are available. The total turbulence intensity is about 0·1 % at medium speeds. Above 300 cm/sec U_1 is obtained from a manometer operated across the contraction and at low speeds an anemometer is available in which the temperature of a 1 mm diameter wire, heated by a constant current, is determined by a thermocouple. The anemometers are calibrated by means of hot-wire measurements of phase in the periodic heat wake of a fine wire heated from the mains. Mean velocities were measured by either total head tube or hot-wire methods. No correction has been made for the finite size of the total head tube in relation to the boundary-layer thickness. Measurements of turbulent quantities were with hot wires of normal length 0·7 mm made from 2·5 μ Wollaston wire. The wire gives an output proportional to $2[\{1+(u/U)^{\frac{1}{2}}\}-1]$ rather than u/U but the difference is usually small. Further, it has been found that heat conduction and convection effects lead to serious errors if hot wires, run at 450 °K, are used closer than 1 mm from a thermally conducting plate in air. These effects limit the accuracy of measurements of skin friction using a hot wire to ± 10 % S.D. Records of the velocity trace were obtained from a photographic drum camera with a film speed up to 200 cm/sec and studies of transient behaviour were by means of a camera and a triggered oscilloscope.

The detection and direct measurement of mean secondary flow was performed with a vortameter (Truitt 1956). This is a very thin vane, normally 1×1 cm, mounted on a spindle so that the vane can rotate. When the spindle is pointed into the wind the vane remains stationary unless there is a component of vorticity parallel to the wind. Rotational speeds were determined stroboscopically.

Turbulent skin friction was determined by the surface-tube method developed by Preston (1954). Provided the surface tube of diameter d lies within the region of wall similarity there exists a relation.

$$d^2\Delta p/\rho\nu^2 = F(\tau_0 d^2/\rho\nu^2).$$

Δp is the pressure difference between the pressure in the surface tube and the local static pressure, and τ_0 is the skin friction. Preston determined the function F by experiment for tubes of inner to outer diameter ratio 0·6. Comparison of the results near an edge, for tubes of different diameter, show that reliable measurements can be made up to one tube diameter from the edge.

Some qualitative experiments were made in the 14 in. water flume of the Engineering Laboratory, Cambridge. A flat plate was immersed in the water in the flume and permanganate solution injected through a narrow slit 4 cm downstream of the leading edge (or more simply by merely sprinkling the plate with dye crystals). This dye later normally remained close to the wall as it was convected downstream but would be quickly broken up by any disturbance to the flow. The detailed motion of such disturbances and in particular that of turbulent spots was clearly revealed by the method.

Throughout this work I have used as a measure of the boundary-layer thickness δ, the distance measured normal to the wall at which the mean velocity $U = 0{\cdot}99U_1$. At first sight this would appear to be a difficult quantity to measure. It is found, however, that if the velocity profile is plotted on probability paper the outer part of the layer generally gives a straight line. This is found to cover a wide range of laminar and turbulent flows and δ can thus be found quite accurately from the straight line drawn through the outer experimental points. It is worth noting that for a laminar Blasius layer $\delta \doteq 5\,(\nu x/U_1)^{\frac{1}{2}}$, whereas for a turbulent layer on a flat plate δ varies from $0{\cdot}02x$ to $0{\cdot}01x$ over the range $R = 10^6$ to 10^9 (Schlichting 1955).

3. Laminar flow

The experimental velocity distribution

Figures 2 and 3 show the distribution of U on a plane x = constant, based on measurements with a 1 mm total head tube made at $x = 20$ cm, $R = 1{\cdot}06 \times 10^5$ for the flat plate of figure 2 and at $x = 37$ cm, $R = 7{\cdot}2 \times 10^4$ for the 2 : 1 rod of figure 3. It is important to notice, especially in comparison with the corresponding turbulent flows below, that the U-distributions are everywhere convex. This is strong evidence that there is no secondary flow other than the diffusive growth of the layer so that even within the boundary layer the flow is nearly unidirectional.

The boundary-layer thickness at the edge of the flat plate is only 0·35 of its value distant from the edge δ_∞ so that as the edge is approached the local skin friction rises. The local skin friction coefficient c_f is defined in terms of the wall

stress τ_0 by $\tau_0 = \frac{1}{2}\rho U_1^2 c_f$. The coefficient distant from the edge will be written $c_{f\infty}$. Experimental values of $c_f/c_{f\infty}$, obtained from hot-wire measurements close to the plate, are shown in figure 4. The points are fitted closely for laminar flow by the empirical functions (accurate to $\pm 10\,\%$ S.D.)

$$c_f/c_{f\infty} = 1{\cdot}53(z/\delta_\infty)^{-\frac{1}{3}}, \quad 0 < z/\delta_\infty < 2,$$
$$= 0{\cdot}78 + 0{\cdot}84\delta_\infty/z, \quad 1{\cdot}3 < z/\delta_\infty < 4.$$

Defining the excess friction factor

$$K = \int_0^\infty (c_f/c_{f\infty} - 1)\, d(z/\delta_\infty),$$

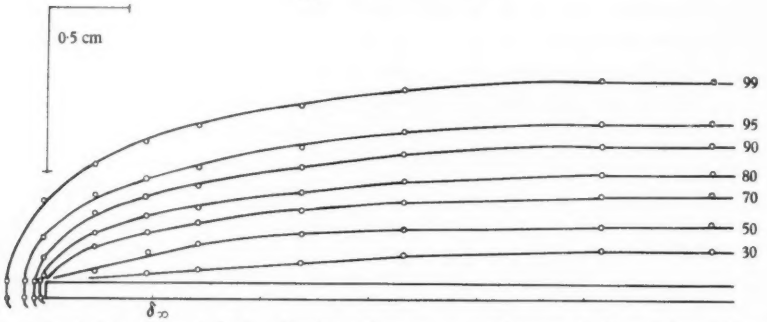

FIGURE 2. Lines of equal U for laminar flow at $x = 20$ cm and $R = 1{\cdot}06 \times 10^5$ on a flat plate. Horizontal scale $= \frac{1}{2} \times$ vertical scale. The contour values are $100\ U/U_1$.

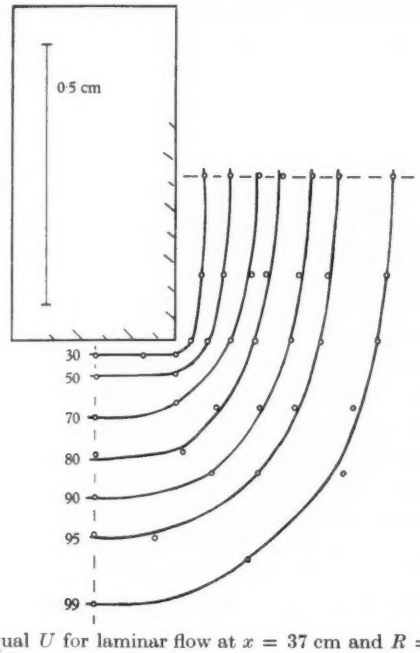

FIGURE 3. Lines of equal U for laminar flow at $x = 37$ cm and $R = 7{\cdot}2 \times 10^4$ on a rod of section 2:1 ($0{\cdot}64 \times 0{\cdot}32$ cm). The contour values are $100\ U/U_1$. Scale 1:1.

we find $K = 1{\cdot}77 \pm 10\,\%$ S.D. Alternatively, the total drag coefficient C_F is such that $(C_F - C_{F\infty})/C_{F\infty} = 53\nu x/U_1 B^2$. This value is greatly in excess of the value $K = 0{\cdot}1$ given by Howarth (1950) in his calculation based on Rayleigh's approximation. The Rayleigh approximation is clearly inadequate. On the other hand Varley's (1958) calculation gives $K = 1{\cdot}43$, only 20 % below the experimental value. This is quite good agreement.

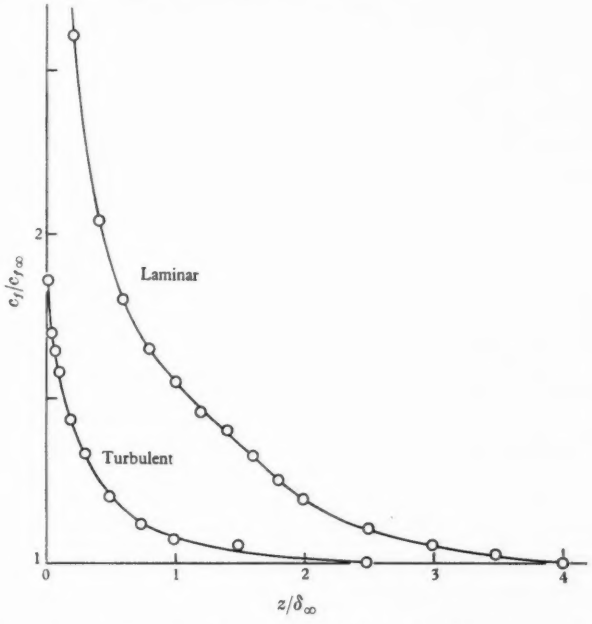

FIGURE 4. Lateral variation of laminar and turbulent skin friction on a flat plate. The turbulent values (discussed in §5) are for a plate of width $B = 6$ cm at $x/B = 10$ and $R = 4 \times 10^5$.

The edge stress

Near the edge the stress rises and will become infinite as the thickness of the plate approaches zero. For example, consider a plate of width B for which the edge cross-section is convex and symmetrical about $y = 0$ but otherwise arbitrary. The shearing force on unit length of this plate is $\oint \mu \dfrac{\partial U}{\partial n} ds$, for a fluid of viscosity μ, where n, s are co-ordinates normal and tangential to the plate cross-section. This expression will be independent of n near the wall where the acceleration of fluid is negligible. Hence, using polar co-ordinates (r,θ) for the edge region, with origin at the centre of curvature corresponding to each element of the edge cross-section and with $z = 0$ corresponding to $\theta = 0, \pi$, say,

$$\frac{1}{2}\oint \mu \frac{\partial U}{\partial n} ds = \int_0^B \mu \frac{\partial U}{\partial y} dz + \int_0^\pi \mu \frac{\partial U}{\partial r} r d\theta$$

$$= \text{constant as } n \to 0.$$

Both integrals are finite so that $r\partial U/\partial r$ is a function of θ as $n \to 0$. Hence near the wall U behaves like $\log r/a$ where a is the local radius of curvature. Unless, however, $\delta \gg a$, so that the region near the wall where the acceleration of fluid is negligible is at least of extent comparable with a, U is not of logarithmic form over a significant portion of the boundary layer but rather, since $\log r/a \doteq (r-a)/a$ when $(r-a)/a \ll 1$, U is of linear form near the wall.

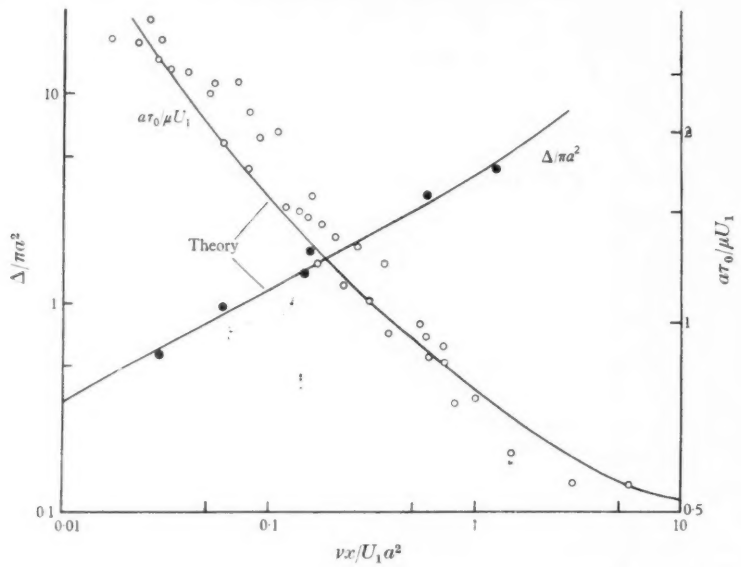

FIGURE 5. Displacement thickness Δ and skin friction τ_0 for laminar flow along a circular cylinder of radius a. Theory by Lighthill & Glauert (1955). Logarithmic scales.

It was Batchelor (1954) who first pointed out the importance of the local lateral radius of curvature in laminar flow along cylinders in his discussion of the corresponding Rayleigh problem. It should be possible to obtain an estimate of the skin friction at an edge by using the results of Lighthill & Glauert (1955) for the axisymmetric flow along a circular cylinder of radius a. Their solution is developed in terms of the parameter $(\nu x/U_1 a^2)^{\frac{1}{2}}$, proportional to the ratio of the flat plate boundary-layer thickness to the cylinder radius. They give expressions for the skin friction τ_0 and the displacement thickness

$$\Delta = 2\int_0^\infty \left(\frac{U}{U_1} - 1\right)(a+y)\,dy.$$

In order to proceed it is desirable to compare these calculations with experiment. Figure 5 compares experimental values of $a\tau_0/\mu U_1$ and $\Delta/\pi a^2$ obtained from hot-wire measurements on the circular cylinder with Lighthill & Glauert's values. The agreement to within 10–20 % is quite good so that we can now calculate the ratio of skin friction on a circular cylinder for a given $(\nu x/U_1 a^2)^{\frac{1}{2}}$ to that at the

same x on an infinite flat plate. The flat plate skin friction is given by $c_{f\infty} = 0{\cdot}664/(U_1x/\nu)^{\frac{1}{2}}$. Typical values are shown below:

$(\nu x/U_1a^2)^{\frac{1}{2}}$	0	1	2	5	10	20
$c_f(a)/c_{f\infty}$	1·0	2·3	3·4	6·1	9·8	16·3

Two experimental values of this ratio, accurate to $\pm 20\,\%$ S.D., were obtained. The first was for the square edge of the flat plate where $a = 0{\cdot}5$ mm, $(\nu x/U_1a^2)^{\frac{1}{2}}$ was 3·6 and the experimental value of $c_f(a)/c_{f\infty}$ was 4·0 compared with the calculated 4·9. The second was the chamfered edge of the plate for which $a = 0{\cdot}15$ mm, $(\nu x/U_1a^2)^{\frac{1}{2}} = 17{\cdot}6$ and the experimental value of $c_f(a)/c_{f\infty}$ was 10 compared with 14·6. This approximate agreement supports the demonstration that the viscous flow near an edge is also governed strongly by the local radius of curvature.

4. Transitional flow

The experimental results

It has been suggested that because of the comparative ease of momentum diffusion near the edge disturbances first become apparent there. This is seen in figure 6 which shows both the U-distribution and the $(\sqrt{u^2}/U)$-distribution from measurements at $x = 51$ cm near the edge of the 20 cm plate and at two values of the Reynolds number, 1·65 and $2{\cdot}70 \times 10^5$. At $R = 1{\cdot}0 \times 10^5$ velocity fluctuations

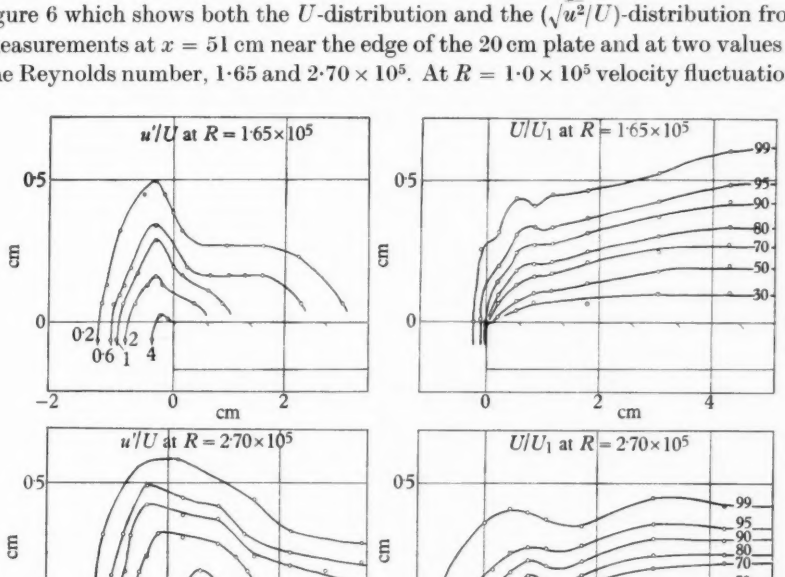

FIGURE 6. Transitional flow distributions of $100\,U/U_1$ and $100\sqrt{u^2}/U$ on a finite flat plate at $x = 51$ cm, $R = 1{\cdot}65$ and $2{\cdot}70 \times 10^5$. Horizontal scale = $\frac{1}{5}\times$ vertical scale.

were barely detectable anywhere on the plate, breakdown to turbulence commenced near the edge at $R = 1{\cdot}7 \times 10^5$, and at $R = 4{\cdot}5 \times 10^5$ the whole plate was turbulent. Also it is seen that associated with the growth of the velocity fluctuations is the growth of the secondary flow discussed in §5.

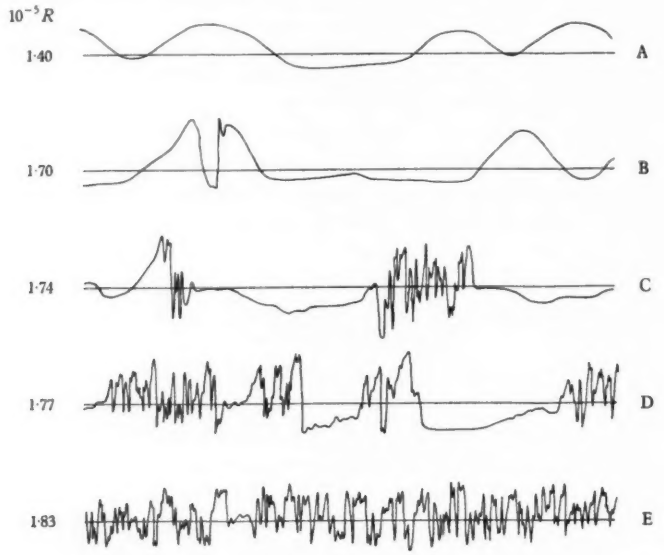

FIGURE 7. Oscillograph traces of u/U at stated values of $10^{-5}R$ and fixed sensitivity. A–E probe near the edge at (51, 0, −0·06) cm. F–G probe distant from the edge at (93, 0·06, 5·2) cm.

The character of the velocity fluctuations can be seen in portions of oscillograph traces shown in figure 7. The traces show u/U as a function of time. Traces A–E are for the probe just below the edge at (51, 0, −0·064,) cm, while traces F, G are for the probe at (97, 0·064, 5·2) cm somewhat distant from the edge. The velocity and time scales are approximately the same for all the traces. Notice that the variation of Reynolds number is obtained by varying the tunnel speed and leaving the probe fixed. Even near the edge the first fluctuations are wave-like disturbances (A). These rather irregular waves grow in amplitude until breakdown occurs (B). From these points of breakdown a turbulent region is initiated, very

small at first but growing nearly linearly in time as it is swept downstream. Two such regions, or spots, are seen in (C). As they proceed downstream the spots begin to merge (D) until the layer is swamped with spots and it is then entirely turbulent (E). Distant from the edge as in (F), (G) a similar sequence occurs, but only at a much higher Reynolds number.

Thus near the edge there is a narrow tongue of disturbed fluid while the bulk of the boundary layer remains relatively undisturbed. Within this tongue transition is obtained by the growth of turbulent spots; spots which are in every way similar to spots hitherto studied on a wide flat plate. It should be noted that spots are characteristic of transition near a wall regardless of the wall cross-section. For example, it was demonstrated both in the wind tunnel and the water channel that turbulent spots are also present during transition in the axisymmetric flow along a circular cylinder. Further, the rate at which the tongue of disturbed fluid encroaches on the surrounding boundary layer can be estimated from the oscillograph traces by reading off the intermittency factor γ, the proportion of time the fluid is turbulent. For example, in trace C, $\gamma = 0{\cdot}27$ and in trace E, $\gamma = 0{\cdot}99$. It is then found that curves of constant intermittency, drawn in the plane of the flat plate, are nearly straight lines which make an angle of $7{\cdot}9°$ to the edge (as sketched in figure 1).

The growth of the turbulent tongue

Dhawan & Narasimha (1958) have shown that Emmons's (1951) description of a transition region in terms of overlapping turbulent spots is in excellent agreement with experiment. They deduce the remarkable fact that breakdown of a laminar boundary layer, while occurring randomly in time, commences in almost point-like areas (of extent $\ll \delta$), all of which (for a plate of infinite width) lie very nearly on a straight line normal to the flow. This immediately suggests that the breakdown responsible for the tongue of disturbed fluid occurs only at a single point—the point P of figure 1. The linear growth of the curves $\gamma =$ constant would then simply be due to the linear growth of individual spots liberated from P, but if this were the case the rate of spread of this tongue ($7{\cdot}9°$) should be similar to the rate of spread of a single spot. The rate of spread of isolated spots has already been given by Schubauer & Klebanoff (1955) as $8{\cdot}6°$ ($U_1 = 300$ cm/sec), and has been independently measured here as $8{\cdot}1°$. This is in excellent agreement with the value of $7{\cdot}9°$. Further, it was directly demonstrated by using two hot-wire probes placed in the tongue of intermittently turbulent fluid upstream of the normal transition zone that turbulence never occurred at the downstream probe without having first occurred at the upstream probe. Thus near an edge breakdown originates near a single point.

The above considerations immediately raise the problem of how the edge tongue will merge with the normal transition region on the portion of the plate distant from the edge. The question reduces to the problem of the interaction of two spots as they grow and merge into one another. In a subsequent paper it will be shown that the area of a plate which is turbulent at any moment is simply the sum of the areas covered by the turbulent spots if each spot grows independently of its neighbours. There are thus two possible forms, sketched in figure 8,

of the transition curve on a plate of finite width. When the disturbance level in the free stream is low (generally at low U_1) the edge transition regions will have overlapped before normal transition occurs. At higher disturbance levels the normal transition region will have moved sufficiently upstream so that both transition regions are present.

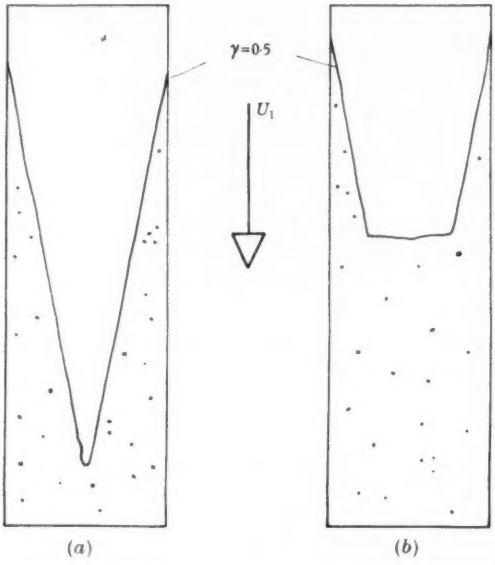

FIGURE 8. A sketch of the transition curve on a finite plate for (*a*) low and (*b*) high free-stream turbulence.

5. Turbulent flow

The secondary flow

Figures 9 and 10 show the distribution of U on a plane x = constant, based on measurements made with the 1 mm total head tube at $x = 97$ cm, $R = 8{\cdot}7 \times 10^5$ for the flat plate of figure 9 and at $x = 92$ cm, $R = 6{\cdot}7 \times 10^5$ for the 2:1 rod of figure 10. The most obvious features, as distinct from the corresponding laminar flows shown in figures 2 and 3, are that the lines of constant U are no longer everywhere convex and that the boundary-layer thickness at the edge is $1{\cdot}28\delta_\infty$ whereas in the laminar flow it was only $0{\cdot}35\delta_\infty$. The distortion of the U-distributions near the edge is strongly suggestive of a secondary flow of Prandtl's second kind in which the flow is produced by the anisotropic Reynolds stresses. But before this can be asserted it is necessary to dispose of the other possibilities. Could the secondary flow be due to the vortex found near the edge of a finite plate which is producing lift because of some error of alignment? First, the flow was symmetrical about $y = 0$. This was directly verified. The lifting vortex is found on one side only and does not therefore produce a symmetrical field. Secondly, the secondary flow is found only when the flow is turbulent whereas a lifting plate has an edge vortex even in laminar flow. This query may be put

even more generally. Is the secondary flow already present in the laminar flow? The U-distribution for laminar flow was always everywhere convex. Thus the explanation of the secondary flow is to be found in the behaviour of the turbulent layer.

A direct demonstration that the secondary flow is due to the Reynolds stresses is obtained with the vortameter, which gives the secondary flow vorticity. The vortameter did not rotate in the laminar field, but immediately transition commenced the vortameter began to rotate. At the same time the U-distribution was no longer everywhere convex. The vortameter readings were anti-symmetric about $y = 0$ and the departures from convexivity developed through the transition region. These phenomena were found for the 30, 22, 6 cm plates and the 12:1 and 2:1 rods so that the phenomena cannot be ascribed to a chance configuration of a single plate.

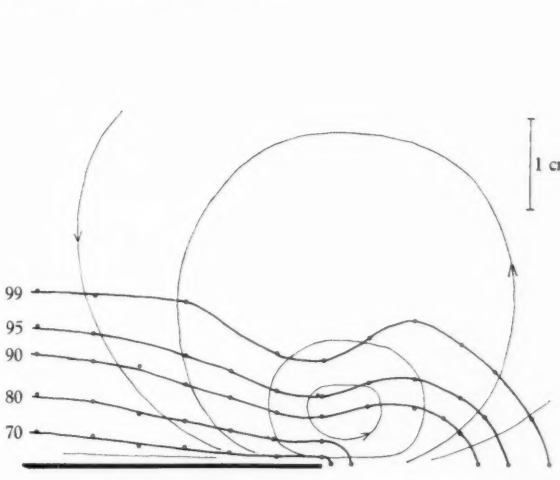

FIGURE 9

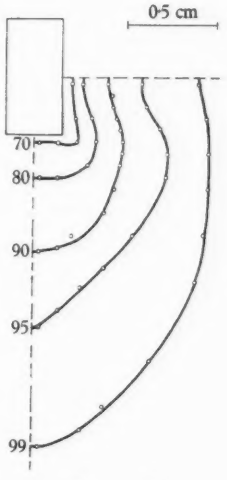

FIGURE 10

FIGURE 9. U-distribution for turbulent flow on a flat plate. Scale 1:1, $B = 30$ cm, $x = 97$ cm, $R = 8{\cdot}7 \times 10^5$. The fine lines are the secondary flow streamlines. Compare with figure 2. The contour values are $100\ U/U_1$.

FIGURE 10. U-distribution for turbulent flow on the rod of section 2:1. Scale 1:1, $x = 92$ cm, $R = 6{\cdot}7 \times 10^5$. Compare with figure 3. The contour values are $100\ U/U_1$.

The secondary flow has been measured with the vortameter for the flow of figure 9. The vortameter rotational frequency n measured in c/s is proportional to the vorticity. The secondary vorticity distribution is shown in figure 11. Notice that not only is the distribution symmetrical about $y = 0$, it is also very nearly symmetrical about a line $z = -0{\cdot}5\,\text{cm} = -0{\cdot}017B$. The flow is such that near the wall fluid is moving away from the plate. A linear relation was found between U_1 and the frequency n at fixed x of the form $\Delta U_1 = 126\Delta n$ and such that $n = 0$ when the transition point is at x. This shows that the mean secondary vortex can be considered to be of constant pitch $= 126\,\text{cm} = 4{\cdot}2B$. Because such

a simple relation exists between U_1 and n it is possible to replace n by the secondary flow stream function ψ defined by

$$\left(\frac{\partial^2}{\partial y^2}+\frac{\partial^2}{\partial z^2}\right)\psi = 4\pi n. \tag{5.1}$$

The stream function has been evaluated from (5·1) and experimental values of n by a relaxation calculation and is shown in figure 12. The stream function has also been drawn in figure 9 (fine lines) where the region outside $\psi/\psi_{\max} = 0{\cdot}2$ has been drawn, taking into account both the calculated values of ψ and the experimental determination of the inclination of the secondary flow vector by means of the observed inclination of a very light vane. The bulk of the secondary flow

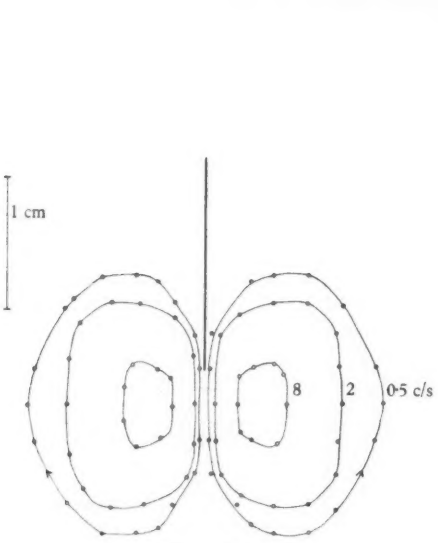

FIGURE 11

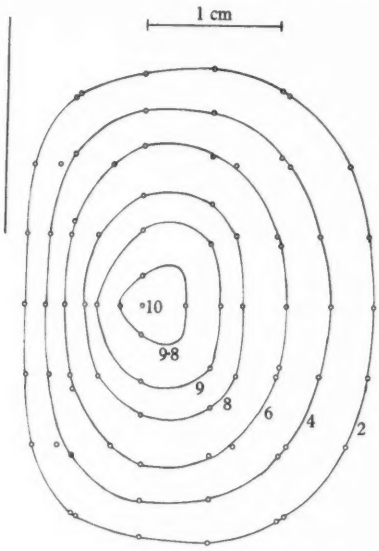

FIGURE 12

FIGURE 11. Secondary flow vorticity distribution n in c/s, near an edge. Maximum value = 8·8 c/s. B = 30 cm, x = 97 cm, $R = 8{\cdot}7\times10^5$. δ = 1·9 cm.

FIGURE 12. Secondary flow stream function ψ of (5·1) normalized to a maximum value of 10.

is seen to be confined to a region of dimensions δ near the edge. From ψ the secondary velocity is easily found. In figure 13 I show the maximum outflow $W = -\partial\psi/\partial y$ evaluated on the line of symmetry $z = -0{\cdot}5$ cm. W is everywhere $< 0{\cdot}037U_1$, so that in fact the secondary flow is quite small.

It would be possible to consider the mean secondary flow from two idealized points of view. First, it could be considered as a vortex, that is a small region of rotational flow outside of which the mean flow is irrotational. If this idea was completely correct the vane would have reversed its direction of rotation as it was moved into the core. In fact as shown in figure 8 such is not the case. Secondly, the secondary flow could be considered as a strong outflow near the wall and a

diffuse inflow over a large portion of plate. This idea also is not borne out by the form of ψ. In fact, ψ shows that the flow is somewhere between the two. Nevertheless, it is important to remember here that the vane was of finite size; a 1·0 cm square. Because of the finite size of the vane it may be argued that the explanation of the unidirectional rotation either side of $y = 0$ is in fact due to a strong outflow at the wall into which the vane is dipping. This assertion is clearly incorrect since the rate of rotation was extremely small even at $z = 0{\cdot}3\delta_\infty$ with the vane almost touching the wall. ψ will certainly need correction due to the finite size of the vane, but unfortunately it is rather difficult to see how this might be done.

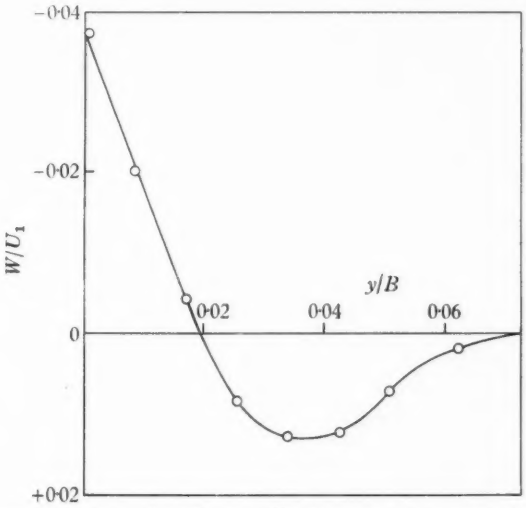

FIGURE 13. Secondary flow profile at $z = -0{\cdot}5$ cm $= -0{\cdot}017B$.
Figures 9, 11, 12, 13 are all for the same flow.

The total drag

Although there is considerable empirical data in the literature on the drag of flat plates, by far the most valuable is that due to Hughes (1954) who proposed an empirical relation for the total drag coefficient C_F of a wide plate of length L and breadth B over the range $R = 0{\cdot}04$ to 250×10^6

$$C_F = 0{\cdot}066\,(-2{\cdot}03 + \log_{10} R)^{-2}(1 + rL/B). \tag{5.2}$$

His data provides overwhelming evidence to support this dependence of C_F on R but the choice of the so-called form factor $1 + rL/B$ is unsatisfactory as the coefficient r varies strongly with both L/B and the Reynolds number $U_1 B/\nu$. It was, in fact, the need to clarify the behaviour of this factor that started the present investigation.

Figure 14 shows the distribution of skin friction obtained with a surface tube near the corner of a finite flat plate of breadth 22 cm at fixed wind speed 1050 cm/sec. The forward edge was square so that transition occurred at $x = 2$ mm, $R = 1300$ in the separated zone of extent 1·1 cm near the edge. The skin friction

rises rapidly from the line of reattachment marked $c_f = 0$ in figure 14 and except for a complex region in the corner $0 < x/B < 2$, $0 < z/B < 0{\cdot}1$ shows the gradual increase towards the side edge already shown for comparison with the laminar case in figure 4 and shown in more detail in figure 15. Note that $c_{f\infty}$ is the skin-friction coefficient for $z = \frac{1}{2}B$. Near the leading edge the behaviour is complex with at first two maxima, both displaced from the edge, then a single maximum displaced from the edge, and for $x/B > 2$ ($R < 3{\cdot}10^5$) a monotonic increase of skin

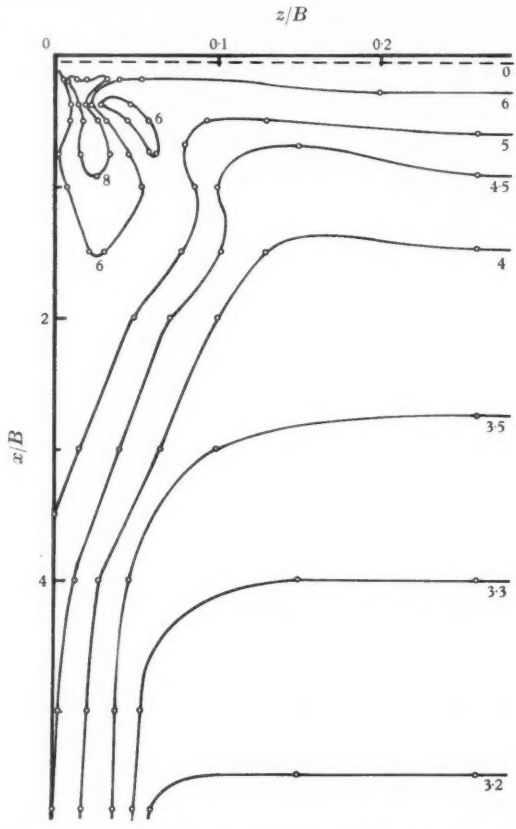

FIGURE 14. Distribution of skin-friction coefficient $10^3\, c_f$ near the corner of a finite flat plate at fixed U_1. $B = 22$ cm, $U_1 B/\nu = 1{\cdot}55 \times 10^5$.

friction to a maximum at the edge where $c_f(0)/c_{f\infty} \doteqdot 1{\cdot}8$ (much smaller than the laminar value). Included on the curve for $x/B = 3$ is the corresponding data for the 6 cm wide plate at $x/B = 10$. The close similarity of the data from the two plates shows that the lateral distribution of c_f is determined by x/B rather than x/δ as it is in the laminar case. Further downstream when δ is comparable with B the variation of c_f is less pronounced and this is illustrated also in figure 14 for $x/B = 20$ on the 2 cm wide plate.

The distribution of skin friction $c_{f\infty}$ along the centre line is shown in figure 16 for two plates of width 6 and 22 cm. Included in figure 16 is $c_{f\infty}$ obtained from

$$\left.\begin{aligned} c_{f\infty} &= R\,dC_{F\infty}/dR, \\ \text{where} \qquad C_{F\infty} &= 0{\cdot}0624\,(-2{\cdot}03+\log_{10}R)^{-} \end{aligned}\right\} \tag{5.3}$$

an expression of similar form to (5·2) but in which the coefficient 0·066 has been replaced by $0{\cdot}0624 \pm 0{\cdot}2\,\%$ S.D. This high accuracy does not refer to the absolute

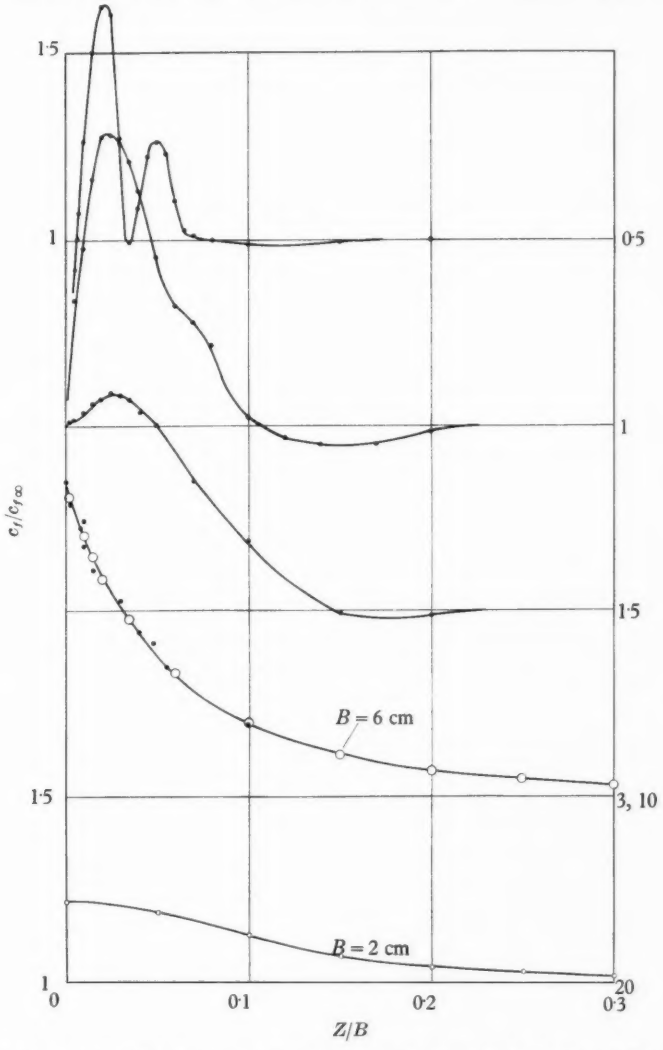

FIGURE 15. Lateral distribution of c_f at values of x/B stated on the right-hand side of the figure. $U_1 = 1050$ cm/sec. •, $B = 22$ cm, $x/B = 0{\cdot}5$, 1, 1·5, 3 (data of figure 14); ○, $B = 6$ cm, $x/B = 10$; ∘, $B = 2$ cm, $x/B = 20$.

accuracy of the coefficient but to the internal consistency of 14 separate determinations of the coefficient over the range $R = 5{\cdot}10^4$ to $5{\cdot}10^5$ for both the 6 and the 22 cm plates. (6 values from the 22 cm plate gave $A = 0{\cdot}0622$ and 8 values from the 6 cm plate gave $A = 0{\cdot}0626$.) The high accuracy does, however, support the functional form given by Hughes for the variation with R and incidentally shows that the total head tube method of measuring skin friction is very reliable. It should be noted that the velocity and stress distribution near the edge was the same for both a square edge and one chamfered to a sharp 10° wedge.

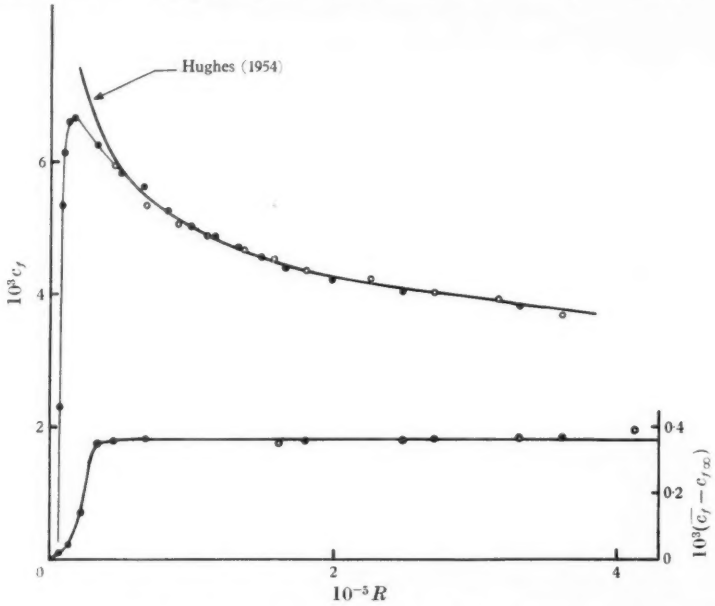

FIGURE 16. c_f along the centre line $z/B = 0{\cdot}5$ of a finite plate compared with values obtained from Hughes (1954) formula (5·3). •, $B = 22$ cm, ○, $B = 6$ cm. Also shown is the mean excess $\overline{c_f} - c_{f\infty}$. The measurements cover $0 < x/B < 10$.

Also given in figure 16 is the mean excess friction $\overline{c_f} - c_{f\infty}$ obtained by computing the mean skin friction $\overline{c_f}$ with respect to z at a fixed x. As is also shown in the behaviour of $c_{f\infty}$, the influence of the leading edge is rapidly lost and the excess rises to a value independent of both R and B. This remarkable result is the key to the differences between various formulations of the drag of a flat plate. This excess will give also an increase in the total drag coefficient of a finite plate over that given by (5·3) and for the data of figure 15 this is given below.

$10^{-5}R$	0·2	0·4	0·6	0·8	1·0	1·2	1·4	1·6
$10^3\Delta C_F$	0·008	0·020	0·037	0·057	0·086	0·120	0·153	0·177

For larger values of R $\qquad \Delta C_F = 3{\cdot}62 \times 10^{-4} - 30/R.$ (5.4)

The excess drag can thus be expressed as the sum of two independent contributions, one due to the finite size of the plate and arising from the flow near the side edges, the other from the particular mode of separation, transition and reattach-

ment near the leading edge. The contribution to the total drag from the leading-edge flow will be independent of x downstream of the edge region in which c_f increases rapidly so that the contribution to C_F will be of the form $-A/R$. In fact $A \doteqdot R_c[C_{FT} - C_{FL}]$, where R_c is the Reynolds number at the end of the leading-edge region, C_{FT} is the turbulent friction coefficient given by (5.3) at R_c and C_{FL} is the actual friction coefficient for the edge region. For natural transition A can easily be as large as 10^3 and through R_c is very dependent on U_1, but in the present case of transition behind a square leading edge A is almost independent of U_1 and the value $A = 30$ given by (5.4) is reasonable.

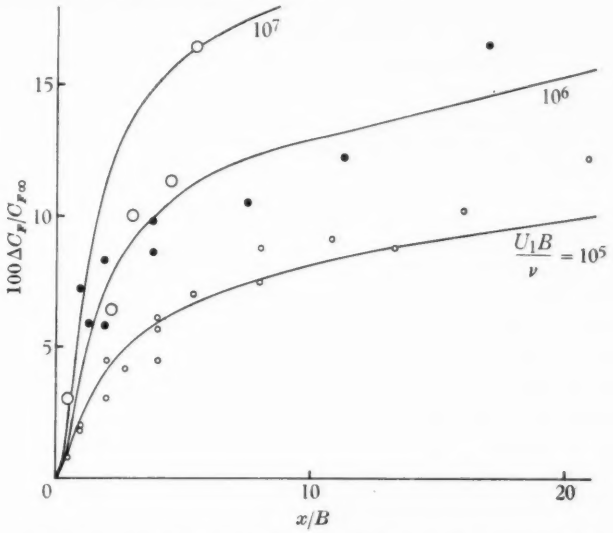

FIGURE 17. The percentage form factor for the total drag as a function of the aspect ratio at various U_1B/ν. The experimental points are given by: ○, Hughes (1954) sheet values, $U_1B/\nu = 2{\cdot}0 \times 10^5$. ●, Hughes (1954) pontoon values, $U_1B/\nu = 1{\cdot}9 \times 10^6$. ○, Allan & Cutland (1953) plank values, $U_1B/\nu = 0{\cdot}81 \times 10^7$.

The determinations of drag reported in the literature are largely for a series of runs at fixed U_1, B with variable plate length x. This data has been collected in figure 17. The curves of constant U_1B/ν are obtained from ΔC_F of (5.4) and C_F of (5.3) at $R = (U_1B/\nu)(x/B)$. The experimental data given by Hughes (1954) for plastic sheets with $U_1B/\nu = 2{\cdot}0 \times 10^5$ and pontoons with $U_1B/\nu = 1{\cdot}9 \times 10^6$ and by Allan & Cutland (1953) for planks with $U_1B/\nu = 0{\cdot}81 \times 10^7$ lie close to the appropriate curves derived from the present data. The sheet values of C_F are accurate to $\pm 1{\cdot}0\,\%$ S.D. and the pontoon values to $\pm 0{\cdot}5\,\%$ S.D. while the consistency of the measurements reported here suggests an accuracy of $\pm 0{\cdot}7\,\%$ S.D. for the total head values of C_F. Thus all this data is consistent to better than $\pm 1\,\%$ S.D.

A number of semi-empirical relations have been given (Schlichting 1955) for C_F, of which the theoretically soundest is that due to Townsend (1956)

$$\sqrt{2}\,kC_F^{-\frac{1}{2}}(1 - R_0/R)^{\frac{1}{2}} = \log RC_F + 1{\cdot}1, \tag{5.5}$$

where $k = 0{\cdot}41$ is the logarithmic velocity profile constant, R_0 is a constant of integration and 1·1 is an empirical constant obtained from the known velocity distribution. If $R_0 = 0$ and the 1·1 is ignored, (5·5) is similar to the widely used Schoenherr (1932) relation

$$0{\cdot}242 C_F^{-\frac{1}{2}} = \log_{10} R C_F. \tag{5.6}$$

The experimental constant 0·242 corresponds to $k = 0{\cdot}394$, considerably different from the accepted value 0·41. As values of C_F are sensitive to the choice of this coefficient (5.6) must be regarded simply as an empirical relation. Schoenherr's data were obtained from the total drag of finite plates and no attempt was made to allow for the effect of aspect ratio. But since by (5.4) the effect of the aspect ratio is merely to increase the drag coefficient by an almost constant amount so that the drag is almost independent of the aspect ratio, then Schoenherr's relation or any other empirical relation obtained by ignoring the effect of aspect ratio should give a good estimate of the total drag of any finite plate. Values given by Schoenherr's relation exceed those of (5.3) by $(1{\cdot}0, 4{\cdot}5, 4{\cdot}1, 3{\cdot}2, 2{\cdot}6) \times 10^{-4}$ at $R = (10^5, 10^6, 10^7, 10^8, 10^9)$, while for the Prandtl–Schlichting relation (Schlichting 1955)

$$C_F = 0{\cdot}455/(\log_{10} R)^{2{\cdot}58}, \tag{5·7}$$

the corresponding values are $(0{\cdot}8, 5{\cdot}1, 4{\cdot}8, 3{\cdot}8, 3{\cdot}2) \times 10^{-4}$. These differences follow quite closely those given by (5.4) with discrepancies in the various values for C_F generally much less than 10^{-4} and certainly not more than the experimental error of rather less than $\pm 1\,\%$ S.D.

In estimating the drag of ship-like bodies the values of C_F given in (5.3) can be used with confidence but due to the presence of a free surface or a keel of large angle the excess friction ΔC_F may differ from (5.4). However, the presence of a free surface does not appear to affect ΔC_F, since the results of Allan & Cutland (1953) who used a semi-submerged plank are consistent with all the other data presented here. The effect of the keel angle on ΔC_F could be obtained by local skin-friction measurements with the surface tube on a body made of two equal finite flat plates at zero incidence and touching each other along an edge.

It should be noted that (5.4) contains a contribution to the drag independent of viscosity. This result was, however, obtained by measurements only up to $R \doteqdot 10^6$ and in spite of being in good agreement with published results up to $R \doteqdot 10^9$ is entirely empirical. It cannot be used with confidence outside the limits of the original data, $R = 10^4$ to 10^9 and in particular cannot contribute to the question of whether or not the drag coefficient of a finite plate at $R = \infty$ is zero or finite. In practice large values of R can only be achieved at large values of δ/B so that the question of drag at $R = \infty$ is best answered by studies of the flow along a long thin wire.

The result that ΔC_F is independent of B is surprising for it may have been supposed that provided B is sufficiently large for the two edge flows not to interact then the contribution of the edge flow to ΔC_F would be of the form (constant)/B. The data clearly show that this is not so, and the edge flows must interact for all values of B. A comparison of the lateral distribution of c_f on the 6 and 22 cm wide plates at $x/B = 10, 3$, respectively, as already given in figure 15 shows that while the rise of c_f at the edge is much the same in the two cases the lateral extent of the

excess edge friction is less for the narrower plate. It is unexpected that in spite of this interaction $c_{f\infty}$ is unaffected. Nevertheless, $c_{f\infty}$ will be affected when the plate is sufficiently narrow for the edge flows to overlap. Any effect is small since the values of A determined from the 6 and 22 cm plates were 0·0626 and 0·0622 with a barely significant difference of 0·7%, while the value obtained from a 2 cm wide plate 0·0600 is still only 2·4 % below the value for a wide plate.

I gratefully acknowledge that my period of research at Cambridge was made possible by my employers, the New Zealand Defence Scientific Corps. Some of the material presented here was described by Dr A. A. Townsend (1958) at the Freiburg symposium on boundary-layer research.

REFERENCES

Allan, J. F. & Cutland, R. S. 1953 *Trans. N.E.C. Inst.*, p. 245.
Batchelor, G. K. 1954 *Quart. J. Mech. Appl. Mech.* **7**, 179.
Charters, A. C. 1943 *N.A.C.A.* TN 891.
Dhawan, S. & Narasimha, R. 1958 *J. Fluid Mech.* **3**, 418.
Emmons, H. W. 1951 *J. Aero. Sci.* **18**, 490.
Howarth, L. 1950 *Proc. Camb. Phil. Soc.* **46**, 127.
Hughes, G. 1954 *Trans. Inst. Naval Arch.* **96**, 314.
Klebanoff, P. S. 1954 *N.A.C.A.* TN 3178.
Lighthill, M. J. & Glauert, M. B. 1955 *Proc. Roy. Soc.* A, **230**, 188.
Moore, F. K. 1956 *Advanc. appl. Mech.* **4**, 159.
Murphy, J. S. & Phinney, R. E. 1951 *J. Aero. Sci.* **18**, 771.
Prandtl, L. 1952 *Essentials of Fluid Dynamics.* London: Blackie.
Preston, J. H. 1954 *J. Aero Sci.* **21**, 109.
Rayleigh, Lord 1911 *Phil. Mag.* (6) **21**, 697.
Schlichting, H. 1955 *Boundary Layer Theory.* London: Pergamon Press.
Schoenherr, K. E. 1932 *Trans. S.N.A.M.E.* **40**, 279.
Schubauer, G. B. & Klebanoff, P. S. 1955 *N.A.C.A.* TN 3489.
Tagori, T. *et al.* 1955 *J. Soc. Nav. Archit. Japan*, **98**, 31.
Townsend, A. A. 1954 *European Shipbuilding*, **3**, 86.
Townsend, A. A. 1956 *The Structure of Turbulent Shear Flow.* Cambridge University Press.
Townsend, A. A. 1958 *Boundary Layer Research.* Proc. Freiburg symposium. Ed. H. Görtler. Berlin: Springer-Verlag.
Truitt, R. W. 1956 *J. Aero. Sci.* **23**, 889.
Varley, E. 1958 *J. Fluid Mech.* **3**, 601.

REVIEWS

The Scientific Papers of G. I. Taylor. Vol. II: Meteorology, Oceanography and Turbulent Flow. Edited by G. K. BATCHELOR. Cambridge University Press, 1960. 515 pp. 75*s.* or $14.50.

This second volume of the collected scientific papers of G. I. Taylor carries the subtitle 'Meteorology, Oceanography and Turbulent Flow', but the whole has a homogeneity of outlook and subject which goes beyond that conveyed by the title and is perhaps not expected knowing the versatility of the author. This common subject is the nature and effects of turbulent flow, in the sea or the atmosphere or the laboratory and, by my count, forty of the forty-five papers relate to turbulence and only the five on tidal oscillations deal wholly with non-turbulent flow. Although there is much of interest for meteorologists and oceanographers, this volume may be regarded as an account of the development of the statistical theory of turbulence and the associated ideas that are fundamental to modern studies of turbulent flow. Acknowledging the importance and originality of this work, it is more interesting to trace the origin and development of the central ideas than simply to applaud the achievement.

When reading these papers, some I regret to say for the first time, I was surprised to see how much of the work on turbulence was published either between 1915 and 1919 or between 1935 and 1938. I formed the impression that G. I. Taylor arrived at his understanding of the nature of turbulent flow during the first period, and put it into mathematical form in the second period when advances in experimental techniques had made possible measurements of fluctuations.

Paper 1 in this volume, 'Eddy motion in the atmosphere', introduces the mixing-length theory of eddy transport, uses it to describe transport of momentum, heat and humidity, derives the variation of wind velocity and direction with height and, in passing, points out that Rayleigh's criterion for flow stability is inapplicable to channel flow because of the no-slip condition at the walls. The second, a discussion of Reynolds's analogy between heat and momentum transfer, describes the motion in the viscous (or 'laminar') sublayer and most of the fundamental concepts of turbulent flow appear in the following papers. Perhaps the most interesting feature is the continual insistence that turbulent motion must be three-dimensional, with its corollaries that vorticity is being produced by continuous extension of vortex-filaments and that the lack of scale effect in turbulent flow depends on a separation in the length-scales of the motions responsible for energy dissipation and for transport of heat and momentum. As far as I can make out, G. I. Taylor has never believed that an adequate description of any kind of turbulent flow could be obtained either by assuming two-dimensional flow or by linearizing the Navier-Stokes equations.

The second period commences with the formulation of the statistical theory of turbulence which has been the model and inspiration for nearly all subsequent investigations of turbulent flow. It is impossible to overrate the importance of

this work but, after reading the papers of the first period, the impression persists that the early work contains the bones of the matter and that the theory was constructed explicitly only when the techniques of fluctuation measurement made the construction not merely a mathematical exercise but a tool for the quantitative investigation of the motion and for the detailed verification of the basic concepts. For this purpose the theory has been extremely successful, but it is curious that the basic simplifying assumption of isotropy now appears more as a catalyst than as an essential ingredient in the theory and survives only in the restricted form of local isotropy. If I were asked to say in what respects we are better informed than we were in 1938, I might point rather doubtfully at the imposing but chaotic mass of experimental material but the only new idea is that the eddies transferring heat and momentum are comparatively stable objects and that randomness and isotropy are characteristic of the dissipative eddies only.

Only two papers of significance in the theory of turbulence seem to have been published outside these periods and one, on turbulent diffusion by continuous movements, is perhaps singular in that no experimental material is presented. The other, on the vorticity transport theory, is most intriguing in its attitude to the mixing-length theory. It is accepted now that the mixing-length theory is wrong and misleading and that no one would use it except engineers and meteorologists who prefer to have some answer rather than none at all, but the case against it has been overstated. For a corrective, read this paper and notice the care taken to form an acceptable model of the diffusion process. Notice also the extreme caution with which Taylor uses the second relation of mixing-length theory which assumes that eddy diffusivity is a function of mean velocity gradient and of position in the flow. In fact, he derives a relation between temperature and velocity in a wake which does not depend on the second relation and which is in much better agreement with recent measurements than the explicit results which do assume the second relation.

One important development which finds no place in these pages is the theory of local isotropy, introduced by Kolmogoroff in 1941 and since then accepted as the proper framework for discussion of the small-scale motion. In some respects, this is a natural extension from the statistical theory and the idea that the motion responsible for eddy transport is not influenced appreciably by the nature of the dissipation process, but the basic assumption of universal equilibrium of the small-eddy motion does not appear to have been anticipated by Taylor and is, I believe, not easily reconciled with his view of the dissipation process as 'the formation of very small regions where the vorticity is very high' (p. 465) caused by continued stretching of vortex lines. This view emphasizes the connexion between motions on large and small scales, and seems to imply that the independence assumed in the theory of local isotropy is not complete and may not extend to some aspects of the motion. Some evidence that very small regions of high vorticity do exist (Sandborn, *J. Fluid Mech.* **6**, 1959, 221) and that the stretching process is persistent (Townsend, *Proc. Roy. Soc.* A, **209**, 1951, 418) confirms the connexion and indicates that universal equilibrium

is not complete. On the other hand, it is difficult to believe that the small eddies of turbulent flow are not in some kind of universal equilibrium with a structure dependent on the rate of energy dissipation and perhaps the length scale of the large eddies. An improved theory of local isotropy which will reconcile our belief in some form of universal equilibrium with an accurate and realistic view of the dissipation process still lies in the future but it is a problem of very great interest.

Some readers of this volume will have other interests than the nature of turbulent flow, and for them I recommend it as a way of watching G. I. Taylor solve complex problems by close combination of theory and observation. Although a reader is denied the characteristic hand-waving (to illustrate extending vortex-filaments, for example), he may notice the clarity of thought, the ability to make an approximate calculation based on inexact measurements and so to produce an unbelievably precise answer, and, of course, the habit of having done the work twenty or more years ago.

A. A. TOWNSEND

Advances in Geophysics. Vol. 6: Atmospheric Diffusion and Air Pollution. Edited by F. N. FRENKIEL and P. A. SHEPPARD. New York: Academic Press, 1959. 471 pp. $12.00.

The study of atmospheric turbulence encompasses phenomena as diverse as the dispersal of radioactive debris in the stratosphere and evaporation from the ground, all of which have a complicated dependence on several variables. Research in such a field is likely to be successful only if it is planned soundly and workers appreciate the significance of what they are doing. The reviewer has found that in many cases this can be achieved most easily by distinguishing three stages in an investigation: first, general exploration; second, definition and exploitation of a simplified model exhibiting the main features of the phenomenon; and third, elaboration of the model to bring it into closer correspondence with reality. Although work on the three stages may proceed simultaneously, their confusion is a common cause of failure.

This point of view may be illustrated by a consideration of flow near the ground. Early exploratory work established the importance of the dynamic effects of a vertical gradient of potential temperature and its associated heat flux, and showed that the shear stress and heat flux often vary little in the first few tens of metres above the surface. This has led to the theoretical study of an idealized flow which is exactly steady in space and time and in which the shear stress and heat flux are constant. With this model and a few plausible assumptions, such as that the roughness length characterizing the surface does not affect the internal mechanism of the flow, it has been possible to deduce a number of important results from dimensional arguments. In particular, all dimensionless properties of the turbulence, such as, for example, the correlation coefficient between temperature and vertical velocity, must be functions of z/L, where L is the length introduced by Monin and Obukhov to represent the dynamical effects of the heat flux and is equal to $\bar{\rho}u_*^3/g\overline{\rho' w'}$ (u_* is the friction

velocity). Of course, conditions in the real atmosphere depart considerably from those assumed in the model, and it is not surprising that observations do not always agree with the theoretical predictions. Indeed, the discrepancies may be of considerable practical importance, and one would not wish to discourage their study. However, it does seem clear that they will be understood only through an extensive quantitative investigation of the manner in which real conditions in individual cases depart from the ideal. At present, while our knowledge of the model flow is sparse, there would seem to be a good case for concentrating research on conditions as near the ideal as possible.

The volume under review contains the proceedings of an international symposium on atmospheric diffusion and air pollution, held at Oxford in August 1958. For a reader with the above background in mind, it may make depressing reading. The aim of the symposium was 'to bring together fluid dynamicists, meteorologists, oceanographers and other scientists in order to discuss atmospheric diffusion and some basic aspects of its application to air pollution studies'; and one might have expected the organizers to have chosen introductory speakers who would provide a clear exposition of the present state of their field and provide a firm framework on which the contributions of the later speakers could be hung. In fact, with the exception of that by A. J. Haagen-Smit, whose lecture on the chemistry of urban air pollution was rather far removed from the main theme of the conference, the introductory reviews were mainly historical and in some cases rather superficial; they failed to show what parts of the subject the speakers regarded as established or where and how it was growing.

The remainder of the meeting consisted of a succession of isolated papers of very variable quality, only a few of which can be mentioned here. F. Gifford made good use of a relatively new method of treating the plume of pollutant from a continuous fixed source: he considered the waving of the plume and the growth of its instantaneous width separately. H. H. Lettau presented the results of an analysis of surface friction in relation to the geostrophic wind and showed the dependence of the drag coefficient on the 'surface Rossby number', $\mathrm{Ro} = V_g/z_0 f$, the importance of which has been known for some time from 'Ekman spiral' calculations.

A number of papers were concerned with measurements of various spectra of turbulence near the ground, but in none of them were the results adequately related to any theoretical model. H. A. Panofsky and R. J. Deland gave a review of present knowledge of one-dimensional Eulerian spectra. H. E. Cramer also reported extensive measurements. He introduced the interesting idea of measuring correlations between quantities filtered so as to include only a narrow band of frequencies, but he made little use of it. J. S. Hay and F. Pasquill examined the relation between Lagrangian and Eulerian spectra, and interpreted their results in terms of a hypothesis that the Lagrangian time spectrum has the same shape as the Eulerian spectrum but with a time-scale differing by a constant factor. In the form in which it was presented this hypothesis is not strictly acceptable, since at a site with a different roughness the flow would be identical except for the superposition of a constant velocity which would alter the Eulerian time-scale but would leave the Lagrangian scale unchanged.

R. W. Davies deserves mention for the enthusiasm with which he organized the photographing of the smoke from a large oil fire.

What was probably the best original idea of the meeting came from E. L. Deacon. He suggested that estimates of the vertical heat flux near the surface might be obtained from measurements of the level of temperature and velocity fluctuations in the small scales of the inertial subrange. This is possible because the mean square velocity difference D_u and the mean square temperature difference D_T between two points a suitable small distance Δ apart are related to the rates of dissipation of mean square velocity (ϵ) and mean square temperature (γ) by

$$D_u = C_1 \epsilon^{\frac{2}{3}} \Delta^{\frac{2}{3}}, \quad D_T = C_2 \gamma \epsilon^{-\frac{1}{3}} \Delta^{\frac{2}{3}}.$$

It is easily seen on dimensional grounds that the heat flux is given by

$$\begin{aligned} \overline{w'T'} &= \gamma^{\frac{1}{2}} \epsilon^{\frac{1}{6}} z^{\frac{2}{3}} f_1(\mathrm{Ri}) \\ &= D_T^{\frac{1}{2}} D_u^{\frac{1}{2}} z^{\frac{2}{3}} \Delta^{-\frac{2}{3}} f(\mathrm{Ri}), \end{aligned}$$

where one may take for Richardson number $gT^{-1}\gamma^{\frac{1}{2}}\epsilon^{-\frac{1}{6}}z^{\frac{2}{3}}$, which is proportional to $gT^{-1}D_T^{\frac{1}{2}}D_u^{\frac{1}{2}}\Delta^{\frac{1}{3}}z^{\frac{2}{3}}$. The function f has to be determined empirically, of course, but this has to be done only once and the most favourable circumstances can be chosen. It is possible that this method for finding the heat flux will be useful at sea, since the motion of a boat or buoy should interfere very much less with measurements of small-scale fluctuations than with the direct determination of the heat flux through the covariance of T' and w'. One hopes that the idea is being pursued.

In short, the Proceedings form a book which is useful mainly as an ephemeral catalogue of current research and which rather few individuals will wish to buy.

T. H. Ellison

Rheology: Theory and Applications. Vol. III. Edited by F. R. Eirich. New York and London: Academic Press, 1960. 680 pp. $12.00.

This is the third of a series of three volumes on the subject of recent advances in rheology. The first two volumes of the treatise have been reviewed earlier in this journal (volume 3, page 110 and volume 5, page 652).

It is characteristic of the subject that there appears not to be general agreement about the meaning of the word *rheology*. 'The science of deformation and flow' is the definition given in volume I and most dictionaries, and it is directly traceable to the original definition when the word was adopted in 1929. By this definition rheology would include most of applied mechanics including elasticity and fluid mechanics as well as kinetic theory. But dictionaries do not establish definitions; they record them. It is usage, illusive though it may sometimes be, that determines the meaning of a word. Today rheology is generally accepted as the science of the deformation and flow of non-ideal matter, i.e. non-Hookean solids and non-Newtonian fluids. The contents of this and other works on rheology attest to this usage as does the lack of mention of the word in most books and papers on elasticity, fluid mechanics, and physics. As another example of accepted usage, we note that in *Applied Mechanics Reviews* Rheology

is given a separate heading under Mechanics of Fluids along with Hydraulics, Incompressible Flow, etc.

As originally planned, volume III was to contain only a survey of general features of industrial rheology and specialized chapters on various materials and processes of technological importance. Rapid advances in the field, however, have tempered the original judgement. The survey chapter 'Rheology in industry' has been omitted and three other chapters added, two of which would probably have been placed in earlier volumes had that been possible. The first of these is 'The normal co-ordinate method for polymer chains', by B. H. Zimm. The author gives a lucid, absorbing introduction to the method of normal co-ordinate analysis as applied to the theory of high polymers. In this method a polymer molecule is idealized as a string of beads separated by springs and attached to them with universal joints. When normal co-ordinates are used, the equations of motion of this chain in a viscous liquid can be decomposed into sets of relatively simple, non-interacting equations. This permits calculation of a relationship between molecular structure and intrinsic viscosity which includes relaxation effects, and the limited calculations performed to date give results in good agreement with theory. This short chapter is a model of perfection of the difficult art of introducing a narrowly specialized subject to a sophisticated audience of widely varying training and interests.

The second of the chapters that might have appeared in an earlier volume is 'The principles of rheometry', by S. Oka. It is a catalogue of mathematical derivations for the behaviour of a wide variety of viscometers. The solutions given are mostly for inelastic, incompressible Newtonian fluids and are, in fact, all obtained from linearized forms of the Navier–Stokes equations. The usefulness of this chapter is severely impaired by lack of any mention of the relative merits of the instruments discussed.

As is to be expected, the remaining chapters vary greatly in style and manner of presentation; some are repetitive and tedious, though most are well-written. They vary even more, however, in the extent to which they are likely to be of interest to the readers of this journal. The subject 'Viscosity and elasticity of interfaces' is fascinating and of growing interest in fluid mechanics, but the chapter by this name is disappointing. Intriguingly incomplete, it is too short to convey adequately the ideas and problems of surface rheology, and it is further handicapped by the author's apparent confusion about units.

'The rheology of printing inks' contains some elementary hydrodynamics and a good description of the process of film splitting by rolls. It also contains a striking last sentence: 'The next decade should provide advances in this field rivaled in practical importance by no other branch of rheology.' The chapter 'Rheology of lubrication and lubricants' is written from the point of view of a physical chemist. To potential contributors to the theory of the fluid mechanics of lubrication, it is recommended as a guide to physical considerations that are relevant to the problem and which could easily be overlooked. Another chapter of interest is entitled 'Viscosity of suspensions of electrically charged particles and solutions of polymeric electrolytes'.

The remaining chapters are of lesser but varying interest to those whose primary work is in fluid mechanics. In order of appearance they are entitled: 'The rheology of Latex', 'Rheology of pastes and paints', 'Atomistic approach to the rheology of sand-water and of clay-water mixtures', 'The rheology of inorganic glasses', 'The rheology of concrete', 'The deformation of crystalline and cross-linked polymers', 'The rheology of adhesion', 'Rheology in moulding', 'Rheology of spinning', and 'Theory of screw extruders'.

This three-volumed treatise on rheology is now complete, and so we are in a position to evaluate its success, which will, of course, depend on the criteria used. A major purpose of a work of this sort is to introduce the scientific reader to various branches of rheology. Save for occasional lapses, this purpose has been well fulfilled both in choice of subject matter and in the manner of presentation. Future advances in rheology, however, will diminish the value of the treatise as introductory matter, and it must then serve as a point of reference for past work. For this purpose, too, it is a success. The impressive list of references in nearly every chapter admirably serve this end. It is likely that rheologists of the future will often turn to this work as an initial guide to past literature.

Another goal of the treatise, avowed in the preface of volume I, is to promote better understanding of the essential unity of rheology. Fortunately, this goal is of secondary importance, for here the work fails. In perusing the chapters one is impressed with the vast diversity of subject matter. On closer reading the diversity of approach becomes evident. Some authors, Weltmann for example, seem to write in a language that is different from that used by most of the others. But such is to be expected when chemists, physicists, engineers, and mathematicians all contribute to so huge a field.

Although the index of each volume is adequate, it is a nuisance to have to use three. If a fourth volume appears, a possibility mentioned in the preface of volume III, a comprehensive index to all four volumes would be a valuable inclusion.

The reviewer notes with pleasure that the cost of this volume is considerably less than that of its predecessors ($20 and $18). It is, in fact, but a few dollars more than seems reasonable to those of us who are at the purchasing end of the business.

C. A. SLEICHER

JOURNAL OF FLUID MECHANICS

Volume 9, Part 1 September 1960

CONTENTS

On the generation of sound by supersonic turbulent shear layers
by O. M. PHILLIPS *page* 1

The propagation of sound in relaxing gases in tubes at low frequencies
by D. H. SMITH and H. J. WINTLE 29

Observations on bubble growths in various superheated liquids
by PAUL DERGARABEDIAN 39

A study of the structure of the magnetohydrodynamic switch-on shock in steady plane motion
by Z. O. BLEVISS 49

A transformation for non-homentropic flows, with an application to large-amplitude motion in the atmosphere
by CHIA-SHUN YIH 68

Transonic rotational flow over a convex corner
by ROBERTO VAGLIO-LAURIN 81

An approximate equation for the spectrum of a conserved scalar quantity in a turbulent fluid
by I. D. HOWELLS 104

Weak thermal vortex rings
by B. R. MORTON 107

The propagation of waves along and through a conducting layer of gas
by G. S. S. LUDFORD 119

The flow past a flat plate of finite width
by J. W. ELDER 133

REVIEWS

The Scientific Papers of G. I. Taylor. Vol. II: Meteorology, Oceanography and Turbulent Flow 154

Advances in Geophysics. Vol. 6: Atmospheric Diffusion and Air Pollution 156

Rheology: Theory and Applications. Vol. III 158

Printed in Great Britain at the University Press, Cambridge
(Brooke Crutchley, University Printer)